Modeling and mathematical analysis of models in oceanography

Ralph Lteif

Université Libanaise
Ecole Doctorale
Sciences et Technologie

Communauté
UNIVERSITÉ Grenoble Alpes

THÈSE

Pour obtenir le grade de

DOCTEUR DE L'UNIVERSITÉ DE GRENOBLE

préparée dans le cadre d'une cotutelle entre l'*Université de Grenoble* et l'*Université Libanaise*

Spécialité : **Mathématiques appliquées**

Arrêté ministérial : le 6 janvier 2005 -7 août 2006

Présentée par

Ralph Lteif

Thèse dirigée par **Stéphane Gerbi et Raafat Talhouk**
et codirigée par **Christian Bourdarias et Samer Israwi**

préparée au sein des **Laboratoires LAMA, Université Savoie Mont Blanc et LM, Université Libanaise**
dans **les Écoles Doctorales MSTII et EDST**

Modélisation et analyse mathématique de modèles en océanographie

Thèse soutenue publiquement le **14 octobre 2016**,
devant le jury composé de :

M. Jean-Claude Saut
Professeur, Université Paris Sud 11, Rapporteur
M. Bernard Di Martino
Maître de conférences HDR, Université de Corse, Rapporteur
M. David Lannes
Directeur de Recherche, CNRS, Examinateur
M. Nicolas Seguin
Professeur, Université de Rennes 1, Examinateur
M. Stéphane Gerbi
Maître de conférences HDR, Université Savoie Mont Blanc, Directeur de thèse
M. Christian Bourdarias
Professeur, Université Savoie Mont Blanc, Co-Directeur de thèse
M. Raafat Talhouk
Professeur, Université Libanaise, Directeur de thèse
M. Samer Israwi
Professeur associé, Université Libanaise, Co-Directeur de thèse

Remerciements

Cette thèse est le résultat d'un travail de recherche qui n'aurait pas vu le jour sans le soutien et le conseil de plusieurs personnes auxquelles j'exprime ici ma sincère gratitude.

Je voudrais adresser en premier lieu ma profonde reconnaissance à mon directeur de thèse Raafat TALHOUK et à mon co-directeur Samer ISRAWI. Je vous remercie vivement pour vos judicieux conseils et pour le temps que vous m'avez consacré durant ces trois ans. Le soutien, l'encouragement et la confiance que vous m'avez accordé m'ont été très précieux.

Je voudrais également remercier mon directeur de thèse du côté Français Stéphane GERBI ainsi que mon co-directeur Christian BOURDARIAS. Vous n'avez pas cessé de m'aider, de me guider et de me motiver tout au long de mon séjour en France. Votre rigueur scientifique, votre grande disponibilité ainsi que votre profonde gentillesse m'ont apporté un cadre de travail très satisfaisant.

Je tiens à remercier chaleureusement Jean-Claude SAUT et Bernard Di MARTINO d'avoir eu l'amabilité d'accepter de rapporter cette thèse. J'exprime également mes sincères remerciements à David LANNES et à Nicolas SEGUIN pour m'avoir fait l'honneur de participer à mon jury.

Un grand remerciement à toutes l'équipes EDPs^2 du LAMA de l'Université Savoie Mont Blanc. Avoir la chance d'intégrer cette équipe m'a permis de riches rencontres tant d'un point de vue scientifique qu'humain. Merci donc à Jimmy GARNIER qui m'a donné la chance de présenter mes travaux dans le groupe de discussion dont la bonne ambiance m'a beaucoup apporté. Je tiens à remercier en particulier Denys DUTYKH pour les discussions fructueuses et pour les idées intéressantes qui m'a offert dans le travail numérique.

Je remercie également tous les collègues avec qui j'ai partagé des beaux moments tout au long de ma thèse. Merci à Bilal, Rodrigo, Jospeh, Lama, Beni, Michel, Marion et Charlotte.

J'exprime ma profonde gratitude à tous mes amis de longue date. Chacun entre vous et à sa manière a contribué à la réalisation de ce travail. Un grand merci à Elias, Jean, Majd, Nancy, Charline et Paul.

Un merci infinie à mes parents et à mes frères Marc et Peter pour leur soutien permanent, leurs encouragements et leur aide inconditionnelle. Sans eux, je ne serais pas ce que je suis aujourd'hui.

Finalement, j'ai une pensée toute particulière pour une personne très chère à mon cœur. Mary qui m'a soutenu durant les moments difficiles et qui m'a poussé à aller plus loin en période de doute. Merci pour tout cela...

Résumé

Modélisation et analyse mathématique de modèles en océanographie

Cette thèse est dédiée à la modélisation et à l'analyse mathématique de modèles asymptotiques utilisés en océanographie décrivant la propagation des ondes internes à l'interface entre deux couches de fluides de densités différentes, soumis à la seule force de gravité. L'objectif de cette thèse est de construire et justifier de nouveaux modèles asymptotiques prenant en compte la variation de la topographie. Pour ce faire, on pose plusieurs hypothèses de petitesse sur la profondeur de l'eau et sur les déformations à l'interface et au fond. On s'intéresse plus particulièrement à deux régimes de variations topographiques, celui de moyenne amplitude et celui de lentes variations de grande amplitude. La première partie de cette thèse consiste à justifier rigoureusement et étudier mathématiquement (existence, unicité, stabilité et convergence de la solution) deux classes de modèles asymptotiques. Une classe de *modèles couplés* et une classe de *modèles scalaires*. Cette dernière classe est caractérisée par la description de la propagation unidirectionnelle des ondes internes. Dans la deuxième partie on propose un schéma numérique pour résoudre le modèle asymptotique couplé dérivé dans la première partie dans le cadre d'un font plat. Ce modèle existant dans la littérature a été reformulé d'une façon plus appropriée pour la résolution numérique en gardant le même ordre de précision que l'original et en améliorant ses propriétés de dispersion. Enfin nous présentons plusieurs simulations numériques pour valider notre schéma.

Mots clés : ondes internes, topographie variable, modèles scalaires, modèles asymptotiques, approximation unidirectionnelle, simulations numériques, équations de Green-Naghdi, régime de Camassa-Holm.

Abstract

Modeling and mathematical analysis of models in oceanography

This thesis is dedicated to the modeling and the mathematical analysis of asymptotic models used in oceanography describing the propagation of internal waves at the interface between two layers of fluids of different densities, under the only influence of gravity. We aim here at constructing and justifying new asymptotic models taking into account variable topography. To this end, we assume several smallness assumptions on the depth of the water and on the deformations at the interface and at the bottom. We are interested in two topographic regimes, one for variations of medium amplitude and one for slow variations with large amplitude. In the first part of this thesis we rigorously justify and mathematically study (existence, uniqueness, stability and convergence of the solution) two classes of asymptotic models. A class of *coupled models* and a class of *scalar models*. The latter class is characterized by the description of the propagation of unidirectional internal waves. In the second part we propose a numerical resolution for the coupled asymptotic model derived in the first part restricted to the flat bottom case. This existing model in the literature has been rewritten under a new formulation more suitable for numerical resolution with the same order of precision as the standard one but with improved frequency dispersion. Finally, we present several numerical simulations to validate our scheme.

Keywords : internal waves, variable topography, asymptotic models, scalar models, unidirectional approximation, numerical simulations, Green-Naghdi equations, Camassa-Holm regime.

Table des matières

Chapitre 1

Introduction générale

Dans ce mémoire, nous nous intéressons à la modélisation et à l'analyse mathématique de problèmes issus de la physique et utilisés en océanographie, plus particulièrement le problème d'évolution des ondes internes intervenant dans l'océan. Les ondes internes se propagent à l'intérieur des fluides stratifiés comme les océans mais elles peuvent aussi intervenir dans l'atmosphère. Dans cette thèse, nous présenterons le problème dans le milieu océanique. En effet, la densité de l'eau des océans n'est pas homogène, elle varie selon sa température et sa salinité, on parle alors de fluide stratifié. Grâce à cette propriété, l'eau de l'océan a tendance à se séparer en deux couches, une couche supérieure d'eau pure qui est moins salée et une couche inférieure ayant une densité plus grande qui est plus fraiche et plus salée. Dans la figure 1.1 de l'expérience faite par l'équipe canadienne SLEIWEX [1] sur les ondes internes intervenant dans l'estuaire de Saint-Laurent au Canada, on peut remarquer notamment des ondes internes de grandes amplitudes. Selon l'équipe SLEIWEX, ces ondes peuvent être générées par les courants de marée stratifiés sur un fond de topographie irrégulière.

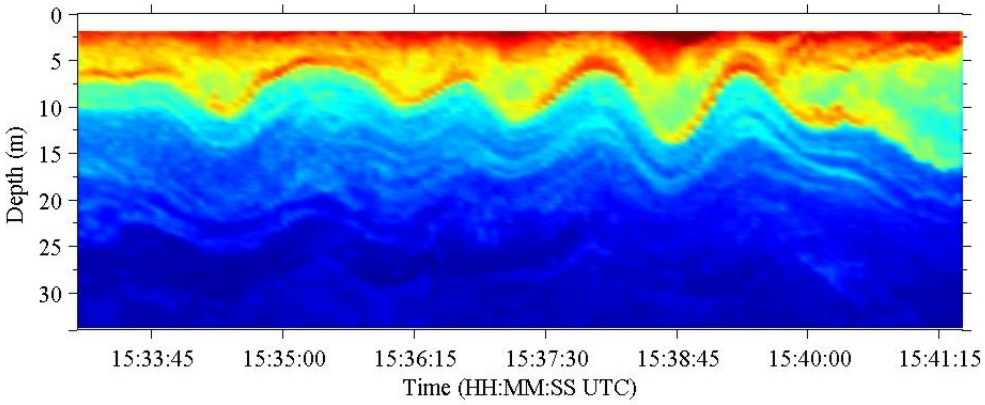

FIGURE 1.1. Stratification, due à la variation de la salinité et de la température.

La mesure des ondes internes solitaires a commencé d'une façon locale depuis les années 1960 à l'aide des chaînes de thermistance. En 1978, des photographies générales obtenues grâce aux observations du satellite SEASAT emportant un radar à synthèse d'ouverture ou "SAR"

1. `http://myweb.dal.ca/kelley/SLEIWEX/index.php`

ont démontré que les ondes internes sont des caractéristiques omniprésentes des eaux côtières (voir [56, 67]). En comparant à des ondes de surface (interface océan/atmosphère), les ondes internes peuvent avoir une grande amplitude de l'ordre de plusieurs centaines de mètres et sont capables de parcourir sous la forme de strie des milliers de kilomètres à travers l'océan. Les ondes internes produisent suffisamment d'effet sur la surface de la mer pour être observées depuis l'espace. On peut remarquer cela dans la figure 1.2 ; cette photographie prise à partir de la Station Spatiale International (ISS) [2], montre la côte nord de la Trinité, une île du sud des Caraïbes. L'effet des ondes internes sur la surface est visible dans cette photographie où on remarque l'interaction de trois ensembles d'ondes. L'ensemble le plus important (l'image en haut à gauche) montre un paquet de plusieurs vagues se déplaçant du nord-ouest en raison de l'écoulement de la marée vers la côte nord de Trinité.

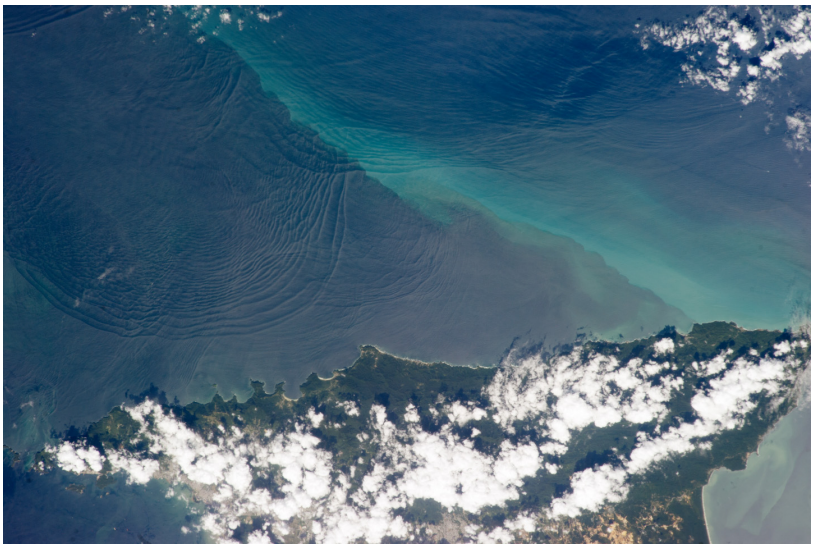

FIGURE 1.2. Paquets d'ondes internes se propageant dans la mer de Trinité, comme vu de l'espace.

La compréhension des ondes internes est un aspect essentiel dans la dynamique des océans. En fait, elles jouent un rôle assez important pour tout ce qui est relatif à la circulation globale (mélange des masses d'eau), l'équilibre des écosystèmes marins (transport de nutriments) et aux mécanismes climatiques (transfert de chaleur). D'autre part, les ondes internes peuvent influer sur la navigation des bateaux dans les eaux stratifiées. En effet, les ondes internes ont été la source d'un phénomène étrange appelé "phénomène des eaux mortes". Bien que déjà connu par les marins, l'explorateur norvégien Fridtjof Nansen a été le premier à décrire ce phénomène précisément dans le rapport de son expédition vers le pôle nord en 1893 à bord de son bateau "Le Fram" [98]. Nansen nous raconte que le bateau était freiné par une force mystérieuse alors que la surface de l'eau était calme [3].

La modélisation des phénomènes d'évolution des ondes internes attire l'attention permanente de plusieurs communautés scientifiques. Cependant, les mathématiciens rencontrent plusieurs

2. `http://earthobservatory.nasa.gov/IOTD/view.php?id=80337`

3. Ce phénomène a été expliqué par Ekman en 1904 par des travaux de recherches durant sa thèse [53]. Il expliqua que cette force est due à la stratification des flots et que l'énergie du bateau est transmise aux ondes internes qui se forment à l'interface entre les deux couches de fluide de différentes densités, ce qui induit une diminution de la vitesse du bateau. L'étude mathématique reliée à ce phénomène ne sera pas le sujet de ce mémoire, le lecteur intéressé pourra consulter [45] et les références incluses.

difficultés pour modéliser précisément les mécanismes physiques en jeu durant la propagation des ondes internes, surtout dans le cadre d'une topographie variable. En effet, l'influence de la variation de la topographie sur les ondes internes est non négligeable, elle peut avoir des conséquences importantes sur leur évolution. De plus, il est plus raisonnable en océanographie de modéliser les phénomènes d'évolution des ondes internes dans le cadre d'une topographie variable. En conséquence, l'influence de la topographie du fond sera traité dans une grande partie de ce mémoire. En général, la modélisation des ondes internes mène à des équations aux dérivées partielles difficiles à résoudre proprement, puisque le domaine d'étude fait partie des inconnues et que le système est fortement non linéaire. Ceci explique l'intérêt de construire des modèles simplifiés dans des régimes physiques spécifiques où plusieurs hypothèses de simplification sur la nature du fluide sont utilisées. Cette approche consiste à chercher des solutions approchées du problème. Les différents modèles sont obtenus à partir d'un développement asymptotique des opérateurs non locaux existant dans le système complet par rapport à des petits paramètres. Les modèles asymptotiques obtenus sont certainement plus agréables à étudier mathématiquement et à justifier rigoureusement. De plus, ils possèdent une structure plus simple pour la résolution numérique.

Le travail présenté dans cette thèse est constitué de deux parties. Dans la première partie nous construisons de nouveaux modèles asymptotiques qui décrivent la propagation des ondes internes unidimensionnelles à l'interface entre deux couches de fluides de densités différentes prenant en compte une topographie variable. Nous nous intéresserons à deux régimes de variations topographiques. Le premier régime sera celui des variations topographiques de moyenne amplitude et le second sera celui des variations topographiques qui peuvent avoir une large amplitude et une grande longueur d'onde, plus précisément on se place dans un régime où le fond peut varier lentement mais avec une grande amplitude. Les modèles simplifiés obtenus sont distingués en deux classes : une classe de *modèles couplés* et une classe de *modèles scalaires*. La dérivation de ces modèles s'appuient sur des hypothèses de petitesse sur la profondeur de l'eau et sur l'amplitude de la déformation de l'interface et du fond. Les solutions de ces deux classes de modèles sont analysées mathématiquement et justifiées rigoureusement comme approximation du modèle exact par des résultats de convergence aux Chapitres 2 et 3. La deuxième partie de cette thèse consiste à résoudre numériquement le modèle asymptotique *couplé* dérivé au Chapitre 2 restreint au cas d'un fond plat. Ce modèle initialement dérivé en [49] a été reformulé d'une façon plus appropriée pour la résolution numérique tout en améliorant sa relation de dispersion à l'aide d'un paramètre à choisir précisément. Enfin, nous présentons une série de validations numériques qui permettent d'évaluer systématiquement le schéma obtenu (voir Chapitre 4). Le corps de cette thèse est formé de trois chapitres au total qui sont l'objet de trois articles publiés ou soumis insérés dans leur forme originale, à part quelques changements mineurs :

• Le Chapitre 2 correspond à un travail en commun avec Samer Israwi et Raafat Talhouk, "An improved result for the full justification of asymptotic models for the propagation of internal waves", publié dans *Communications on pure and applied analysis*, 14(6) :2203–2230, 2015.

• Le Chapitre 3 correspond à un travail en commun avec Samer Israwi, "Coupled and scalar asymptotic models for internal waves over variable topography", *à soumettre*.

• Le Chapitre 4 correspond à un travail en commun avec Stéphane Gerbi et Christian Bourdarias, "A numerical scheme for an improved Green-Naghdi model in the Camassa-Holm regime for the propagation of internal waves", *à soumettre*.

Dans ce premier chapitre introductif, nous présentons le système d'équations qui gouvernent la propagation des ondes internes. Tout d'abord, on considère les hypothèses simplificatrices sur la nature du fluide, permettant ainsi la mise en place d'un cadre physique spécifique. Une deuxième étape consiste à reformuler le système d'équations à l'aide de l'introduction des opérateurs non locaux réduisant ainsi le nombre d'inconnues et la dimension de l'espace considéré. Le système d'équations obtenu demeure très difficile à résoudre. A cet effet, on l'écrit sous forme adimensionnée afin de faire apparaitre des petits paramètres sans dimension que nous détaillons permettant ainsi de réaliser dans la suite des développements asymptotiques. La construction des modèles asymptotiques est établi dans la Section 1.2. On commence par donner le sens de la justification rigoureuse des modèles asymptotiques en tant qu'une approximation du système complet. Après avoir présenté l'état de l'art sur les principaux modèles asymptotiques, on s'attache au développement asymptotique des opérateurs non locaux afin de dériver le modèle approché de type Green-Naghdi. Enfin, dans la Section 1.3 nous exposons plus en détails le contenu des différents Chapitres ainsi que les principaux résultats obtenus.

1.1 Les équations régissant le système

1.1.1 Système d'Euler complet

Le système que nous étudions est composé de deux couches de fluides non miscibles, homogènes et de densités différentes délimités supérieurement par un toit rigide et inférieurement par un fond variable. On note $X \in \mathbb{R}^d$ la variable horizontale de dimension $d = 1$ ou 2 et $z \in \mathbb{R}$ la variable verticale. La variable du temps est noté t. On suppose que l'interface et le fond sont paramétrisés par les graphes de deux fonctions $\zeta(t, X)$ et $b(X)$ désignant respectivement les déviations par rapport à leurs états de repos $z = 0$ et $z = -d_2$ (voir Figure 1.3). Les deux domaines occupés par le fluide supérieur et le fluide inférieur à l'instant $t \geq 0$ sont notés respectivement par :

$$\Omega_1 = \{(X, z) \in \mathbb{R}^d \times \mathbb{R} \ ; \ \zeta(t, X) \ \leq \ z \ \leq \ d_1\},$$
$$\Omega_2 = \{(X, z) \in \mathbb{R}^d \times \mathbb{R} \ ; \ -d_2 + b(X) \ \leq \ z \ \leq \ \zeta(t, X)\}.$$

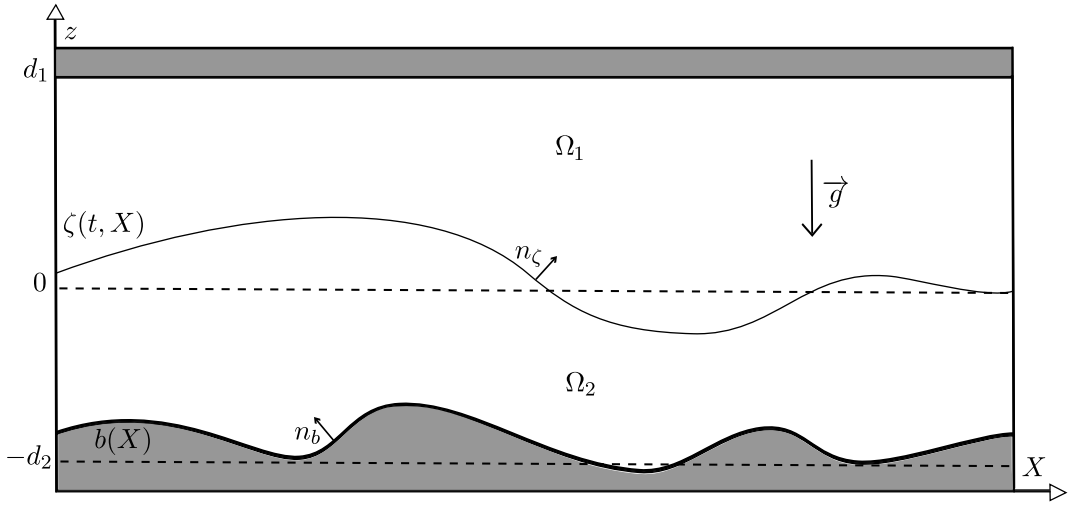

FIGURE 1.3. Domaine d'étude.

Précisons maintenant les hypothèses sur la nature et le domaine du fluide, afin de déterminer les équations qui gouvernent la propagation des ondes internes. Ce type d'hypothèse raisonnable est utilisé couramment en océanographie (voir [42]).

• Le domaine occupé par chaque fluide reste strictement connexe.
On supposera ainsi une profondeur minimale des deux couches de fluides c'est à dire il existe une constante strictement positive h_0 tel que pour tout $t > 0$ et pour tout $X \in \mathbb{R}^d$ on a :

$$d_1 - \zeta(t, X) \geq h_0 > 0 \quad \text{et} \quad \zeta(t, X) + d_2 - b(X) \geq h_0 > 0. \tag{1.1}$$

• Les fluides sont incompressibles et l'écoulement est irrotationnel.
L'incompressibilité d'un fluide se traduit par une masse volumique constante. On note par (ρ_i, v_i) la masse volumique et le champ de vitesse du fluide, avec $i = 1$ pour le fluide supérieur et $i = 2$ pour le fluide inférieur. L'équation de conservation des masses prend alors la forme suivante :

$$\text{div } \mathrm{v}_i = 0 \quad \text{dans} \quad \Omega_i. \tag{1.2}$$

L'hypothèse d'écoulement irrotationnel signifie que les particules de fluides ne tourne pas autour d'elle même. En fait, on se place loin des zones de surf et de swash, notamment dans la zone d'avant plage où les effets rotationnels sont négligeables. Un champ de vitesse irrotationnel s'écrit comme le gradient d'un potentiel, d'où l'existence des potentiels de vitesse ϕ_i tel que $\mathrm{v}_i = \nabla_{X,z}\phi_i$ dans Ω_i. Alors on peut déduire que ces potentiels vérifient également l'équation de Laplace à l'intérieur de chaque fluide :

$$\Delta_{X,z}\phi_i = 0 \quad \text{dans} \quad \Omega_i. \tag{1.3}$$

• Les fluides sont parfaits, non visqueux et soumis à la seule force de gravité.
L'évolution des potentiels de vitesse s'écrit à l'aide de l'équation de Bernoulli :

$$\partial_t\phi_i + \frac{1}{2}|\nabla_{X,z}\phi_i|^2 = -\frac{P}{\rho_i} - gz \quad \text{dans} \quad \Omega_i, \tag{1.4}$$

où g est l'accélération de la pesanteur et P la pression à l'intérieur du fluide.

• La surface, l'interface et le fond sont imperméables.
Plus précisément, aucune particule de fluide ne traverse la surface, l'interface et le fond. En notant n le vecteur normal à la surface concernée dans la direction ascendante, on peut écrire les conditions cinématiques suivantes :

$$\partial_z\phi_1 = 0 \qquad \text{sur} \qquad \{z = d_1\}, \tag{1.5}$$
$$\partial_t\zeta = \sqrt{1 + |\nabla\zeta|^2}\partial_n\phi_1 = \sqrt{1 + |\nabla\zeta|^2}\partial_n\phi_2 \qquad \text{sur} \qquad \{z = \zeta(t, X)\}, \tag{1.6}$$
$$\partial_n\phi_2 = 0 \qquad \text{sur} \qquad \{z = -d_2 + b(X)\}, \tag{1.7}$$

avec $\partial_n = n.\nabla_{X,z}$ la dérivée normale dans la direction du vecteur n concerné.
Notons $n_\zeta = \dfrac{1}{\sqrt{1 + |\nabla\zeta|^2}}(-\nabla\zeta, 1)^T$ et $n_b = \dfrac{1}{\sqrt{1 + |\nabla b|^2}}(-\nabla b, 1)^T$. Quand il y a aucun risque de confusion nous notons ∇_X par ∇.

• Le tenseur des contraintes est continue à l'interface,

$$[\![P(t, x)]\!] \equiv \lim_{\varepsilon \to 0} \Big(P(t, x, \zeta(t, x) + \varepsilon) - P(t, x, \zeta(t, x) - \varepsilon) \Big) = -\sigma k(\zeta), \tag{1.8}$$

où $k(\zeta) = -\nabla.\Big(\frac{1}{\sqrt{1+|\nabla\zeta|^2}}\nabla\zeta\Big)$ représente la courbure moyenne de l'interface et σ le coefficient de tension à l'interface.

En tout, les équations (1.2)- (1.8) qui décrivent notre problème sont récapitulées dans le système suivant :

$$\begin{cases} \Delta_{X,z}\phi_i \;=\; 0 & \text{dans } \Omega_i,\ i=1,2,\\ \partial_t\phi_i + \frac{1}{2}|\nabla_{x,z}\phi_i|^2 = -\frac{P}{\rho_i} - gz & \text{dans } \Omega_i,\ i=1,2,\\ \partial_z\phi_1 \;=\; 0 & \text{sur } \{z=d_1\},\\ \partial_t\zeta \;=\; \sqrt{1+|\nabla\zeta|^2}\partial_n\phi_1 \;=\; \sqrt{1+|\nabla\zeta|^2}\partial_n\phi_2 & \text{sur } \{z=\zeta(t,x)\},\\ \partial_n\phi_2 \;=\; 0 & \text{sur } \{z=-d_2+b(X)\},\\ [\![P(t,x)]\!] \;=\; -\sigma k(\zeta) & \text{sur } \{z=\zeta(t,x)\}, \end{cases} \tag{1.9}$$

Ce système est communément appelé *système d'Euler complet* et les solutions de ce système seront considérées comme solutions exactes de notre problème. Néanmoins, l'étude théorique de ce système est extrêmement difficile. A cause de la complexité de ces équations, leurs solutions sont très difficiles à décrire et sont difficilement calculables d'un point de vue numérique. En fait, on a un problème à frontière libre autrement dit le domaine est lui même une des inconnues.

1.1.2 Reformulation de Zakharov

Face à cette complexité, une idée intéressante due à Craig et Sulem [40, 39] consiste à reformuler le système d'équations (1.9) à l'aide de l'introduction d'un opérateur de Dirichlet-Neumann réduisant ainsi le nombre d'inconnues et la dimension de l'espace considéré. Cette idée est basée sur une remarque de Zakharov [115] qui consiste à dire "la connaissance du fluide à l'interface ou à la surface est suffisante pour déterminer le fluide dans tout le domaine". Cette reformulation a été adaptée au cas de deux couches avec une surface libre dans [38], avec toit rigide dans [10, 36].

Introduisons tout d'abord la trace du potentiel du fluide supérieure ϕ_1 à l'interface, que l'on notera ψ :

$$\psi \equiv \phi_1(t, X, \zeta(t, X)).$$

En effet, ϕ_1 et ϕ_2 sont définies de manière unique à partir de (ζ, ψ) comme solutions des problèmes de Laplace suivant [4] :

$$\begin{cases} \Delta_{X,z}\phi_1 = 0 & \text{dans } \Omega_1,\\ \partial_z\phi_1 = 0 & \text{sur } \{(X,z)\in\mathbb{R}^{d+1},\ z=d_1\},\\ \phi_1 = \psi & \text{sur } \{(X,z)\in\mathbb{R}^{d+1},\ z=\zeta\}, \end{cases} \tag{1.10}$$

$$\begin{cases} \Delta_{X,z}\phi_2 = 0 & \text{dans } \Omega_2,\\ \partial_n\phi_2 = \partial_n\phi_1 & \text{sur } \{(X,z)\in\mathbb{R}^{d+1},\ z=\zeta\},\\ \partial_n\phi_2 = 0 & \text{sur } \{(X,z)\in\mathbb{R}^{d+1},\ z=-d_2+b(X)\}. \end{cases} \tag{1.11}$$

L'écoulement est ainsi caractérisé par l'évolution des seules quantités (ζ, ψ) localisées à l'interface entre les deux couches de fluides. La description de cette évolution est due à l'introduction des opérateurs de Dirichlet-Neumann qu'on définit comme suit :

4. Les arguments classiques utilisés pour montrer l'existence et l'unicité d'une solution de (1.10)- (1.11) et donc le caractère bien posé des opérateurs de Dirichlet-Neumann sont détaillés dans [84].

Definition 1.1.1 (Opérateurs de Dirichlet-Neumann)**.** Soient $\zeta, b \in H^{t_0+1}(\mathbb{R}^d)$, $t_0 > d/2$, tel que (1.1) soit vérifié et soient $\psi \in L^2_{\text{loc}}(\mathbb{R}^d)$, $\nabla\psi \in H^{1/2}(\mathbb{R}^d)$, alors on définit :

$$\begin{aligned} G[\zeta]\psi &\equiv \sqrt{1+|\nabla\zeta|^2}\big(\partial_n\phi_1\big)\,|_{z=\zeta} = -(\nabla\zeta)(\nabla\phi_1)\,|_{z=\zeta} + (\partial_z\phi_1)\,|_{z=\zeta}\,, \\ H[\zeta,b]\psi &\equiv \nabla\big(\phi_2\,|_{z=\zeta}\,\big) = (\nabla\phi_2)\,|_{z=\zeta} + (\nabla\zeta)(\partial_z\phi_2)\,|_{z=\zeta}\,, \end{aligned}$$

avec ϕ_1 et ϕ_2 uniquement définis comme solutions dans $H^2(\mathbb{R}^d)$ des problèmes de Laplace (1.10) et (1.11).

En utilisant la condition cinématique (1.6) et en prenant la trace de l'équation de Bernoulli (1.4) à l'interface, le *système d'Euler complet* (1.9) peut se reformuler [5] en fonction des seules variables canoniques (ζ, ψ) comme un système d'équations d'évolutions définies sur $\mathbb{R}^d$:

$$\left\{\begin{array}{l} \partial_t\zeta \;-\; G[\zeta]\psi \;=\; 0, \\ \\ \partial_t\Big(\rho_2 H[\zeta,b]\psi - \rho_1\nabla\psi\Big) \;+\; g(\rho_2-\rho_1))\nabla\zeta \;+\; \dfrac{1}{2}\nabla\Big(\rho_2|H[\zeta,b]\psi|^2 - \rho_1|\nabla\psi|^2\Big) \\ \qquad\qquad\qquad\qquad\qquad\qquad = \;\nabla\mathcal{N}(\zeta,\psi) + \sigma\nabla(k(\zeta)), \end{array}\right. \tag{1.12}$$

avec :

$$\mathcal{N}(\zeta,\psi) \;\equiv\; \frac{\rho_2\big(G[\zeta]\psi + \nabla\zeta H[\zeta,b]\psi\big)^2 \;-\; \rho_1\big(G[\zeta]\psi + (\nabla\zeta)(\nabla\psi)\big)^2}{2(1+|\nabla\zeta|^2)}.$$

1.1.3 Système adimensionné

Bien que la "reformulation de Zakharov" a abouti à un système d'équations réduit (1.12), la description de ces solutions d'un point de vue qualitatif et quantitatif demeure très complexe. Un remède à cette situation passe par la construction des modèles asymptotiques simplifiés, donc la recherche des solutions approchées du système complet. Ces modèles approchés permettent de décrire d'une manière assez précise le comportement du système complet dans un régime physique spécifique. Ceci exige un adimensionnement du système afin de faire apparaître des petits paramètres sans dimension qui permettent de réaliser des développements asymptotiques des opérateurs non locaux (Dirichlet-Neumann), négligeant ainsi les termes dont l'influence est minime. L'ordre de grandeur de ces paramètres permet ainsi d'identifier le régime physique considéré. Nous commençons par définir les grandeurs caractéristiques du système (voir Figure 1.4).

• Une longueur d'onde typique de l'interface λ.

• Une amplitude maximale de la déformation de l'interface a.

• Une amplitude maximale de la déformation du fond a_b.

5. En utilisant la règle de dérivation en chaine et la continuité de la pression à l'interface.

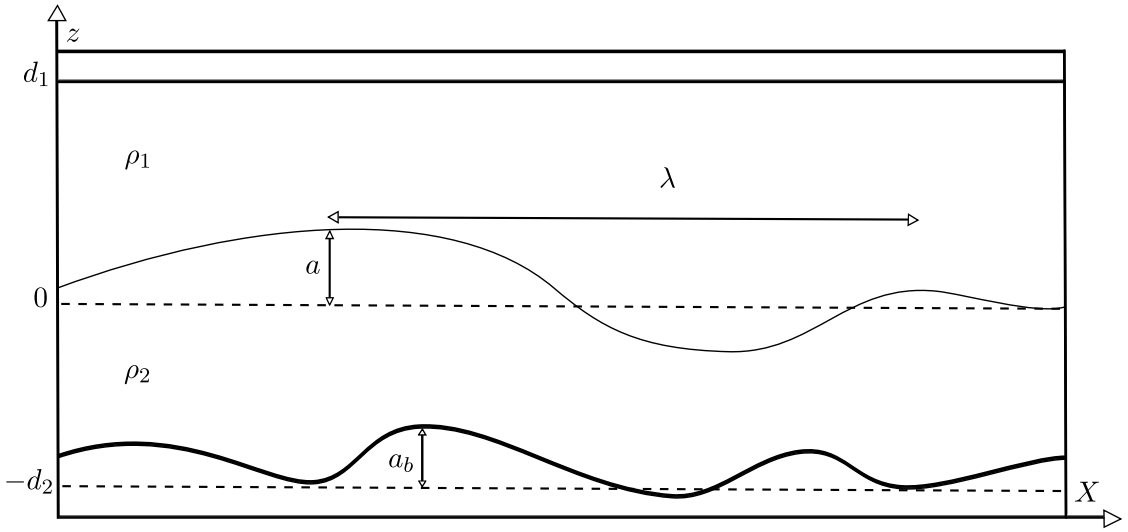

FIGURE 1.4. Grandeurs caractéristiques.

La longueur caractéristique λ est supposé identique dans les deux directions si $d = 2$. La longueur verticale de référence choisie est d_1 (profondeur du fluide supérieur). Rappelons que d_2 est la profondeur du fluide inférieur. La vitesse d'onde caractéristique est donnée par :

$$c_0 \;=\; \sqrt{g\frac{(\rho_2-\rho_1)d_1d_2}{\rho_2 d_1+\rho_1 d_2}}.$$

On définit alors les variables et les inconnues sans dimension suivantes [6] :

$$\tilde{z} \;\equiv\; \frac{z}{d_1}, \qquad \tilde{X} \;\equiv\; \frac{X}{\lambda}, \qquad \tilde{t} \;\equiv\; \frac{c_0}{\lambda}t,$$

et

$$\tilde{\zeta}(\tilde{t},\tilde{X}) \;\equiv\; \frac{\zeta(t,X)}{a}, \quad \tilde{b}(\tilde{X}) \;\equiv\; \frac{b(X)}{a_b}, \quad \tilde{\phi_i}(\tilde{t},\tilde{X},\tilde{z}) \;\equiv\; \frac{d_1}{a\lambda c_0}\phi_i(t,X,z) \quad (i=1,2).$$

Le choix de la vitesse caractéristique des ondes c_0 pour adimensionner la variable de temps et le potentiel des vitesses est motivé par l'étude du système linéarisé de (1.12) autour de l'état de repos $(\zeta,\psi)=(0,0)$ avec un fond plat (voir [83, Appendice A] pour plus de détails). Introduisons maintenant les différents paramètres sans dimension :

$$\mu \;\equiv\; \frac{d_1^2}{\lambda^2}, \quad \epsilon \;\equiv\; \frac{a}{d_1}, \quad \beta \;\equiv\; \frac{a_b}{d_1}, \quad \gamma \;=\; \frac{\rho_1}{\rho_2}, \quad \delta \;\equiv\; \frac{d_1}{d_2}, \quad \mathrm{Bo} \;=\; \frac{g(\rho_2-\rho_1)\lambda^2}{\sigma}.$$

Avant de réécrire le système sans dimension, nous donnons dans ce qui suit la signification de chaque paramètre :

• μ représente le carré du rapport de la longueur verticale de référence à la longueur d'onde

6. Dans le Chapitre 3 on effectue un changement de variable légèrement différent de celui présenté ici. En fait, l'adimensionnement du fond suppose que la longueur d'onde de la variation de la topographie est différente de celle de l'interface (voir Section 3.2 du Chapitre 3, page 68).

interne. Ce paramètre communément appelé paramètre de dispersion ou "*shallowness parameter*", mesure le caractère de faible profondeur. En effet, on s'intéresse dans notre étude au régime d'eaux peu profondes ou "*shallow water regime*" où ce paramètre est supposé très petit :

$$\mu \ll 1.$$

Cette hypothèse est essentielle afin de pouvoir faire des développements asymptotiques permettant ainsi la dérivation de modèles approchés.

• ϵ représente l'amplitude de l'onde interne. Il est souvent appelé paramètre de non linéarité. Dans la suite de notre étude, la dérivation des modèles asymptotiques s'appuiera sur une hypothèse de petitesse sur ce paramètre. Plus précisément, on suppose $\epsilon = \mathcal{O}(\sqrt{\mu})$, ce qui correspond au régime souvent appelé "*Camassa-Holm regime*".

• β représente l'amplitude de la variation topographique. Dans ce qui suit, on dérive plusieurs modèles asymptotiques *couplés* et *scalaires*, prenant en compte la variation topographique. On distinguera deux cas :
-Le premier cas est traité dans le Chapitre 2 et correspond à une variation topographique de moyenne amplitude, où on s'appuie sur l'hypothèse de petitesse $\beta = \mathcal{O}(\sqrt{\mu})$.
-Le deuxième cas est traité dans le Chapitre 3 et peut correspondre à une variation topographique lente de large amplitude [7]. En fait, on suppose cette fois que $\beta\alpha = \mathcal{O}(\sqrt{\mu})$ avec α le rapport de la longueur d'onde de la variation de l'interface à la longueur d'onde de la variation du fond.

• γ représente le rapport de la densité du fluide supérieur à la densité du fluide inférieur. On suppose que le fluide est stratifié de manière stable, notamment pas de phénomène de convection c'est à dire que le fluide plus dense sera au dessous du fluide moins dense. On fixe $\gamma \in (0, 1)$.

• δ représente le rapport de la profondeur du fluide supérieur à la profondeur du fluide inférieur. On suppose que les deux couches de fluide admettent une profondeur similaire, notamment δ ne s'approche pas de zéro ou de l'infini.

• Bo représente le rapport des forces de gravité aux forces capillaires. Ce paramètre est appelé "*Bond number*". Par contre, dans la suite on utilisera $\mathrm{bo} = \mu\mathrm{Bo} = \dfrac{\mathrm{g}(\rho_2 - \rho_1)\mathrm{d}_1^2}{\sigma}$ cela revient à supposer que $\mathrm{Bo}^{-1} = \mathcal{O}(\mu)$.

Il est important de comprendre qu'on se place dans un régime physique spécifique ("*shallow water regime*) où la profondeur des deux couches de fluides est faible par rapport à la longueur d'onde caractéristique. Ceci n'empêche pas que la profondeur peut atteindre l'ordre d'un kilomètre. De plus les hypothèses sur l'amplitude de l'onde interne et sur celle du fond sont considérées petites par rapport à la profondeur des couches de fluide. Ce régime asymptotique ainsi que les hypothèses de petitesse s'appliquent dans différents domaines physiques, ils permettent de considérer la propagation des ondes internes dans les zones côtières et dans les mers profondes. Par exemple, les observations et mesures dans les zones côtières de la baie de Massachusetts font apparaitre la propagation d'ondes internes de 10 m d'amplitude avec une longueur d'onde de 300 m sur une

7. Dans ce régime particulier, plusieurs équations de type KdV pour les ondes de surface unidirectionnelles au fond variable ont été dérivées dans la littérature, citons [95, 102, 71], (voir aussi [28] pour les systèmes de type Boussinesq).

profondeur de 30 m. De même, des paquets d'ondes internes de large amplitude (80 m) et de longueur d'onde d'environ 2000 m ont été mesurés dans la mer d'Andaman situé dans l'océan indien sur une profondeur de 500 m dans une eau de profondeur 1500 m.(voir [66, 67] et leurs références).

L'introduction de ces différents variables, inconnues et paramètres sans dimension permet d'écrire la forme adimensionnée de notre système. En omettant les tildes pour des raisons de lisibilité, on introduit les domaines adimensionnés des deux fluides :

$$\Omega_1 = \{(X,z) \in \mathbb{R}^d \times \mathbb{R} \ ; \ \epsilon\zeta(t,X) \ \leq \ z \ \leq \ 1\},$$

$$\Omega_2 = \{(X,z) \in \mathbb{R}^d \times \mathbb{R} \ ; \ -\frac{1}{\delta} + \beta b(X) \ \leq \ z \ \leq \ \epsilon\zeta(t,X)\}.$$

La condition de profondeur minimale devient la suivante :

$$1 - \epsilon\zeta(t,X) \geq h_0 > 0 \quad \text{et} \quad 1/\delta + \epsilon\zeta(t,X) - \beta b(X)) \geq h_0 > 0, \tag{1.13}$$

et les problèmes de Laplace adimensionnés :

$$\begin{cases} (\mu\Delta_X + \partial_z^2)\phi_1 = 0 & \text{dans } \ \Omega_1, \\ \partial_z\phi_1 = 0 & \text{sur } \{(X,z) \in \mathbb{R}^{d+1}, \ z = 1\}, \\ \phi_1 = \psi & \text{sur } \{(X,z) \in \mathbb{R}^{d+1}, \ z = \epsilon\zeta\}, \end{cases} \tag{1.14}$$

$$\begin{cases} (\mu\Delta_X + \partial_z^2)\phi_2 = 0 & \text{dans } \ \Omega_2, \\ \partial_n\phi_2 = \partial_n\phi_1 & \text{sur } \{(X,z) \in \mathbb{R}^{d+1}, \ z = \epsilon\zeta\}, \\ \partial_n\phi_2 = 0 & \text{sur } \{(X,z) \in \mathbb{R}^{d+1}, \ z = -\frac{1}{\delta} + \beta b(X)\}. \end{cases} \tag{1.15}$$

À partir de ϕ_1 et ϕ_2 adimensionnés solutions des problèmes de Laplace (1.14) et (1.15), on définit également les opérateurs de Dirichlet-Neumann adimensionnés.

$$\begin{aligned} G^\mu\psi \ &\equiv \ G[\epsilon\zeta]\psi \equiv \sqrt{1+\mu|\epsilon\nabla\zeta|^2}\big(\partial_n\phi_1\big)\,|_{z=\epsilon\zeta} = -\mu\epsilon(\nabla\zeta)(\nabla\phi_1)\,|_{z=\epsilon\zeta} + (\partial_z\phi_1)\,|_{z=\epsilon\zeta}\,, \\ H^{\mu,\delta}\psi \ &\equiv \ H[\epsilon\zeta,\beta b]\psi \equiv \nabla\big(\phi_2\,|_{z=\epsilon\zeta}\,\big) = (\nabla\phi_2)\,|_{z=\epsilon\zeta} + \epsilon(\nabla\zeta)(\partial_z\phi_2)\,|_{z=\epsilon\zeta}\,. \end{aligned}$$

Enfin la forme adimensionnée du *système d'Euler complet* est la suivante :

$$\begin{cases} \partial_t\zeta \ - \ \dfrac{1}{\mu}G^\mu\psi \ = \ 0, \\ \partial_t\Big(H^{\mu,\delta}\psi - \gamma\nabla\psi\Big) \ + \ (\gamma+\delta)\nabla\zeta \ + \ \dfrac{\epsilon}{2}\nabla\Big(|H^{\mu,\delta}\psi|^2 - \gamma|\nabla\psi|^2\Big) \\ \qquad\qquad = \ \mu\epsilon\nabla\mathcal{N}^{\mu,\delta} - \mu\dfrac{(\gamma+\delta)}{\mathrm{bo}}\dfrac{\nabla(k(\epsilon\sqrt{\mu}\zeta))}{\epsilon\sqrt{\mu}}, \end{cases} \tag{1.16}$$

avec :

$$\mathcal{N}^{\mu,\delta} \ \equiv \ \frac{\big(\frac{1}{\mu}G^\mu\psi + \epsilon\nabla\zeta H^{\mu,\delta}\psi\big)^2 \ - \ \gamma\big(\frac{1}{\mu}G^\mu\psi + \epsilon(\nabla\zeta)(\nabla\psi)\big)^2}{2(1+\mu|\epsilon\nabla\zeta|^2)}.$$

Des résultats antérieurs ont montré que le problème de Cauchy associé au *système d'Euler complet* (1.16) est mal posé dans les espaces de Sobolev (au moins en dimension $d = 1$) en absence de tension de surface à cause des instabilités de types Kelvin-Helmholtz et Rayleigh-Taylor, citons [109, 108, 52, 69, 89, 78]. Ajouter un terme de tension de surface permet d'obtenir un caractère bien posé mais pour un temps d'existence très faible (voir [4, 5, 106]). Grâce à un

critère de stabilité, Lannes a démontré dans [83] que le problème devient bien posé (dans le cas d'un fond plat) en prenant en considération le terme de tension de surface dans le système. Le temps d'existence de la solution de ce système reste raisonnable même si le terme de tension de surface est très petit. Cependant, ces résultats sont valables dans le cadre d'un fond plat et à notre connaissance il n'existe aucun résultat de caractère bien posé dans le cas où le fond est variable.

Comme nous l'avons mentionné ci-dessus, l'étude théorique ainsi que la résolution numérique du *système d'Euler complet* demeurent très difficiles. Dès lors, nous nous intéresserons dans la section suivante à la construction des modèles asymptotiques réduits.

1.2 Construction des modèles asymptotiques

Justification rigoureuse des modèles asymptotiques.

Avant de construire les différents modèles asymptotiques, donnons un sens à leur justification rigoureuse en tant qu'approximation du *système d'Euler complet* (1.16). Suivant la terminologie de [84, 83], la justification rigoureuse d'un modèle asymptotique (S_a) consiste en trois étapes :

• **Consistance** : Le *système d'Euler complet* (1.16) est consistant avec le modèle asymptotique (S_a), si toute solution bornée et suffisamment régulière $U = (\zeta, \psi)$ de (1.16) telle que (1.13) est vérifiée, satisfait (S_a) jusqu'à un petit résidu, indiquant la *précision* du modèle asymptotique.

Dans ce mémoire, la précision d'ordre $\mathcal{O}_{L^\infty}(\varepsilon)$ sera comprise au sens de la norme L^∞, i.e. le reste est borné en norme L^∞. Cependant, la précision d'ordre $\mathcal{O}(\varepsilon)$ sera comprise au sens des normes $L^\infty H^s$, i.e. le reste est borné en norme H^s, uniformément par rapport au temps t. La consistance en norme H^s est plus forte que celle en norme L^∞ et elle permet de justifier rigoureusement le modèle asymptotique.

• **Caractère bien posé** : Le *système d'Euler complet* (1.16) et le modèle asymptotique (S_a) ayant des données initiales identiques suffisamment régulières, doivent être bien posés [8].

• **Convergence** : La solution $U_a = (\zeta_a, v_a)$ du modèle asymptotique (S_a) approche la solution $U = (\zeta, \psi)$ du *système d'Euler complet* (1.16) avec une précision d'ordre $\mathcal{O}(\varepsilon)$, si pour une même donnée initiale, la différence entre les deux solutions est bornée en norme H^s, uniformément par rapport au temps t. Plus précisément, on a l'estimation suivante :

$$|(\zeta, \psi) - (\zeta_a, v_a)|_{L^\infty([0,T],H^s)} \leq C\ \varepsilon,$$

avec C indépendant de ε.

A partir des deux premières étapes de la procédure (consistance et caractère bien posé) on peut conclure la convergence grâce à un résultat de stabilité des solutions du modèle asymptotique (S_a) par rapport aux perturbations des équations.

Présentons maintenant l'état de l'art sur la dérivation, l'analyse mathématique et la résolution numérique de plusieurs modèles asymptotiques dans différents régimes.

8. Comme nous l'avons dit, à notre connaissance il n'existe aucun résultat d'existence et d'unicité de solution pour le *système d'Euler complet* (1.16) dans le cas où le fond est variable. Pour la suite de notre étude, on supposera que ce dernier admet une unique solution.

1.2.1 État de l'art sur les modèles asymptotiques

La dérivation des modèles asymptotiques dans le régime d'eaux peu profondes ($\mu \ll 1$) et dans le cadre des ondes de gravité (une couche de fluide à surface libre) remonte à la fin du XIXème siècle. Saint-Venant [41] a dérivé le modèle qui porte son nom en négligeant les termes du premier ordre $\mathcal{O}(\mu)$. Ceci correspond à supposer que la vitesse horizontale est constante sur toute la profondeur du fluide. Un modèle faiblement non linéaire a été dérivé par Boussineq [20, 21] afin de décrire la propagation des ondes de gravité de petite amplitude et de grandes longueurs d'ondes ($\epsilon = \mathcal{O}(\mu)$). Un modèle d'ordre supérieur $\mathcal{O}(\mu^2)$ traitant les vagues ayant une plus grande amplitude que le modèle de type Boussinesq a été introduit plus tard par Serre [105] et Green, Naghdi [60]. Ce modèle prend en compte les termes à effet dispersif négligés par le modèle de Saint-Venant. La justification du modèle de Boussinesq a été achevée et améliorée plus tard dans les travaux suivants [35, 12, 14, 104, 25]. Finalement, Alvarez-Samaniego et Lannes [2] ont démontré le caractère bien posé du *système d'Euler complet* pour un temps large dans le cas d'une couche de fluide en dimension ($d = 1, 2$) et avec un fond variable. De plus, ils ont justifié rigoureusement plusieurs modèles asymptotiques de type Saint-Venant, Boussineq et Green-Naghdi. L'influence de la topographie sur les ondes de surface a été traitée dans [28], où plusieurs modèles asymptotiques ont été construits et étudiés en dimension $d = 1, 2$ considérant deux régime topographiques sur le fond : un régime de faible amplitude et un régime de large amplitude. Voir aussi [70, 72] où la solution des équations de Green-Naghdi avec fond variable a été construite par un schéma itératif de Picard de sorte qu'il n'y ait pas de perte de régularité de la solution par rapport à l'état initial.

Tous ces travaux sont limités au cas d'une couche de fluide. Cependant, les modèles bi-couche possèdent la même structure. En fait, on peut retrouver les modèles dans le cas d'une couche de fluide à partir des modèles bi-couche en supposant que la densité du premier fluide est nulle et que le rapport des deux profondeurs est égale à 1. Introduisons quelques résultats antérieures traitant le cas de deux couches de fluide. Plusieurs modèles asymptotiques pour le système bi-fluide ont été dérivés et étudiés sous l'hypothèse de toit rigide, citons [97, 92, 93, 31, 32, 38]. Plus tard, dans le même cadre (bi-couche et toit rigide) une large classe de modèles dans différents régimes a été dérivée et justifiée dans le sens de consistance (voir [16]). Dans [65], les auteurs ont montré que le système de Saint-Venant bi-couche est bien posé en dimension $d = 2$ et sans tension de surface sous certaines conditions raisonnables sur les données initiales. Ce résultat a été généralisé par Bresch et Renardy [22] au cas non-irrotationnel. Récemment, Duchêne, Israwi et Talhouk [49] ont dérivé un nouveau modèle de type Green-Naghdi dans le *régime de Camassa-Holm* décrivant la propagation des ondes internes de moyenne amplitude ($\epsilon = \mathcal{O}(\sqrt{\mu})$) délimité par un toit rigide et un fond plat. Ils ont justifié rigoureusement leur modèle asymptotique comme approximation du modèle exact par un résultat de convergence. De plus, leur modèle permet de justifier rigoureusement tout modèle asymptotique bien posé et consistant. Ce résultat sera étendu dans le Chapitre 2 au cas de fond variable de moyenne amplitude et dans le Chapitre 3 au cas de fond variable de large amplitude et de grandes longueurs d'ondes.

Cependant, le cas de fond variable a été moins exploré dans la littérature d'ondes internes. Présentons quelques résultats remarquables dans ce cadre. Un modèle asymptotique bi-fluide a été dérivé dans [103] afin d'étudier l'interaction des ondes internes non linéaires avec une topographie variable de grande amplitude. Suivant la méthode initiée dans [16] basée sur le développement asymptotique des opérateurs non locaux, Anh dérive dans [6] plusieurs modèles asymptotiques pour une grande classe de régimes prenant en compte la tension de surface. Suivant la même méthode Duchêne [44] dérive des modèles asymptotiques pour la propagation des ondes de surface

et des ondes internes en dimension $d = 1, 2$. L'évolution des ondes internes bidimensionnelles de grandes amplitudes dans un système bi-couche avec fond variable a été étudié dans [7] à l'aide d'un nouveau modèle asymptotique qui régularise les instabilités de type Kelvin-Helmholtz. Un modèle de type Green-Naghdi qui décrit la propagation des ondes internes bidimensionnelles ($d = 2$) sur un fond variable a été dérivé et justifié en terme de consistance dans [48]. Les travaux mentionnés précédemment sont limités au niveau formel. En fait, les modèles dérivés dans ces papiers sont systématiquement justifiés par un résultat de consistance, et ne fournissent pas une justification rigoureuse contrairement à [90].

Dans tous les travaux énoncés précédemment, les modèles dérivés consistent en deux équations d'évolution couplées. Tous ces modèles se réduisent à l'ordre inférieur de précision à une équation d'onde de vitesse ± 1 et toute perturbation de la donnée initiale de l'interface conduit à une division de l'interface en deux ondes se propageant dans des directions opposées. Dès lors, un intérêt particulier est accordé à l'étude de modèle unidirectionnel caractérisé par une équation scalaire qui décrit la propagation de l'onde dans une direction donnée. Plus précisément, l'attention est apportée à une seule direction après que l'onde se divise. L'équation de Korteweg-de Vries [81] est l'exemple le plus fameux d'un tel modèle. Cette équation dispersive non-linéaire modélise la propagation unidirectionnelle d'une onde solitaire au dessus d'une couche de fluide homogène en eau peu profonde. A partir de cette équation on peut retrouver par exemple l'équation de Benjamin-Bona-Mahony (BBM) [9]. Plusieurs généralisations de ces modèles ont été proposées dans la littérature, voir [27, 75]. Pour une généralisation au cas $d = 2$ pour les ondes faiblement transverses voir [76]. Ces modèles sont une approximation au premier ordre des équations de Boussinesq. Leur justification rigoureuse a été démontrée plus tard dans les travaux de [14, 87, 29, 34, 71] (voir [46] pour le cas de deux couches de fluide).

Une différence importante se manifeste dans le cas de deux couches de fluides. En fait, les coefficients dépendent maintenant de la situation (deux couches, fond variable) et le terme de non linéarité peut s'éliminer pour un certain coefficient critique. Face à cette situation, plusieurs modèles contenant un terme non linéaire cubique ont été dérivés dans [77, 43, 100] et étudiés dans [61, 101]. Ces modèles ont été souvent motivés par des expériences, citons [80, 68, 94]. Des modèles d'ordres élevés ont été dérivés et justifiés dans le *régime de Camassa-Holm* ($\epsilon = \mathcal{O}(\sqrt{\mu})$) dans [34] pour le cas d'une couche de fluide. De tels modèles sont dérivés pour le cas de deux couches de fluides avec fond plat et toit rigide dans [32], avec surface libre dans [62, 38]. La justification rigoureuse de tels modèles d'ordres élevés a été achevée dans [47] dans le cas d'un fond plat. A notre connaissance il n'existe aucun travail de justification rigoureuse de modèles unidirectionnels qui décrivent la propagation d'ondes internes sur un fond variable. Dès lors, on proposera dans le Chapitre 3 plusieurs modèles unidirectionnels dans plusieurs régimes prenant en compte la variation topographique.

La résolution numérique de ces modèles asymptotiques a aussi connu une très grande activité depuis quelques années. Présentons tout d'abord quelques travaux récents qui traitent numériquement plusieurs systèmes de type Green-Naghdi (dénoté GN dans la suite) dans le cas d'une couche de fluide. Un schéma numérique de type Godunov préservant la dynamique des ondes solitaires de surface a été utilisé dans [88] afin de résoudre numériquement un système de type GN écrit en terme de nouvelles variables de potentiel. Une nouvelle formulation du système de type GN a été donnée dans [17] dans le but d'améliorer les propriétés de dispersion en fonction d'un paramètre (voir aussi [30] où une famille de trois paramètres de système de type GN a été dérivée). Ensuite les auteurs proposent un schéma de "splitting" qui traite séparément la partie hyperbolique avec une méthode de volumes finis et la partie dispersive avec une méthode de différences finies. Cette stratégie a été utilisée antérieurement dans [55] pour décrire les solutions

des équations de type Boussinesq (voir aussi [110] où cette stratégie a été développée pour traiter le déferlement). Un schéma numérique basé sur une méthode de Galerkin/éléments-finis est présenté dans [96] pour résoudre le système de Serre. Récemment, Lannes et Marche [86] ont adapté le schéma de "splitting" pour une nouvelle classe d'équations non linéaires et faiblement dispersives de type GN en dimension $d = 2$ prenant en compte la variation de la topographie.

Pour autant que nous sachions, la résolution numérique du système de type GN dans le cas des ondes internes à l'interface entre deux couches de fluide avec un toit rigide a été moins étudiée. Dans ce cadre, la validité des modèles faiblement non-linéaires (Boussinesq) et fortement non-linéaires (Saint-Venant et Green-Naghdi) est examinée dans [26] à partir d'une comparaison des résultats analytiques et numériques des modèles asymptotiques fortement non-linéaires dérivés par Choi et Camassa [32] avec des simulations numériques des équations d'Euler et des données expérimentales présentées dans [94, 63]. Guyenne [64] compare les solutions numériques d'ondes solitaires internes de grande amplitude d'un modèle hamiltonien avec les solutions de modèles faiblement et fortement non-linéaires. Un modèle de type Boussinesq pour la propagation des ondes internes dans deux sens avec toit rigide a été dérivé dans [99], où les auteurs étudient numériquement la propagation ainsi que la collision d'ondes solitaires. Récemment, Duchêne *et al.* [50] ont étudié numériquement plusieurs classes de modèles modifiés de type GN afin de montrer comment les différentes propriétés de dispersion des modèles modifiés peuvent affecter l'apparition des instabilités de type Kelvin-Helmholtz. Dans le Chapitre 4, nous allons comparer numériquement le modèle dérivé dans le Chapitre 2, après reformulation, dans le cadre d'un fond plat [9] aux différentes classes de modèles de type GN modifiés obtenus dans [50]. Cette comparaison mettra en évidence l'amélioration des propriétés de dispersion et de stabilisation qu'offre cette nouvelle formulation.

Après avoir exposé l'état de l'art, nous présentons d'une manière résumée la méthode qui permet d'obtenir les développements asymptotiques des opérateurs de Dirichlet-Neumann afin de construire les différents modèles asymptotiques dans le cas de deux couches de fluides avec fond variable.

1.2.2 Développements asymptotiques des opérateurs de Dirichlet-Neumann

L'ingrédient essentielle pour la construction de modèles approchés consiste dans le développement asymptotique des opérateurs de Dirichlet-Neumann. Il s'agit de remplacer ces opérateurs dans le *système d'Euler complet* (1.16) par leurs approximations pour obtenir les différents modèles asymptotiques. Tout d'abord il faut se placer dans un régime physique spécifique, où on considère une hypothèse de petitesse sur un des paramètres du système. Comme nous l'avons dit, on s'intéresse dans notre étude au régime d'eaux peu profondes où on suppose que le paramètre de dispersion est très petit :

$$\mu \ll 1.$$

Nous commençons par définir u_1 (resp. u_2) la vitesse horizontale du fluide moyennée verticalement sur la couche du fluide supérieur (resp. inférieur).

Definition 1.2.1. Soient $\psi \in L^2_{\mathrm{loc}}(\mathbb{R}^d)$, tel que $\nabla\psi \in H^{1/2}(\mathbb{R}^d)$ et $\zeta, b \in H^{t_0+1}(\mathbb{R}^d)$ avec $t_0 > d/2$. Soient $h_1 \equiv 1 - \epsilon\zeta$ et $h_2 \equiv \delta^{-1} + \epsilon\zeta - \beta b$ les profondeurs du fluide supérieur et du fluide inférieur

9. Ce modèle correspond exactement au modèle dérivé dans [48].

respectivement. On suppose qu'il existe $h_0 > 0$ avec $h_1, h_2 \geq h_0 > 0$. Alors on définit :

$$u_1(t,x) = \frac{1}{h_1(t,X)} \int_{\epsilon\zeta(t,X)}^{1} \nabla\phi_1(X,z)\ dz,$$
$$u_2(t,x) = \frac{1}{h_2(t,X)} \int_{-\frac{1}{\delta}+\beta b(X)}^{\epsilon\zeta(t,X)} \nabla\phi_2(X,z)\ dz,$$

avec ϕ_1 and ϕ_2 solutions des problèmes de Laplace (1.14) et (1.15).

Proposition 1. *Soient ζ, ψ, b satisfaisant l'hypothèse de la Définition 1.2.1. Alors on a les identités suivantes :*

$$G^\mu[\epsilon\zeta]\psi \ = \ \mu\nabla\cdot(h_1u_1) \ = \ -\mu\nabla\cdot(h_2u_2). \tag{1.17}$$

Idée de la preuve. La preuve de cette proposition est basée sur un calcul simple par l'intégration des équations de Laplace satisfaites par ϕ_1 et ϕ_2 après les avoir multiplié par une fonction test. Utilisant l'identité de Green et le fait que $\partial_n\phi_1 = \partial_n\phi_2 = (1+\mu|\epsilon\nabla\zeta|^2)^{-1/2}G^\mu[\epsilon\zeta]\psi$, on peut facilement déduire les identités. Pour le calcul détaillé voir [47, Section 2.2]. □

Donnons maintenant le développement asymptotique des opérateurs de Dirichlet-Neumann dans les deux propositions suivantes. On rappelle que ces deux propositions étendent le résultat obtenu en [16] au second ordre. On peut déduire ces deux résultats à partir des développements asymptotiques obtenus en [12, 13, 14, 84] traitant le cas d'une couche de fluide [10]. Pour plus de détails sur la description de cette méthode consulter [48, Section 3].

Proposition 2. *Soient $t_0 > d/2$, $s \geq 0$ et soient $\psi \in L^2_{\text{loc}}(\mathbb{R}^d)$, tel que $\nabla\psi \in H^{s+4}(\mathbb{R}^d)^d$ et $\zeta, b \in H^{t_0+2}(\mathbb{R}^d) \cap H^{s+4}(\mathbb{R}^d)$. Soient $h_1 \equiv 1-\epsilon\zeta$ et $h_2 \equiv \delta^{-1}+\epsilon\zeta-\beta b$ tel qu'il existe $h_0 > 0$ avec $h_1, h_2 \geq h_0 > 0$. Alors :*

$$\big|u_1 \ - \ \nabla\psi\big|_{H^s} \quad \leq \quad \mu M(s+2)\big|\nabla\psi\big|_{H^{s+2}}, \tag{1.18}$$
$$\big|u_1 \ - \ \nabla\psi \ + \ \mu\mathcal{T}[h_1,0]\nabla\psi\big|_{H^s} \quad \leq \quad \mu^2 M(s+4)\big|\nabla\psi\big|_{H^{s+4}}, \tag{1.19}$$
$$\big|\nabla\psi \ - \ u_1 \ - \ \mu\mathcal{T}[h_1,0]u_1\big|_{H^s} \quad \leq \quad \mu^2 M(s+4)\big|\nabla\psi\big|_{H^{s+4}}. \tag{1.20}$$

Proposition 3. *Soient $t_0 > d/2$, $s \geq 0$ et soient $\psi \in L^2_{\text{loc}}(\mathbb{R}^d)$, tel que $\nabla\psi \in H^{s+5}(\mathbb{R}^d)^d$ et $\zeta, b \in H^{t_0+2}(\mathbb{R}^d) \cap H^{s+11/2}(\mathbb{R}^d)$. Soient $h_1 \equiv 1-\epsilon\zeta$ et $h_2 \equiv \delta^{-1}+\epsilon\zeta-\beta b$ tel qu'il existe $h_0 > 0$ avec $h_1, h_2 \geq h_0 > 0$. Alors :*

$$\big|u_2 - H^{\mu,\delta}\psi\big|_{H^s} \quad \leq \quad \mu M(s+7/2)\big|\nabla\psi\big|_{H^{s+3}}, \tag{1.21}$$
$$\big|H^{\mu,\delta}\psi - u_2 - \mu\mathcal{T}[h_2,\beta b]u_2\big|_{H^s} \quad \leq \quad \mu^2 M(s+11/2)\big|\nabla\psi\big|_{H^{s+5}}. \tag{1.22}$$

10. La stratégie adoptée dans le cas d'une couche de fluide pour obtenir les développements asymptotiques de l'opérateur de Dirichlet-Neumann consiste à étudier asymptotiquement le potentiel ϕ sachant que l'opérateur est explicitement défini en fonction du potentiel. L'idée est de redresser le domaine à l'aide d'un difféomorphisme admissible afin de transformer l'équation de Laplace posée sur un domaine en mouvement en une équation elliptique à coefficients variables (ζ, b) posée sur un domaine fixe et plat (voir [2]). Sachant que l'opérateur elliptique admet un développement asymptotique en μ, on peut déduire le développement asymptotique du potentiel ϕ en résolvant le problème elliptique à chaque ordre. Le fait que la différence entre la solution exacte et l'approximation à l'ordre voulu vérifie l'équation elliptique sur le domaine plat et que l'opérateur est coercif permet de contrôler la norme H^s de cette différence, d'où l'obtention des estimations sur l'opérateur. Cette stratégie a été étendue au cas de deux couches de fluides avec un fond plat et toit rigide dans [16], avec un fond variable et surface libre dans [44]. Dans le cas de fond variable, le choix du difféomorphisme exige une certaine régularité sur la paramétrisation du fond (voir [84, Section 2.5.3]).

avec

$$\mathcal{T}[h,b]V \equiv \frac{-1}{3h}\nabla(h^3\nabla V) + \frac{1}{2h}[\nabla(h^2(\nabla b)V) - h^2(\nabla b)(\nabla V)] + (\nabla b)^2 V$$

et

$$M(s) \;=\; C(h_0^{-1}, \big|\zeta\big|_{H^{\max(s,t_0+1)}}, \big|b\big|_{H^{\max(s,t_0+1)}}).$$

A partir de la Proposition 1, la première équation du *système d'Euler complet* (1.16) devient :

$$\partial_t\zeta \;=\; \nabla\cdot(h_1u_1) \;=\; -\nabla\cdot(h_2u_2). \tag{1.23}$$

En utilisant les développements asymptotiques au second ordre des Propositions 2 et 3 dans la deuxième équation du *système d'Euler complet* (1.16) et en négligeant tous les termes d'ordre $\mathcal{O}(\mu^2)$, on obtient

$$\begin{aligned}\partial_t\Big(u_2 - \gamma u_1 + \mu\mathcal{T}[h_2,\beta b]u_2 - \mu\gamma\mathcal{T}[h_1,0]u_1\Big)&\\ +(\gamma+\delta)\nabla\zeta + \frac{\epsilon}{2}\nabla\Big(|u_2+\mu\mathcal{T}[h_2,\beta b]u_2|^2 - \gamma|u_1+\mu\mathcal{T}[h_1,0]u_1|^2\Big)&\\ = \mu\epsilon\nabla\mathcal{N}_0^{\mu,\delta} - \mu\frac{(\gamma+\delta)}{\mathrm{bo}}\frac{\nabla\big(k(\epsilon\sqrt{\mu}\zeta)\big)}{\epsilon\sqrt{\mu}} + \mathcal{O}(\mu^2),&\end{aligned} \tag{1.24}$$

avec

$$\begin{aligned}\mathcal{N}_0^{\mu,\delta} &\equiv \frac{\big(\nabla\cdot(h_2u_2) + \epsilon(\nabla\zeta)\cdot(u_2)\big)^2 - \gamma\big(\nabla\cdot(h_1u_1) + \epsilon(\nabla\zeta)\cdot(u_1)\big)^2}{2}\\ &\equiv \frac{\big(-h_2\nabla u_2 + \beta(\nabla b)\cdot(u_2)\big)^2 - \gamma\big(h_1\nabla\cdot u_1\big)^2}{2}.\end{aligned}$$

Les équations (1.23) et (1.24) sont très similaires au système obtenu dans [32] et la consistance de ces deux équations avec les équations d'Euler (1.16) est montrée dans [48, Proposition 6].

Afin de réduire les équations (1.23) et (1.24) à un système d'équations d'évolution couplées, on introduit une nouvelle variable v, qui satisfait la relation suivante :

$$\nabla\cdot(\frac{h_1h_2}{h_1+\gamma h_2}v) \;=\; -\nabla\cdot(h_1u_1) \;=\; \nabla\cdot(h_2u_2). \tag{1.25}$$

En dimension $d=1$ et en supposant que $v\to 0$ quand $|x|\to\infty$ (le fluide est au repos à l'infini), l'identité (1.25) définit uniquement v comme la vitesse moyenne suivante communément appelée "*shear mean velocity*" :

$$\partial_x(\frac{h_1h_2}{h_1+\gamma h_2}v) \;=\; -\partial_x(h_1u_1) \;=\; \partial_x(h_2u_2) \quad \text{si et seulement si} \quad v \;=\; u_2-\gamma u_1. \tag{1.26}$$

Cependant, cette identité n'est plus valable en dimension $d=2$. Afin de pouvoir définir v comme étant l'unique solution de (1.25), il faut utiliser l'opérateur non local [11] suivant introduit dans [16].

Definition 1.2.2. Soit $\zeta\in L^\infty(\mathbb{R}^d)$ tel que $|\zeta|_{L^\infty}<1$. Alors pour tout $W\in L^2(\mathbb{R}^d)^d$:

• il existe un unique $V\in L^2(\mathbb{R}^d)^d$ tel que

$$\nabla\cdot\big((1+\zeta)V\big) = \nabla\cdot W,$$

11. Duchêne [44] a démontré que cet opérateur spécifique aux ondes internes bidimensionnelles ($d=2$) est la conséquence de l'hypothèse de toit rigide.

et $\Pi V = V$, avec $\Pi = \frac{\nabla\nabla^\top}{|D|^2}$ est le projecteur orthogonal sur le champ de vecteur gradient de $L^2(\mathbb{R}^d)^d$;

• on a $V = \mathfrak{Q}[\zeta]W$, avec $\mathfrak{Q}[\zeta] : L^2(\mathbb{R}^d)^d \to L^2(\mathbb{R}^d)^d$ défini par

$$\mathfrak{Q}[\zeta] : U \mapsto \sum_{n=0}^{\infty}(-1)^n\big(\Pi(\zeta\Pi\cdot)\big)^n(\Pi U);$$

• si $\zeta \in H^s(\mathbb{R}^d)$ et $W \in H^s(\mathbb{R}^d)^d$ avec $s \geq t_0 + 1$, $t_0 > d/2$, alors $\mathfrak{Q}[\zeta]W \in H^s(\mathbb{R}^d)^d$ et

$$\big|\mathfrak{Q}[\zeta]W\big|_{H^s} \leq C\Big(|\zeta|_{H^s}, \frac{1}{1-|\zeta|_{L^\infty}}\Big)\big|W\big|_{H^s}.$$

Comme nous l'avons dit, l'utilisation de cet opérateur permet de définir v comme unique solution de (1.25) et d'établir ainsi des développements asymptotiques des opérateurs de Dirichlet-Neumann en fonction de v. Pour plus de détails, le lecteur intéressé peut consulter [48] où les auteurs démontrent que le *système d'Euler complet* (1.16) est consistant avec le système de type Green-Naghdi généralisé (dimension $d = 2$ et fond variable) avec comme inconnues ζ et v .

Jusqu'ici on a travaillé avec $d = 2$. Dès lors, nous restreignons notre étude au cas unidimensionnelle ($d = 1$) sachant que dans tout ce mémoire on s'intéressera aux modèles asymptotiques qui décrivent la propagation des ondes internes unidimensionnelles ($d = 1$).

1.2.3 Le système de type Green-Naghdi unidimensionnel

Plusieurs variables de vitesse ont été utilisées dans la littérature pour exprimer les équations de type Green-Naghdi. Par exemple, dans [16] les auteurs choisissent d'utiliser une variable v, le cisaillement ou "*shear velocity* défini par

$$v \equiv \partial_x((\phi_2 - \gamma\phi_1)|_{z=\epsilon\zeta}) = H^{\mu,\delta}\psi - \gamma\partial_x\psi.$$

Malheureusement, avec ce choix, le système linéarisé est conditionnellement mal posé. Le choix de la variable de vitesse v comme définie dans (1.26) et que nous choisirons dans la suite de notre étude a été utilisé dans [31, 32]. Ce choix admet deux avantages principaux. Premièrement, l'équation qui décrit l'évolution de la déformation de l'interface est une équation exacte et non pas une approximation d'ordre $\mathcal{O}(\mu^2)$. De plus, ce choix assure que le système (1.27) soit linéairement bien posé (voir [47, Section 2.2]). Après certains calculs simples et en utilisant la variable de vitesse v comme défini dans (1.26), les équations (1.23) et (1.24) se réduisent en dimension ($d = 1$) au système d'équations d'évolution couplées suivant :

$$\begin{cases} \partial_t\zeta \;+\; \partial_x\Big(\dfrac{h_1h_2}{h_1+\gamma h_2}v\Big) \;=\; 0, \\[2ex] \partial_t\Big(v \;+\; \mu\overline{\mathcal{Q}}[h_1,h_2]v\Big) \;+\; (\gamma+\delta)\partial_x\zeta \;+\; \dfrac{\epsilon}{2}\partial_x\Big(\dfrac{h_1^2-\gamma h_2^2}{(h_1+\gamma h_2)^2}v^2\Big) \;= \\[2ex] \qquad\qquad \mu\epsilon\partial_x\big(\overline{\mathcal{R}}[h_1,h_2]v\big) + \mu\dfrac{\gamma+\delta}{\mathrm{bo}}\partial_x^3\zeta, \end{cases} \tag{1.27}$$

où l'on note $h_1 = 1 - \epsilon\zeta$ et $h_2 = \delta^{-1} + \epsilon\zeta - \beta b$ et on définit :

$$\begin{aligned}\overline{\mathcal{Q}}[h_1,h_2]v =&\mathcal{T}[h_2,\beta b]\Big(\frac{h_1 v}{h_1+\gamma h_2}\Big) - \gamma\mathcal{T}[h_1,0]\Big(\frac{-h_2 v}{h_1+\gamma h_2}\Big),\\ =&-\frac{1}{3h_2}\partial_x\Big(h_2^3\partial_x\big(\frac{h_1 v}{h_1+\gamma h_2}\big)\Big)\\ &+\frac{1}{2h_2}\beta\Big[\partial_x\Big(h_2^2(\partial_x b)\frac{h_1 v}{h_1+\gamma h_2}\Big) - h_2^2(\partial_x b)\partial_x\big(\frac{h_1 v}{h_1+\gamma h_2}\big)\Big]\\ &+\beta^2(\partial_x b)^2\big(\frac{h_1 v}{h_1+\gamma h_2}\big) - \gamma\Big[\frac{1}{3h_1}\partial_x\Big(h_1^3\partial_x\big(\frac{h_2 v}{h_1+\gamma h_2}\big)\Big)\Big],\end{aligned} \tag{1.28}$$

$$\begin{aligned}\overline{\mathcal{R}}[h_1,h_2]v =&\frac{1}{2}\Big(-h_2\partial_x\big(\frac{h_1 v}{h_1+\gamma h_2}\big)+\beta(\partial_x b)\big(\frac{h_1 v}{h_1+\gamma h_2}\big)\Big)^2 - \frac{\gamma}{2}\Big(h_1\partial_x\big(\frac{-h_2 v}{h_1+\gamma h_2}\big)\Big)^2\\ &-\big(\frac{h_1 v}{h_1+\gamma h_2}\big)\mathcal{T}[h_2,\beta b]\Big(\frac{h_1 v}{h_1+\gamma h_2}\Big)+\gamma\big(\frac{-h_2 v}{h_1+\gamma h_2}\big)\mathcal{T}[h_1,0]\Big(\frac{-h_2 v}{h_1+\gamma h_2}\Big).\end{aligned} \tag{1.29}$$

L'existence et l'unicité des solutions du système de type Green-Naghdi (1.27) ont été montrées dans [50, Section 5] dans le cas d'un fond plat ($\beta = 0$). Leur méthode est similaire à celle utilisée pour le *système d'Euler complet* avec tension de surface par Lannes [83].

Donnons maintenant le résultat de consistance du *système d'Euler complet* (1.16) avec le système de type Green-Naghdi unidimensionnel (1.27). Comme nous l'avons dit ci-dessus, ce résultat a été démontré dans [48] dans le cas généralisé ($d = 2$). Ainsi la proposition suivante dans le cas unidimensionnel suit sans aucune difficulté sachant que le terme de tension de surface se traite de la manière suivante :

$$\left|\frac{-\mu}{\mathrm{bo}}\frac{\partial_x\big(k(\epsilon\sqrt{\mu}\zeta)\big)}{\epsilon\sqrt{\mu}} - \frac{\mu}{\mathrm{bo}}\partial_x^3\zeta\right|_{H^s} \leq \frac{\mu^2\epsilon^2}{\mathrm{bo}}\, C(\mu\epsilon^2, |\zeta|_{H^{s+2}}).$$

Proposition 4. *Soit $U \equiv (\zeta,\psi)^\top$ solution du système d'Euler complet* (1.16) *(avec $d = 1$) tel qu'il existe $T > 0$, $s \geq 0$ avec $(\zeta, \partial_x\psi)^\top$ borné dans $L^\infty([0,T);H^{s+N})^2$ (N suffisamment grand). De plus, on suppose que $b \in H^{s+N}$ et qu'il existe $h_0 > 0$ tel que* (1.13) *soit vérifié. Définissons v comme dans 1.26. Alors (ζ, v) satisfait le système de type Green-Naghdi* (1.27) *jusqu'à un reste $R = (r_1, r_2)^\top$, tel que*

$$\|r_2\|_{L^\infty([0,T);H^s)} \leq \mu^2\, C,$$

avec C indépendant de μ.

A partir du système de type Green-Naghdi unidimensionnel (1.27), on construira dans la suite de ce mémoire plusieurs modèles asymptotiques *couplés* et *scalaires* équivalents (au sens de la consistance). Les modèles obtenus possèdent une structure agréable pour l'étude mathématique (existence, unicité et stabilité de la solution) et pour la résolution numérique.

Dans cette section, nous avons choisi d'exposer le contenu des différents chapitres ainsi que les principaux résultats obtenus dans ce mémoire. Malgré tout, l'énoncé exact des résultats ne sera pas présenté dans ce chapitre introductif et sera reporté au corps de ce mémoire.

1.3 Résultats principaux

1.3.1 Partie I : Analyse mathématique et justification rigoureuse de modèles asymptotiques

Dans le Chapitre 2 (travail en commun avec Samer Israwi et Raafat Talhouk), on étend le résultat de justification rigoureuse du nouveau modèle de type Green-Naghdi dans le *régime de Camssa-Holm* (interface de moyenne amplitude, $\epsilon = \mathcal{O}(\sqrt{\mu})$) obtenu par Duchêne, Israwi et Talhouk en [49] au cas de fond variable. Pour ce faire, on se place dans un régime de variation topographique d'amplitude moyenne ($\beta = \mathcal{O}(\sqrt{\mu})$). A partir des hypothèses de petitesse sur les déformations de l'interface et du fond, on effectue un développement asymptotique des opérateurs $\overline{\mathcal{Q}}$ et $\overline{\mathcal{R}}$ définis dans (1.28) et (1.29). En utilisant ces développements asymptotiques dans le système de type Green-Naghdi (1.27) et en négligeant tous les termes d'ordre $\mathcal{O}(\mu^2, \mu\epsilon^2, \mu\beta^2, \mu\epsilon\beta)$, on construit en suivant la même stratégie initiée dans [49, Section 4.2] un modèle équivalent (dans le sens de la consistance) qui possède une structure similaire à celle d'un système quasi-linéaire symétrisable. Suivant la théorie classique des systèmes hyperboliques et en se basant sur des estimations d'énergie du système linéaire, on montre que notre modèle est bien posé (au sens de Hadamard) dans des espaces de Sobolev en utilisant un schéma itératif de Picard de sorte qu'on ne perd pas de régularité par rapport aux données initiales [12]. Grâce à une estimation d'énergie de la différence de deux solutions du modèle, on montre que notre modèle est stable par rapport aux perturbations des équations. Indépendamment de leurs nécessités pour la dérivation du modèle, les hypothèses de petitesse sur les déformations de l'interface et du fond peuvent être annulées pour les résultats d'existence, d'unicité et de stabilité en adaptant le symétriseur du système. Finalement, on peut déduire que les solutions de notre modèle approchent les solutions du *système d'Euler complet* avec une précision d'ordre $\mathcal{O}(\mu^2)$.

Donnons tout d'abord le nouveau modèle obtenu. La construction de ce modèle est détaillée au Chapitre 2, section 2.3 page 43.

$$\begin{cases} \partial_t\zeta + \partial_x\left(\dfrac{h_1h_2}{h_1+\gamma h_2}v\right) = 0, \\ \\ \mathfrak{T}[\epsilon\zeta,\beta b]\left(\partial_t v + \epsilon\varsigma v\partial_x v\right) + (\gamma+\delta)q_1(\epsilon\zeta,\beta b)\partial_x\zeta \\ +\frac{\epsilon}{2}q_1(\epsilon\zeta,\beta b)\partial_x\left(\frac{h_1^2-\gamma h_2^2}{(h_1+\gamma h_2)^2}|v|^2 - \varsigma|v|^2\right) = -\mu\epsilon\tfrac{2}{3}\alpha_1\partial_x\big((\partial_x v)^2\big) + \mu\beta\omega(\partial_x\zeta)(\partial_x^2 b), \end{cases} \tag{1.30}$$

L'opérateur différentiel symétrique $\mathfrak{T}[\epsilon\zeta,\beta b]$ est défini par :

$$\mathfrak{T}[\epsilon\zeta,\beta b]V = q_1(\epsilon\zeta,\beta b)V - \mu\nu\partial_x\Big(q_2(\epsilon\zeta,\beta b)\partial_x V\Big),$$

avec $q_i(X,Y) \equiv 1+\kappa_i X+\omega_i Y$ $(i=1,2)$ et $\nu,\kappa_1,\kappa_2,\omega_1,\omega_2,\varsigma$ des paramètres fixés dépendant des paramètres sans dimension γ, δ et bo^{-1} (voir section 2.3 du Chapitre 2 page 44). Dans la suite de ce mémoire on démontre que l'opérateur $\mathfrak{T}$ est uniformément continu, coercif et bijectif sous certaines conditions (voir Chapitre 2 section 2.4 page 47).

Avant de donner les résultats principaux de ce chapitre on rappelle qu'on se place dans le régime suivant :

$$\epsilon = \mathcal{O}(\sqrt{\mu}) \quad \text{et} \quad \beta = \mathcal{O}(\sqrt{\mu}).$$

12. Une stratégie similaire a été utilisée dans [72] pour le système de type Green-Naghdi dans le cas d'une couche de fluide avec fond variable, et dans [114] dans le cas de deux couches de fluide avec surface libre et fond plat. Dans ces travaux, les résultats de caractère bien posé des systèmes évitent l'utilisation de la technique de Nash-Moser introduite dans [3] et ne comportent pas de perte de dérivées.

Le développement des opérateurs $\overline{\mathcal{Q}}$ et $\overline{\mathcal{R}}$ nous permet de déduire facilement, à partir de la Proposition 4, le résultat suivant :

Proposition 5. (Consistance) *Le système d'Euler complet* (1.16) *est consistant avec le nouveau modèle asymptotique* (1.30) *avec une précision d'ordre* $\mathcal{O}(\mu^2)$.

L'énoncé exact et la preuve de cette proposition sont précisés en détails au Chapitre 2 à la section 2.3 page 45.

Suivant la théorie classique des systèmes hyperboliques et en se basant sur des estimations d'énergie, nous montrons que notre système (1.30) est bien posé (au sens de Hadamard) sur un temps de l'ordre $\mathcal{O}(\frac{1}{\max(\epsilon,\beta)})$ dans l'espace d'énergie $X^s = H^s(\mathbb{R}) \times H^{s+1}(\mathbb{R})$, muni de la norme

$$\forall\, U = (\zeta, v)^\top \in X^s, \quad |U|^2_{X^s} \equiv |\zeta|^2_{H^s} + |v|^2_{H^s} + \mu|\partial_x v|^2_{H^s}.$$

Après avoir montré que notre modèle est stable par rapport aux perturbations des équations, on déduit finalement le résultat de convergence suivant :

Theorem 1.3.1. (Convergence) *La solution du nouveau modèle asymptotique* (1.30) *approche la solution du système d'Euler complet* (1.16) *avec une précision d'ordre* $\mathcal{O}(\mu^2)$.

Les énoncés exacts et les preuves des théorèmes de caractère bien posé, de stabilité et de convergence du système (1.30) sont donnés en détails au Chapitre 2 à la section 2.6 page 61.

Le Chapitre 3 est divisé en deux parties. Dans la première partie on généralise le résultat de justification rigoureuse obtenu dans [48] et [90, Chap. 2], au cas d'une topographie variable qui peut avoir une large amplitude et une grande longueur d'onde. Plus précisément, on suppose cette fois $\beta\alpha = \mathcal{O}(\sqrt{\mu})$ avec α le rapport de la longueur d'onde de la variation de l'interface à la longueur d'onde de la variation du fond. En partant du système de Green-Naghdi (1.27), on effectue à partir des hypothèses de petitesse sur l'interface et sur le fond ($\epsilon = \mathcal{O}(\sqrt{\mu})$ et $\beta\alpha = \mathcal{O}(\sqrt{\mu})$) un développement asymptotique des opérateurs $\overline{\mathcal{Q}}$ et $\overline{\mathcal{R}}$ définis dans (1.28) et (1.29). Suivant les mêmes techniques que dans les travaux mentionnés ci-dessus on construit un nouveau modèle équivalent (au sens de la consistance). Des restrictions raisonnables sur la déformation du fond sont nécessaires afin de garantir la validité de notre modèle. Admettant une structure hyperbolique, le caractère bien posé de notre modèle est établi comme dans le Chapitre 2. On utilise une technique de symétrisation qui permet d'effectuer des estimations d'énergie dans l'espace approprié. Enfin, la consistance et la stabilité des équations du modèle nous permettent de justifier ce dernier en tant qu'une approximation du *système d'Euler complet* par un résultat de convergence.

Présentons tout d'abord le nouveau modèle obtenu :

$$\begin{cases} \partial_t\zeta + \partial_x\left(\dfrac{h_1h_2}{h_1+\gamma h_2}v\right) = 0, \\ \\ \mathfrak{T}[\epsilon\zeta, \beta b^{(\alpha)}]\left(\partial_t v + \epsilon\varsigma v\partial_x v\right) + (\gamma+\delta)q_1\partial_x\zeta + \frac{\epsilon}{2}q_1\partial_x\left(\frac{h_1^2-\gamma h_2^2}{(h_1+\gamma h_2)^2}|v|^2\right) - q_1(\epsilon\varsigma v\partial_x v) \\ \qquad\qquad = \mu\dfrac{2\epsilon}{3}(1+\omega_1)(\gamma-1)g^2\partial_x\big((\partial_x v)^2\big) + \mu\beta(\gamma+\delta)(1+\omega_1)\eta_1\alpha^2(\partial_x^2 b)^{(\alpha)}\partial_x\zeta, \end{cases} \tag{1.31}$$

avec $h_1 = 1-\epsilon\zeta$, $h_2 = 1/\delta+\epsilon\zeta-\beta b^{(\alpha)}$ et $q_i \equiv 1+\epsilon\kappa_i(\beta b^{(\alpha)})\zeta+\omega_i(\beta b^{(\alpha)})$ $(i=1,2)$ où $\kappa_1, \kappa_2, \omega_1, \omega_2$ et ς sont des fonctions qui dépendent de $\beta b^{(\alpha)}$ avec $b^{(\alpha)}(x) = b(\alpha x)$ représente la déformation

du fond. La définition de ces fonctions nécessite certaines conditions sur le fond (voir Chapitre 3 section 3.3 page 74). L'opérateur différentiel symétrique $\mathfrak{T}[\epsilon\zeta, \beta b^{(\alpha)}]$ est défini par :

$$\mathfrak{T}[\epsilon\zeta, \beta b]V \;=\; q_1 V \;-\; \mu\partial_x\Big(\nu q_2 \partial_x V\Big)$$

où ν, g et η_1 sont aussi des fonctions qui dépendent de $\beta b^{(\alpha)}$. Par souci de lisibilité, on ne détaille pas les expressions exactes des fonctions qui dépendent du fond. Pour plus de détails sur ces dernières et sur la construction du modèle (1.31), le lecteur intéressé pourra consulter la section 3.3 du Chapitre 3.

A partir des hypothèses $\epsilon = \mathcal{O}(\sqrt{\mu})$ et $\beta\alpha = \mathcal{O}(\sqrt{\mu})$, le développement asymptotique des opérateurs ainsi que le résultat de la Proposition 4 nous permettent de déduire de manière triviale le résultat de consistance suivant :

Proposition 6. (Consistance) *Le système d'Euler complet* (1.16) *est consistant avec le nouveau modèle asymptotique* (1.31) *avec une précision d'ordre* $\mathcal{O}(\mu^2)$.

Le nouveau système obtenu (1.31) admet une structure quasi-linéaire symétrisable qui nous permet d'utiliser des méthodes d'énergie afin de montrer son caractère bien posé ainsi que le résultat suivant :

Theorem 1.3.2. (Convergence) *La solution du nouveau modèle asymptotique* (1.31) *approche la solution du système d'Euler complet* (1.16) *avec une précision d'ordre* $\mathcal{O}(\mu^2)$.

Les énoncés exactes des résultats de consistance, de caractère bien posé et de convergence sont donnés en détails au Chapitre 3, section 3.6 page 79.

De plus, notre modèle permet de justifier rigoureusement d'autres modèles bien posés. En effet, il suffit de montrer la consistance de n'importe quel modèle bien posé avec le modèle (1.31) pour déduire directement la convergence vers le *système d'Euler complet* (1.16). On applique cette stratégie à d'autres modèles unidirectionnels dans la deuxième partie de ce Chapitre. En fait, les deux nouveaux modèles dérivés dans le Chapitre 2 et dans la première partie du Chapitre 3 sont des *modèles couplés*. Cependant, en négligeant les termes du premier ordre, tous ces modèles se réduisent à une simple équation d'onde de vitesse ± 1 et toute perturbation initiale de l'interface mène à une division en deux ondes se propageant dans des directions opposées. Suivant la même stratégie utilisée pour les ondes de surface dans [34] et pour les ondes internes (fond plat) dans [47], nous nous intéresserons dès lors à la dérivation de *modèles asymptotiques scalaires* qui décrivent la propagation unidirectionnelle des ondes internes sur une topographie variable. Tout d'abord, nous étudions notre approximation unidirectionnelle dans le régime de Camassa-Holm ($\epsilon = \mathcal{O}(\sqrt{\mu})$). En fait, nous montrons que les familles de solutions de l'approximation unidirectionnelle satisfont le système Green-Naghdi (1.27) sous des conditions appropriées sur les variations de la topographie, à un petit reste près. Notre deuxième résultat sur cette équation d'évolution scalaire, concerne le caractère bien posé du problème de Cauchy en temps long démontré grâce à des estimations d'énergie et à l'aide d'un schéma itératif de Picard. Nous montrons aussi que le déferlement de la solution se produit dans le régime de Camassa-Holm pour certaines conditions particulières sur les paramètres et dans un régime de variation topographique lente. Finalement, un résultat de justification rigoureuse est obtenu sous des hypothèses fortes sur la topographie. De plus, on récupère et on justifie rigoureusement l'approximation unidirectionnelle dans un régime plus restreint d'ondes longues ($\epsilon = \mathcal{O}(\mu)$).

Partant du système de Green-Naghdi (1.27) et après certains calculs se basant sur un développement asymptotique des opérateurs existant, on dérive l'approximation unidirectionnelle sous forme de l'équation scalaire suivante :

$$\partial_t\zeta + \alpha_0\partial_x\zeta + \frac{1}{2}\partial_x(\alpha_0)\zeta + \epsilon\alpha_1\zeta\partial_x\zeta + \epsilon^2\alpha_2\zeta^2\partial_x\zeta + \epsilon^3\alpha_3\zeta^3\partial_x\zeta + \mu\varrho^{\theta,\lambda}\partial_x^3\zeta - \mu(\theta+\lambda)\partial_x^2\partial_t\zeta \\ +\mu\beta\alpha\omega^{\theta,\lambda}(\partial_x b)^{(\alpha)}\partial_x^2\zeta + \mu\epsilon\partial_x\big(\varkappa_1^{\theta,\lambda}\zeta\partial_x^2\zeta + \varkappa_2^{\theta,\lambda}(\partial_x\zeta)^2\big) = 0, \qquad (1.32)$$

où pour tout $\theta, \lambda \in \mathbb{R}$, α_i $(i = 0, 1, 2, 3)$, $\varrho^{\theta,\lambda}$, $\omega^{\theta,\lambda}$, $\varkappa_1^{\theta,\lambda}$ et $\varkappa_2^{\theta,\lambda}$ sont des fonctions qui dépendent de $\beta b^{(\alpha)}$ avec $\underline{v}$ défini comme suit :

$$\underline{v} = \alpha_0\zeta - \frac{1}{2}\int_{-\infty}^{x}\partial_x(\alpha_0)\zeta dx + \epsilon\frac{\alpha_1}{2}\zeta^2 + \epsilon^2\frac{\alpha_2}{3}\zeta^3 + \epsilon^3\frac{\alpha_3}{4}\zeta^4 + \mu\varrho\partial_x^2\zeta \\ +\mu\beta\alpha\omega(\partial_x b)^{(\alpha)}\partial_x\zeta + \mu\epsilon\big(\varkappa_1\zeta\partial_x^2\zeta + \varkappa_2(\partial_x\zeta)^2\big). \qquad (1.33)$$

Pour plus de détails, sur la dérivation de l'équation scalaire et sur l'expression exacte des fonctions qui dépendent du fond, voir Chapitre 3, section 3.7.

En se plaçant dans le régime suivant :

$$\epsilon = \mathcal{O}(\sqrt{\mu}), \quad \beta\alpha = \mathcal{O}(\sqrt{\mu}), \quad \beta\alpha^{3/2} = \mathcal{O}(\mu^2), \quad \beta\alpha\epsilon = \mathcal{O}(\mu^2),$$

nous montrons que toutes familles de solutions de l'approximation unidirectionnelle (1.32) satisfont le système de type Green-Naghdi (1.27) à un petit résidu près d'ordre $\mathcal{O}_{L^\infty}(\mu^2)$. Une étude précise des estimations d'énergie du système linéarisé nous permet de démontrer l'existence et l'unicité de la famille de solutions de l'équation (1.32). On choisit de ne pas donner les énoncés exacts de ces deux résultats dans ce chapitre introductif. Le lecteur intéressé pourra consulter Chapitre 3, sections 3.8.1 et 3.8.2 pages 86 et 88 respectivement. Afin d'obtenir un résultat de justification rigoureuse on se restreint au régime suivant :

$$\epsilon = \mathcal{O}(\sqrt{\mu}), \quad \beta\alpha = \mathcal{O}(\mu^2).$$

Dès lors, on peut donner les deux résultats suivants (pour plus de détails sur les énoncés exactes voir Chapitre 3 section 3.8.4 page 92) :

Proposition 7. (Consistance) *Le nouveau modèle asymptotique couplé* (1.31) *est consistant avec l'approximation unidirectionnelle scalaire* (1.32) *avec une précision d'ordre* $\mathcal{O}(\mu^2)$.

Theorem 1.3.3. (Convergence) *La solution de l'approximation unidirectionnelle scalaire* (1.32) *approche la solution du nouveau modèle asymptotique couplé* (1.31) *avec une précision d'ordre* $\mathcal{O}(\mu^2)$.

A partir de ce dernier résultat on peut déduire facilement que la solution de l'approximation unidirectionnelle scalaire (1.32) approche la solution du *système d'Euler complet* (1.16) avec une précision d'ordre $\mathcal{O}(\mu^2)$.

Finalement, on récupère et on justifie rigoureusement à la section 3.9 du Chapitre 3, l'approximation unidirectionnelle dans un régime plus restreint d'ondes longues, $\epsilon = \mathcal{O}(\mu)$.

1.3.2 Partie II : Résolution numérique

Dans le Chapitre 4, nous résolvons numériquement le modèle (1.30) dans le cadre d'un fond plat ($\beta = 0$). Ce modèle a été initialement dérivé et justifié rigoureusement en [49] et étendu au cas de topographie variable en [90, Chap. 2]. Rappelons que ce modèle décrit la propagation unidimensionnelle d'ondes internes à l'interface entre deux couches de fluide avec un toit rigide et un fond plat. Ce modèle a été reformulé d'une façon plus appropriée pour la résolution numérique. Plus précisément, on obtient un modèle ayant le même ordre de précision que le modèle originale ($\mathcal{O}(\mu^2)$) ainsi que les propriétés suivantes :

• L'opérateur différentiel d'ordre deux ne dépend plus du temps et sera inversé une seule fois durant le calcul tout en gardant son effet de stabilisation.

• Le nouveau modèle admet des propriétés de dispersion améliorées grâce à un choix précis d'un nouveau paramètre introduit dans le modèle.

• La nouvelle formulation ne contient pas des dérivées d'ordre trois.

Afin de faciliter la lecture, nous avons choisi de ne pas détailler la reformulation et la présentation du nouveau modèle. Malgré tout, le lecteur intéressé pourra se reporter à la section 4.3.1 du Chapitre 4 page 106.

La méthode numérique développée pour résoudre le nouveau modèle suit la même stratégie adoptée en [18, 86]. On propose un schéma de "splitting" d'ordre deux séparant la partie hyperbolique et la partie dispersive du modèle. L'approximation $U^{n+1} = (\zeta^{n+1}, v^{n+1})$ est calculée à l'instant $t^{n+1} = t^n + \Delta t$ où ζ représente la déformation de l'interface et v représente la vitesse moyenne définie par l'équation (1.26), en fonction de l'approximation U^n à l'instant t^n en résolvant

$$U^{n+1} = S_1(\Delta t/2)S_2(\Delta t)S_1(\Delta t/2)U^n,$$

où $S_1(.)$ est l'opérateur associé à la partie hyperbolique et $S_2(.)$ est l'opérateur associé à la partie dispersive du modèle.

Pour le calcul numérique de $S_1(.)$, on utilise la méthode des volumes finis. On commence par un schéma VFRoe (voir [24, 57, 58]). Malheureusement ce schéma semble être très diffusif. Un remède à cette situation passe par l'extension à l'ordre deux en espace suivant la méthode "MUSCL" [112]. Enfin, nous mettons en œuvre une reconstruction "WENO" d'ordre cinq [74, 107] afin d'atteindre une précision d'ordre supérieur dans les régions régulières et une bonne résolution autour des discontinuités. D'autre part, $S_2(.)$ est calculé numériquement en utilisant un schéma aux différences finies discrétisé en utilisant des formules centrées d'ordre deux et quatre, alors que pour la discrétisation en temps, nous utilisons des méthodes classiques de Runge-Kutta d'ordre deux et quatre conformément à la discrétisation en espace considérée. Nous traitons uniquement les conditions aux bords de type périodiques et réflexives. Les méthodes numériques utilisées pour résoudre le nouveau modèle sont détaillées au Chapitre 4 section 4.4 page 118.

Finalement, plusieurs simulations numériques sont effectuées dans le cas d'une couche et de deux couches de fluide montrant ainsi l'efficacité, la precision et la capacité de notre schéma à réduire la dissipation et la dispersion numérique et à traiter les discontinuités. De plus, nous soulignons l'importance du choix du nouveau paramètre introduit dans le modèle en comparant celui-ci à des données numériques issues de [50]. Pour plus de détails sur les simulations numériques effectuées voir Chapitre 4 section 4.5 page 128.

Notations

Dans cette section, nous donnons les notations utilisées tout au long du mémoire. Ces notations sont respectées dans l'introduction et rappelées dans chaque chapitre.

Notations générales.
• C_0 toute constante positive dont l'expression exacte n'a pas d'importance.
• $a \lesssim b$ signifie que $a \leq C_0\ b$ et on écrit $A = \mathcal{O}(B)$ si $A \leq C_0\ B$.
• $C(\lambda_1, \lambda_2, \dots)$ indique une constante positive dépendant seulement des paramètres $\lambda_1, \lambda_2, \ldots$dont la dépendance en λ_j est supposée non décroissante.
• $A_s = B_s + \langle C_s \rangle_{s>\underline{s}}$, pour exprimer que $A_s = B_s$ si $s \leq \underline{s}$ et $A_s = B_s + C_s$ si $s > \underline{s}$.

Variables et opérateurs standards.
• $X \in \mathbb{R}^d$, $d = 1, 2$ désigne toujours la variable horizontale. $X = x$ si $d = 1$.
• $z \in \mathbb{R}$ désigne toujours la variable verticale.
• ∂_t désigne la dérivée partielle par rapport au temps t. ∂_x (resp. ∂_z) désigne la dérivée partielle par rapport à la variable d'espace x (resp. z).
• $\nabla \equiv (\partial_x, \partial_y)^T$ si $d = 2$ et $\nabla_{X,z} \equiv \begin{pmatrix} \nabla \\ \partial_z \end{pmatrix}$.
• Soit $F \equiv (f_1, \cdots, f_d) : [0, T] \times \mathbb{R}^d \to \mathbb{R}^d$, div$F$ est la divergence définie par :

$$\text{div}F \equiv \sum_{i=1}^{d} \partial_{x_i} f_i \equiv \ \nabla \cdot F.$$

• $\partial_n \equiv n.\nabla_{X,z}$ la dérivée normale dans la direction du vecteur n concerné.
• $\Delta_X \equiv \partial_x^2 + \partial_y^2$ si $d = 2$ et $\Delta_{X,z} \equiv \Delta_X + \partial_z^2$.
• Λ est l'opérateur défini comme suit : $\Lambda = (1 + |D|^2)^{1/2}$.

Espaces fonctionnels sur $\mathbb{R}^d$.
• $L^p \equiv L^p(\mathbb{R}^d)$ $(1 \leq p < \infty)$ désigne l'espace de Lebesgue des fonctions mesurables f sur $\mathbb{R}^d$, muni de la norme :

$$|f|_{L^p} \equiv \big(\int_{\mathbb{R}^d} |f(x)|^p dx \big)^{1/p} < \infty.$$

• $L^\infty \equiv L^\infty(\mathbb{R}^d)$ désigne l'espace de Lebesgue des fonctions mesurables f bornées presque partout par une constante finie, muni de la norme :

$$|f|_{L^\infty} \equiv \sup \text{ess}\, |f(x)| < \infty.$$

• Le produit scalaire de deux fonctions f_1 et f_2 dans l'espace de Hilbert $L^2(\mathbb{R}^d)$ est désigné par :

$$(f_1, f_2) \equiv \int_{\mathbb{R}^d} f_1(x) f_2(x) dx.$$

• $W^{k,\infty}(\mathbb{R}^d)$ est défini pour tout $k \in \mathbb{N}$ par

$$W^{k,\infty}(\mathbb{R}^d) = \{f \in L^\infty, |f|_{W^{k,\infty}} < \infty\},$$

avec $|f|_{W^{k,\infty}} = \sum_{\alpha \in \mathbb{N}^d, \alpha \leq k} |\partial^\alpha f|_{L^\infty}$, où $\partial^\alpha = \partial_x^{\alpha_1} \partial_y^{\alpha_2}$ si $d = 2$ et $\partial^\alpha = \partial_x^\alpha$ si $d = 1$.

• $H^s \equiv H^s(\mathbb{R}^d)$ (pour toute constante réelle $s \geq 0$), désigne l'espace de Sobolev de toutes les distributions tempérées f de $\mathbb{R}^d$ muni de la norme :

$$|f|_{H^s} = |\Lambda^s f|_{L^2} < \infty.$$

• Soit $\mu > 0$, on désigne par $H^{s+1}_\mu(\mathbb{R}^d)$ l'espace $H^{s+1}(\mathbb{R}^d)$ muni de la norme

$$\left| \cdot \right|^2_{H^{s+1}_\mu} \equiv \left| \cdot \right|^2_{H^s} + \mu \left| \cdot \right|^2_{H^{s+1}} .$$

• On note $L^\infty([0,T); H^s(\mathbb{R}^d))$ l'espace de fonctions tel que $u(t,\cdot)$ est bornée dans $H^s(\mathbb{R}^d)$, uniformément par rapport au temps $t \in [0,T)$. L'espace est muni de la norme :

$$\left\|u\right\|_{L^\infty([0,T);H^s(\mathbb{R}^d))} = \sup_{t\in[0,T)} \operatorname{ess} |u(t,\cdot)|_{H^s} < \infty.$$

• $C^k([0,T); H^s(\mathbb{R}^d))$ désigne l'espace des fonctions u k-fois différentiables sur $\mathbb{R}^d$ à valeurs dans $H^s(\mathbb{R}^d)$ dont toutes les dérivées jusqu'à l'ordre k sont continues dans $\mathbb{R}^d$.

• Pour tout opérateur fermé T défini sur un espace de Banach, le commutateur $[T, f]$ est défini par $[T, f]g = T(fg) - fT(g)$ avec f, g et fg appartenant au domaine de T.

Première partie

Analyse mathématique et justification rigoureuse de modèles asymptotiques

Chapitre 2

An improved result for the full justification of asymptotic models for the propagation of internal waves

We are interested in asymptotic models that describes the one-dimensional propagation of internal waves located at the interface between two ideal fluids of different densities delimited by a rigid lid from above and a variable bottom from below. The aim of this chapter is to show that the full justification by a convergence result of the model obtained by Duchêne, Israwi and Talhouk [*SIAM J. Math. Anal.*, 47(1), 240—290], can be improved in two directions. The first direction is taking into account medium amplitude topography variations and the second direction is allowing strong nonlinearity using a new pseudo-symmetrizer, thus canceling out the smallness assumptions of the Camassa-Holm regime for the well-posedness and stability results.

2.1 Introduction

2.1.1 Motivation

The study of internal waves in a two-fluid system attract the attention of many scientific communities because of the challenging modeling, mathematical and numerical issues that arise in the analysis of this system. Such a configuration is commonly used in oceanography, where variations of temperature and salinity induce a density stratification. Internal ocean waves, can interact with the bottom topography and submerged structures as well as surface waves. Many authors have set a good theoretical background for this problem in the flat bottom case. The case of uneven bottoms has been less investigated.

The mathematical theory for this system of equation the so-called *full Euler system* derived in [6], [16] and [47] are fully nonlinear, and their direct study and computation remain a real obstacle. In particular, the well-posedness of the equations in Sobolev space is challenging. Unlike the water wave problem (air-water interface), the Cauchy problem associated with waves at the interface of two fluids of positive different densities over a flat bottom is known to be ill-posed in Sobolev spaces in the absence of surface tension, as Kelvin–Helmholtz instabilities appear. However, when adding a small amount of surface tension, Lannes [83] proved that, thanks to a stability criterion, the problem becomes well-posed with a time of existence that does not vanish

as the surface tension goes to zero and thus is consistent with the observations. Consequently, a very large amount of work has been dedicated to the derivation of simplified, asymptotic models, aiming at capturing the main characteristics of the flow with much simpler equations, on the condition that the size of given parameters are small, thus reducing the framework to more specific physical regimes, see Definition 1.1.

Many models for a two-fluid system have already been derived and studied. Systems under the rigid-lid assumption have first been investigated (see [92] or [97], for example). Weakly and strongly nonlinear regimes have been derived by Matsuno [93], Choi and Camassa [31, 32], generalizing the classical Green–Naghdi model (see [60]). Among other works, we would like to mention [16] where many asymptotic models are presented and rigorously justified, in a wide range of regimes following the same strategy introduced in [12, 13]. In [65], the well-posedness and stability results have been proved for bi-fluidic shallow-water system without surface tension and under reasonable assumptions on the flow. Recently, Duchêne, Israwi and Talhouk derived in [49], an asymptotic model for the propagation of internal waves in the one-dimensional setting. They assume the fluids to be limited by a flat rigid lid from above and a flat bottom from below. The authors presented a well-posed new Green-Naghdi type model in the Camassa-Holm (or medium amplitude) regime which has been fully justified by a convergence result. Moreover, their system constitute an intermediary to fully justify lower order models provided that they are consistent and well-posed. They applied this strategy to the extension of the famous Korteweg-de Vries equation in the Camassa-Holm regime, called the Constantin-Lannes approximation (see [47]).
All the aforementioned works considered the case of a flat bottom. As a matter of fact, topography plays an important role for internal waves. Indeed, in the ocean, internal waves are often propagating over variable topography, and this can cause many transformations in the internal waves. In this chapter we extend the result of full justification obtained in [49] to the more complex case of non-flat topography, which is more reasonable in oceanography.

Let us introduce some earlier results dealing with non-flat topography. A higher-order nonlinear model for a two-layer fluid of finite depth, is derived in [103] to study the interaction of nonlinear internal waves with large amplitude bottom topography that might vary rapidly over the characteristic length scale of internal waves. Duchêne derived in [44] asymptotic models for the propagation of two and three dimensional gravity waves at the free surface and the interface between two layers of immiscible fluids of different densities over an uneven bottom, following a method introduced by Bona, Lannes, and Saut in [16] based on the expansion of the involved Dirichlet-to-Neumann operators. The same strategy was followed by Anh in [6] to derive asymptotic models but taking into account surface tension, variable topography and for a large class of scaling regimes, furthermore the consistency of these asymptotic systems with the full Euler equations is established. To study the evolution of two-dimensional large amplitude internal waves in a two-layer system with variable bottom topography, a new asymptotic model is derived by Barros and Choi in [7], the model is regularized to remove ill-posedness due to shear instability and it is further extended to include the effects of bottom topography and it is asymptotically equivalent to the strongly nonlinear model proposed by Choi and Camassa [32]. Finally, a bi-dimensional Green-Naghdi model for the two-layers case over a non-flat bottom, is derived and justified (in the sense of consistency) in [48], following the results obtained in the one-layer case. The models derived in these papers are justified formally by a consistency result, and do not provide the full justification, contrarily to the present work.

2.1.2 Outline of the chapter

This chapter deals with the propagation of one dimensional internal waves between two layers of fluids of different densities over an uneven bottom under the following assumptions: the fluids are homogeneous, immiscible, ideal, incompressible, irrotationnal, and under the only influence of gravity. We assume that the surface is confined by a flat rigid lid.

The main idea of this chapter is to improve the result of full justification of the Green-Naghdi type model in the Camassa-Holm (or medium amplitude) regime obtained by Duchêne, Israwi and Talhouk in [49] in two directions. Since the aforementioned work is restricted to the case of a flat topography, the first direction is to relax this assumption by taking into account medium amplitude topography variations, which is more reasonable in oceanography. To this end, we introduce a new parameter β to characterize the shape of the bottom. Moreover we assume that $\beta = \mathcal{O}(\sqrt{\mu})$ which corresponds to the physical case of a bottom with medium variations in amplitude. In the linear analysis of the model obtained in [49], the smallness assumption of the Camassa-Holm regime, $\epsilon = \mathcal{O}(\sqrt{\mu})$ is used in the construction of the model and stands in the proof of the energy estimates [49, Lemma 6.5]. As a matter of fact, the second direction of our improvement is to construct a new pseudo-symmetrizer that allows to cancel the use of the Camassa-Holm regime assumptions ($\epsilon = \mathcal{O}(\sqrt{\mu})$ and $\beta = \mathcal{O}(\sqrt{\mu})$) from the energy estimate proof. Therefore these assumptions can be relaxed for the well-posedness and stability results, regardless of their necessity for the derivation of the model. Our new model possesses a structure similar to symmetrizable quasilinear systems that allows to use the energy estimates method for the linearized system, thus allowing its full justification, following the classical theory of hyperbolic systems. Firstly, we prove that our model is consistent with the full Euler system. Then we prove its well-posedness (in the sense of Hadamard) in Sobolev spaces. Finally, thanks to a stability result we prove that the solutions of our system and the solutions of the full Euler system remain close over the time scale.

2.1.3 Organization of the chapter

This chapter is organized as follows. We start by introducing in Section 2 the non-dimensionalized full Euler system and the Green-Naghdi model. In Section 3 we construct the new asymptotic model. Sections 4 and 5 contain the necessary ingredients for the proof of our results. In Section 6, we explain the full justification of asymptotic models and we state its main ingredients.

Notations. $C(\lambda_1, \lambda_2, \dots)$ denotes a positive constant depending on the parameters λ_1, λ_2,... . C_0 denotes any nonnegative constant whose exact expression is of no importance.
The notation $a \lesssim b$ means that $a \leq C_0\, b$ and we write $A = \mathcal{O}(B)$ if $A \leq C_0\, B$.

$$A_s = B_s + \langle C_s \rangle_{s>\underline{s}},$$

signify that $A_s = B_s$ if $s \leq \underline{s}$ and $A_s = B_s + C_s$ if $s > \underline{s}$.
$L^p = L^p(\mathbb{R})$ $(1 \leq p < \infty)$ denotes the space of all Lebesgue-measurable functions f with the standard norm

$$|f|_{L^p} = \big(\int_{\mathbb{R}} |f(x)|^p dx \big)^{1/p} < \infty.$$

$L^\infty = L^\infty(\mathbb{R})$ consists the space of all essentially bounded, Lebesgue-measurable functions f with the norm

$$|f|_{L^\infty} = \operatorname{ess\,sup} |f(x)| < \infty.$$

$W^{k,\infty} = W^{k,\infty}(\mathbb{R}) = \{f \in L^\infty, |f|_{W^{k,\infty}} < \infty\}$ for $k \in \mathbb{N}$, where $|f|_{W^{k,\infty}} = \sum_{\alpha\in\mathbb{N},\alpha\leq k} |\partial_x^\alpha f|_{L^\infty}$.
$H^s = H^s(\mathbb{R})$ (for any real constant $s \geq 0$), denotes the Sobolev space of all tempered distributions f with the norm $|f|_{H^s} = |\Lambda^s f|_{L^2} < \infty$, where Λ is the following differential operator $\Lambda = (1 - \partial_x^2)^{1/2}$.
For a given $\mu > 0$, we denote by $H^{s+1}_\mu(\mathbb{R})$ the space $H^{s+1}(\mathbb{R})$ endowed with the norm

$$\left| \cdot \right|^2_{H^{s+1}_\mu} \equiv \left| \cdot \right|^2_{H^s} + \mu \left| \cdot \right|^2_{H^{s+1}} .$$

We denote $L^\infty([0,T); H^s(\mathbb{R}))$ the space of functions such that $u(t,\cdot)$ is controlled in H^s, uniformly for $t \in [0,T)$:

$$\left\|u\right\|_{L^\infty([0,T);H^s(\mathbb{R}))} = \operatorname*{ess\,sup}_{t\in[0,T)} |u(t,\cdot)|_{H^s} < \infty.$$

Finally, $C^k(\mathbb{R})$ denote the space of k-times continuously differentiable functions.
The commutator $[T, f]$ is defined by $[T, f]g = T(fg) - fT(g)$ with f, g and fg belonging to the domain of the closed operator T, defined on a Banach space.

Let us now define the regimes that appear in this work.

Definition 2.1.1. *(Regimes).* We define the so-called *shallow water regime* for two layers of comparable depths the set of parameters:

$$\mathcal{P}_{\mathrm{SW}} \equiv \Big\{(\mu,\epsilon,\delta,\gamma,\beta,\mathrm{bo}) : 0 < \mu \leq \mu_{\max},\ 0 \leq \epsilon \leq 1,\ \delta \in (\delta_{\min},\delta_{\max}),\ 0 \leq \gamma < 1,\ 0 \leq \beta \leq \beta_{\max},\ \mathrm{bo}_{\min} \leq \mathrm{bo} \leq \infty \Big\}, \quad (2.1)$$

with given $0 \leq \mu_{\max}, \delta_{\min}^{-1}, \delta_{\max}, \mathrm{bo}_{\min}^{-1}, \beta_{\max} < \infty$.

The additional key restrictions for the validity of the model (2.16) are as follows:

$$\mathcal{P}_{\mathrm{CH}} \equiv \Big\{(\mu,\epsilon,\delta,\gamma,\beta,\mathrm{bo}) \in \mathcal{P}_{\mathrm{SW}} : \epsilon \leq \mathrm{M}\sqrt{\mu},\quad \beta \leq \mathrm{M}\sqrt{\mu} \quad \text{and} \quad \nu \equiv \frac{1+\gamma\delta}{3\delta(\gamma+\delta)} - \frac{1}{\mathrm{bo}} \geq \nu_0 \Big\}, \quad (2.2)$$

with given $0 \leq M, \nu_0^{-1} < \infty$.

We denote for convenience

$$M_{\mathrm{SW}} \equiv \max\left\{\mu_{\max}, \delta_{\min}^{-1}, \delta_{\max}, \mathrm{bo}_{\min}^{-1}, \beta_{\max}\right\}, \quad \mathrm{M_{CH}} \equiv \max\left\{\mathrm{M_{SW}}, \mathrm{M}, \nu_0^{-1}\right\}.$$

2.2 Previously obtained models

2.2.1 The full Euler system

We briefly recall the governing equations of a two-layer flow in the aforementioned configuration, that we call *full Euler system* (using non-dimensionalized variables and the Zakharov/Craig-Sulem formulation) [39, 115]. We let the reader refer to [6, 16, 47] for more details.

$$\begin{cases} \partial_t\zeta \ - \ \dfrac{1}{\mu}G^\mu\psi \ = \ 0, \\ \partial_t\Big(H^{\mu,\delta}\psi - \gamma\partial_x\psi\Big) \ + \ (\gamma+\delta)\partial_x\zeta \ + \ \dfrac{\epsilon}{2}\partial_x\Big(|H^{\mu,\delta}\psi|^2 - \gamma|\partial_x\psi|^2\Big) \\ \qquad\qquad = \mu\epsilon\partial_x\mathcal{N}^{\mu,\delta} - \mu\frac{\gamma+\delta}{\mathrm{bo}}\frac{\partial_x\big(k(\epsilon\sqrt{\mu}\zeta)\big)}{\epsilon\sqrt{\mu}} \ , \end{cases} \tag{2.3}$$

where we denote

$$\mathcal{N}^{\mu,\delta} \ \equiv \ \frac{\big(\frac{1}{\mu}G^\mu\psi + \epsilon(\partial_x\zeta)H^{\mu,\delta}\psi\big)^2 \ - \ \gamma\big(\frac{1}{\mu}G^\mu\psi + \epsilon(\partial_x\zeta)(\partial_x\psi)\big)^2}{2(1+\mu|\epsilon\partial_x\zeta|^2)}.$$

$\zeta(t,x)$ represent the deformation of the interface between the two layers and $b(x)$ represent the deformation of the bottom, ψ is the trace of the velocity potential of the upper-fluid at the interface.

The function $k(\zeta) = -\partial_x\Big(\frac{1}{\sqrt{1+|\partial_x\zeta|^2}}\partial_x\zeta\Big)$ denotes the mean curvature of the interface.

Let a(resp. a_b) be the maximal vertical deformation of the interface(resp. bottom). We denote by λ the wavelength of the interface; d_1 (resp. d_2) the deepness of the upper (resp. lower) fluid; and ρ_1 (resp. ρ_2) is the mass density of the upper (resp. lower) fluid, g the gravitational acceleration, σ the interfacial tension coefficient. In the following we use $\mathrm{bo} = \mu\mathrm{Bo}$ instead of *the classical Bond number*, Bo which measures the ratio of gravity forces over surface tension forces. Consequently we introduce the following dimensionless parameters

$$\mu \ \equiv \ \frac{d_1^2}{\lambda^2}, \quad \epsilon \ \equiv \ \frac{a}{d_1}, \quad \beta \ \equiv \ \frac{a_b}{d_1}, \quad \delta \ \equiv \ \frac{d_1}{d_2}, \quad \gamma \ = \ \frac{\rho_1}{\rho_2}, \quad \mathrm{bo} \ = \ \frac{\mathrm{g}(\rho_2-\rho_1)\mathrm{d}_1^2}{\sigma}, \tag{2.4}$$

where ϵ (resp. β) measures the amplitude of the deformation at the interface (resp. bottom) with respect to the depth of the upper layer of fluid, and μ is the shallowness parameter.

Finally, G^μ and $H^{\mu,\delta}$ are the so-called Dirichlet-Neumann operators, defined as follows:

Definition 2.2.1 (Dirichlet-Neumann operators)**.** Let $\zeta, b \in H^{t_0+1}(\mathbb{R})$, $t_0 > 1/2$, such that there exists $h_0 > 0$ with $h_1 \ \equiv \ 1-\epsilon\zeta \geq h_0 > 0$ and $h_2 \ \equiv \ \frac{1}{\delta} + \epsilon\zeta - \beta b \geq h_0 > 0$, and let $\psi \in L^2_{\mathrm{loc}}(\mathbb{R})$, $\partial_x\psi \in H^{1/2}(\mathbb{R})$. Then we define

$$G^\mu\psi \equiv G^\mu[\epsilon\zeta]\psi \equiv \sqrt{1+\mu|\epsilon\partial_x\zeta|^2}\big(\partial_n\phi_1\big)\,|_{z=\epsilon\zeta} = -\mu\epsilon(\partial_x\zeta)(\partial_x\phi_1)\,|_{z=\epsilon\zeta} + (\partial_z\phi_1)\,|_{z=\epsilon\zeta} \ ,$$

$$H^{\mu,\delta}\psi \equiv H^{\mu,\delta}[\epsilon\zeta,\beta b]\psi \equiv \partial_x\big(\phi_2\,|_{z=\epsilon\zeta}\,\big) = (\partial_x\phi_2)\,|_{z=\epsilon\zeta} + \epsilon(\partial_x\zeta)(\partial_z\phi_2)\,|_{z=\epsilon\zeta} \ ,$$

where ϕ_1 and ϕ_2 are uniquely defined (up to a constant for ϕ_2) as the solutions in $H^2(\mathbb{R})$ of the Laplace's problems:

$$\begin{cases} \big(\ \mu\partial_x^2 \ + \ \partial_z^2\ \big)\ \phi_1 = 0 & \text{in } \Omega_1 \equiv \{(x,z)\in\mathbb{R}^2,\ \epsilon\zeta(x) < z < 1\}, \\ \partial_z\phi_1 = 0 & \text{on } \Gamma_{\mathrm{t}} \equiv \{(x,z)\in\mathbb{R}^2,\ z=1\}, \\ \phi_1 = \psi & \text{on } \Gamma \equiv \{(x,z)\in\mathbb{R}^2,\ z=\epsilon\zeta\}, \end{cases} \tag{2.5}$$

$$\begin{cases} \big(\ \mu\partial_x^2 \ + \ \partial_z^2\ \big)\ \phi_2 = 0 & \text{in } \Omega_2 \equiv \{(x,z)\in\mathbb{R}^2,\ -\frac{1}{\delta} + \beta b(x) < z < \epsilon\zeta\}, \\ \partial_n\phi_2 = \partial_n\phi_1 & \text{on } \Gamma, \\ \partial_n\phi_2 = 0 & \text{on } \Gamma_{\mathrm{b}} \equiv \{(x,z)\in\mathbb{R}^2,\ z=-\frac{1}{\delta}+\beta b(x)\}. \end{cases} \tag{2.6}$$

The well-posedness of the Laplace's problems (2.5)-(2.6) as well as the one of the Dirichlet-Neumann operators are detailed in [84].

2.2.2 The Green-Naghdi model

In the following, we construct Green-Naghdi type model for the system (2.3), that is asymptotic model with precision $\mathcal{O}(\mu^2)$, in the sense of consistency. The construction of shallow water asymptotic models relies heavily on the expansion of the Dirichlet-Neumann operators given in [44, 48], with respect to the shallowness parameter, μ. When replacing the Dirichlet-to-Neumann operators by their truncated expansion, and after straightforward computations, one is able to deduce the Green-Naghdi model, that we disclose below. This model has been introduced in [47] (with a flat bottom) and generalized in [48]. It is also convenient to introduce a new velocity variable, namely the shear mean velocity v is equivalently defined as

$$v \equiv u_2 - \gamma u_1 \tag{2.7}$$

where u_1 and u_2 are the horizontal velocities integrated across each layer:

$$u_1(t,x) = \frac{1}{h_1(t,x)} \int_{\epsilon\zeta(t,x)}^{1} \partial_x \phi_1(t,x,z)\ dz$$

and

$$u_2(t,x) = \frac{1}{h_2(t,x)} \int_{-\frac{1}{\delta}+\beta b(x)}^{\epsilon\zeta(t,x)} \partial_x \phi_2(t,x,z)\ dz,$$

where ϕ_1 and ϕ_2 are the solutions to the Laplace's problems (2.5)-(2.6).

The expansions of the Dirichlet-Neumann operators may be written in terms of the new variable v.

Plugging the expansions given in [48] into the full Euler system (2.3), and withdrawing all $\mathcal{O}(\mu^2)$ terms yields (in the unidimensional case $d = 1$),

$$\begin{cases} \partial_t \zeta \ + \ \partial_x\Big(\dfrac{h_1 h_2}{h_1+\gamma h_2} v\Big) \ = \ 0, \\ \\ \partial_t\Big(v \ + \ \mu \overline{\mathcal{Q}}[h_1,h_2]v\Big) \ + \ (\gamma+\delta)\partial_x\zeta \ + \ \dfrac{\epsilon}{2}\partial_x\Big(\dfrac{h_1^2-\gamma h_2^2}{(h_1+\gamma h_2)^2} v^2\Big) \ = \\ \qquad\qquad \mu\epsilon\partial_x\big(\overline{\mathcal{R}}[h_1,h_2]v\big) + \mu\dfrac{\gamma+\delta}{\mathrm{bo}}\partial_x^3\zeta, \end{cases} \tag{2.8}$$

where we denote $h_1 = 1-\epsilon\zeta$ and $h_2 = \delta^{-1}+\epsilon\zeta-\beta b$, as well as

$$\begin{aligned} \overline{\mathcal{Q}}[h_1,h_2]v =& \mathcal{T}[h_2,\beta b]\Big(\frac{h_1 v}{h_1+\gamma h_2}\Big) - \gamma\mathcal{T}[h_1,0]\Big(\frac{-h_2 v}{h_1+\gamma h_2}\Big), \\ =& -\frac{1}{3h_2}\partial_x\Big(h_2^3\partial_x\big(\frac{h_1 v}{h_1+\gamma h_2}\big)\Big) \\ &+ \frac{1}{2h_2}\beta\Big[\partial_x\Big(h_2^2(\partial_x b)\frac{h_1 v}{h_1+\gamma h_2}\Big) - h_2^2(\partial_x b)\partial_x\big(\frac{h_1 v}{h_1+\gamma h_2}\big)\Big] \\ &+ \beta^2(\partial_x b)^2\big(\frac{h_1 v}{h_1+\gamma h_2}\big) - \gamma\Big[\frac{1}{3h_1}\partial_x\Big(h_1^3\partial_x\big(\frac{h_2 v}{h_1+\gamma h_2}\big)\Big)\Big]. \end{aligned}$$

$$\overline{\mathcal{R}}[h_1,h_2]v = \frac{1}{2}\Big(- h_2\partial_x(\frac{h_1 v}{h_1+\gamma h_2}) + \beta(\partial_x b)(\frac{h_1 v}{h_1+\gamma h_2})\Big)^2 - \frac{\gamma}{2}\Big(h_1\partial_x(\frac{-h_2 v}{h_1+\gamma h_2})\Big)^2 - (\frac{h_1 v}{h_1+\gamma h_2})\mathcal{T}[h_2,\beta b]\Big(\frac{h_1 v}{h_1+\gamma h_2}\Big) + \gamma(\frac{-h_2 v}{h_1+\gamma h_2})\mathcal{T}[h_1,0]\Big(\frac{-h_2 v}{h_1+\gamma h_2}\Big),$$

with

$$\mathcal{T}[h,b]V \equiv \frac{-1}{3h}\partial_x(h^3\partial_x V) + \frac{1}{2h}[\partial_x(h^2(\partial_x b)V) - h^2(\partial_x b)(\partial_x V)] + (\partial_x b)^2 V.$$

2.3 Construction of the new model

In the following section, we will construct an equivalent model (in the sense of consistency) using many transformations. The obtained model possesses a structure similar to quasilinear hyperbolic systems.
In what follows we restrict ourselves to the so-called Camassa-Holm regime, that is to say we use two additional assumptions $\epsilon = \mathcal{O}(\sqrt{\mu})$ and $\beta = \mathcal{O}(\sqrt{\mu})$ (deformation of the interface and the one of the bottom are of medium amplitude). We manipulate the Green-Naghdi system (2.8), systematically withdrawing $\mathcal{O}(\mu^2, \mu\epsilon^2, \mu\beta^2, \mu\epsilon\beta)$ terms, in order to recover our model.
Firstly, let us give the following expansions:

$$\begin{aligned}
\overline{\mathcal{Q}}[h_1,h_2]v &= -\lambda\partial_x^2 v - \epsilon\frac{\gamma+\delta}{3}\left((\theta_1-\alpha_1)v\partial_x^2\zeta + (\alpha_1+2\theta_1)\partial_x(\zeta\partial_x v) - \theta_1\zeta\partial_x^2 v\right)\\
&+ \beta\frac{\gamma+\delta}{3}\left((\frac{\alpha_2}{2}+\theta_2)v\partial_x^2 b + (\alpha_2+2\theta_2)\partial_x(b\partial_x v) - \theta_2 b\partial_x^2 v\right)\\
&+ \mathcal{O}(\epsilon^2,\beta^2,\epsilon\beta),\\
\overline{\mathcal{R}}[h_1,h_2]v &= \alpha_1\left(\frac{1}{2}(\partial_x v)^2 + \frac{1}{3}v\partial_x^2 v\right) + \mathcal{O}(\epsilon,\beta).
\end{aligned}$$

with

$$\lambda = \frac{1+\gamma\delta}{3\delta(\gamma+\delta)}\ , \quad \alpha_1 = \frac{1-\gamma}{(\gamma+\delta)^2} \quad \text{and} \quad \theta_1 = \frac{(1+\gamma\delta)(\delta^2-\gamma)}{\delta(\gamma+\delta)^3}\ ,$$

and

$$\alpha_2 = \frac{1}{(\gamma+\delta)^2} \quad \text{and} \quad \theta_2 = \frac{\delta(1+\gamma\delta)}{(\gamma+\delta)^3}\ .$$

Plugging these expansions into system (2.8) and using the same techniques as in [49, Section 4.2] but with a different symmetric operator $\mathfrak{T}[\epsilon\zeta,\beta b]$ defined below, yields a reduced equivalent model (same order of precision) in the Camassa-Holm regime.
Let us first introduce the operator $\mathfrak{T}[\epsilon\zeta,\beta b]$.

$$\mathfrak{T}[\epsilon\zeta,\beta b]V \ = \ q_1(\epsilon\zeta,\beta b)V \ - \ \mu\nu\partial_x\Big(q_2(\epsilon\zeta,\beta b)\partial_x V\Big), \tag{2.9}$$

with $q_i(X,Y) \equiv 1 + \kappa_i X + \omega_i Y$ $(i=1,2)$ and $\nu, \kappa_1, \kappa_2, \omega_1, \omega_2, \varsigma$ are constants to be determined.

Choosing ν properly allows to withdraw the first order $\mathcal{O}(\mu)$ terms since the second equation of the Green-Naghdi model (2.8) yields

$$\partial_t v = -(\gamma+\delta)\partial_x\zeta - \frac{\epsilon}{2}\partial_x\Big(\frac{\delta^2-\gamma}{(\gamma+\delta)^2}|v^2|\Big) + \mathcal{O}(\epsilon^2,\mu,\epsilon\beta).$$

Indeed it follows that

$$\begin{aligned}\frac{\gamma+\delta}{\mathrm{bo}}\partial_x^3\zeta = &-\frac{1}{\mathrm{bo}}\partial_x^2\partial_t v - \frac{3\epsilon}{2\mathrm{bo}}\frac{\delta^2-\gamma}{(\gamma+\delta)^2}\partial_x((\partial_x v)^2)\\ &-\frac{\epsilon}{\mathrm{bo}}\frac{\delta^2-\gamma}{(\gamma+\delta)^2}v\partial_x^3 v + \mathcal{O}(\epsilon^2,\mu,\epsilon\beta).\end{aligned} \tag{2.10}$$

Using again that (2.8) yields $\partial_t v = -(\gamma+\delta)\partial_x\zeta + \mathcal{O}(\epsilon,\beta,\mu)$ and $\partial_t\zeta = \frac{-1}{\gamma+\delta}\partial_x v + \mathcal{O}(\epsilon,\beta,\mu)$, it becomes clear, that one can adjust $\kappa_1,\ \kappa_2,\ \omega_1,\ \omega_2 \in \mathbb{R}$ so that all terms containing ζ and its higher-order derivatives are canceled.

In order to deal with $(v\partial_x^3 v)$ terms, $\varsigma \in \mathbb{R}$ is to be determined. In fact, these terms appear after replacing the term $\dfrac{\gamma+\delta}{\mathrm{bo}}\partial_x^3\zeta$ of the second equation of (2.8) by its expression given in (2.10). Thus one defines the constants $\nu, \kappa_1, \kappa_2, \omega_1, \omega_2, \varsigma$ as follow:

$$\nu \ = \ \lambda - \frac{1}{\mathrm{bo}} \ = \ \frac{1+\gamma\delta}{3\delta(\gamma+\delta)} - \frac{1}{\mathrm{bo}}, \tag{2.11}$$

$$(\lambda - \frac{1}{\mathrm{bo}})\kappa_1 \ = \ \frac{\gamma+\delta}{3}(2\theta_1-\alpha_1), \quad (\lambda - \frac{1}{\mathrm{bo}})\kappa_2 \ = \ (\gamma+\delta)\theta_1, \tag{2.12}$$

$$(\lambda - \frac{1}{\mathrm{bo}})\omega_1 \ = \ -\theta_2\frac{(\gamma+\delta)}{3}, \quad (\lambda - \frac{1}{\mathrm{bo}})\omega_2 \ = \ -\frac{(\gamma+\delta)}{3}(\alpha_2+2\theta_2), \tag{2.13}$$

$$(\lambda - \frac{1}{\mathrm{bo}})\varsigma \ = \ \frac{2\alpha_1-\theta_1}{3} \ - \ \frac{1}{\mathrm{bo}}\frac{\delta^2-\gamma}{(\delta+\gamma)^2}. \tag{2.14}$$

Finally, one can check that

$$\begin{aligned}&\mathfrak{T}[\epsilon\zeta,\beta b](\partial_t v + \epsilon\varsigma v\partial_x v) - q_1(\epsilon\zeta,\beta b)\partial_t\Big(v \ + \ \mu\overline{\mathcal{Q}}[h_1,h_2]v\Big)\\ &\qquad + \mu q_1(\epsilon\zeta,\beta b)\Big(\frac{\gamma+\delta}{\mathrm{bo}}\partial_x^3\zeta + \epsilon\partial_x\big(\overline{\mathcal{R}}[h_1,h_2]v\big)\Big)\\ &= \epsilon\varsigma q_1(\epsilon\zeta,\beta b)v\partial_x v - \mu\epsilon\frac{2\alpha_1}{3}\partial_x\big((\partial_x v)^2\big) + \mu\beta\omega(\partial_x\zeta)(\partial_x^2 b) + \mathcal{O}(\mu^2,\mu\epsilon^2,\mu\beta^2,\mu\epsilon\beta)\end{aligned} \tag{2.15}$$

where we denote $\omega = \dfrac{(\gamma+\delta)^2}{3}\big(\dfrac{\alpha_2}{2}+\theta_2\big)$.

Plugging the estimate (2.15) in (2.8), and multiplying the second equation by $q_1(\epsilon\zeta,\beta b)$, yields the following model:

$$\begin{cases}\partial_t\zeta + \partial_x\left(\dfrac{h_1h_2}{h_1+\gamma h_2}v\right) \ = \ 0,\\[2ex] \mathfrak{T}[\epsilon\zeta,\beta b]\left(\partial_t v + \epsilon\varsigma v\partial_x v\right) + (\gamma+\delta)q_1(\epsilon\zeta,\beta b)\partial_x\zeta\\ +\frac{\epsilon}{2}q_1(\epsilon\zeta,\beta b)\partial_x\left(\frac{h_1^2-\gamma h_2^2}{(h_1+\gamma h_2)^2}|v|^2 - \varsigma|v|^2\right) = -\mu\epsilon\frac{2}{3}\alpha_1\partial_x\big((\partial_x v)^2\big) + \mu\beta\omega(\partial_x\zeta)(\partial_x^2 b),\end{cases} \tag{2.16}$$

Proposition 8 (Consistency). *For* $\mathsf{p} = (\mu, \epsilon, \delta, \gamma, \beta, \mathrm{bo}) \in \mathcal{P}_{\mathrm{SW}}$, *let* $U^{\mathsf{p}} = (\zeta^{\mathsf{p}}, \psi^{\mathsf{p}})^\top$ *be a family of solutions of the full Euler system* (2.3) *such that there exists* $T > 0$, $s \geq s_0 + 1$, $s_0 > 1/2$ *for which* $(\zeta^{\mathsf{p}}, \partial_x \psi^{\mathsf{p}})^\top$ *is bounded in* $L^\infty([0,T); H^{s+N})^2$ *with sufficiently large* N, *and uniformly with respect to* $\mathsf{p} \in \mathcal{P}_{\mathrm{SW}}$. *Moreover assume that* $b \in H^{s+N}$ *and there exists* $h_{01} > 0$ *such that*

$$h_1 = 1 - \epsilon\zeta^{\mathsf{p}} \geq h_{01} > 0, \quad h_2 = 1/\delta + \epsilon\zeta^{\mathsf{p}} - \beta b \geq h_{01} > 0.$$

Define v^{p} *as in* (2.7). *Then* $(\zeta^{\mathsf{p}}, v^{\mathsf{p}})^\top$ *satisfies* (2.16) *up to a remainder term,* $R = (0, r)^\top$, *bounded by*

$$\|r\|_{L^\infty([0,T);H^s)} \leq (\mu^2 + \mu\epsilon^2 + \mu\beta^2 + \mu\epsilon\beta)C,$$

with $C = C(h_{01}^{-1}, M_{\mathrm{SW}}, |b|_{H^{s+N}}, \|(\zeta^{\mathsf{p}}, \partial_x\psi^{\mathsf{p}})^\top\|_{L^\infty([0,T);H^{s+N})^2})$.

Proof. Let $U = (\zeta, \psi)^\top$ satisfy the hypothesis above withdrawing the explicit dependence with respect to parameters p for the sake of readability. We know from [48, Proposition 3.14] that $(\zeta, v)^\top$ satisfies the system (2.8) up to a remainder $R_0 = (0, r_0)^\top$ bounded by,

$$\|r_0\|_{L^\infty([0,T);H^s)} \leq \mu^2 C_1,$$

with $C_1 = C(h_{01}^{-1}, M_{\mathrm{SW}}, |b|_{H^{s+N}}, \|(\zeta^{\mathsf{p}}, \partial_x\psi^{\mathsf{p}})^\top\|_{L^\infty([0,T);H^{s+N})^2})$, uniformly with respect to $\mathsf{p} \in \mathcal{P}_{\mathrm{SW}}$.
However, all the neglected terms in the above manipulations can be estimated identically. Let us now precise the bound on the remaining terms. One has

$$\Big|\partial_t\big(\overline{\mathcal{Q}}[h_1,h_2]v\big) - \big[-\lambda\partial_x^2\partial_t v - \epsilon\frac{\gamma+\delta}{3}\partial_t\left((\beta-\alpha_1)v\partial_x^2\zeta + (\alpha_1+2\beta)\partial_x(\zeta\partial_x v) - \beta\zeta\partial_x^2 v\right) + \beta\frac{\gamma+\delta}{3}\partial_t\left((\frac{\alpha_2}{2}+\theta_2)v\partial_x^2 b + (\alpha_2+2\theta_2)\partial_x(b\partial_x v) - \theta_2 b\partial_x^2 v\right)\big]\Big|_{H^s} \leq (\epsilon^2+\beta^2+\epsilon\beta)C(s+3),$$

with $C(s+3) \equiv C\Big(M_{\mathrm{SW}}, h_{01}^{-1}, |\zeta|_{H^{s+3}}, |\partial_t\zeta|_{H^{s+2}}, |v|_{H^{s+3}}, |\partial_t v|_{H^{s+2}}, |b|_{H^{s+3}}\Big)$, and

$$\Big|\partial_x\big(\overline{\mathcal{R}}[h_1,h_2]v\big) - \partial_x\big[\alpha_1\big(\frac{1}{2}(\partial_x v)^2 + \frac{1}{3}v\partial_x^2 v\big)\big]\Big|_{H^s} \leq (\epsilon+\beta)C(s+3).$$

Then, since (ζ, v) satisfies (2.8), up to the remainder R_0, one has

$$|\partial_t v + (\gamma+\delta)\partial_x\zeta|_{H^s} + \Big|\partial_t\zeta + \frac{1}{\gamma+\delta}\partial_x v\Big|_{H^s} \leq (\epsilon+\beta)C(s+3) + |R_0|_{H^s}.$$

It follows that (2.15) is valid up to a remainder R_1, bounded by

$$|R_1|_{H^s} \leq (\mu^2 + \mu\epsilon^2 + \mu\beta^2 + \mu\epsilon\beta)C(s+3) + \mu(\epsilon+\beta+\mu)|R_0|_{H^s}$$

Finally, (ζ, v) satisfies (2.16) up to a remainder R, bounded by

$$|R|_{H^s} \leq |R_0 + R_1|_{H^s} \leq (\mu^2 + \mu\epsilon^2 + \mu\beta^2 + \mu\epsilon\beta)C.$$

where we use that

$$|v|_{H^{s+3}} + |\partial_t v|_{H^{s+2}} \leq C.$$

The estimate on v follows directly from the identity $\partial_x\Big(\frac{h_1h_2}{h_1+\gamma h_2}v\Big) = -\frac{1}{\mu}G^{\mu,\epsilon}\psi = \partial_t\zeta$. The estimate on $\partial_t v$ can be proved, for example, following [44, Prop. 2.12]. This concludes the proof of Proposition 8.

□

2.4 Preliminary results

In this section, we recall the operator $\mathfrak{T}[\epsilon\zeta, \beta b]$, defined in (2.9):

$$\mathfrak{T}[\epsilon\zeta, \beta b]V \;=\; q_1(\epsilon\zeta, \beta b)V \;-\; \mu\nu\partial_x\Big(q_2(\epsilon\zeta, \beta b)\partial_x V\Big).$$

with $\nu, \kappa_1, \kappa_2, \omega_1, \omega_2$ are constants and $\nu = \dfrac{1+\gamma\delta}{3\delta(\gamma+\delta)} - \dfrac{1}{\mathrm{bo}} \geq \nu_0 > 0$.
The operator $\mathfrak{T}[\epsilon\zeta, \beta b]$, has exactly the same structure as the one introduced in [49] but it depends also on the deformation of the bottom and plays an important role in the energy estimate and the local well-posednees of the system (2.16).
The ellipticity of the operator $\mathfrak{T}$ requires some sufficient conditions in order to provide the well-posedness and continuity of the inverse $\mathfrak{T}^{-1}$. More precisely, one has to assume that deformations at the interface and the bottom are not too large. For fixed $\zeta \in L^\infty$ and $b \in L^\infty$, we assume that $\epsilon_{\max}\big|\zeta\big|_{L^\infty} + \beta_{\max}|b|_{L^\infty}$ with $\epsilon_{\max}, \beta_{\max} = \min(M\sqrt{\mu_{\max}}, 1)$, so that (H1)-(H2) hold uniformly with respect to $(\mu, \epsilon, \delta, \gamma, \beta, \mathrm{bo}) \in \mathcal{P}_{\mathrm{CH}}$.

Let us recall the non-zero depth condition

$$\exists\; h_{01} > 0, \quad \text{such that} \quad \inf_{x\in\mathbb{R}} h_1 \geq h_{01} > 0, \quad \inf_{x\in\mathbb{R}} h_2 \geq h_{01} > 0. \tag{H1}$$

where $h_1 = 1 - \epsilon\zeta$ and $h_2 = 1/\delta + \epsilon\zeta - \beta b$ are the depth of respectively the upper and the lower layer of the fluid.

For all $(\mu, \epsilon, \delta, \gamma, \beta, \mathrm{bo}) \in \mathcal{P}_{\mathrm{CH}}$, the following condition

$$\epsilon_{max}|\zeta|_{L^\infty} + \beta_{max}|b|_{L^\infty} < \min(1, \frac{1}{\delta_{max}})$$

is sufficient to define $h_{01} > 0$ such that (H1) is valid independently of $(\mu, \epsilon, \delta, \gamma, \beta, \mathrm{bo})$
$\in \mathcal{P}_{\mathrm{CH}}$.
Let us now introduce now the ellipticity condition,

$$\begin{aligned} \exists\; h_{02} > 0,\ \text{such that} \quad & \inf_{x\in\mathbb{R}} (1 + \epsilon\kappa_1\zeta + \beta\omega_1 b) \geq h_{02} \;>\; 0\;; \\ & \inf_{x\in\mathbb{R}} (1 + \epsilon\kappa_2\zeta + \beta\omega_2 b) \geq h_{02} \;>\; 0. \end{aligned} \tag{H2}$$

The conditions (H1) and (H2) are imposed only on the initial data, and then they are automatically satisfied over the relevant time scale. The interested reader is referred to the proof of Theorem 2.6.1.

Now the preliminary results proved in [49, Section 5] remain valid for the operator $\mathfrak{T}[\epsilon\zeta, \beta b]$. Let us recall now that the quantity $|\cdot|_{H^1_\mu}$ is defined as follows

$$\forall\; v \in H^1(\mathbb{R}), \quad |\; v \;|^2_{H^1_\mu} \;=\; |\; v \;|^2_{L^2} \;+\; \mu \;|\; \partial_x v \;|^2_{L^2},$$

equivalently to the $H^1(\mathbb{R})$-norm and depending on μ. We define by, $H^1_\mu(\mathbb{R})$ the space $H^1(\mathbb{R})$ endowed with this norm and $(H^1_\mu(\mathbb{R}))^\star$ the space $H^{-1}(\mathbb{R})$ the dual space of $H^1_\mu(\mathbb{R})$.

The following lemma gives an important invertibility result on $\mathfrak{T}$.

Lemma 2.4.1. *Let $(\mu,\epsilon,\delta,\gamma,\beta,\mathrm{bo}) \in \mathcal{P}_{\mathrm{CH}}$ and $\zeta \in L^\infty(\mathbb{R})$, $b \in L^\infty(\mathbb{R})$ such that* (H2) *is satisfied. Then the operator*

$$\mathfrak{T}[\epsilon\zeta,\beta b] : H^1_\mu(\mathbb{R}) \longrightarrow (H^1_\mu(\mathbb{R}))^\star$$

is uniformly continuous and coercive. More precisely, there exists $c_0 > 0$ such that

$$\begin{aligned}(\mathfrak{T}u,v) &\leq c_0|u|_{H^1_\mu}|v|_{H^1_\mu};\\ (\mathfrak{T}u,u) &\geq \frac{1}{c_0}|u|^2_{H^1_\mu}\end{aligned}$$

with $c_0 = C(M_{\mathrm{CH}}, h_{02}^{-1}, \epsilon\big|\zeta\big|_{L^\infty}, \beta\big|b\big|_{L^\infty})$.

Moreover, the following estimates hold: Let $s_0 > \frac{1}{2}$ and $s \geq 0$,

(i) If $\zeta, b \in H^{s_0}(\mathbb{R}) \cap H^s(\mathbb{R})$ and $u \in H^{s+1}(\mathbb{R})$ and $v \in H^1(\mathbb{R})$, then:

$$\begin{aligned}\big|\big(\Lambda^s\mathfrak{T}[\epsilon\zeta,\beta b]u,v\big)\big| \leq & C_0\Big((\epsilon|\zeta|_{H^{s_0}}+\beta|b|_{H^{s_0}})\big|u\big|_{H^{s+1}_\mu}\\ &+\big\langle(\epsilon|\zeta|_{H^s}+\beta|b|_{H^s})\big|u\big|_{H^{s_0+1}_\mu}\big\rangle_{s>s_0}\Big)\big|v\big|_{H^1_\mu}.\end{aligned}$$

(ii) If $\zeta, b \in H^{s_0+1} \cap H^s(\mathbb{R})$, $u \in H^s(\mathbb{R})$ and $v \in H^1(\mathbb{R})$, then:

$$\begin{aligned}\big|\big(\big[\Lambda^s,\mathfrak{T}[\epsilon\zeta,\beta b]\big]u,v\big)\big| &\leq C_0\Big((\epsilon|\zeta|_{H^{s_0+1}}+\beta|b|_{H^{s_0+1}})\big|u\big|_{H^s_\mu}\\ &\qquad+\big\langle(\epsilon|\zeta|_{H^s}+\beta|b|_{H^s})\big|u\big|_{H^{s_0+1}_\mu}\big\rangle_{s>s_0+1}\Big)\big|v\big|_{H^1_\mu}\\ &\leq \max(\epsilon,\beta)C_0\Big((|\zeta|_{H^{s_0+1}}+|b|_{H^{s_0+1}})\big|u\big|_{H^s_\mu}\\ &\qquad+\big\langle(|\zeta|_{H^s}+|b|_{H^s})\big|u\big|_{H^{s_0+1}_\mu}\big\rangle_{s>s_0+1}\Big)\big|v\big|_{H^1_\mu},\end{aligned}$$

where $C_0 = C(M_{\mathrm{CH}}, h_{02}^{-1})$.

The following lemma then gives some properties of the inverse operator $\mathfrak{T}^{-1}$.

Lemma 2.4.2. *Let $(\mu,\epsilon,\delta,\gamma,\beta,\mathrm{bo}) \in \mathcal{P}_{\mathrm{CH}}$ and $\zeta \in L^\infty(\mathbb{R})$, $b \in L^\infty(\mathbb{R})$ such that* (H2) *is satisfied. Then the operator*

$$\mathfrak{T}[\epsilon\zeta,\beta b] : H^2(\mathbb{R}) \longrightarrow L^2(\mathbb{R})$$

is one-to-one and onto. In addition, the following estimates holds:

(i) $(\mathfrak{T}[\epsilon\zeta,\beta b])^{-1} : L^2 \to H^1_\mu(\mathbb{R})$ is continuous. More precisely, one has

$$\| \mathfrak{T}^{-1} \|_{L^2(\mathbb{R})\to H^1_\mu(\mathbb{R})} \leq c_0,$$

with $c_0 = C(M_{\mathrm{CH}}, h_{02}^{-1}, \epsilon\big|\zeta\big|_{L^\infty}, \beta\big|b\big|_{L^\infty})$.

(ii) Additionally, if $\zeta, b \in H^{s_0+1}(\mathbb{R})$ with $s_0 > \frac{1}{2}$, then one has for any $0 < s \leq s_0 + 1$,

$$\| \mathfrak{T}^{-1} \|_{H^s(\mathbb{R})\to H^{s+1}_\mu(\mathbb{R})} \leq c_{s_0+1}.$$

(iii) If $\zeta, b \in H^s(\mathbb{R})$ *with* $s \geq s_0 + 1,\ s_0 > \frac{1}{2}$*, then one has*

$$\| \mathfrak{T}^{-1} \|_{H^s(\mathbb{R}) \to H^{s+1}_\mu(\mathbb{R})} \leq\ c_s$$

where $c_{\bar{s}} = C(M_{\mathrm{CH}}, h_{02}^{-1}, \epsilon|\zeta|_{H^{\bar{s}}}, \beta|b|_{H^{\bar{s}}})$*, thus uniform with respect to* $(\mu, \epsilon, \delta, \gamma, \beta, \mathrm{bo}) \in \mathcal{P}_{\mathrm{CH}}$.

A technical estimate is necessary for the next sections.

Corollary 1. *Let* $(\mu, \epsilon, \delta, \gamma, \beta, \mathrm{bo}) \in \mathcal{P}_{\mathrm{CH}}$ *and* $\zeta, b \in H^s(\mathbb{R})$ *with* $s \geq s_0 + 1,\ s_0 > \frac{1}{2}$*, such that* (H2) *is satisfied. Suppose that* $u \in H^{s-1}(\mathbb{R})$ *and that* $v \in H^1(\mathbb{R})$*. Then one has*

$$\begin{aligned}\left|\left(\left[\Lambda^s, \mathfrak{T}^{-1}[\epsilon\zeta, \beta b]\right]u, \mathfrak{T}[\epsilon\zeta, \beta b]v\right)\right| &= \left|\left(\left[\Lambda^s, \mathfrak{T}[\epsilon\zeta, \beta b]\right]\mathfrak{T}^{-1}u, v\right)\right| \\ &\leq \max(\epsilon, \beta) C(M_{\mathrm{CH}}, h_{02}^{-1}, |\zeta|_{H^s}, |b|_{H^s}) |u|_{H^{s-1}} |v|_{H^1_\mu}\end{aligned}$$

2.5 Linear analysis

This section is devoted to the energy estimate study of the linearized system associated to our nonlinear asymptotic system (2.16), following the classical theory of quasilinear hyperbolic systems. More precisely, we establish new linear estimates independent of the Camassa-Holm assumptions $\epsilon = \mathcal{O}(\sqrt{\mu})$ and $\beta = \mathcal{O}(\sqrt{\mu})$. To establish these estimates we propose a new pseudo-symmetrizer of the system that allows us to cancel the use of the smallness assumptions of the Camassa-Holm regime in the proof of Lemma 5.18, in fact the assumption on the deformation of the interface $\epsilon = \mathcal{O}(\sqrt{\mu})$ was necessary for the proof of [49, Lemma 6.5]. Therefore, these assumptions can be relaxed for the well-posedness and stability results (Theorem 6.1 and Theorem 6.6 respectively), regardless of their necessity for the derivation of the model (2.16).

Let us recall the system (2.16).

$$\begin{cases} \partial_t \zeta + \partial_x \left(\dfrac{h_1 h_2}{h_1 + \gamma h_2} v \right) \ = \ 0, \\ \\ \mathfrak{T}[\epsilon\zeta, \beta b]\left(\partial_t v + \epsilon\varsigma v \partial_x v\right) + (\gamma + \delta) q_1(\epsilon\zeta, \beta b) \partial_x \zeta \\ + \frac{\epsilon}{2} q_1(\epsilon\zeta, \beta b) \partial_x \left(\frac{h_1^2 - \gamma h_2^2}{(h_1 + \gamma h_2)^2} |v|^2 - \varsigma |v|^2 \right) = -\mu\epsilon\frac{2}{3}\alpha_1 \partial_x \big((\partial_x v)^2 \big) + \mu\beta\omega(\partial_x\zeta)(\partial_x^2 b), \end{cases}$$

with $h_1 = 1 - \epsilon\zeta$, $h_2 = 1/\delta + \epsilon\zeta - \beta b$, $q_i(X, Y) = 1 + \kappa_i X + \omega_i Y$ $(i = 1, 2)$, $\kappa_i, \omega_i, \varsigma$ defined in (2.12),(2.13),(2.14), and

$$\mathfrak{T}[\epsilon\zeta, \beta b]V = q_1(\epsilon\zeta, \beta b)V - \mu\nu\partial_x \left(q_2(\epsilon\zeta, \beta b)\partial_x V \right).$$

The definition of the following functions allows to simplify the reading

$$f : X \to \frac{(1 - X)(\delta^{-1} + X - \beta b)}{1 - X + \gamma(\delta^{-1} + X - \beta b)},$$

and

$$g : X \to \Big(\frac{(1 - X)}{1 - X + \gamma(\delta^{-1} + X - \beta b)} \Big)^2.$$

so that one can write

$$f(\epsilon\zeta) \;=\; \frac{h_1h_2}{h_1+\gamma h_2}, \qquad f'(\epsilon\zeta) \;=\; \frac{h_1^2-\gamma h_2^2}{(h_1+\gamma h_2)^2} \quad \text{and} \quad g(\epsilon\zeta)=\Big(\frac{h_1}{h_1+\gamma h_2}\Big)^2.$$

Additionally, let us denote

$$\kappa=\frac{2}{3}\alpha_1=\frac{2}{3}\frac{1-\gamma}{(\delta+\gamma)^2} \quad \text{and} \quad q_3(\epsilon\zeta)=\frac{1}{2}\big(\frac{h_1^2-\gamma h_2^2}{(h_1+\gamma h_2)^2}-\varsigma\big),$$

and finally one obtains the following model,

$$\left\{\begin{array}{l} \partial_t\zeta+f(\epsilon\zeta)\partial_x v+\epsilon\partial_x\zeta f'(\epsilon\zeta)v-\beta\partial_x b g(\epsilon\zeta)v \;=\; 0,\\[2ex] \mathfrak{T}\Big(\partial_t v+\dfrac{\epsilon}{2}\varsigma\partial_x(v^2)\Big)+(\gamma+\delta)q_1(\epsilon\zeta,\beta b)\partial_x\zeta+\epsilon q_1(\epsilon\zeta,\beta b)\partial_x(q_3(\epsilon\zeta)v^2)\\ \qquad\qquad =-\mu\epsilon\kappa\partial_x\big((\partial_x v)^2\big)+\mu\beta\omega(\partial_x\zeta)(\partial_x^2 b). \end{array}\right. \tag{2.17}$$

with $\partial_x(q_3(\epsilon\zeta))=\dfrac{-\gamma\epsilon\partial_x\zeta(h_1+h_2)^2+\gamma\beta\partial_x b h_1(h_1+h_2)}{(h_1+\gamma h_2)^3}$.

We apply $\mathfrak{T}^{-1}$ to the second equation in (2.17) so as the system of equations is written by

$$\partial_t U+A[U]\partial_x U+B[U] \;=\; 0,$$

with

$$A[U]=\begin{pmatrix} \epsilon f'(\epsilon\zeta)v & f(\epsilon\zeta)\\ \mathfrak{T}^{-1}(Q_0(\epsilon\zeta,\beta b)\cdot+\epsilon^2 Q_1(\epsilon\zeta,\beta b,v)\cdot) & \epsilon\mathfrak{T}^{-1}(\mathfrak{Q}[\epsilon\zeta,\beta b,v]\cdot)+\epsilon\varsigma v\end{pmatrix} \tag{2.18}$$

$$B[U]=\begin{pmatrix} -\beta\partial_x b g(\epsilon\zeta)v\\ \epsilon\mathfrak{T}^{-1}\Big(\dfrac{\gamma\beta q_1(\epsilon\zeta,\beta b)h_1(h_1+h_2)v^2}{(h_1+\gamma h_2)^3}\partial_x b\Big)\end{pmatrix}$$

where $Q_0(\epsilon\zeta,\beta b), Q_1(\epsilon\zeta,\beta b,v)$ are defined as

$$\begin{aligned} Q_0(\epsilon\zeta,\beta b)&=(\gamma+\delta)q_1(\epsilon\zeta,\beta b)-\mu\beta\omega\partial_x^2 b,\\ Q_1(\epsilon\zeta,\beta b,v)&=-\gamma q_1(\epsilon\zeta,\beta b)\frac{(h_1+h_2)^2}{(h_1+\gamma h_2)^3}v^2 \end{aligned}$$

and the operator $\mathfrak{Q}[\epsilon,\beta b,v]$ defined by

$$\mathfrak{Q}[\epsilon\zeta,\beta b,v]f \;\equiv\; 2q_1(\epsilon\zeta,\beta b)q_3(\epsilon\zeta)vf+\mu\kappa\partial_x(f\partial_x v).$$

The following sections are devoted to the proof of energy estimates for the following initial value problem around some reference state $\underline{U}=(\underline{\zeta},\underline{v})^\top$:

$$\left\{\begin{array}{l} \partial_t U+A[\underline{U}]\partial_x U+B[\underline{U}]=0;\\ U_{|_{t=0}}=U_0. \end{array}\right. \tag{2.19}$$

2.5.1 Energy space

The structure of the system of equations allows to give the new pseudo-symmetrizer

$$Z[\underline{U}] = \begin{pmatrix} \frac{Q_0(\epsilon\underline{\zeta},\beta b)+\epsilon^2 Q_1(\epsilon\underline{\zeta},\beta b,\underline{v})}{f(\epsilon\underline{\zeta})} & 0 \\ 0 & \mathfrak{T}[\epsilon\underline{\zeta},\beta b] \end{pmatrix} \tag{2.20}$$

Note however that one should add an additional assumption in order to ensure that our pseudo-symmetrizer is defined and positive which is:

$$\exists\ h_{03}>0 \ \text{ such that } \ Q_0(\epsilon\underline{\zeta},\beta b)+\epsilon^2 Q_1(\epsilon\underline{\zeta},\beta b,\underline{v})\geq h_{03}>0. \tag{H3}$$

Let us now define X^s the energy space of this problem as $X^s = H^s(\mathbb{R})\times H^{s+1}(\mathbb{R})$, with the following norm

$$\forall\, U=(\zeta,v)^\top\in X^s,\quad |U|^2_{X^s}\equiv|\zeta|^2_{H^s}+|v|^2_{H^s}+\mu|\partial_x v|^2_{H^s},$$

while X^s_T stands for the space of $U=(\zeta,v)$ such that $U\in C^0([0,\frac{T}{\max(\epsilon,\beta)}];X^s)$, and $\partial_t U\in L^\infty([0,\frac{T}{\max(\epsilon,\beta)}]\times\mathbb{R})$, endowed with the canonical norm

$$\|U\|_{X^s_T}\equiv \sup_{t\in[0,T/\max(\epsilon,\beta)]}|U(t,\cdot)|_{X^s}+\operatorname*{ess\,sup}_{t\in[0,T/\max(\epsilon,\beta)],x\in\mathbb{R}}|\partial_t U(t,x)|.$$

The initial value problem (2.19) has the following energy problem:

$$\begin{aligned} E^s(U)^2=(\Lambda^s U,Z[\underline{U}]\Lambda^s U)=&(\Lambda^s\zeta,\frac{Q_0(\epsilon\underline{\zeta},\beta b)+\epsilon^2Q_1(\epsilon\underline{\zeta},\beta b,\underline{v})}{f(\epsilon\underline{\zeta})}\Lambda^s\zeta)\\ &+\left(\Lambda^s v,\mathfrak{T}[\epsilon\underline{\zeta},\beta b]\Lambda^s v\right).\end{aligned}$$

In order to ensure the equivalency of X^s with the energy of the pseudo-symmetrizer it requires to add the additional assumption given in (H3).

In the following lemma we prove that $E^s(U)$ and $|\cdot|_{X^s}$-norm are equivalent.

Lemma 2.5.1. *Let* $\mathsf{p}=(\mu,\epsilon,\delta,\gamma,\beta,\mathrm{bo})\in\mathcal{P}_{\mathrm{CH}}$, $s\geq 0$, $\underline{U}\in L^\infty(\mathbb{R})$ *and* $b\in W^{2,\infty}(\mathbb{R})$, *satisfying* (H1), (H2), *and* (H3). *The* $E^s(U)$ *is equivalent to the* $|\cdot|_{X^s}$*-norm.*
More precisely, there exists $c_0=C(M_{\mathrm{CH}},h_{01}^{-1},h_{02}^{-1},h_{03}^{-1},\epsilon|\underline{U}|_{L^\infty},\beta|b|_{W^{2,\infty}})>0$ *such that*

$$\frac{1}{c_0}E^s(U)\ \leq\ \left|U\right|_{X^s}\ \leq\ c_0E^s(U).$$

Proof. Using Lemma 2.4.1 and the fact that for $Q_0(\epsilon\underline{\zeta},\beta b)+\epsilon^2Q_1(\epsilon\underline{\zeta},\beta b,\underline{v})\geq h_{03}>0$ and $f(\epsilon\underline{\zeta})>0$, one has

$$\begin{aligned}\inf_{x\in\mathbb{R}}\frac{Q_0(\epsilon\underline{\zeta},\beta b)+\epsilon^2Q_1(\epsilon\underline{\zeta},\beta b,\underline{v})}{f(\epsilon\underline{\zeta})}&\geq\inf_{x\in\mathbb{R}}\Big(Q_0(\epsilon\underline{\zeta},\beta b))+\epsilon^2Q_1(\epsilon\underline{\zeta},\beta b,\underline{v})\Big)\Big(\sup_{x\in\mathbb{R}}f(\epsilon\underline{\zeta})\Big)^{-1},\\ \sup_{x\in\mathbb{R}}\frac{Q_0(\epsilon\underline{\zeta},\beta b)+\epsilon^2Q_1(\epsilon\underline{\zeta},\beta b,\underline{v})}{f(\epsilon\underline{\zeta})}&\leq\sup_{x\in\mathbb{R}}\Big(Q_0(\epsilon\underline{\zeta},\beta b)+\epsilon^2Q_1(\epsilon\underline{\zeta},\beta b,\underline{v})\Big)\Big(\inf_{x\in\mathbb{R}}f(\epsilon\underline{\zeta})\Big)^{-1}.\end{aligned}$$

where we recall that if (H1) is satisfied then, $\underline{h_1}=1-\epsilon\underline{\zeta},\underline{h_2}=1/\delta+\epsilon\underline{\zeta}-\beta b$ satisfy

$$\inf_{x\in\mathbb{R}}\underline{h_1}\geq h_{01},\quad \sup_{x\in\mathbb{R}}|\underline{h_1}|\leq 1+1/\delta,\quad \inf_{x\in\mathbb{R}}\underline{h_2}\geq h_{01},\quad \sup_{x\in\mathbb{R}}|\underline{h_2}|\leq 1+1/\delta.$$

□

Lemma 2.5.2. *Let* $\mathsf{p} = (\mu, \epsilon, \delta, \gamma, \beta, \mathrm{bo}) \in \mathcal{P}_{\mathrm{CH}}$*, and let* $U = (\zeta_u, u)^\top \in L^\infty$*,* $b \in W^{2,\infty}$ *satisfies* (H1),(H2) *and* (H3)*. Then for any* $V, W \in X^0$*, one has*

$$\Big| \Big(Z[U]V \ , \ W \Big) \Big| \ \leq \ C \ |V|_{X^0} |W|_{X^0}, \tag{2.21}$$

with $C = C(M_{\mathrm{CH}}, h_{01}^{-1}, h_{02}^{-1}, \epsilon|U|_{L^\infty}, \beta|b|_{W^{2,\infty}})$.

Moreover, if $U \in X^s, b \in H^{s+2}, V \in X^{s-1}$ *with* $s \geq s_0 + 1$*,* $s_0 > 1/2$*, then one has*

$$\Big| \Big(\ [\Lambda^s, Z[U]]V \ , \ W \ \Big) \Big| \quad \leq \quad C \ |V|_{X^{s-1}} |W|_{X^0} \tag{2.22}$$

$$\Big| \Big(\ [\Lambda^s, Z^{-1}[U]]V \ , \ Z[U]W \ \Big) \Big| \quad \leq \quad C \ |V|_{H^{s-1} \times H^{s-1}} |W|_{X^0} \tag{2.23}$$

with $C = C(M_{\mathrm{CH}}, h_{01}^{-1}, h_{02}^{-1}, \epsilon|U|_{X^s}, \beta|b|_{H^{s+2}})$.

Proof. The Lemma 5.13 is proved using Cauchy-Schwarz inequality, Lemma 4.2 and Corollary 4.8. We omit the proof here, and refer to [49, Lemma 6.4]. □

2.5.2 Energy estimates

In this section we study the energy estimates of our linear system. To this end we modify the linear system by adding a right-hand-side term F. Thus one obtains the following system

$$\begin{cases} \partial_t U + A[\underline{U}]\partial_x U + B[\underline{U}] = F; \\ U_{|t=0} = U_0. \end{cases} \tag{2.24}$$

Starting with the X^0 energy estimate, we extend this result later to the X^s space ($s > 3/2$).

Lemma 2.5.3 (X^0 energy estimate)**.** *Set* $(\mu, \epsilon, \delta, \gamma, \beta, \mathrm{bo}) \in \mathcal{P}_{\mathrm{CH}}$*. Let* $T > 0$*,* $s_0 > 1/2$ *and* $U \in L^\infty([0, T/\max(\epsilon, \beta)]; X^0)$ *and* $\underline{U}, \partial_x \underline{U} \in L^\infty([0, T/\max(\epsilon, \beta)] \times \mathbb{R})$ *and* $b \in H^{s_0+3}$ *such that* $\partial_t \underline{U} \in L^\infty([0, T/\max(\epsilon, \beta)] \times \mathbb{R})$ *and* $\underline{U}, b$ *satisfies* (H1),(H2)*, and* (H3) *and* $U, \underline{U}$ *satisfy system* (2.24)*, with a right hand side,* F*, such that*

$$\big(F, Z[\underline{U}]U\big) \ \leq \ C_F \ \max(\epsilon, \beta)|U|_{X^0}^2 \ + \ f(t) \ |U|_{X^0},$$

with C_F *a constant and* f *a positive integrable function on* $[0, T/\max(\epsilon, \beta)]$*.*
Then there exists $\lambda, C_1 \equiv C(\|\partial_t \underline{U}\|_{L^\infty}, \|\underline{U}\|_{L^\infty}, \|\partial_x \underline{U}\|_{L^\infty}, \|b\|_{H^{s_0+3}}, C_F)$ *such that*

$$\begin{aligned} \forall t \in [0, \frac{T}{\max(\epsilon, \beta)}], \qquad E^0(U)(t) \leq & e^{\max(\epsilon,\beta)\lambda t} E^0(U_0) \\ & + \int_0^t e^{\max(\epsilon,\beta)\lambda(t-t')} \Big(f(t') + \max(\epsilon, \beta) C_1 \Big) dt', \end{aligned} \tag{2.25}$$

The constants λ *and* C_1 *are independent of* $\mathsf{p} = (\mu, \epsilon, \delta, \gamma, \beta, \mathrm{bo}) \in \mathcal{P}_{\mathrm{CH}}$*, but depend on* $M_{\mathrm{CH}}, h_{01}^{-1}, h_{02}^{-1}$*, and* h_{03}^{-1}*.*

Proof. The first step of this proof is to take the L^2 inner product of (2.24) by $Z[\underline{U}]U$:

$$\big(\partial_t U, Z[\underline{U}]U\big) \ + \ \big(A[\underline{U}]\partial_x U, Z[\underline{U}]U\big) \ + \ \big(B[\underline{U}], Z[\underline{U}]U\big) \ = \ \big(F, Z[\underline{U}]U\big) \ .$$

Since $Z[\underline{U}]$ is symmetric, one can deduces from the definition of $E^s(u)$ the following

$$\frac{1}{2}\frac{d}{dt}E^0(U)^2 = \frac{1}{2}\big(U, \big[\partial_t, Z[\underline{U}]\big]U\big) - \big(Z[\underline{U}]A[\underline{U}]\partial_x U, U\big) - \big(B[\underline{U}], Z[\underline{U}]U\big) + \big(F, Z[\underline{U}]U\big). \quad (2.26)$$

Let us first estimate $\big(B[\underline{U}], Z[\underline{U}]U\big)$. One has

$$\begin{aligned}\big(B[\underline{U}], Z[\underline{U}]U\big) =& \Big(- g(\epsilon\underline{\zeta})\underline{v}\beta\partial_x b, \frac{Q_0(\epsilon\underline{\zeta},\beta b) + \epsilon^2 Q_1(\epsilon\underline{\zeta},\beta b,\underline{v})}{f(\epsilon\underline{\zeta})}\zeta\Big)\\ &+ \Big(\epsilon\mathfrak{T}^{-1}\big(\frac{\gamma\beta q_1(\epsilon\underline{\zeta},\beta b)h_1(h_1+h_2)\underline{v}^2\partial_x b}{(h_1+\gamma h_2)^3}\big), \mathfrak{T}[\epsilon\underline{\zeta},\beta b]v\Big).\end{aligned}$$

$$\begin{aligned}&\Big(- g(\epsilon\underline{\zeta})\underline{v}\beta\partial_x b, \frac{Q_0(\epsilon\underline{\zeta},\beta b) + \epsilon^2 Q_1(\epsilon\underline{\zeta},\beta b,\underline{v})}{f(\epsilon\underline{\zeta})}\zeta\Big)\\ &\qquad \le \beta C\big(\big\|\underline{U}\big\|_{L^\infty}, \|b\|_{W^{2,\infty}}, \|\partial_x b\|_{L^2}\big)\big|U\big|_{X^0}.\end{aligned}$$

Using the symmetry property of $\mathfrak{T}[\epsilon\underline{\zeta},\beta b]$, we write

$$\begin{aligned}&\Big(\epsilon\mathfrak{T}^{-1}\big(\frac{\gamma\beta q_1(\epsilon\underline{\zeta},\beta b)h_1(h_1+h_2)\underline{v}^2\partial_x b}{(h_1+\gamma h_2)^3}\big), \mathfrak{T}[\epsilon\underline{\zeta},\beta b]v\Big)\\ &\qquad = \epsilon\Big(\frac{\gamma\beta q_1(\epsilon\underline{\zeta},\beta b)h_1(h_1+h_2)\underline{v}^2\partial_x b}{(h_1+\gamma h_2)^3}, v\Big).\end{aligned}$$

From Cauchy-Schwarz inequality, one deduces

$$\epsilon\Big(\frac{\gamma\beta q_1(\epsilon\underline{\zeta},\beta b)h_1(h_1+h_2)\underline{v}^2\partial_x b}{(h_1+\gamma h_2)^3}, v\Big) \le \beta C\big(\big\|\underline{U}\big\|_{L^\infty}, \|\partial_x b\|_{L^2}\big)\big|U\big|_{X^0}.$$

Altogether, one has

$$\big(B[\underline{U}], Z[\underline{U}]U\big) \le \beta C_1\big|U\big|_{X^0} \le \max(\epsilon,\beta)C_1\big|U\big|_{X^0}. \quad (2.27)$$

Now we have,

$$Z[\underline{U}]A[\underline{U}] = \begin{pmatrix} \epsilon\frac{Q_0(\epsilon\underline{\zeta},\beta b)+\epsilon^2 Q_1(\epsilon\underline{\zeta},\beta b,\underline{v})}{f(\epsilon\underline{\zeta})}f'(\epsilon\underline{\zeta})\underline{v} & Q_0(\epsilon\underline{\zeta},\beta b) + \epsilon^2 Q_1(\epsilon\underline{\zeta},\beta b,\underline{v}) \\ Q_0(\epsilon\underline{\zeta},\beta b) + \epsilon^2 Q_1(\epsilon\underline{\zeta},\beta b,\underline{v}) & \epsilon\mathfrak{Q}[\epsilon\underline{\zeta},\beta b,\underline{v}] + \epsilon_{\mathfrak{S}}\mathfrak{T}[\epsilon\underline{\zeta},\beta b](\underline{v}.) \end{pmatrix}$$

One has,

$$\begin{aligned}\big(Z[\underline{U}]A[\underline{U}]\partial_x U, U\big) &= \Big(\epsilon\frac{Q_0(\epsilon\underline{\zeta},\beta b) + \epsilon^2 Q_1(\epsilon\underline{\zeta},\beta b,\underline{v})}{f(\epsilon\underline{\zeta})}f'(\epsilon\underline{\zeta})\underline{v}\partial_x\zeta, \zeta\Big)\\ &+ \Big(Q_0(\epsilon\underline{\zeta},\beta b)\partial_x v, \zeta\Big) + \Big(\epsilon^2 Q_1(\epsilon\underline{\zeta},\beta b,\underline{v})\partial_x v, \zeta\Big)\\ &+ \Big(Q_0(\epsilon\underline{\zeta},\beta b)\partial_x\zeta, v\Big) + \Big(\epsilon^2 Q_1(\epsilon\underline{\zeta},\beta b,\underline{v})\partial_x\zeta, v\Big)\\ &+ \Big(\epsilon\mathfrak{Q}[\epsilon\underline{\zeta},\beta b,\underline{v}]\partial_x v, v\Big) + \epsilon_{\mathfrak{S}}\Big(\mathfrak{T}[\epsilon\underline{\zeta},\beta b](\underline{v}\partial_x v), v\Big).\end{aligned}$$

One deduces that,

$$\begin{aligned}\big(Z[\underline{U}]A[\underline{U}]\partial_x U, U\big) &= -\frac{1}{2}\Big(\epsilon\partial_x\big(\frac{Q_0(\epsilon\underline{\zeta},\beta b)+\epsilon^2 Q_1(\epsilon\underline{\zeta},\beta b,\underline{v})}{f(\epsilon\underline{\zeta})}f'(\epsilon\underline{\zeta})\underline{v}\big)\zeta,\zeta\Big)\\ &- \Big(\partial_x\big(Q_0(\epsilon\underline{\zeta},\beta b)\big)\zeta,v\Big)-\epsilon^2\Big(\partial_x\big(Q_1(\epsilon\underline{\zeta},\beta b,\underline{v})\big)\zeta,v\Big)\\ &+ \Big(\epsilon\mathfrak{Q}[\epsilon\underline{\zeta},\beta b,\underline{v}]\partial_x v,v\Big)+\epsilon\varsigma\Big(\mathfrak{T}[\epsilon\underline{\zeta},\beta b](\underline{v}\partial_x v),v\Big).\end{aligned}$$

One can easily remark that we didn't use the smallness assumption of the Camassa-Holm regime $\epsilon=\mathcal{O}(\sqrt{\mu})$ since we do not have anymore $\partial_x v$ in the third term of the above identity.

One make use of the identity below,

$$\begin{aligned}\big(\mathfrak{T}[\epsilon\underline{\zeta},\beta b](\underline{v}\partial_x V),V\big) =&\big(\ q_1(\epsilon\underline{\zeta},\beta b)\underline{v}\partial_x V-\mu\nu\partial_x(q_2(\epsilon\underline{\zeta},\beta b)\partial_x(\underline{v}\partial_x V))\ ,\ V\ \big)\\ =&-\frac{1}{2}\big(\ \partial_x(q_1(\epsilon\underline{\zeta},\beta b)\underline{v})V,V\big)+\mu\nu\big(\ q_2(\epsilon\underline{\zeta},\beta b)\partial_x(\underline{v}\partial_x V),\partial_x V\big)\\ =&-\frac{1}{2}\big(\partial_x(q_1(\epsilon\underline{\zeta},\beta b)\underline{v})V,V\big)+\mu\nu\big(q_2(\epsilon\underline{\zeta},\beta b)(\partial_x\underline{v})\partial_x V,\partial_x V\big)\\ &-\mu\nu\frac{1}{2}\big(\partial_x(q_2(\epsilon\underline{\zeta},\beta b)\underline{v})\partial_x V,\partial_x V\big).\end{aligned}$$

From Cauchy-Schwarz inequality, one deduces

$$\Big|\big(Z[\underline{U}]A[\underline{U}]\partial_x U,U\big)|\le\max(\epsilon,\beta)C\Big(\big\|\underline{U}\big\|_{L^\infty}+\big\|\partial_x\underline{U}\big\|_{L^\infty}+\big\|b\big\|_{W^{3,\infty}}\Big)|U|^2_{X^0}. \tag{2.28}$$

The last term to estimate is $\big(U,\big[\partial_t,Z[\underline{U}]\big]U\big)$.

One has

$$\begin{aligned}\big(U,\big[\partial_t,Z[\underline{U}]\big]U\big)\equiv&(v,\Big[\partial_t,\underline{\mathfrak{T}}\Big]v)+(\zeta,\Big[\partial_t,\frac{Q_0(\epsilon\underline{\zeta},\beta b)+\epsilon^2Q_1(\epsilon\underline{\zeta},\beta b,\underline{v})}{f(\epsilon\underline{\zeta})}\Big]\zeta)\\ =&\Big(v,\big(\partial_t q_1(\epsilon\underline{\zeta},\beta b)\big)v\Big)-\mu\nu\Big(v,\partial_x\big((\partial_t q_2(\epsilon\underline{\zeta},\beta b))(\partial_x v)\big)\Big)\\ &+\Big(\zeta,\partial_t\Big(\frac{Q_0(\epsilon\underline{\zeta},\beta b)+\epsilon^2Q_1(\epsilon\underline{\zeta},\beta b,\underline{v})}{f(\epsilon\underline{\zeta})}\Big)\zeta\Big).\end{aligned}$$

From Cauchy-Schwarz inequality and since $\underline{\zeta}$ and b satisfies (H1), one deduces

$$\begin{aligned}\Big|\ \frac{1}{2}\big(U,\big[\partial_t,Z[\underline{U}]\big]U\big)\ \Big|\ &\le\epsilon C(\big\|\partial_t\underline{U}\big\|_{L^\infty},\big\|\underline{U}\big\|_{L^\infty})|U|^2_{X^0}\\ &\le\max(\epsilon,\beta)C(\big\|\partial_t\underline{U}\big\|_{L^\infty},\big\|\underline{U}\big\|_{L^\infty})|U|^2_{X^0}.\end{aligned} \tag{2.29}$$

Plugging (2.27), (2.28) and (2.29) into (2.26), and using the assumption on F given by the Lemma, one has

$$\frac{1}{2}\frac{d}{dt}E^0(U)^2\ \le\ \max(\epsilon,\beta)\ C_1E^0(U)^2+\Big(f(t)+\max(\epsilon,\beta)C_1\Big)E^0(U),$$

where $C_1\equiv C(\big\|\partial_t\underline{U}\big\|_{L^\infty},\big\|\underline{U}\big\|_{L^\infty},\big\|\partial_x\underline{U}\big\|_{L^\infty},\|b\|_{H^{s_0+3}},C_F)$. Consequently

$$\frac{d}{dt}E^0(U)\ \le\ \max(\epsilon,\beta)C_1E^0(U)+\Big(f(t)+\max(\epsilon,\beta)C_1\Big).$$

For any $\lambda \in \mathbb{R}$, one has

$$e^{\max(\epsilon,\beta)\lambda t}\partial_t(e^{-\max(\epsilon,\beta)\lambda t}E^0(U)) = -\max(\epsilon,\beta)\lambda E^0(U) + \frac{d}{dt}E^0(U).$$

We choose $\lambda = C_1$, so that for all $t \in [0, \frac{T}{\max(\epsilon,\beta)}]$, the above inequality becomes

$$\frac{d}{dt}(e^{-\max(\epsilon,\beta)\lambda t}E^0(U)) \ \leq \ \Big(f(t) + \max(\epsilon,\beta)C_1\Big)e^{-\max(\epsilon,\beta)\lambda t}.$$

By integration one can deduce

$$\begin{aligned}\forall t \in [0, \frac{T}{\max(\epsilon,\beta)}], \qquad E^0(U)(t) \leq & e^{\max(\epsilon,\beta)\lambda t}E^0(U_0) \\ & + \int_0^t e^{\max(\epsilon,\beta)\lambda(t-t')}\Big(f(t') + \max(\epsilon,\beta)C_1\Big)dt'.\end{aligned}$$

This proves the energy estimate (2.25). □

Let us give now the X^s energy estimates.

Lemma 2.5.4 (X^s energy estimate)**.** *Set $(\mu,\epsilon,\delta,\gamma,\beta,\mathrm{bo}) \in \mathcal{P}_{\mathrm{CH}}$, and $s \geq s_0 + 1$, $s_0 > 1/2$. Let $U = (\zeta, v)^\top$ and $\underline{U} = (\underline{\zeta}, \underline{v})^\top$ be such that $U, \underline{U} \in L^\infty([0, T/\max(\epsilon,\beta)]; X^s)$, $\partial_t\underline{U} \in L^\infty([0, T/\max(\epsilon,\beta)]\times\mathbb{R})$, $b \in H^{s+2}$ and $\underline{U}$ satisfies* (H1),(H2)*, and* (H3) *uniformly on $[0, T/\max(\epsilon,\beta)]$, and such that system* (2.24) *holds with a right hand side, F, with*

$$\big(\Lambda^s F, Z[\underline{U}]\Lambda^s U\big) \ \leq \ C_F \ \max(\epsilon,\beta)\big|U\big|^2_{X^s} \ + \ f(t) \ \big|U\big|_{X^s},$$

where f is an integrable function on $[0, T/\max(\epsilon,\beta)]$ and C_F is a constant.

Then there exists $\lambda, C_2 = C(\big\|\underline{U}\big\|_{X^s_T}, \big\|b\big\|_{H^{s+2}}, C_F)$ such that:

$$E^s(U)(t) \leq e^{\max(\epsilon,\beta)\lambda t}E^s(U_0) + \int_0^t e^{\max(\epsilon,\beta)\lambda(t-t')}\big(f(t') + \max(\epsilon,\beta)C_2\big)dt'. \tag{2.30}$$

The constants λ and C_2 are independent of $\mathsf{p} = (\mu,\epsilon,\delta,\gamma,\beta,\mathrm{bo}) \in \mathcal{P}_{\mathrm{CH}}$, but depend on $M_{\mathrm{CH}}, h_{01}^{-1}, h_{02}^{-1}$, and h_{03}^{-1}.

Remark 1. In what follows the norm $\big\|\underline{U}\big\|_{X^s_T}$ is to be understood as essential sup:

$$\|U\|_{X^s_T} \equiv \operatorname*{ess\,sup}_{t\in[0,T/\max(\epsilon,\beta)]}|U(t,\cdot)|_{X^s} + \operatorname*{ess\,sup}_{t\in[0,T/\max(\epsilon,\beta)],x\in\mathbb{R}}|\partial_t U(t,x)|.$$

Proof. Let us multiply the system (2.24) on the right by $\Lambda^s Z[\underline{U}]\Lambda^s U$, and integrate by parts. One obtains

$$\begin{aligned}\big(\Lambda^s\partial_t U, Z[\underline{U}]\Lambda^s U\big) + \big(\Lambda^s A[\underline{U}]\partial_x U, Z[\underline{U}]\Lambda^s U\big) + \big(\Lambda^s B[\underline{U}], Z[\underline{U}]\Lambda^s U\big) \\ = \big(\Lambda^s F, Z[\underline{U}]\Lambda^s U\big).\end{aligned}$$

Using the fact that $Z[\underline{U}]$ is symmetric, as well as the definition of $E^s(U)$ we deduce:

$$\begin{aligned}\frac{1}{2}\frac{d}{dt}E^s(U)^2 = & \frac{1}{2}\big(\Lambda^s U, \big[\partial_t, Z[\underline{U}]\big]\Lambda^s U\big) - \big(Z[\underline{U}]A[\underline{U}]\partial_x\Lambda^s U, \Lambda^s U\big) \\ & - \big(\big[\Lambda^s, A[\underline{U}]\big]\partial_x U, Z[\underline{U}]\Lambda^s U\big) - \big(\Lambda^s B[\underline{U}], Z[\underline{U}]\Lambda^s U\big) \\ & + \big(\Lambda^s F, Z[\underline{U}]\Lambda^s U\big).\end{aligned} \tag{2.31}$$

Let us now estimate each component of the r.h.s of the above identity.

• *Estimate of* $\big(\Lambda^s B[\underline{U}], Z[\underline{U}]\Lambda^s U\big)$,

$$\begin{aligned}\big(\Lambda^s B[\underline{U}], Z[\underline{U}]\Lambda^s U\big) = \Big(\Lambda^s\big(-g(\epsilon\underline{\zeta})\underline{v}\beta\partial_x b\big), \frac{Q_0(\epsilon\underline{\zeta},\beta b)+\epsilon^2 Q_1(\epsilon\underline{\zeta},\beta b,\underline{v})}{f(\epsilon\underline{\zeta})}\Lambda^s\zeta\Big)\\ +\epsilon\Big(\Lambda^s\underline{\mathfrak{T}}^{-1}\big(\frac{\gamma\beta q_1(\epsilon\underline{\zeta},\beta b)h_1(h_1+h_2)\underline{v}^2}{(h_1+\gamma h_2)^3}\partial_x b\big), \mathfrak{T}[\epsilon\underline{\zeta},\beta b]\Lambda^s v\Big).\end{aligned}$$

Using Cauchy-Schwarz inequality, Lemma 4.2 and Lemma 4.7 one has,

$$\big|\big(\Lambda^s B[\underline{U}], Z[\underline{U}]\Lambda^s U\big)\big| \leq \beta C\big(\big\|\underline{U}\big\|_{X^s_T}, \|b\|_{H^{s+1}}\big)|U|_{X^s} \leq \max(\epsilon,\beta)C_2|U|_{X^s}. \tag{2.32}$$

• *Estimate of* $\big(Z[\underline{U}]A[\underline{U}]\partial_x\Lambda^s U, \Lambda^s U\big)$.

Thanks to Sobolev embedding, one has for $s > s_0+1, s_0 > 1/2$

$$C(\|\underline{U}\|_{L^\infty} + \|\partial_x\underline{U}\|_{L^\infty}) \leq C(\big\|\underline{U}\big\|_{X^s_T}).$$

Using the L^2 estimate derived in (2.28), applied to $\Lambda^s U$, one deduces

$$\Big|\big(Z[\underline{U}]A[\underline{U}]\partial_x\Lambda^s U, \Lambda^s U\big)\Big| \leq \max(\epsilon,\beta)C\Big(\big\|\underline{U}\big\|_{X^s_T} + \big\|b\big\|_{W^{3,\infty}}\Big)|U|^2_{X^s}. \tag{2.33}$$

• *Estimate of* $\big(\big[\Lambda^s, A[\underline{U}]\big]\partial_x U, Z[\underline{U}]\Lambda^s U\big)$. Using the definition of $A[\cdot]$ and $Z[\cdot]$ in (2.18) and (2.20), one has

$$\begin{aligned}\big(\big[\Lambda^s, A[\underline{U}]\big]\partial_x U, Z[\underline{U}]\Lambda^s U\big) =& \Big([\Lambda^s, \epsilon f'(\epsilon\underline{\zeta})\underline{v}]\partial_x\zeta + [\Lambda^s, f(\epsilon\underline{\zeta})]\partial_x v, \frac{Q(\epsilon\underline{\zeta},\beta b,\underline{v})}{f(\epsilon\underline{\zeta})}\Lambda^s\zeta\Big)\\ &+\Big([\Lambda^s, \underline{\mathfrak{T}}^{-1}\big(Q(\epsilon\underline{\zeta},\beta b,\underline{v})\big)]\partial_x\zeta\ ,\ \underline{\mathfrak{T}}\Lambda^s v\Big)\\ &+\epsilon\Big([\Lambda^s, \underline{\mathfrak{T}}^{-1}\mathfrak{Q}[\epsilon\underline{\zeta},\beta b,\underline{v}] + \varsigma\underline{v}]\partial_x v, \underline{\mathfrak{T}}\Lambda^s v\Big).\end{aligned}$$

For the sake of simplicity, we denote here and in what follows $\underline{\mathfrak{T}} \equiv \mathfrak{T}[\epsilon\underline{\zeta},\beta b]$ and $Q(\epsilon\underline{\zeta},\beta b,\underline{v}) = Q_0(\epsilon\underline{\zeta},\beta b)+\epsilon^2 Q_1(\epsilon\underline{\zeta},\beta b,\underline{v})$.

Using the same techniques as in [49, Lemma 6.6] and since $\underline{\zeta}$ and b satisfies (H1), we proved

$$\Big|\big(\big[\Lambda^s, A[\underline{U}]\big]\partial_x U, Z[\underline{U}]\Lambda^s U\big)\Big| \leq \max(\epsilon,\beta)C\Big(\big\|\underline{U}\big\|_{X^s_T} + \big\|b\big\|_{H^{s+2}}\Big)|U|^2_{X^s}. \tag{2.34}$$

• *Estimate of* $\frac{1}{2}\big(\Lambda^s U, \big[\partial_t, Z[\underline{U}]\big]\Lambda^s U\big)$. One has

$$\begin{aligned}\big(\Lambda^s U, \big[\partial_t, Z[\underline{U}]\big]\Lambda^s U\big) \equiv&(\Lambda^s v, \Big[\partial_t, \underline{\mathfrak{T}}\Big]\Lambda^s v)\\ &+ (\Lambda^s \zeta, \Big[\partial_t, \frac{Q_0(\epsilon\underline{\zeta}, \beta b) + \epsilon^2 Q_1(\epsilon\underline{\zeta}, \beta b, \underline{v})}{f(\epsilon\underline{\zeta})}\Big]\Lambda^s \zeta)\\ =&\Big(\Lambda^s v, \big(\partial_t q_1(\epsilon\underline{\zeta}, \beta b)\big)\Lambda^s v\Big)\\ &- \mu\nu\Big(\Lambda^s v, \partial_x\big((\partial_t q_2(\epsilon\underline{\zeta}, \beta b))(\partial_x\Lambda^s v)\big)\Big)\\ &+ \Big(\Lambda^s\zeta, \partial_t\Big(\frac{Q_0(\epsilon\underline{\zeta}, \beta b) + \epsilon^2 Q_1(\epsilon\underline{\zeta}, \beta b, \underline{v})}{f(\epsilon\underline{\zeta})}\Big)\Lambda^s\zeta\Big)\\ =&\epsilon\kappa_1\Big(\Lambda^s v, (\partial_t\underline{\zeta})\Lambda^s v\Big) + \mu\nu\epsilon\kappa_2\Big(\Lambda^s\partial_x v, (\partial_t\underline{\zeta})\Lambda^s\partial_x v\Big)\\ &+ \Big(\Lambda^s\zeta, \partial_t\Big(\frac{Q_0(\epsilon\underline{\zeta}, \beta b) + \epsilon^2 Q_1(\epsilon\underline{\zeta}, \beta b, \underline{v})}{f(\epsilon\underline{\zeta})}\Big)\Lambda^s\zeta\Big).\end{aligned}$$

From Cauchy-Schwarz inequality and since $\underline{\zeta}$ and b satisfies (H1), one deduces

$$\begin{aligned}\Big|\ \frac{1}{2}\big(\Lambda^s U, \big[\partial_t, Z[\underline{U}]\big]\Lambda^s U\big)\ \Big| &\le \epsilon C(\big\|\partial_t\underline{U}\big\|_{L^\infty}, \big\|\underline{U}\big\|_{L^\infty})\big|U\big|_{X^s}^2\\ &\le\ \max(\epsilon,\beta)C(\big\|\partial_t\underline{U}\big\|_{L^\infty}, \big\|\underline{U}\big\|_{L^\infty})\big|U\big|_{X^s}^2.\end{aligned}$$

and continuous Sobolev embedding yields,

$$\Big|\ \frac{1}{2}\big(\Lambda^s U, \big[\partial_t, Z[\underline{U}]\big]\Lambda^s U\big)\ \Big| \le\ \max(\epsilon,\beta)C\big(\big\|\underline{U}\big\|_{X^s_T}\big)\big|U\big|_{X^s}^2. \tag{2.35}$$

We conclude now the proof of the X^s energy estimate. Plugging (2.32), (2.33), (2.34) and (2.35) into (2.31), and using the assumption on F given by the Lemma, one deduces

$$\frac{1}{2}\frac{d}{dt}E^s(U)^2\ \le\ \max(\epsilon,\beta)C_2E^s(U)^2 + E^s(U)\big(f(t) + \max(\epsilon,\beta)C_2\big),$$

with $C_2 = C(\big\|\underline{U}\big\|_{X^s_T}, \big\|b\big\|_{H^{s+2}}, C_F)$, and consequently

$$\frac{d}{dt}E^s(U)\ \le\ \max(\epsilon,\beta)C_2E^s(U) + \big(f(t) + \max(\epsilon,\beta)C_2\big).$$

For any $\lambda\in\mathbb{R}$, one has

$$e^{\max(\epsilon,\beta)\lambda t}\partial_t(e^{-\max(\epsilon,\beta)\lambda t}E^s(U)) = -\max(\epsilon,\beta)\lambda E^s(U) + \frac{d}{dt}E^s(U).$$

Thus with $\lambda = C_2$, one has for all $t\in[0, \frac{T}{\max(\epsilon,\beta)}]$,

$$\frac{d}{dt}(e^{-\max(\epsilon,\beta)\lambda t}E^s(U))\ \le\ \big(f(t) + \max(\epsilon,\beta)C_2\big)e^{-\max(\epsilon,\beta)\lambda t}.$$

Integrating this differential inequality yields,

$$E^s(U)(t) \le e^{\max(\epsilon,\beta)\lambda t}E^s(U_0) + \int_0^t e^{\max(\epsilon,\beta)\lambda(t-t')}\big(f(t') + \max(\epsilon,\beta)C_2\big)dt'.$$

□

2.5.3 Well-posedness of the linearized system

Proposition 9. *Let* $\mathsf{p} = (\mu, \epsilon, \delta, \gamma, \beta, \mathrm{bo}) \in \mathcal{P}_{\mathrm{CH}}$ *and* $s \geq s_0 + 1$ *with* $s_0 > 1/2$, *and let* $\underline{U} = (\underline{\zeta}, \underline{v})^\top \in X^s_T$, $b \in H^{s+2}$ *be such that* (H1),(H2), *and* (H3) *are satisfied for* $t \in [0, T/\max(\epsilon, \beta)]$, *uniformly with respect to* $\mathsf{p} \in \mathcal{P}_{\mathrm{CH}}$. *For any* $U_0 \in X^s$, *there exists a unique solution to* (2.19), $U^{\mathsf{p}} \in C^0([0, T/\max(\epsilon,\beta)]; X^s) \cap C^1([0, T/\max(\epsilon,\beta)]; X^{s-1}) \subset X^s_T$,
with $\lambda_T, C_0 = C(\|\underline{U}\|_{X^s_T}, T, M_{\mathrm{CH}}, h_{01}^{-1}, h_{02}^{-1}, h_{03}^{-1}, \|b\|_{H^{s+2}})$, *independent of* $\mathsf{p} \in \mathcal{P}_{\mathrm{CH}}$, *such that the following energy estimates holds*

$$\begin{aligned}
\forall\ 0 \leq t \leq \frac{T}{\max(\epsilon,\beta)}, \quad E^s(U^{\mathsf{p}})(t) \leq & e^{\max(\epsilon,\beta)\lambda_T t} E^s(U_0) \\
& + \max(\epsilon,\beta) C_0 \int_0^t e^{\max(\epsilon,\beta)\lambda_T (t-t')} dt' \\
\textit{and} \quad E^{s-1}(\partial_t U^{\mathsf{p}}) \leq & C_0 e^{\max(\epsilon,\beta)\lambda_T t} E^s(U_0) \\
& + \max(\epsilon,\beta) C_0^2 \int_0^t e^{\max(\epsilon,\beta)\lambda_T (t-t')} dt' + \max(\epsilon,\beta) C_0.
\end{aligned}$$

Proof. The well-posedness of the initial value problem (2.19) follows from energy estimates techniques, namely from the estimate (2.30) in Lemma 2.5.4 with $F = 0$:

$$E^s(U)(t) \leq e^{\max(\epsilon,\beta)\lambda_T t} E^s(U_0) + \max(\epsilon,\beta) C_0 \int_0^t e^{\max(\epsilon,\beta)\lambda_T (t-t')} dt', \tag{2.36}$$

An energy estimate on the time-derivative of the solution can be deduced using the system of equation (2.19). In fact, one has

$$\begin{aligned}
\big|\partial_t U\big|_{X^{s-1}} =& \big| - A[\underline{U}]\partial_x U - B[\underline{U}]\big|_{X^{s-1}} \\
\leq& \big|\epsilon f'(\epsilon\underline{\zeta})\underline{v}\partial_x\zeta + f(\epsilon\underline{\zeta})\partial_x v + \beta\partial_x b g(\epsilon\underline{\zeta})\underline{v}\big|_{H^{s-1}} \\
& + \big|\mathfrak{T}[\epsilon\underline{\zeta}, \beta b]^{-1}\Big(Q_0(\epsilon\underline{\zeta}, \beta b)\partial_x\zeta + \epsilon\mathfrak{Q}[\epsilon\underline{\zeta}, \beta b, \underline{v}]\partial_x v + \epsilon^2 Q_1(\epsilon\underline{\zeta}, \beta b, \underline{v})\partial_x\zeta \\
& + \epsilon\frac{\gamma\beta q_1(\epsilon\underline{\zeta}, \beta b) h_1(h_1+h_2)\underline{v}^2\partial_x b}{(h_1+\gamma h_2)^3}\Big) + \epsilon\varsigma\underline{v}\partial_x v\big|_{H^s_\mu} \\
\leq& C(|\underline{U}|_{X^s}, |b|_{H^{s+1}})|U|_{X^s} + \beta C_0 \\
\leq& C_0 E^s(U)(t) + \beta C_0 \\
\leq& C_0 e^{\max(\epsilon,\beta)\lambda_T t} E^s(U_0) \\
& + \max(\epsilon,\beta) C_0^2 \int_0^t e^{\max(\epsilon,\beta)\lambda_T (t-t')} dt' + \max(\epsilon,\beta) C_0.
\end{aligned} \tag{2.37}$$

To complete the proof we proceed by constructing a solution to (2.19). We use a sequence of Friedrichs mollifiers, defined by $J_\nu \equiv (1 - \nu\partial_x^2)^{-1/2}$ ($\nu > 0$) in order to reduce our system to ordinary differential equation systems on X^s, which are solved uniquely by Cauchy-Lipschitz theorem. Estimates (2.36),(2.37) hold for each $U_\nu \in C^0([0, T/\max(\epsilon,\beta)]; X^s)$, uniformly in $\nu > 0$. One deduces that a subsequence converges towards $U \in L^2([0, T/\max(\epsilon,\beta)]; X^s)$, a (weak) solution of the Cauchy problem (2.19). Taking a regular initial data, one can show that the solution $U \in C^0([0, T/\max(\epsilon,\beta)]; X^s) \cap C^1([0, T/\max(\epsilon,\beta)]; X^{s-1})$ is actually a strong solution. Applying the estimate (2.36) to the difference of two solutions having the same initial data (i.e $U_0 \equiv 0$) one can deduce the uniqueness. □

2.5.4 A priori estimate

In this section, we control the difference of two solutions of the nonlinear system, with different right-hand sides and initial data.

Proposition 10. *Let* $(\mu,\epsilon,\delta,\gamma,\beta,\mathrm{bo}) \in \mathcal{P}_{\mathrm{CH}}$ *and* $s \geq s_0+1$, $s_0 > 1/2$, *and assume that there exists* U_i *for* $i \in \{1,2\}$, *such that* $U_i = (\zeta_i, v_i)^\top \in X^s_T$, $U_2 \in L^\infty([0,T/\max(\epsilon,\beta)]; X^{s+1})$, $b \in H^{s+2}$, U_1 *satisfy* (H1),(H2) *and* (H3) *on* $[0,T/\max(\epsilon,\beta)]$, *with* $h_{01},h_{02},h_{03}>0$, *and* U_i *satisfy*

$$\begin{aligned} \partial_t U_1 \ + \ A[U_1]\partial_x U_1 \ + \ B[U_1] \ &= \ F_1 \ , \\ \partial_t U_2 \ + \ A[U_2]\partial_x U_2 \ + \ B[U_2] \ &= \ F_2 \ , \end{aligned}$$

with $F_i \in L^1([0,T/\max(\epsilon,\beta)]; X^s)$.

Then there exists constants:
$C_0 = C(M_{\mathrm{CH}}, h_{01}^{-1}, h_{02}^{-1}, h_{03}^{-1}, \max(\epsilon,\beta)\big|U_1\big|_{X^s}, \max(\epsilon,\beta)\big|U_2\big|_{X^s}, |b|_{H^{s+2}})$
and $\lambda_T = \big(C_0 \times C(|U_2|_{L^\infty([0,T/\max(\epsilon,\beta)];X^{s+1})}) + C_0\big)$ *such that for all* $t \in [0, \frac{T}{\max(\epsilon,\beta)}]$,

$$\begin{aligned} E^s(U_1-U_2)(t) \leq & e^{\max(\epsilon,\beta)\lambda_T t} E^s(U_1\,|_{t=0} - U_2\,|_{t=0}) \\ & + C_0 \int_0^t e^{\max(\epsilon,\beta)\lambda_T (t-t')} E^s(F_1-F_2)(t')dt'. \end{aligned}$$

Proof. We multiply on the left by $Z[U_i]$ the equations satisfied by U_i, one obtains

$$\begin{aligned} Z[U_1]\partial_t U_1 + \Sigma[U_1]\partial_x U_1 + Z[U_1]B[U_1] \ &= \ Z[U_1]F_1 \\ Z[U_2]\partial_t U_2 + \Sigma[U_2]\partial_x U_2 + Z[U_2]B[U_2] \ &= \ Z[U_2]F_2; \end{aligned}$$

with $\Sigma[U] = Z[U]A[U]$. When we subtract the above equations, and after defining a new variable V as $V = U_1 - U_2 \equiv (\zeta, v)^\top$ one obtains

$$\begin{aligned} Z[U_1]\partial_t V + \Sigma[U_1]\partial_x V + (Z[U_1]B[U_1] - Z[U_2]B[U_2]) \\ = Z[U_1](F_1-F_2) - (\Sigma[U_1]-\Sigma[U_2])\partial_x U_2 \\ -(Z[U_1]-Z[U_2])(\partial_t U_2 - F_2). \end{aligned}$$

Applying $Z^{-1}[U_1]$ to the above equation, one deduces the following system:

$$\begin{cases} \partial_t V + A[U_1]\partial_x V + Z^{-1}[U_1]\big(Z[U_1]B[U_1] - Z[U_2]B[U_2]\big) = F \\ V(0) = (U_1-U_2)\,|_{t=0}\ , \end{cases} \tag{2.38}$$

$$\begin{aligned} \text{where,} \quad F \equiv & F_1 - F_2 - Z^{-1}[U_1]\big(\Sigma[U_1]-\Sigma[U_2]\big)\partial_x U_2 \\ & - Z^{-1}[U_1]\big(Z[U_1]-Z[U_2]\big)(\partial_t U_2 - F_2). \end{aligned} \tag{2.39}$$

We would like to use the energy estimate given in Lemma 2.5.4 to the linear system (2.38).

The additional term now is $Z^{-1}[U_1]\big(Z[U_1]B[U_1] - Z[U_2]B[U_2]\big)$.

So we have to control,

$$\big(\Lambda^s Z^{-1}[U_1]\big(Z[U_1]B[U_1] - Z[U_2]B[U_2]\big), Z[U_1]\Lambda^s V\big) = B.$$

One has,

$$\begin{aligned} B =&\big(\Lambda^s\big(Z[U_1]B[U_1]-Z[U_2]B[U_2]\big),\Lambda^s V\big)\\ &+\big(\big[\Lambda^s,Z^{-1}[U_1]\big]Z[U_1]B[U_1]-Z[U_2]B[U_2],Z[U_1]\Lambda^s V\big)\\ =&B_1+B_2 \end{aligned}$$

Now we have to estimate the terms (B_1) and (B_2).

$$\begin{aligned} B_1 = \Big(\Lambda^s\big(\frac{-Q(\epsilon\zeta_1,\beta b,v_1)\beta\partial_x bg(\epsilon\zeta_1)v_1}{f(\epsilon\zeta_1)}+\frac{Q(\epsilon\zeta_2,\beta b,v_2)\beta\partial_x bg(\epsilon\zeta_2)v_2}{f(\epsilon\zeta_2)}\big),\Lambda^s\zeta_v\Big)\\ +\Big(\Lambda^s\big(\frac{\epsilon\gamma\beta q_1(\epsilon\zeta_1,\beta b)h_1(h_1+h_2)v_1^2\partial_x b}{(h_1+\gamma h_2)^3}-\frac{\epsilon\gamma\beta q_1(\epsilon\zeta_2,\beta b)h_1(h_1+h_2)v_2^2\partial_x b}{(h_1+\gamma h_2)^3}\big),\Lambda^s v\Big) \end{aligned}$$

With $Q(\epsilon\zeta_i,\beta b,v_i)=Q_0(\epsilon\zeta_i,\beta b)+\epsilon^2Q_1(\epsilon\zeta_i,\beta b,v_i)$ for $i=1,2$.

In order to control (B_1) we use the following decompositions,

- $$\begin{aligned} &\Big(\frac{-Q_0(\epsilon\zeta_1,\beta b)\beta\partial_x bg(\epsilon\zeta_1)v_1}{f(\epsilon\zeta_1)}+\frac{Q_0(\epsilon\zeta_2,\beta b)\beta\partial_x bg(\epsilon\zeta_2)v_2}{f(\epsilon\zeta_2)}\Big)\\ &\qquad=\Big(\frac{-Q_0(\epsilon\zeta_1,\beta b)g(\epsilon\zeta_1)}{f(\epsilon\zeta_1)}+\frac{Q_0(\epsilon\zeta_2,\beta b)g(\epsilon\zeta_2)}{f(\epsilon\zeta_2)}\Big)(\beta\partial_x bv_1)\\ &\qquad\qquad-\beta(v_1-v_2)\frac{Q_0(\epsilon\zeta_2,\beta b)g(\epsilon\zeta_2)\partial_x b}{f(\epsilon\zeta_2)}. \end{aligned}$$

- $$\begin{aligned} &\beta\Big(\frac{-\epsilon^2Q_1(\epsilon\zeta_1,\beta b,v_1)\partial_x bg(\epsilon\zeta_1)v_1}{f(\epsilon\zeta_1)}+\frac{\epsilon^2Q_1(\epsilon\zeta_2,\beta b,v_2)\partial_x bg(\epsilon\zeta_2)v_2}{f(\epsilon\zeta_2)}\Big)\\ &\qquad=\Big(\frac{-\epsilon^2Q_1(\epsilon\zeta_1,\beta b,v_1)g(\epsilon\zeta_1)}{f(\epsilon\zeta_1)}+\frac{\epsilon^2Q_1(\epsilon\zeta_2,\beta b,v_2)g(\epsilon\zeta_2)}{f(\epsilon\zeta_2)}\Big)(\beta\partial_x bv_1)\\ &\qquad\qquad-\beta(v_1-v_2)\frac{\epsilon^2Q_1(\epsilon\zeta_2,\beta b,v_2)g(\epsilon\zeta_2)\partial_x b}{f(\epsilon\zeta_2)}. \end{aligned}$$

- $$\begin{aligned} &\Big(\frac{\epsilon\gamma\beta q_1(\epsilon\zeta_1,\beta b)h_1(h_1+h_2)v_1^2\partial_x b}{(h_1+\gamma h_2)^3}-\frac{\epsilon\gamma\beta q_1(\epsilon\zeta_2,\beta b)h_1(h_1+h_2)v_2^2\partial_x b}{(h_1+\gamma h_2)^3}\Big)\\ &\qquad=\Big(\frac{\epsilon v_1\gamma q_1(\epsilon\zeta_1,\beta b)h_1(h_1+h_2)}{(h_1+\gamma h_2)^3}-\frac{\epsilon v_1\gamma q_1(\epsilon\zeta_2,\beta b)h_1(h_1+h_2)}{(h_1+\gamma h_2)^3}\Big)(\beta\partial_x bv_1)\\ &\qquad\qquad+\Big(\frac{\epsilon\gamma q_1(\epsilon\zeta_2,\beta b)h_1(h_1+h_2)\partial_x b}{(h_1+\gamma h_2)^3}\Big)\beta(v_1^2-v_2^2). \end{aligned}$$

Using the fact that, $\epsilon^2Q_1(\epsilon\zeta_i,\beta b,v_i)=Q_1(\epsilon\zeta_i,\beta b,\epsilon v_i)$, one deduces,

$$
\begin{aligned}
|B_1| \leq & C(\beta|v_1|_{H^s}, |b|_{H^{s+2}})\epsilon|\zeta_1-\zeta_2|_{H^s}|\zeta_v|_{H^s} \\
& + C(\epsilon|\zeta_2|_{H^s}, |b|_{H^{s+2}})\beta|v_1-v_2|_{H^s}|\zeta_v|_{H^s} \\
& + C(\beta|v_1|_{H^s}, |b|_{H^{s+1}})\epsilon|\zeta_1-\zeta_2|_{H^s}|\zeta_v|_{H^s} \\
& + C(\epsilon|\zeta_2|_{H^s}, \epsilon|v_2|_{H^s}, |b|_{H^{s+1}})\beta|v_1-v_2|_{H^s}|\zeta_v|_{H^s} \\
& + C(\beta|v_1|_{H^s}, \epsilon|v_1|_{H^s}, |b|_{H^{s+1}})\epsilon|\zeta_1-\zeta_2|_{H^s}|v|_{H^s} \\
& + C(\epsilon|\zeta_2|_{H^s}, \epsilon|v_1|_{H^s}, \epsilon|v_2|_{H^s}, |b|_{H^{s+1}})\beta|v_1-v_2|_{H^s}|v|_{H^s} \\
\leq & \max(\epsilon,\beta)C_0E^s(U_1-U_2)E^s(V) \\
\leq & \max(\epsilon,\beta)C_0E^s(V)^2.
\end{aligned}
$$

with $C_0 = C(M_{\mathrm{CH}}, h^{-1}, h_{03}^{-1}, \max(\epsilon,\beta)\big|U_1\big|_{X^s}, \max(\epsilon,\beta)\big|U_2\big|_{X^s}, |b|_{H^{s+2}})$.

The contribution of (B_2) is immediately bounded using Lemma 2.5.2:

$$
\begin{aligned}
|B_2| = & \big(\ \big[\Lambda^s, Z^{-1}[U_1]\big]\big(Z[U_1]B[U_1]-Z[U_2]B[U_2]\big) \ , \ Z[U_1]\Lambda^s V \ \big) \\
\leq & C|Z[U_1]B[U_1]-Z[U_2]B[U_2]|_{H^{s-1}\times H^{s-1}}|V|_{X^s} \\
\leq & C\Big(\Big|\frac{-Q(\epsilon\zeta_1,\beta b,v_1)\beta\partial_x bg(\epsilon\zeta_1)v_1}{f(\epsilon\zeta_1)} + \frac{Q(\epsilon\zeta_2,\beta b,v_2)\beta\partial_x bg(\epsilon\zeta_2)v_2}{f(\epsilon\zeta_2)}\Big|_{H^{s-1}} \\
& + \Big|\epsilon\gamma\beta\partial_x b\Big(\frac{q_1(\epsilon\zeta_1,\beta b)h_1(h_1+h_2)v_1^2}{(h_1+\gamma h_2)^3} - \frac{q_1(\epsilon\zeta_2,\beta b)h_1(h_1+h_2)v_2^2}{(h_1+\gamma h_2)^3}\Big)\Big|_{H^{s-1}}\Big)|V|_{X^s} \\
\leq & \max(\epsilon,\beta)C_0E^s(U_1-U_2)E^s(V) \\
\leq & \max(\epsilon,\beta)C_0E^s(V)^2.
\end{aligned}
$$

So we have,

$$|B| \leq C_0 \max(\epsilon,\beta)E^s(V)^2.$$

Now one needs to control accordingly the right hand side F.

To this end, we introduce the following Lemma.

Lemma 2.5.5. *Let $(\mu,\epsilon,\delta,\gamma,\beta,\mathrm{bo}) \in \mathcal{P}_{\mathrm{CH}}$ and $s \geq s_0 > 1/2$. Let $V = (\zeta_v, v)^\top$, $W = (\zeta_w, w)^\top \in X^s$ and $U_1 = (\zeta_1, v_1)^\top$, $U_2 = (\zeta_2, v_2)^\top \in X^s$, $b \in H^{s+2}$ such that there exists $h > 0$ with*

$$1-\epsilon\zeta_1 \geq h > 0, \quad 1-\epsilon\zeta_2 \geq h > 0, \quad \frac{1}{\delta}+\epsilon\zeta_1-\beta b \geq h > 0, \quad \frac{1}{\delta}+\epsilon\zeta_2-\beta b \geq h > 0.$$

Then one has

$$
\begin{aligned}
\Big|\ \Big(\ \Lambda^s\big(Z[U_1]-Z[U_2]\big)V \ , \ W\ \Big)\ \Big| \quad &\leq \quad \epsilon\ C\ \big|U_1-U_2\big|_{X^s}\big|V\big|_{X^s}\big|W\big|_{X^0} \\
\Big(\ \Lambda^s\big(Z[U_1]A[U_1]-Z[U_2]A[U_2]\big)V \ , \ W\ \Big) \quad &\leq \quad \epsilon\ C\ \big|U_1-U_2\big|_{X^s}\big|V\big|_{X^s}\big|W\big|_{X^0}
\end{aligned}
$$

with $C = C(M_{\mathrm{CH}}, h^{-1}, \epsilon\big|U_1\big|_{X^s}, \epsilon\big|U_2\big|_{X^s}, |b|_{H^{s+2}})$.

Proof. We prove the Lemma 5.40 using the same techniques as in the Proof of [49, Lemma 7.2], adapted to our pseudo-symmetrizer as $\epsilon^2 Q_1(\epsilon\zeta_i, \beta b, v_i) = Q_1(\epsilon\zeta_i, \beta b, \epsilon v_i)$. □

Proceeding in the proof of Proposition 10, we estimate F defined in (2.39), and therefore we would like to estimate the following

$$\begin{aligned}\big(\ \Lambda^s F\ ,\ Z[U_1]\Lambda^s V\ \big) =&\big(\ \Lambda^s F_1 - \Lambda^s F_2\ ,\ Z[U_1]\Lambda^s V\big)\\ &-\big(\ \Lambda^s(\Sigma[U_1]-\Sigma[U_2])\partial_x U_2\ ,\ \Lambda^s V\big)\\ &-\big(\ \big[\Lambda^s, Z^{-1}[U_1]\big](\Sigma[U_1]-\Sigma[U_2])\partial_x U_2\ ,\ Z[U_1]\Lambda^s V\big)\\ &-\big(\ \Lambda^s\big(Z[U_1]-Z[U_2]\big)(\partial_t U_2 - F_2)\ ,\ \Lambda^s V\big)\\ &-\big(\ \big[\Lambda^s, Z^{-1}[U_1]\big](Z[U_1]-Z[U_2])(\partial_t U_2 - F_2)\ ,\ Z[U_1]\Lambda^s V\big)\\ =&(I)+(II)+(III)+(IV)+(V).\end{aligned}$$

The contribution of (I) is immediately bounded using Lemma 5.13. The contributions of (II) and (IV) follow Lemma 5.40. Finally, we control (III) and (V) using Lemma 5.13 (2.23). All together, we proved using Lemma 5.12 that F as defined in (2.39), satisfies

$$\begin{aligned}|(\Lambda^s F, Z[U_1]\Lambda^s V)| \leq&\epsilon C\times(|\partial_x U_2|_{X^s}+|\partial_t U_2 - F_2|_{X^s})E^s(V)^2 + CE^s(V)E^s(F_1-F_2)\\ \leq&\max(\epsilon,\beta)C\times(|\partial_x U_2|_{X^s}+|\partial_t U_2 - F_2|_{X^s})E^s(V)^2\\ &+CE^s(V)E^s(F_1-F_2).\end{aligned}$$

with $C = C(M_{\mathrm{CH}}, h^{-1}, h_{03}^{-1}, \epsilon\big|U_1\big|_{X^s}, \epsilon\big|U_2\big|_{X^s}, |b|_{H^{s+2}})$.

Then one has

$$\begin{aligned}|(\Lambda^s F, Z[U_1]\Lambda^s V)| \leq&\max(\epsilon,\beta)C_0\times(|\partial_x U_2|_{X^s}+|\partial_t U_2 - F_2|_{X^s})E^s(V)^2\\ &+C_0E^s(V)E^s(F_1-F_2).\end{aligned}$$

We can now conclude by Lemma 2.5.4, and the proof of Proposition 10 is complete. □

2.6 Full justification of the asymptotic model

Following the terminology of [84]), the full justification of an asymptotic model consist in proving the well-posedness of the Cauchy problem for both the full Euler system and the asymptotic model and in proving that their solutions with similar initial data remain close. We conclude our work by fully justifying our model.

Theorem 2.6.1 (Existence and uniqueness)**.** *Let* $\mathsf{p} = (\mu, \epsilon, \delta, \gamma, \beta, \mathrm{bo}) \in \mathcal{P}_{\mathrm{CH}}$ *and* $s \geq s_0 + 1$, $s_0 > 1/2$, *and assume* $U_0 = (\zeta_0, v_0)^\top \in X^s$, $b \in H^{s+2}$ *satisfies* (H1),(H2), *and* (H3). *Then there exists a maximal time* $T_{\max} > 0$, *uniformly bounded from below with respect to* $\mathsf{p} \in \mathcal{P}_{\mathrm{CH}}$, *such that the system of equations* (2.16) *admits a unique strong solution* $U = (\zeta, v)^\top \in C^0([0, T_{\max}); X^s) \cap C^1([0, T_{\max}); X^{s-1})$ *with the initial value* $(\zeta, v)\,|_{t=0} = (\zeta_0, v_0)$, *and preserving the conditions* (H1),(H2) *and* (H3) *(with different lower bounds) for any* $t \in [0, T_{\max})$.

Moreover, there exists $\lambda, C_0 = C(h_{01}^{-1}, h_{02}^{-1}, h_{03}^{-1}, M_{\mathrm{CH}}, T, \big|U_0\big|_{X^s}, |b|_{H^{s+2}})$, *independent of* $\mathsf{p} \in \mathcal{P}_{\mathrm{CH}}$, *such that* $T_{\max} \geq T/\max(\epsilon,\beta)$, *and one has the energy estimates*

$$\forall\ 0 \leq t \leq \tfrac{T}{\max(\epsilon,\beta)},$$

$$\begin{aligned}\big|U(t,\cdot)\big|_{X^s}\ +\ \big|\partial_t U(t,\cdot)\big|_{X^{s-1}} \leq&C_0 e^{\max(\epsilon,\beta)\lambda t}\\ &+\max(\epsilon,\beta)C_0^2\int_0^t e^{\max(\epsilon,\beta)\lambda(t-t')}dt' + \max(\epsilon,\beta)C_0\end{aligned}$$

If $T_{\max} < \infty$*, one has*

$$|U(t,\cdot)|_{X^s} \longrightarrow \infty \quad as \quad t \longrightarrow T_{\max},$$

or one of the conditions (H1),(H2), (H3) *ceases to be true as* $t \longrightarrow T_{\max}$.

Proof. Let $(U^n = (\zeta^n, v^n))_{n\geq 0}$ a sequence of approximate solution of the following linear system

$$U^0 = U_0, \quad \text{and} \quad \forall n \in \mathbb{N}, \quad \begin{cases} \partial_t U^{n+1} + A[U^n]\partial_x U^{n+1} + B[U^n] = 0; \\ U^{n+1}_{|t=0} = U_0. \end{cases} \tag{2.40}$$

By Proposition 9, there exists
$U^{n+1} \in C^0([0, \frac{T_{n+1}}{\max(\epsilon,\beta)}]; X^s) \cap C^1([0, \frac{T_{n+1}}{\max(\epsilon,\beta)}]; X^{s-1})$ unique solution to (2.40) if $U^n \in C^0([0, \frac{T_n}{\max(\epsilon,\beta)}]; X^s) \cap C^1([0, \frac{T_n}{\max(\epsilon,\beta)}]; X^{s-1}) \subset X^s_T$, and satisfies (H1),(H2) and (H3).

Let us continue by proving the existence and the control of U^n. In the following we prove by induction the existence of $T' > 0$ such that the sequence U^n is uniquely defined, controlled in $X^s_{T'}$, and satisfies (H1),(H2) and (H3), uniformly with respect to $n \in \mathbb{N}$.

Proposition 9 yields

$$E^s(U^{n+1})(t) \leq e^{\max(\epsilon,\beta)\lambda_n t} E^s(U_0) + \max(\epsilon,\beta) C_n \int_0^t e^{\max(\epsilon,\beta)\lambda_n (t-t')} dt'.$$

$$\begin{aligned} \left|\partial_t U^{n+1}(t,\cdot)\right|_{X^{s-1}} \leq & C_n E^s(U^{n+1})(t) + \max(\epsilon,\beta) C_n \\ \leq & C_n e^{\max(\epsilon,\beta)\lambda_n t} E^s(U_0) + \max(\epsilon,\beta) C_n^2 \int_0^t e^{\max(\epsilon,\beta)\lambda_n (t-t')} dt' \\ & + \max(\epsilon,\beta) C_n, \end{aligned}$$

with $C_n, \lambda_n = C(M_{\mathrm{CH}}, h_{01,n}^{-1}, h_{02,n}^{-1}, T_n, \left\|U^n\right\|_{X^s_{T_n}}, |b|_{H^{s+2}})$, provided $U^n \in X^s_{T_n}$ satisfies (H1),(H2) and (H3) with positive constants $h_{01,n}, h_{02,n}$, and $h_{03,n}$ on $[0, T_n/\max(\epsilon,\beta)]$.

As a consequence of the work [49, Theorem 7.3] and by taking into account the topographic variation, we impose the assumptions (H1) and (H2) only on the initial data and then we show that they are automatically satisfied over the time scale. We omit the proof here and only detail the proof for the new assumption (H3),

Since $U^n = (\zeta^n, v^n)^\top$ satisfies (2.40), one has

$$\partial_t \zeta^{n+1} = -f(\epsilon\zeta^n)\partial_x v^{n+1} - \epsilon f'(\epsilon\zeta^n) v^n \partial_x \zeta^{n+1} + \beta \partial_x b g(\epsilon\zeta^n) v^n,$$

and

$$\begin{aligned} \partial_t v^{n+1} = & -\mathfrak{T}[\epsilon\zeta^n, \beta b]^{-1} \Big(Q_0(\epsilon\zeta^n, \beta b)\partial_x \zeta^{n+1} + \epsilon \mathfrak{Q}[\epsilon\zeta^n, \beta b, v^n]\partial_x v^{n+1} \\ & + \epsilon^2 Q_1(\epsilon\zeta^n, \beta b, v^n)\partial_x \zeta^{n+1} + \epsilon \frac{\gamma\beta q_1(\epsilon\zeta^n, \beta b) h_1(h_1+h_2) {v^n}^2 \partial_x b}{(h_1+\gamma h_2)^3} \Big) \\ & - \epsilon\varsigma v^n \partial_x v^{n+1}. \end{aligned}$$

Using the embedding of H^{s-1} into L^∞ ($s-1>1/2$), and since U^n satisfies (H1),(H2) with $h_{01,n}, h_{02,n}$ on $[0, T_n/\max(\epsilon,\beta)]$, one deduces that

$$|\partial_t \zeta^{n+1}|_{L^\infty} \leq C(M_{\mathrm{CH}}, h_{01,n}^{-1}, h_{02,n}^{-1}, \beta|b|_{H^s})\left\|U^n\right\|_{X^s_{T_n}}, \tag{2.41}$$

and

$$|\partial_t v^{n+1}|_{L^\infty} \leq C(M_{\mathrm{CH}}, h_{01,n}^{-1}, h_{02,n}^{-1}, \beta|b|_{H^{s+1}})\left\|U^n\right\|_{X^s_{T_n}}. \tag{2.42}$$

Let $g^{n+1} = a_1(\epsilon\zeta^{n+1}, \beta b) + a_2(\epsilon\zeta^{n+1}, \beta b)\epsilon^2 (v^{n+1})^2$, where

$$\begin{aligned} a_1(\epsilon\zeta^{n+1}, \beta b) &= (\gamma+\delta) q_1(\epsilon\zeta^{n+1}, \beta b) - \mu\beta\omega\partial_x^2 b, \\ a_2(\epsilon\zeta^{n+1}, \beta b) &= -\gamma q_1(\epsilon\zeta^{n+1}, \beta b)\frac{(h_1+h_2)^2}{(h_1+\gamma h_2)^3}. \end{aligned}$$

One has,

$$\begin{aligned} g^{n+1} =& g^{n+1}\,|_{t=0} + \int_0^t \partial_t a_1(\epsilon\zeta^{n+1}, \beta b) + \epsilon^2 \int_0^t \partial_t a_2(\epsilon\zeta^{n+1}, \beta b)(v^{n+1})^2 \\ &+ 2\epsilon^2 \int_0^t a_2(\epsilon\zeta^{n+1}, \beta b) v^{n+1}\partial_t v^{n+1} \\ =& g^{n+1}\,|_{t=0} + (\gamma+\delta)\epsilon\kappa_1 \int_0^t \partial_t \zeta^{n+1} + \epsilon^3 \int_0^t a_2'(\epsilon\zeta^{n+1}, \beta b)\partial_t\zeta^{n+1}(v^{n+1})^2 \\ &+ 2\epsilon^2 \int_0^t a_2(\epsilon\zeta^{n+1}, \beta b) v^{n+1}\partial_t v^{n+1} \end{aligned}$$

so that (2.41) and (2.42) yields

$$\left|g^{n+1} - g^{n+1}\,|_{t=0}\,\right|_{L^\infty} \leq \epsilon t \times C(M_{\mathrm{CH}}, h_{01,n}^{-1}, h_{02,n}^{-1}, |b|_{H^{s+2}})\left\|U^n\right\|_{X^s_{T_n}}.$$

Now, one has $g^{n+1}\,|_{t=0} \equiv g^0\,|_{t=0} \geq h_{03,0} > 0$, independent of n. By induction one can easily prove that we can chose $T' > 0$ such that $g^{n+1} > \dfrac{h_{03}}{2}$ holds on $[0, T'/\max(\epsilon,\beta)]$, and the above energy estimates remain satisfied uniformly with respect to n, on $[0, T'/\max(\epsilon,\beta)]$.

More precisely, one has that U^n satisfies (H3) with $\dfrac{h_{03}}{2} > 0$ and the estimates

$$\begin{aligned} E^s(U^n)(t) &\leq e^{\max(\epsilon,\beta)\lambda t} E^s(U_0) + \max(\epsilon,\beta) C_0 \int_0^t e^{\max(\epsilon,\beta)\lambda(t-t')} dt' \\ \left|\partial_t U^n(t,\cdot)\right|_{X^{s-1}} &\leq C_0 E^s(U^n)(t) + \max(\epsilon,\beta) C_0 \\ &\leq C_0 e^{\max(\epsilon,\beta)\lambda t} E^s(U_0) \\ &\quad + \max(\epsilon,\beta) C_0^2 \int_0^t e^{\max(\epsilon,\beta)\lambda(t-t')} dt' + \max(\epsilon,\beta) C_0. \end{aligned}$$

on $[0, T'/\max(\epsilon,\beta)]$, where $C_0, \lambda = C(M_{\mathrm{CH}}, h_{01}^{-1}, h_{02}^{-1}, h_{03}^{-1}, T', \left|U_0\right|_{X^s}, |b|_{H^{s+2}})$ are uniform with respect to n.

For the completion of the proof, one has to prove the convergence of U^n to a solution of the non-linear problem we use the same techniques as in the proof of [49, Theorem 7.3](see e.g. [1]). The uniqueness of U follows from the priori estimate result of Proposition 10 with $F_1 \equiv F_2 \equiv 0$. □

Theorem 2.6.2 (Stability). *Let* $\mathsf{p} = (\mu, \epsilon, \delta, \gamma, \beta, \mathrm{bo}) \in \mathcal{P}_{\mathrm{CH}}$ *and* $s \geq s_0 + 1$ *with* $s_0 > 1/2$*, and assume* $U_{1,0} = (\zeta_{1,0}, v_{1,0})^\top \in X^s$*,* $U_{2,0} = (\zeta_{2,0}, v_{2,0})^\top \in X^{s+1}$*, and* $b \in H^{s+2}$ *satisfies* (H1),(H2)*, and* (H3)*. Denote* U_j *the solution to* (2.16) *with* $U_j \,|_{t=0} = U_{j,0}$*.*
Then there exists $T, \lambda, C_0 = C(M_{\mathrm{CH}}, h_{01}^{-1}, h_{02}^{-1}, h_{03}^{-1}, \big|U_{1,0}\big|_{X^s}, |U_{2,0}|_{X^{s+1}}, |b|_{H^{s+2}})$ *such that* $\forall t \in [0, \frac{T}{\max(\epsilon,\beta)}]$*,*

$$\big|(U_1 - U_2)(t,\cdot)\big|_{X^s} \leq C_0 e^{\max(\epsilon,\beta)\lambda t} \big|U_{1,0} - U_{2,0}\big|_{X^s}.$$

Proof. Thanks to Theorem 2.6.1, one can prove the existence of the solution U_1 (resp. U_2) in $L^\infty([0, T/\max(\epsilon,\beta)]; X^s)$ (resp. $L^\infty([0, T/\max(\epsilon,\beta)]; X^{s+1})$), as well as their uniform control. As a consequence of the priori estimate of Proposition 10, with $F_1 = F_2 = 0$, and Lemma 2.5.1 we complete the proof. □

Finally, we conclude by a "convergence result" stating that the solutions of our system and the ones of the full Euler system, reamin close.

Theorem 2.6.3 (Convergence). *Let* $\mathsf{p} = (\mu, \epsilon, \delta, \gamma, \beta, \mathrm{bo}) \in \mathcal{P}_{\mathrm{CH}}$*(see* (2.2)*) and* $s \geq s_0 + 1$ *with* $s_0 > 1/2$*, and let* $U^0 \equiv (\zeta^0, \psi^0)^\top \in H^{s+N}(\mathbb{R})^2$*,* $b \in H^{s+N}$ *satisfy the hypotheses* (H1),(H2)*, and* (H3)*, with* N *sufficiently large. We suppose* $U \equiv (\zeta, \psi)^\top$ *a unique solution to the full Euler system* (2.3) *with initial data* $(\zeta^0, \psi^0)^\top$*, defined on* $[0, T_1]$ *for* $T_1 > 0$ [1]*, and we suppose that* $U \equiv (\zeta, \psi)^\top$ *satisfies the assumptions of our consistency result, Proposition 8. Then there exists* $C, T > 0$*, independent of* p*, such that*

- *There exists a unique solution* $U_a \equiv (\zeta_a, v_a)^\top$ *to our new model* (2.16)*, defined on* $[0, T]$ *and with initial data* $(\zeta^0, v^0)^\top$ *(provided by Theorem 2.6.1);*
- *With* v*, defined as in* (2.7)*, one has for any* $t \in [0, T]$*,*

$$\big|(\zeta, v) - (\zeta_a, v_a)\big|_{L^\infty([0,t];X^s)} \leq C\ \mu^2\ t.$$

Proof. Thank to Theorem 2.6.1 one can prove the existence of U_a solution to the asymptotic model (where T is chosen as the minimum of the existence time of both solutions). Assuming that $U \equiv (\zeta, \psi)^\top$ satisfies the assumptions of our consistency result, Proposition 8, therefore $(\zeta, v)^\top$ solves (2.16) up to a residual $R = (r_1, r_2)^\top$, with $\big|R\big|_{L^\infty([0,T];H^s)} \leq C(M_{\mathrm{SW}}, h_{01}^{-1}, |b|_{H^{s+N}}, \big|U^0\big|_{H^{s+N}})(\mu^2 + \mu\epsilon^2 + \mu\beta^2 + \mu\epsilon\beta)$. As a matter of fact, since $\mathsf{p} \in \mathcal{P}_{\mathrm{CH}}$ therefore the residual is now bounded by μ^2. The result follows from the stability Proposition 10, with $F_1 = (r_1, \mathfrak{T}[\epsilon\zeta]^{-1} r_2)^\top$ and $F_2 = 0$. □

1. To our knowledge, the local well-posedness of the full Euler system in the two-fluid configuration over a variable topography seems to be an open problem.

Chapitre 3

Coupled and scalar asymptotic models for internal waves over variable topography

The Green-Naghdi type model in the Camassa-Holm regime derived in [*Comm. Pure Appl. Anal.*, 14(6):2203–2230, 2015]/Chapter 2, for the description of medium amplitude internal waves at the interface of two layers of immiscible fluids of different densities and taking into account medium amplitude topography variations is fully justified by a convergence result. In this chapter, we generalize this result by constructing a fully justified coupled asymptotic model in a more complex physical case of variable topography. In addition, our system permit the full justification of other model of lower order provided that it is consistent and well-posed. We apply the procedure to scalar models driven by simple unidirectional equations in the Camassa-Holm and long wave regimes and under some restrictions on the topography variations. We also show that, wave breaking of solutions to such equations, occurs in the Camassa-Holm regime with slow topography variations and for a specific set of parameters.

3.1 Introduction

The oceans are not a solitary, uniform waterway. In fact, they really comprise a number of specific water masses described by different densities because of variations in temperature, saltiness, and pressure. Indeed, ocean water get to be stratified, one regularly watches the limit between colder, saltier water beneath and hotter, less-salty water above. Internal waves might be produced by stratified tidal streams over base topographic components. It is thought that such waves play a key role in Earth's climate, ocean ecosystems, circulation and pollutant dispersal.

This chapter treat the internal waves issue for uneven bottoms which involve the description of the movement of the interface between two layers of immiscible liquids of various densities, and also the velocity flow inside the two layers of liquid, under the accompanying assumptions: the liquid is homogeneous, perfect, incompressible, irrotational and under the main impact of gravity. The domain of the two layers is endless in the flat unidimensional space variable. The bottom on which both fluids rest is presumed to be non-flat while the top is limited by the rigid lid assumption. The governing equations of such a system are called the "*full Euler system*", we briefly recall the system in section 2.1 below, and refer to [6, 16, 47, 48] for more details. The

mathematical study of this system is extremely complicated as the interface boundary is part of the unknowns and since the system is strongly nonlinear. Very often, additional smallness assumptions are made on some given dimensionless parameters that describe the nature of the flow and the regime under consideration in order to obtain simpler asymptotic models.

Prior works have set a good theoretical environment for this issue and various models for a bi-fluid system have already been derived and studied in the flat bottom case see [97, 93, 31, 32, 16, 65] and references therein. Recently, Duchêne, Israwi and Talhouk derived in [49], a new Green-Naghdi type model, under the rigid lid assumption, with a flat bottom and in the so-called Camassa-Holm regime, that is to say, making use of an additional smallness assumption on the deformation of the interface between the two layers of fluids, $\epsilon = \mathcal{O}(\sqrt{\mu})$. In addition to its full justification, the authors proved that their model permit the full justification of other lower order model provided that it is consistent and well-posed. They applied this strategy to the Constantin-Lannes approximation [47]. The case of uneven bottoms has been less explored. Some of the noteworthy references dealing with non-flat topography are [103, 6, 44, 7, 48], where many bi-fluidic models that allows a non-flat topography are derived and justified by a consistency result. However, the preceding works do not provide the full justification, contrarily to [90] where the result of full justification obtained in [49], have been improved recently in [90] taking into account medium amplitude topography variations.

In all the previously stated works, the subsequent model consists in two relatively simple evolution equations coupling the shear speed and the interface deformation. However, if one chooses precisely the initial perturbation so as the flow moves in a single direction, then the flow can be approximated as a solution of a scalar evolution equation. This means in a physical way, that we pay particular attention on a given direction of the two counter-propagating waves after they have split. This strategy has been developed in [14] in order to fully justify the famous Korteweg-de Vries equation (see [81]) that describes the propagation of long surface waves ($\epsilon = \mathcal{O}(\mu)$) and the extension of this result to the two-layers system has been done by Duchêne in [46]. Constantin and Lannes, introduced and fully justified higher order models in [34], for the water-wave problem in the Camassa-Holm regime ($\epsilon = \mathcal{O}(\sqrt{\mu})$), (see [47] for the internal wave problem). Let us note that the Camassa-Holm regime is more interesting than the long wave regime, since it allows larger amplitude waves and yields models that can create singularities in limited time as wave breaking [34]. However, all these results only hold for flat bottoms. For the situation of an uneven bottom, various generalizations of the KdV equation in the context of propagation of surface gravity waves have been derived and justified in [71], using the same scaling as in [34] but under appropriate conditions on the topographical variations.

In this chapter, we generalize the result of full justification obtained in [49] and [90] to a more complex case of variable topography. To this end, we introduce two new parameters β and α, where β characterize the shape of the bottom and α is the ratio of the interface wave-length to the bottom wave-length. Moreover we assume that $\beta\alpha = \mathcal{O}(\sqrt{\mu})$ which can correspond to a physical case of a slowly varying bottom with large amplitude. We construct a new model that possesses a pleasant structure similar to symmetrizable quasilinear systems that allows to study the properties, in particular energy estimates, for the linearized system, thus allowing its full justification, following the classical theory of hyperbolic systems. Additional key restrictions on the deformation of the bottom are needed to ensure the validity of our model, see (3.10) and (H0). Moreover, our new model allows to fully justify other well-posed models. In fact, proving the

consistency of any well-posed model with our new model ensure its convergence to the full Euler system. We try to apply this procedure to other unidirectional models. Using a strategy initiated in [34], we construct in this chapter, an approximate solution to the Green-Naghdi system, driven by a simple unidirectional scalar equation for the propagation of internal waves over variable topography. First, we study our unidirectional approximation in the Camassa-Holm regime. In fact, we show that, families of solutions of the unidirectional approximation satisfy the Green-Naghdi system under appropriate conditions on the topography variations, up to a small residual. Our second result regarding this scalar evolution equation, concerns the long time well-posedness of the Cauchy problem; we also show that wave breaking of the solution occurs in the Camassa-Holm regime for some particular conditions on the parameters and under slow topography variations. Finally, a full justification result is given after making stronger assumptions on the topography. In addition, we recover and fully justify the unidirectional approximation designated as the KdV equation in the more restrictive long wave scaling.

Outline of the chapter We start by the introduction of the non-dimensionalized full Euler system and the Green-Naghdi model in Section 2. We derive in Section 3 the new coupled asymptotic model. Section 4 contains some preliminary results. Section 5 contains the "linearized" system. In Section 6, we explain the full justification of asymptotic models and we state its main ingredients. In Section 7, we derive an approximate solution to the Green-Naghdi driven by a simple unidirectional scalar equation. Section 8 is dedicated to the mathematical analysis of the unidirectional approximation in the Camassa-Holm regime, where we study its accuracy in Section 8.1, prove its well-posedness in Section 8.2 and give the explosion conditions in Section 8.3. We give a full justification result in Section 8.4. Finally, we give a full justification result for the unidirectional approximation in the long wave regime in Section 9.

Notations. In what follows, C_0 denotes any positive constant whose accurate expression is of no significance. The notation $A = \mathcal{O}(B)$ signify that $A \leq C_0\ B$.
$C(\lambda_1, \lambda_2, \dots)$ indicate a positive constant depending on the parameters λ_1, λ_2,... such that the dependence on the λ_j is non-decreasing.
$L^p = L^p(\mathbb{R})$ $(1 \leq p < \infty)$ is the space of Lebesgue-measurable functions f with the standard norm $|f|_{L^p} = \big(\int_{\mathbb{R}} |f(x)|^p dx\big)^{1/p} < \infty$.

$(u, v) = \int_{\mathbb{R}} u(x)v(x)dx$ denotes the real inner product of any functions u and v in the Hilbert space $L^2(\mathbb{R})$.

$L^\infty = L^\infty(\mathbb{R})$ is the space of all essentially bounded, Lebesgue-measurable functions f with the norm $|f|_{L^\infty} = \operatorname{ess\,sup}_{x\in\mathbb{R}} |f(x)| < \infty$.

For $k \in \mathbb{N}$, we denote by $W^{k,\infty} = W^{k,\infty}(\mathbb{R}) = \{f \in L^\infty, |f|_{W^{k,\infty}} < \infty\}$, where $|f|_{W^{k,\infty}} = \sum_{\alpha\in\mathbb{N},\alpha\leq k} |\partial_x^\alpha f|_{L^\infty}$.
$H^s = H^s(\mathbb{R})$ $(s \geq 0)$ denotes the Sobolev space with the norm $|f|_{H^s} = |\Lambda^s f|_{L^2} < \infty$, where Λ is the following operator $\Lambda = (1 - \partial_x^2)^{1/2}$.

$L^\infty([0,T); H^s(\mathbb{R}))$ denotes the space of functions such that $u(t,\cdot)$ is bounded in H^s, uniformly with respect to $t \in [0,T)$: $\big\|u\big\|_{L^\infty([0,T);H^s(\mathbb{R}))} = \operatorname*{ess\,sup}_{t\in[0,T)} |u(t,\cdot)|_{H^s} < \infty$.

$C^k([0,T);H^s(\mathbb{R}))$ denotes the space of k-times continuously differentiable functions u with values in $H^s(\mathbb{R})$ with the norm, $\|u\|_{C^k([0,T);H^s(\mathbb{R}))} = \max\limits_{0\leq i\leq k}\sup\limits_{t\in[0,T)}|\partial_x^i u(t,\cdot)|_{H^s} < \infty$.

The commutator $[T,f]$ is defined by $[T,f]g = T(fg) - fT(g)$ with T a closed operator defined on a Banach space and f, g and fg belongs to $D(T)$ (domain of T).

3.2 Green-Naghdi system

In this section, we first briefly recall the so-called *"full Euler system"* (3.2), governing the evolution of the deformation of the interface and the trace of a velocity potential at the interface and refer to [6, 16, 47] for more details.

In the shallow-water scaling ($\mu \ll 1$), one can derive the Green-Naghdi model after replacing the Dirichlet-to-Neumann operators by their truncated expansion with respect to the shallowness parameter, μ. This asymptotic model is justified by a consistency result, that is to say the solutions of the full Euler system satisfy the Green-Naghdi asymptotic model up to a small remainder, of size $\mathcal{O}(\mu^2)$.

3.2.1 Full Euler system

We review that the framework comprises two layers of immiscible, homogeneous, perfect, incompressible liquids just affected by gravity, (see Figure 3.1). We confine ourselves to the bi-dimensional case, *i.e.* the horizontal dimension $d = 1$.

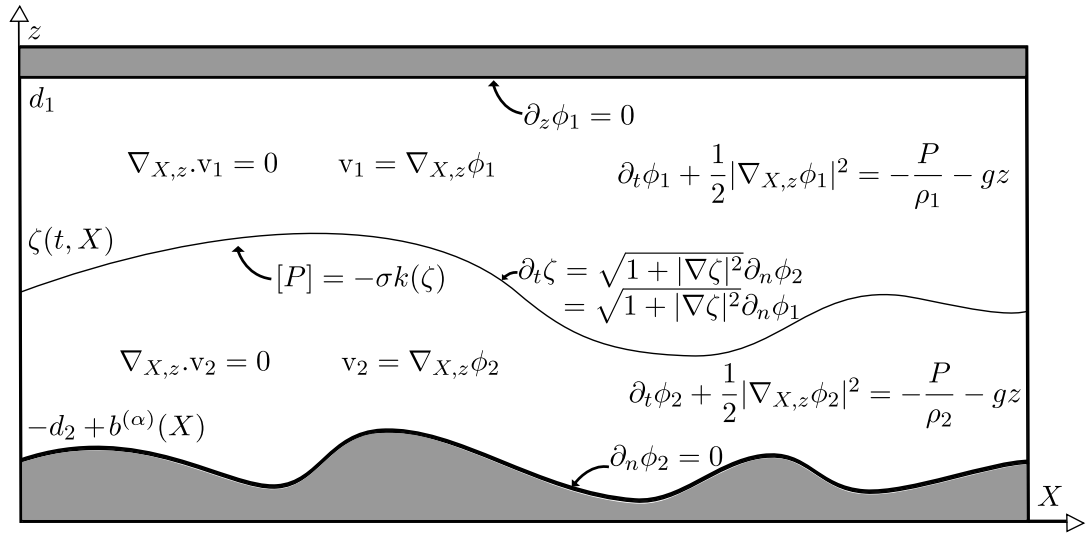

Figure 3.1. Governing equations and domain of the study

The study of the asymptotic dynamics is made accessible by the nondimensionalization of the equations [1]. To this end we introduce dimensionless variables and unknowns that reduce the

1. The adapted re-scaling is motivated by the study of the linearized system (3.2) around the rest state $(\zeta,\psi) = (0,0)$ and over a flat topography done in [83].

setting to the physical regime under consideration:

$$\tilde{z} \equiv \frac{z}{d_1}, \qquad \tilde{X} \equiv \frac{X}{\lambda}, \qquad \tilde{t} \equiv \frac{c_0}{\lambda}t,$$

and

$$\tilde{\zeta}(\tilde{t},\tilde{X}) \equiv \frac{\zeta(t,X)}{a}, \quad \tilde{b}(\alpha\tilde{X}) \equiv \frac{b(X)}{a_b}, \quad \tilde{\phi}_i(\tilde{t},\tilde{X},\tilde{z}) \equiv \frac{d_1}{a\lambda c_0}\phi_i(t,X,z) \quad (i=1,2),$$

where the typical internal wave velocity is given by

$$c_0 = \sqrt{g\frac{(\rho_2-\rho_1)d_1d_2}{\rho_2 d_1+\rho_1 d_2}}.$$

Now we introduce the following dimensionless parameters

$$\mu \equiv \frac{d_1^2}{\lambda^2}, \quad \epsilon \equiv \frac{a}{d_1}, \quad \beta \equiv \frac{a_b}{d_1}, \quad \delta \equiv \frac{d_1}{d_2}, \quad \gamma = \frac{\rho_1}{\rho_2}, \quad \mathrm{Bo} = \frac{\mathrm{g}(\rho_2-\rho_1)\lambda^2}{\sigma}, \tag{3.1}$$

where a (resp. a_b) is the maximal amplitude of the defotmation at the interface (resp. bottom); λ is the wavelength of the interface; λ/α is the wave-length of the bottom variations; d_1 (resp. d_2) is the deepness of the upper (resp. lower) fluid; and ρ_1 (resp. ρ_2) is the density of the upper (resp. lower) layer, g the gravitational acceleration, σ the interfacial tension coefficient and Bo *the classical Bond number*, measuring the ratio of gravity forces over surface tension forces.
In the following we use $\mathrm{bo} = \mu\mathrm{Bo} = \dfrac{\mathrm{g}(\rho_2-\rho_1)\mathrm{d}_1^2}{\sigma}$ instead of *the standard Bond number*, Bo. The parameter ϵ is often called non linearity parameter while μ is the shallowness parameter.

The equations governing the evolution of the aforedescribed system in the introduction read (using non-dimensionalized variables and the Zakharov/Craig-Sulem formulation) [39, 115]:

$$\begin{cases} \partial_t\zeta - \dfrac{1}{\mu}G^\mu\psi = 0, \\ \partial_t\Big(H^{\mu,\delta}\psi - \gamma\partial_x\psi\Big) + (\gamma+\delta)\partial_x\zeta + \dfrac{\epsilon}{2}\partial_x\Big(|H^{\mu,\delta}\psi|^2 - \gamma|\partial_x\psi|^2\Big) \\ \qquad\qquad = \mu\epsilon\partial_x\mathcal{N}^{\mu,\delta} - \mu\frac{\gamma+\delta}{\mathrm{bo}}\frac{\partial_x\Big(k(\epsilon\sqrt{\mu}\zeta)\Big)}{\epsilon\sqrt{\mu}}, \end{cases} \tag{3.2}$$

where we denote

$$\mathcal{N}^{\mu,\delta} \equiv \frac{\big(\frac{1}{\mu}G^\mu\psi + \epsilon(\partial_x\zeta)H^{\mu,\delta}\psi\big)^2 - \gamma\big(\frac{1}{\mu}G^\mu\psi + \epsilon(\partial_x\zeta)(\partial_x\psi)\big)^2}{2(1+\mu|\epsilon\partial_x\zeta|^2)}.$$

$\zeta(t,x)$ represents the deformation of the interface between the two layers and $b^{(\alpha)}(x) = b(\alpha x)$ represents the deformation of the bottom, ψ is the trace of the velocity potential of the upper-fluid at the interface.

The function $k(\zeta) = -\partial_x\Big(\frac{1}{\sqrt{1+|\partial_x\zeta|^2}}\partial_x\zeta\Big)$ denotes interface curvature and σ the surface (or interfacial) tension coefficient.

System (3.2) will be referred as the *full Euler system*, and its solutions will be exact solutions of the problem.

Finally, we define the so-called Dirichlet-Neumann operators G^μ and $H^{\mu,\delta}$ as follows:

Definition 3.2.1 (Dirichlet-Neumann operators)**.** Let $\zeta, b \in H^{t_0+1}(\mathbb{R})$, $t_0 > 1/2$, such that there exists $h_0 > 0$ with $h_1 \equiv 1 - \epsilon\zeta \geq h_0 > 0$ and $h_2 \equiv \frac{1}{\delta} + \epsilon\zeta - \beta b^{(\alpha)} \geq h_0 > 0$, and let $\psi \in L^2_{\rm loc}(\mathbb{R})$, $\partial_x\psi \in H^{1/2}(\mathbb{R})$. Then we define

$$\begin{aligned} G^\mu\psi &\equiv G^\mu[\epsilon\zeta]\psi \equiv \sqrt{1+\mu|\epsilon\partial_x\zeta|^2}\big(\partial_n\phi_1\big)\,|_{z=\epsilon\zeta} = -\mu\epsilon(\partial_x\zeta)(\partial_x\phi_1)\,|_{z=\epsilon\zeta} + (\partial_z\phi_1)\,|_{z=\epsilon\zeta}\,, \\ H^{\mu,\delta}\psi &\equiv H^{\mu,\delta}[\epsilon\zeta,\beta b^{(\alpha)}]\psi \equiv \partial_x\big(\phi_2\,|_{z=\epsilon\zeta}\,\big) = (\partial_x\phi_2)\,|_{z=\epsilon\zeta} + \epsilon(\partial_x\zeta)(\partial_z\phi_2)\,|_{z=\epsilon\zeta}\,, \end{aligned}$$

where ϕ_1 and ϕ_2 are uniquely defined (up to a constant for ϕ_2) as the solutions in $H^2(\mathbb{R})$ of the Laplace's problems:

$$\left\{\begin{array}{ll} \big(\,\mu\partial_x^2 \,+\, \partial_z^2\,\big)\;\phi_1 = 0 & \text{in } \Omega_1 \equiv \{(x,z)\in\mathbb{R}^2,\ \epsilon\zeta(x) < z < 1\}, \\ \partial_z\phi_1 = 0 & \text{on } \Gamma_{\rm t} \equiv \{(x,z)\in\mathbb{R}^2,\ z = 1\}, \\ \phi_1 = \psi & \text{on } \Gamma \equiv \{(x,z)\in\mathbb{R}^2,\ z = \epsilon\zeta\}, \end{array}\right. \tag{3.3}$$

$$\left\{\begin{array}{ll} \big(\,\mu\partial_x^2 \,+\, \partial_z^2\,\big)\;\phi_2 = 0 & \text{in } \Omega_2 \equiv \{(x,z)\in\mathbb{R}^2,\ -\frac{1}{\delta} + \beta b^{(\alpha)}(x) < z < \epsilon\zeta\}, \\ \partial_n\phi_2 = \partial_n\phi_1 & \text{on } \Gamma, \\ \partial_n\phi_2 = 0 & \text{on } \Gamma_{\rm b} \equiv \{(x,z)\in\mathbb{R}^2,\ z = -\frac{1}{\delta} + \beta b^{(\alpha)}(x)\}. \end{array}\right. \tag{3.4}$$

The well-posedness of (3.3)-(3.4) and of the Dirichlet-Neumann operators are detailed in [84].. We let the reader check [48, Section 2] for more details on the construction of the system.

3.2.2 Green-Naghdi model

In this section, we develop the asymptotic Green-Naghdi model with accuracy $\mathcal{O}(\mu^2)$. Our construction is based on replacing the Dirichlet-to-Neumann operators by their asymptotic expansions, with respect to the shallowness parameter, μ, (see [44, 48]). Following [31, 32], we choose to write the equations using the *shear layer-mean velocity* as unknown, which is equivalently defined as

$$v \equiv \frac{1}{h_2(t,x)}\int_{-\frac{1}{\delta}+\beta b^{(\alpha)}(x)}^{\epsilon\zeta(t,x)} \partial_x\phi_2(t,x,z)\;dz - \frac{\gamma}{h_1(t,x)}\int_{\epsilon\zeta(t,x)}^{1}\partial_x\phi_1(t,x,z)\;dz. \tag{3.5}$$

As discussed in [47], two main advantages follow the use of such a choice. First, the equation describing the interface evolution is an exact equation, and not a $\mathcal{O}(\mu^2)$ approximation. In fact, as shown in [47] one has that

$$\frac{1}{\mu}G^\mu\psi = -\partial_x\Big(\frac{h_1h_2}{h_1+\gamma h_2}v\Big).$$

This choice yields also to a much better behavior concerning the linear well-posedness. For the unidimensional case and over uneven bottoms these equations couple the deformation of the interface ζ to the *shear mean velocity* v, and can be written as:

$$\left\{\begin{array}{l} \partial_t\zeta \;+\; \partial_x\Big(\dfrac{h_1h_2}{h_1+\gamma h_2}v\Big) \;=\; 0, \\[2ex] \partial_t\Big(v \;+\; \mu\overline{\mathcal{Q}}[h_1,h_2]v\Big) \;+\; (\gamma+\delta)\partial_x\zeta \;+\; \dfrac{\epsilon}{2}\partial_x\Big(\dfrac{h_1^2-\gamma h_2^2}{(h_1+\gamma h_2)^2}v^2\Big) \;= \\[2ex] \qquad\qquad \mu\epsilon\partial_x\big(\overline{\mathcal{R}}[h_1,h_2]v\big) + \mu\dfrac{\gamma+\delta}{\rm bo}\partial_x^3\zeta, \end{array}\right. \tag{3.6}$$

where we denote $h_1 = 1 - \epsilon\zeta$ and $h_2 = \delta^{-1} + \epsilon\zeta - \beta b^{(\alpha)}$, as well as

$$\begin{aligned}
\overline{\mathcal{Q}}[h_1,h_2]v &= \mathcal{T}[h_2,\beta b^{(\alpha)}]\Big(\frac{h_1 v}{h_1+\gamma h_2}\Big) - \gamma\mathcal{T}[h_1,0]\Big(\frac{-h_2 v}{h_1+\gamma h_2}\Big),\\
&= -\frac{1}{3h_2}\partial_x\Big(h_2^3\partial_x\big(\frac{h_1 v}{h_1+\gamma h_2}\big)\Big)\\
&\quad + \frac{1}{2h_2}\beta\alpha\Big[\partial_x\Big(h_2^2(\partial_x b)^{(\alpha)}\frac{h_1 v}{h_1+\gamma h_2}\Big) - h_2^2(\partial_x b)^{(\alpha)}\partial_x\big(\frac{h_1 v}{h_1+\gamma h_2}\big)\Big]\\
&\quad + \alpha^2\beta^2((\partial_x b)^{(\alpha)})^2\big(\frac{h_1 v}{h_1+\gamma h_2}\big) - \gamma\Big[\frac{1}{3h_1}\partial_x\Big(h_1^3\partial_x\big(\frac{h_2 v}{h_1+\gamma h_2}\big)\Big)\Big], \qquad (3.7)
\end{aligned}$$

$$\begin{aligned}
\overline{\mathcal{R}}[h_1,h_2]v &= \frac{1}{2}\Big(-h_2\partial_x\big(\frac{h_1 v}{h_1+\gamma h_2}\big) + \beta\alpha(\partial_x b)^{(\alpha)}\big(\frac{h_1 v}{h_1+\gamma h_2}\big)\Big)^2 - \frac{\gamma}{2}\Big(h_1\partial_x\big(\frac{-h_2 v}{h_1+\gamma h_2}\big)\Big)^2\\
&\quad - \big(\frac{h_1 v}{h_1+\gamma h_2}\big)\mathcal{T}[h_2,\beta b^{(\alpha)}]\Big(\frac{h_1 v}{h_1+\gamma h_2}\Big) + \gamma\big(\frac{-h_2 v}{h_1+\gamma h_2}\big)\mathcal{T}[h_1,0]\Big(\frac{-h_2 v}{h_1+\gamma h_2}\Big) \qquad (3.8)
\end{aligned}$$

with,

$$\mathcal{T}[h,b^{(\alpha)}]V \equiv \frac{-1}{3h}\partial_x(h^3\partial_x V) + \alpha\frac{1}{2h}[\partial_x(h^2(\partial_x b)^{(\alpha)}V) - h^2(\partial_x b)^{(\alpha)}(\partial_x V)] + \alpha^2((\partial_x b)^{(\alpha)})^2 V.$$

Remark 2. We would like to mention that the well posedness result for the original Green-Naghdi model (3.6), has been proved in [50, Section 5] in the flat bottom case with an adaptive change of variable. Their strategy is similar to the one used for the full Euler system with surface tension by Lannes [83]. The main tool of the analysis is the control of a space-time energy.

In what follows, we restrict our study to the following set of dimensionless parameters:

$$\begin{aligned}
\mathcal{P} \equiv \Big\{\mathsf{p} = (\mu,\epsilon,\delta,\gamma,\beta,\alpha,\mathrm{bo}) :\ & 0 < \mu \le \mu_{\max},\ 0 \le \epsilon \le 1,\ \delta \in (\delta_{\min},\delta_{\max}),\\
& 0 \le \gamma < 1,\ 0 \le \beta \le \beta_{\max},\ 0 \le \alpha \le \alpha_{\max},\ \mathrm{bo}_{\min} \le \mathrm{bo} \le \infty\Big\}, \qquad (3.9)
\end{aligned}$$

with given $0 \le \mu_{\max}, \delta_{\min}^{-1}, \delta_{\max}, \mathrm{bo}_{\min}^{-1}, \beta_{\max}, \alpha_{\max} < \infty$.

We close this section by stating the first rigorous justification of the two-layers Green-Naghdi model by a consistency result. Let us define exactly what we assign by consistency throughout this chapter.

Definition 3.2.2. We say that $(\zeta^{\mathsf{p}}, v^{\mathsf{p}})_{\mathsf{p}\in\mathcal{P}}$ is L^∞-consistent (resp. H^s-consistent of order $s \ge 0$) on $[0,T]$ with the Green-Naghdi system (3.6) at precision $\mathcal{O}(\mu^2)$, if for all $\mathsf{p} \in \mathcal{P}$, $(\zeta^{\mathsf{p}}, v^{\mathsf{p}})$ satisfies, for μ^2 sufficiently small,

$$\begin{cases}
\partial_t\zeta^{\mathsf{p}} + \partial_x\Big(\dfrac{h_1 h_2}{h_1+\gamma h_2}v^{\mathsf{p}}\Big) = \mu^2 r_1,\\[2ex]
\partial_t\Big(v^{\mathsf{p}} + \mu\overline{\mathcal{Q}}[h_1,h_2]v^{\mathsf{p}}\Big) + (\gamma+\delta)\partial_x\zeta^{\mathsf{p}} + \dfrac{\epsilon}{2}\partial_x\Big(\dfrac{h_1^2-\gamma h_2^2}{(h_1+\gamma h_2)^2}(v^{\mathsf{p}})^2\Big)\\
\qquad\qquad -\mu\epsilon\partial_x\big(\overline{\mathcal{R}}[h_1,h_2]v^{\mathsf{p}}\big) - \mu\dfrac{\gamma+\delta}{\mathrm{bo}}\partial_x^3\zeta^{\mathsf{p}} = \mu^2 r_2,
\end{cases}$$

where $h_1 = 1 - \epsilon\zeta^{\mathsf{p}}$ and $h_2 = \delta^{-1} + \epsilon\zeta^{\mathsf{p}} - \beta b^{(\alpha)}$ and with (r_1, r_2) bounded in $L^\infty([0,T]\times\mathbb{R})^2$ (resp. in $L^\infty([0,T], H^s(\mathbb{R}))^2$.

Remark 3. Since $H^s(\mathbb{R})$ is continuously embedded in $L^\infty(\mathbb{R})$ when $s > 1/2$, the H^s-consistency implies the L^∞-consistency. The notion of H^s-consistency is stronger then the notion of L^∞-consistency and allows a full justification of the asymptotic models.

Proposition 11 (Consistency)**.** *For $\mathsf{p} \in \mathcal{P}$, let $U^{\mathsf{p}} = (\zeta^{\mathsf{p}}, \psi^{\mathsf{p}})^\top$ be a family of solutions of the full Euler system (3.2) such that there exists $T > 0$, $s \geq s_0 + 1$, $s_0 > 1/2$ for which $(\zeta^{\mathsf{p}}, \partial_x\psi^{\mathsf{p}})^\top$ is bounded in $L^\infty([0,T); H^{s+N})^2$ with sufficiently large N, and uniformly with respect to $\mathsf{p} \in \mathcal{P}$. Moreover assume that $b \in H^{s+N}$ and there exists $h_{01} > 0$ such that*

$$h_1 = 1 - \epsilon\zeta^{\mathsf{p}} \geq h_{01} > 0, \quad h_2 = 1/\delta + \epsilon\zeta^{\mathsf{p}} - \beta b^{(\alpha)} \geq h_{01} > 0. \tag{H1}$$

Define v^{p} as in (3.5). Then $(\zeta^{\mathsf{p}}, v^{\mathsf{p}})$ is H^s-consistent with (3.6), on $[0,T]$ with precision $\mathcal{O}(\mu^2)$.

Proof. The proof of this proposition is obtained as in the proof of [48, Proposition 3.14]. We omit it here. □

3.3 Construction of the new coupled model

In the following section, we construct a new asymptotic model that shares the same order of precision as the standard one under some restrictions on the set of parameters $\mathsf{p} \in \mathcal{P}$, but have a mathematical structure more suitable for the study of its well-posedness. To this end, we use additional assumptions on the deformation of the interface and the deformation of the bottom. The assumptions are as follows:

$$\epsilon = \mathcal{O}(\sqrt{\mu}) \quad \text{and} \quad \beta\alpha = \mathcal{O}(\sqrt{\mu}). \tag{3.10}$$

The following expansions formally hold:

$$\frac{h_1}{h_1 + \gamma h_2} = \frac{\delta}{\gamma + \delta - \gamma\delta\beta b^{(\alpha)}}\Big(1 - \epsilon\zeta + \frac{\epsilon\zeta\delta(1-\gamma)}{\gamma + \delta - \gamma\delta\beta b^{(\alpha)}} + \mathcal{O}(\epsilon^2)\Big),$$

$$\frac{h_2}{h_1 + \gamma h_2} = \frac{\delta}{\gamma + \delta - \gamma\delta\beta b^{(\alpha)}}\Big(\delta^{-1} + \epsilon\zeta - \beta b^{(\alpha)} + \frac{(1 - \delta\beta b^{(\alpha)})\epsilon\zeta(1-\gamma)}{\gamma + \delta - \gamma\delta\beta b^{(\alpha)}} + \mathcal{O}(\epsilon^2)\Big).$$

Plugging these expansions into $\overline{\mathcal{Q}}[h_1, h_2]v$ and $\overline{\mathcal{R}}[h_1, h_2]v$, one can check the following:

$$\begin{aligned}
\overline{\mathcal{Q}}[h_1, h_2]v &= -d\partial_x^2 v \\
&+ \epsilon\left(\eta\ v\partial_x^2\zeta + \big(2\eta + (\gamma-1)g\big)\ \partial_x\zeta\partial_x v + \big(\eta + \frac{2}{3}(\gamma-1)g\big)\ \zeta\partial_x^2 v\right) \\
&+ \beta\left(\eta_1\ \alpha^2(\partial_x^2 b)^{(\alpha)} v + 2\eta_1\ \alpha(\partial_x b)^{(\alpha)}\partial_x v + \big(\frac{\gamma}{3}f + \frac{2}{3}\delta^{-1}f\big)\ b^{(\alpha)}\partial_x^2 v\right) \\
&+ \beta^2\left(\frac{2\gamma}{3}f'\ b^{(\alpha)}\alpha(\partial_x b)^{(\alpha)}\partial_x v - \frac{1}{3}f\ {b^{(\alpha)}}^2\partial_x^2 v\right) \\
&+ \mathcal{O}(\epsilon^2, \epsilon\beta\alpha, \beta^2\alpha^2),
\end{aligned}$$

$$\overline{\mathcal{R}}[h_1, h_2]v = (1-\gamma)g^2\left(\frac{1}{2}(\partial_x v)^2 + \frac{1}{3}v\partial_x^2 v\right) + \mathcal{O}(\epsilon, \beta\alpha),$$

with

$$d = d(\beta b^{(\alpha)}) = \frac{1+\gamma\delta}{3\delta(\gamma+\delta-\gamma\delta\beta b^{(\alpha)})}, \qquad f = f(\beta b^{(\alpha)}) = \frac{\delta}{(\gamma+\delta-\gamma\delta\beta b^{(\alpha)})}, \tag{3.11}$$

$$f' = f'(\beta b^{(\alpha)}) = \frac{\gamma\delta^2}{(\gamma+\delta-\gamma\delta\beta b^{(\alpha)})^2}, \qquad g = g(\beta b^{(\alpha)}) = \frac{1-\delta\beta b^{(\alpha)}}{(\gamma+\delta-\gamma\delta\beta b^{(\alpha)})} \tag{3.12}$$

$$\eta = \eta(\beta b^{(\alpha)}) = \frac{1}{3}(\delta^{-1}-\beta b^{(\alpha)})^2 f - \frac{1}{3}(\delta^{-1}-\beta b^{(\alpha)})^2(1-\gamma)f^2 - \frac{\gamma}{3}f - \frac{\gamma}{3}fg(1-\gamma), \tag{3.13}$$

$$\eta_1 = \eta_1(\beta b^{(\alpha)}) = -\frac{1}{3}(\delta^{-1}-\beta b^{(\alpha)})^2 f' + \frac{(\delta^{-1}-\beta b^{(\alpha)})}{2}f - \frac{\gamma}{3}\delta^{-1}f' + \frac{\gamma}{3}f, \tag{3.14}$$

Actually, thanks to the non-zero depth condition (H1) that we assume, one has $h_1 + h_2 > 0$, which is equivalent to say that $\beta b^{(\alpha)} < 1 + 1/\delta$. Since $\gamma < 1$, one has $\beta b^{(\alpha)} < \dfrac{\gamma+\delta}{\gamma\delta}$, so one can deduce that the above functions are well defined under the non-zero depth condition.

Plugging the expansions of $\overline{\mathcal{Q}}[h_1,h_2]v$ and $\overline{\mathcal{R}}[h_1,h_2]v$ into system (3.6) yields a streamlined model, with the same order of accuracy of the original model (that is $\mathcal{O}(\mu^2)$). We will use yet a few extra changes, keeping in mind that the end goal is to create an equivalent model (again, in the sense of consistency), which has a structure like symmetrizable quasilinear systems.

Firstly, we introduce the following second-order differential operator,

$$\mathfrak{T}[\epsilon\zeta,\beta b^{(\alpha)}]V \;=\; q_1 V \;-\; \mu\partial_x\Big(\nu q_2\partial_x V\Big), \tag{3.15}$$

where $q_1 \equiv 1+\epsilon\kappa_1(\beta b^{(\alpha)})\zeta+\omega_1(\beta b^{(\alpha)})$ and $q_2 \equiv 1+\epsilon\kappa_2(\beta b^{(\alpha)})\zeta+\omega_2(\beta b^{(\alpha)})$ and $\nu,\kappa_1,\kappa_2,\omega_1,\omega_2$ are functions of $\beta b^{(\alpha)}$ to be determined (here and for the rest of the chapter, we omit the dependence on $\beta b^{(\alpha)}$ for the sake of readability) so as to write,

$$\begin{aligned}
\mathfrak{T}[\epsilon\zeta,\beta b]\partial_t v \;-\; q_1\partial_t\Big(v \;+\; \mu\overline{\mathcal{Q}}[h_1,h_2]v\Big) + q_1\mu\frac{\gamma+\delta}{\mathrm{bo}}\partial_x^3\zeta \\
= -\mu\partial_x\nu\partial_x\partial_t v - \mu\nu\partial_x^2\partial_t v - \mu\partial_x(\nu\epsilon\kappa_2\zeta\partial_x\partial_t v) - \mu\partial_x(\nu\omega_2\partial_x\partial_t v) \\
- \mu\partial_t\overline{\mathcal{Q}}[h_1,h_2]v - \mu\epsilon\kappa_1\zeta\partial_t\overline{\mathcal{Q}}[h_1,h_2]v - \mu\omega_1\partial_t\overline{\mathcal{Q}}[h_1,h_2]v \\
+ \mu\frac{\gamma+\delta}{\mathrm{bo}}\partial_x^3\zeta + \mu\epsilon\kappa_1\zeta\frac{\gamma+\delta}{\mathrm{bo}}\partial_x^3\zeta + \mu\omega_1\frac{\gamma+\delta}{\mathrm{bo}}\partial_x^3\zeta + \mathcal{O}(\mu^2,\mu\epsilon^2,\mu\epsilon\beta\alpha,\mu\beta^2\alpha^2).
\end{aligned} \tag{3.16}$$

In order to cancel the first order ($\mu\partial_x^2\partial_t v$) terms, one has to choose properly ν, making use of the fact that the second equation of system (3.6) yields

$$\partial_t v = -(\gamma+\delta)\partial_x\zeta \;-\; \frac{\epsilon}{2}(f^2-\gamma g^2)\partial_x\Big(|v|^2\Big) + \mathcal{O}(\epsilon^2,\epsilon\beta\alpha,\mu).$$

Indeed, it follows that

$$\mu\frac{\gamma+\delta}{\mathrm{bo}}\partial_x^3\zeta \;=\; \frac{-\mu}{\mathrm{bo}}\partial_x^2\partial_t v - \frac{\mu\epsilon}{2\mathrm{bo}}(f^2-\gamma g^2)\partial_x^3\Big(|v|^2\Big) + \mathcal{O}(\mu\epsilon^2,\mu\epsilon\beta\alpha,\mu^2).$$

After replacing the term $\mu\frac{\gamma+\delta}{\mathrm{bo}}\partial_x^3\zeta$ of the equation (3.16) by its expression given above and taking the identification of $\partial_t\overline{\mathcal{Q}}[h_1,h_2]v$ using (3.7), thus one defines

$$\nu \;=\; \nu(\beta b^{(\alpha)}) \;=\; d - \frac{1}{\mathrm{bo}}. \tag{3.17}$$

Using again that (3.6) yields $\partial_t v = -(\gamma+\delta)\partial_x\zeta \ + \mathcal{O}(\epsilon,\mu)$ and $\partial_t\zeta = -g\partial_x v + \mathcal{O}(\epsilon,\beta\alpha,\mu)$, we adjust $\kappa_1,\kappa_2,\omega_1,\omega_2$ in order to withdraw all terms containing ζ and its higher order derivatives. More specifically we set,

$$\kappa_2 \ = \ \kappa_2(\beta b^{(\alpha)}) \ = \ \frac{-\big(3\eta+(\gamma-1)g\big)(1+\omega_1)}{\nu}, \tag{3.18}$$

so that $\partial_x\zeta\partial_x^2\zeta$ terms are withdrawn.

In order to deal with the $\zeta\partial_x^3\zeta$ terms we set κ_1 so that,

$$\nu\kappa_2 + (1+\omega_1)\big(\eta+\frac{2}{3}(\gamma-1)g\big) - \nu\kappa_1 + \beta b^{(\alpha)}\kappa_1\big(\frac{\gamma}{3}f+\frac{2}{3}\delta^{-1}f\big) - \beta^2 {b^{(\alpha)}}^2\kappa_1\frac{f}{3} = 0$$

Using (3.18), one defines

$$\kappa_1 \ = \ \kappa_1(\beta b^{(\alpha)}) \ = \ \frac{\big(-2\eta-\frac{(\gamma-1)}{3}g\big)\big(1+\omega_1\big)}{\nu-\beta b^{(\alpha)}\big(\frac{\gamma}{3}f+\frac{2}{3}\delta^{-1}f\big)+\frac{\beta^2{b^{(\alpha)}}^2}{3}f}, \tag{3.19}$$

In order to deal with the $\partial_x^3\zeta$ terms, ω_1 is determined as follows,

$$\omega_1 \ = \ \omega_1(\beta b^{(\alpha)}) \ = \ \frac{\nu\omega_2+\beta b^{(\alpha)}\big(\frac{\gamma}{3}f+\frac{2}{3}\delta^{-1}f\big)-\frac{\beta^2{b^{(\alpha)}}^2}{3}f}{\nu-\beta b^{(\alpha)}\big(\frac{\gamma}{3}f+\frac{2}{3}\delta^{-1}f\big)+\frac{\beta^2{b^{(\alpha)}}^2}{3}f}, \tag{3.20}$$

The $(\partial_x b)^{(\alpha)}\partial_x^2\zeta$ terms may be canceled with the proper choice of ω_2 solution of the following first order linear differential equation.

$$\nu'\omega_2+\nu\omega_2' \ = \ -\nu' - 2\eta_1(1+\omega_1) - \frac{2\gamma}{3}f'\beta b^{(\alpha)}(1+\omega_1). \tag{3.21}$$

Making use of (3.20), one can easily remark that (3.21) can be written as:

$$\begin{aligned}\omega_2' \ + \ \left(\frac{\nu'}{\nu}+\frac{(2\eta_1+\beta b^{(\alpha)}\frac{2\gamma}{3}f')}{\nu-\beta b^{(\alpha)}\big(\frac{\gamma}{3}f+\frac{2}{3}\delta^{-1}f\big)+\frac{\beta^2{b^{(\alpha)}}^2}{3}f}\right)\omega_2 \\ = -\frac{\nu'}{\nu} - \frac{\Big(2\eta_1+\beta b^{(\alpha)}\frac{2\gamma}{3}f'\Big)\beta b^{(\alpha)}\Big(\frac{\gamma}{3}f+\frac{2}{3}\delta^{-1}f-\frac{\beta b^{(\alpha)}}{3}f\Big)}{\nu\big[\nu-\beta b^{(\alpha)}\big(\frac{\gamma}{3}f+\frac{2}{3}\delta^{-1}f\big)+\frac{\beta^2{b^{(\alpha)}}^2}{3}f\big]} \\ -\frac{2\eta_1}{\nu}-\frac{2\gamma}{3\nu}f'\beta b^{(\alpha)},\end{aligned} \tag{3.22}$$

In order to solve (3.22) and to define κ_1, κ_2, ω_1 and ω_2 we seek for sufficient conditions. Let us shortly detail these conditions namely (H0).

Since $\gamma\geq 0$, $\delta>0$ and bo $>>6$ then the discriminant of $\big[\nu-\beta b^{(\alpha)}\big(\frac{\gamma}{3}f+\frac{2}{3}\delta^{-1}f\big)+\frac{\beta^2{b^{(\alpha)}}^2}{3}f\big]$ is $\big[\gamma^2\delta^4\text{bo}(\text{bo}-6)+12\delta^4\text{bo}+9\gamma^2\delta^4\big]>0$ thus one needs:

$$\nu(\beta b^{(\alpha)})\neq 0 \quad\text{and}\quad \beta b^{(\alpha)}\neq\frac{2\delta\text{bo}+\gamma\delta^2\text{bo}-3\gamma\delta^2\pm\sqrt{\gamma^2\delta^4\text{bo}(\text{bo}-6)+12\delta^4\text{bo}+9\gamma^2\delta^4}}{2\delta^2\text{bo}}. \tag{H0}$$

Indeed, the definition of κ_1, κ_2, ω_1 and ω_2 prevent these values as for the deformation of the bottom. These conditions simply consist in assuming additional restrictions on the deformation of the bottom.

However, terms involving three derivatives on v remains in (3.16), as well as in $\partial_x\big(\overline{\mathcal{R}}[h_1,h_2]v\big)$. Dealing with these terms requires the introduction of $\mathfrak{T}[\epsilon\zeta,\beta b^{(\alpha)}](\epsilon\varsigma v\partial_x v)$ where, again, ς is a function of $\beta b^{(\alpha)}$ to be determined. More precisely, one has

$$\begin{aligned}\mathfrak{T}[\epsilon\zeta,\beta b^{(\alpha)}](\epsilon\varsigma v\partial_x v) \;+\; \mu\epsilon q_1\partial_x\Big(\overline{\mathcal{R}}[h_1,h_2]v\Big) \;=\; q_1(\epsilon\varsigma v\partial_x v) \;-\; \mu\partial_x\Big(\nu q_2\partial_x(\epsilon\varsigma v\partial_x v)\Big)\\ +\; \mu\epsilon q_1\partial_x\Big(\overline{\mathcal{R}}[h_1,h_2]v\Big) \qquad .\end{aligned} \tag{3.23}$$

Combining (3.16) with (3.23), one can check that if we adjust ς so that the following identity is satisfied

$$\begin{aligned}\nu(1+\omega_2)\varsigma = \frac{(1-\gamma)g^2}{3}(1+\omega_1) - \frac{1}{\mathrm{bo}}(f^2-\gamma g^2) + \eta g(1+\omega_1)\\ +\nu\omega_2(f^2-\gamma g^2) + (1+\omega_1)\big[\beta b^{(\alpha)}(\frac{\gamma}{3}f+\frac{2}{3}\delta^{-1}f)(f^2-\gamma g^2)\big]\\ -(1+\omega_1)\big[\beta^2 {b^{(\alpha)}}^2\frac{1}{3}f(f^2-\gamma g^2)\big] - \omega_1 d(f^2-\gamma g^2),\end{aligned} \tag{3.24}$$

then the following approximation holds (withdrawing $\mathcal{O}(\mu^2,\mu\epsilon^2,\mu\epsilon\beta\alpha,\mu\beta^2\alpha^2)$ terms):

$$\begin{aligned}\mathfrak{T}(\partial_t v+\epsilon\varsigma v\partial_x v) - q_1\partial_t\Big(v \;+\; \mu\big(\overline{\mathcal{Q}}[h_1,h_2]v\big)\Big) + q_1\mu\frac{\gamma+\delta}{\mathrm{bo}}\partial_x^3\zeta + \mu\epsilon q_1\partial_x\Big(\overline{\mathcal{R}}[h_1,h_2]v\Big)\\ = q_1(\epsilon\varsigma v\partial_x v) + \mu\frac{2\epsilon}{3}(1+\omega_1)(\gamma-1)g^2\partial_x\big((\partial_x v)^2\big)\\ +\mu\beta(\gamma+\delta)(1+\omega_1)\eta_1\alpha^2(\partial_x^2 b)^{(\alpha)}\partial_x\zeta + \mathcal{O}(\mu^2,\mu\epsilon^2,\mu\epsilon\beta\alpha,\mu\beta^2\alpha^2).\end{aligned} \tag{3.25}$$

After multiplying the second equation of (3.6) by q_1 and plugging the estimate (3.25), we get the following model:

$$\begin{cases}\partial_t\zeta+\partial_x\left(\dfrac{h_1h_2}{h_1+\gamma h_2}v\right) \;=\; 0,\\[2ex] \mathfrak{T}[\epsilon\zeta,\beta b]\left(\partial_t v+\epsilon\varsigma v\partial_x v\right)+(\gamma+\delta)q_1\partial_x\zeta+\frac{\epsilon}{2}q_1\partial_x\left(\frac{h_1^2-\gamma h_2^2}{(h_1+\gamma h_2)^2}|v|^2\right)-q_1(\epsilon\varsigma v\partial_x v)\\ \qquad = \mu\dfrac{2\epsilon}{3}(1+\omega_1)(\gamma-1)g^2\partial_x\big((\partial_x v)^2\big)+\mu\beta(\gamma+\delta)(1+\omega_1)\eta_1\alpha^2(\partial_x^2 b)^{(\alpha)}\partial_x\zeta\end{cases} \tag{3.26}$$

We will refer to (3.26) as the new Green-Naghdi model.

Remark 4. After setting $\beta=0$ in (3.26), we recover the model obtained and fully justified by Duchêne, Israwi and Talhouk in [49]. If we take $\beta=\mathcal{O}(\sqrt{\mu})$ and $\alpha=1$ in (3.26), we recover the model obtained and fully justified in [90].

3.4 Preliminary results

The ellipticity of the operator $\mathfrak{T}$ requires some sufficient conditions in order to provide the well-posedness and continuity of the inverse $\mathfrak{T}^{-1}$. We recall the operator $\mathfrak{T}[\epsilon\zeta,\beta b]$, defined in (3.15):

$$\mathfrak{T}[\epsilon\zeta,\beta b^{(\alpha)}]V \;=\; q_1V \;-\; \mu\partial_x\Big(\nu q_2\partial_x V\Big), \tag{3.27}$$

with $\nu, \kappa_1, \kappa_2, \omega_1, \omega_2$ functions depending on $\beta b^{(\alpha)}$ and in what follows we assume that $\nu(\beta b^{(\alpha)}) > 0$ is bounded from below (by hypothesis):

$$\nu(\beta b^{(\alpha)}) = d(\beta b^{(\alpha)}) - \frac{1}{\mathrm{bo}} \geq \nu_0 > 0.$$

Let us recall the minimum depth condition

$$\exists\ h_{01} > 0, \quad \text{such that} \quad \inf_{x\in\mathbb{R}} h_1 \geq h_{01} > 0, \quad \inf_{x\in\mathbb{R}} h_2 \geq h_{01} > 0, \tag{H1}$$

with $h_1 = 1 - \epsilon\zeta$ and $h_2 = \frac{1}{\delta} + \epsilon\zeta - \beta b^{(\alpha)}$.

We also introduce the condition

$$\exists\ h_{02} > 0,\ \text{such that} \quad \inf_{x\in\mathbb{R}} q_1 \geq h_{02} > 0; \qquad \inf_{x\in\mathbb{R}} q_2 \geq h_{02} > 0. \tag{H2}$$

Assuming that the deformations at the interface and the ones at the bottom are not too large is sufficient to ensure the conditions (H1) and (H2), for more details see [49] where it is proved in the flat bottom case. We believe that this could be applied easily in the variable bottom case, we omit it here. Let us introduce now $H^{s+1}_\mu(\mathbb{R})$ the space $H^{s+1}(\mathbb{R})$ endowed with the norm

$$\left|\ \cdot\ \right|^2_{H^{s+1}_\mu} \ \equiv\ \left|\ \cdot\ \right|^2_{H^s} \ +\ \mu\left|\ \cdot\ \right|^2_{H^{s+1}}\ .$$

For $s = 0$, $|\cdot|_{H^1_\mu}$ is defined as

$$\forall\ v \in H^1(\mathbb{R}), \quad |\ v\ |^2_{H^1_\mu} \ =\ |\ v\ |^2_{L^2} \ +\ \mu\ |\ \partial_x v\ |^2_{L^2},$$

and is equivalent to the $H^1(\mathbb{R})$-norm but not uniformly with respect to μ. We define by $(H^1_\mu(\mathbb{R}))^\star$ the space $H^{-1}(\mathbb{R})$ the dual space of $H^1_\mu(\mathbb{R})$.

The preliminary results proved in [49, Section 5] remain valid for the operator $\mathfrak{T}[\epsilon\zeta, \beta b^{(\alpha)}]$. Let us recall the strong ellipticity and invertibility results on $\mathfrak{T}$.

Lemma 3.4.1. *Let* $\mathsf{p} \in \mathcal{P}$ *satisfy* (3.10) *and* $\zeta \in L^\infty(\mathbb{R})$, $b^{(\alpha)} \in L^\infty(\mathbb{R})$ *such that* (H2) *is satisfied. Then the operator*

$$\mathfrak{T}[\epsilon\zeta, \beta b^{(\alpha)}] : H^1_\mu(\mathbb{R}) \longrightarrow (H^1_\mu(\mathbb{R}))^\star$$

is uniformly continuous and coercive. More precisely, there exists $c_0 > 0$ *such that*

$$(\mathfrak{T}u, v) \quad \leq \quad c_0 |u|_{H^1_\mu} |v|_{H^1_\mu}; \tag{3.28}$$

$$(\mathfrak{T}u, u) \quad \geq \quad \frac{1}{c_0} |u|^2_{H^1_\mu} \tag{3.29}$$

with $c_0 = C(M_{\mathrm{CH}}, h_{02}^{-1}, \epsilon\big|\zeta\big|_{L^\infty}, \beta\big|b^{(\alpha)}\big|_{L^\infty})$.

Proof. Defining the following bilinear form

$$a(u, v) = \big(\ \mathfrak{T}u\ ,\ v\ \big) = \big(\ (1 + \epsilon\kappa_1\zeta + \omega_1)u\ ,\ v\ \big) + \mu\big(\ \nu(1 + \epsilon\kappa_2\zeta + \omega_2)\partial_x u\ ,\ \partial_x v\ \big),$$

where $\big(\ \cdot\ ,\ \cdot\ \big)$ denotes the L^2 inner product. The following estimation holds without any difficulties

$$\big|a(u,v)\big| \leq \sup_{x\in\mathbb{R}} |1+\epsilon\kappa_1\zeta+\omega_1|\big(\ u\ ,\ v\ \big) + \mu \sup_{x\in\mathbb{R}} |\nu(1+\epsilon\kappa_2\zeta+\omega_2)|\big(\ \partial_x u\ ,\ \partial_x v\ \big),$$

so that (3.28) can be deduced using the Cauchy-Schwarz inequality.

The $H^1_\mu(\mathbb{R})$-coercivity of $a(\cdot,\cdot)$, inequality (3.29), is a consequence of condition (H2):

$$\begin{aligned} a(u,u) = \big(\ \mathfrak{T}u\ ,\ u\ \big) &= \int_{\mathbb{R}} (1+\epsilon\kappa_1\zeta+\omega_1)|u|^2\,dx + \mu\int_{\mathbb{R}} \nu(1+\epsilon\kappa_2\zeta+\omega_2)|u_x|^2\,dx \\ &\geq h_{02}\min(1,\nu_0)|u|^2_{H^1_\mu}. \end{aligned}$$

□

Lemma 3.4.2. *Let* $\mathsf{p}\in\mathcal{P}$ *satisfy* (3.10) *and* $\zeta\in L^\infty(\mathbb{R})$, $b^{(\alpha)}\in L^\infty(\mathbb{R})$ *such that* (H2) *is satisfied. Then the operator*

$$\mathfrak{T}[\epsilon\zeta,\beta b^{(\alpha)}] : H^2(\mathbb{R}) \longrightarrow L^2(\mathbb{R})$$

is bijective.

Proof. The invertibility of the operator $\mathfrak{T}$ is shown using the Lax-Milgram theorem. The following bilinear form

$$a(u,v) = \big(\ \mathfrak{T}u\ ,\ v\ \big) = \big(\ (1+\epsilon\kappa_1\zeta+\omega_1)u\ ,\ v\ \big) + \mu\big(\ \nu(1+\epsilon\kappa_2\zeta+\omega_2)\partial_x u\ ,\ \partial_x v\ \big)$$

is continuous and coercive on $H^1_\mu(\mathbb{R})$ (previous lemma). For any $\mu>0$, the dual of $H^1_\mu(\mathbb{R})$ is $H^{-1}(\mathbb{R})$, of whom $L^2(\mathbb{R})$ is a subspace, and one has $\big(f,g\big)\leq \big|f\big|_{H^1_\mu}\big|g\big|_{L^2}$, *independently of* $\mu>0$. Therefore, using Lax-Milgram lemma, for all $f\in L^2(\mathbb{R})$, there exists a unique $u\in H^1_\mu(\mathbb{R})$ such that, for all $v\in H^1_\mu(\mathbb{R})$

$$a(u,v) = (f,v);$$

that is to say, there exist a unique solution to the following equation

$$\mathfrak{T}u = f. \tag{3.30}$$

The definition of $\mathfrak{T}$ give us:

$$\mu\nu\,(1+\epsilon\kappa_2\zeta+\omega_2)\,\partial_x^2 u = (1+\epsilon\kappa_1\zeta+\omega_1)u - \mu\partial_x\big(\nu q_2\big)\partial_x u - f. \tag{3.31}$$

Now, using condition (H2), and since $u\in H^1(\mathbb{R})$, $\zeta\in L^\infty(\mathbb{R})$ and $f\in L^2(\mathbb{R})$, we deduce that $\partial_x^2 u\in L^2(\mathbb{R})$, and thus $u\in H^2(\mathbb{R})$. We proved that $\mathfrak{T}[\epsilon\zeta,\beta b^{(\alpha)}] : H^2(\mathbb{R}) \longrightarrow L^2(\mathbb{R})$ is one-to-one and onto. □

3.5 Linearized system

Let us recall the system (3.26).

$$\begin{cases} \partial_t\zeta + \partial_x\left(\dfrac{h_1h_2}{h_1+\gamma h_2}v\right) = 0, \\[2ex] \mathfrak{T}[\epsilon\zeta,\beta b^{(\alpha)}]\,(\partial_t v + \epsilon\varsigma v\partial_x v) + (\gamma+\delta)q_1\partial_x\zeta + \frac{\epsilon}{2}q_1\partial_x\left(\frac{h_1^2-\gamma h_2^2}{(h_1+\gamma h_2)^2}|v|^2\right) - q_1(\epsilon\varsigma v\partial_x v) \\ \qquad = \mu\dfrac{2\epsilon}{3}(1+\omega_1)(\gamma-1)g^2\partial_x\big((\partial_x v)^2\big) + \mu\beta(\gamma+\delta)(1+\omega_1)\eta_1\alpha^2(\partial_x^2 b)^{(\alpha)}\partial_x\zeta, \end{cases} \tag{3.32}$$

with $h_1 = 1 - \epsilon\zeta$, $h_2 = 1/\delta + \epsilon\zeta - \beta b^{(\alpha)}$, $q_1 \equiv 1 + \epsilon\kappa_1(\beta b^{(\alpha)})\zeta + \omega_1(\beta b^{(\alpha)})$ and $q_2 \equiv 1+\epsilon\kappa_2(\beta b^{(\alpha)})\zeta+\omega_2(\beta b^{(\alpha)})$ where $\kappa_1, \kappa_2, \omega_1, \omega_2$ and ς are defined in (3.19),(3.18),(3.20),(3.21),(3.24), and

$$\mathfrak{T}[\epsilon\zeta, \beta b]V \;=\; q_1 V \;-\; \mu\partial_x\Big(\nu q_2 \partial_x V\Big).$$

We define the following functions in order to simplify the reading,

$$H : X \to \frac{(1-X)(\delta^{-1} + X - \beta b^{(\alpha)})}{1 - X + \gamma(\delta^{-1} + X - \beta b^{(\alpha)})},$$

and

$$G : X \to \Big(\frac{(1-X)}{1 - X + \gamma(\delta^{-1} + X - \beta b^{(\alpha)})}\Big)^2.$$

One has

$$H(\epsilon\zeta) \;=\; \frac{h_1 h_2}{h_1 + \gamma h_2}, \qquad H'(\epsilon\zeta) \;=\; \frac{h_1^2 - \gamma h_2^2}{(h_1 + \gamma h_2)^2} \quad \text{and} \quad G(\epsilon\zeta) = \Big(\frac{h_1}{h_1 + \gamma h_2}\Big)^2.$$

One can rewrite,

$$\begin{cases} \partial_t\zeta + H(\epsilon\zeta)\partial_x v + \epsilon\partial_x\zeta H'(\epsilon\zeta)v - \beta\partial_x b G(\epsilon\zeta)v \;=\; 0, \\ \\ \mathfrak{T}\Big(\partial_t v + \dfrac{\epsilon}{2}\varsigma\partial_x(v^2)\Big) + (\gamma+\delta)q_1\partial_x\zeta + \epsilon q_1\big(H'(\epsilon\zeta) - \varsigma\big)v\partial_x v + \epsilon q_1\partial_x\big(\dfrac{H'(\epsilon\zeta)}{2}\big)v^2 \\ \qquad\qquad = \mu\dfrac{2\epsilon}{3}(1+\omega_1)(\gamma-1)g^2\partial_x\big((\partial_x v)^2\big) + \mu\beta(\gamma+\delta)(1+\omega_1)\eta_1\alpha^2(\partial_x^2 b)^{(\alpha)}\partial_x\zeta. \end{cases} \tag{3.33}$$

with $\partial_x(\dfrac{H'(\epsilon\zeta)}{2}) = \dfrac{-\gamma\epsilon\partial_x\zeta(h_1+h_2)^2 + \gamma\beta\alpha(\partial_x b)^{(\alpha)}h_1(h_1+h_2)}{(h_1+\gamma h_2)^3}$.

We apply $\mathfrak{T}^{-1}$ to the second equation in (3.33), thus we can write the equations as follows

$$\partial_t U + A[U]\partial_x U + B[U] \;=\; 0, \tag{3.34}$$

with

$$A[U] = \begin{pmatrix} \epsilon H'(\epsilon\zeta)v & H(\epsilon\zeta) \\ \mathfrak{T}^{-1}(Q_0(\epsilon\zeta, \beta b^{(\alpha)}) + \epsilon^2 Q_1(\epsilon\zeta, \beta b^{(\alpha)}, v)\cdot) & \mathfrak{T}^{-1}(\mathfrak{Q}[\epsilon\zeta, \beta b^{(\alpha)}, v]\cdot) + \epsilon\varsigma v \end{pmatrix}, \tag{3.35}$$

$$B[U] = \begin{pmatrix} -\alpha\beta(\partial_x b)^{(\alpha)}G(\epsilon\zeta)v \\ \mathfrak{T}^{-1}\Big(\dfrac{\gamma\epsilon\beta\alpha q_1 h_1(h_1+h_2)(\partial_x b)^{(\alpha)}}{(h_1+\gamma h_2)^3}v^2\Big) \end{pmatrix} \tag{3.36}$$

where $Q_0(\epsilon\zeta, \beta b^{(\alpha)}), Q_1(\epsilon\zeta, \beta b^{(\alpha)}, v)$ are defined as

$$\begin{aligned} Q_0(\epsilon\zeta, \beta b^{(\alpha)}) \;&=\; (\gamma+\delta)q_1 - \mu\beta(\gamma+\delta)(1+\omega_1)\eta_1\alpha^2(\partial_x^2 b)^{(\alpha)}, \\ Q_1(\epsilon\zeta, \beta b^{(\alpha)}, v) &= -\gamma q_1(\epsilon\zeta, \beta b^{(\alpha)})\frac{(h_1+h_2)^2}{(h_1+\gamma h_2)^3}v^2 \end{aligned}$$

and the operator $\mathfrak{Q}[\epsilon, \beta b^{(\alpha)}, v]$ defined by

$$\mathfrak{Q}[\epsilon\zeta, \beta b^{(\alpha)}, v]f \;\equiv\; \epsilon q_1(H'(\epsilon\zeta) - \varsigma)vf - \mu\frac{2\epsilon}{3}(1+\omega_1)(\gamma-1)g^2\partial_x(\partial_x v f). \tag{3.37}$$

Taking after the traditional theory of quasilinear hyperbolic systems, the existence and uniqueness result of the initial value problem of the above system will depend on some precise energy estimates for the following linearized system $\underline{U} = (\underline{\zeta}, \underline{v})^\top$:

$$\begin{cases} \partial_t U + A[\underline{U}]\partial_x U + B[\underline{U}] = 0; \\ U_{|_{t=0}} = U_0. \end{cases} \tag{3.38}$$

The symmetrizer of the system is given by

$$Z[\underline{U}] = \begin{pmatrix} \frac{Q_0(\epsilon\underline{\zeta}, \beta b^{(\alpha)}) + \epsilon^2 Q_1(\epsilon\underline{\zeta}, \beta b^{(\alpha)}, \underline{v})}{H(\epsilon\underline{\zeta})} & 0 \\ 0 & \mathfrak{T}[\epsilon\underline{\zeta}, \beta b^{(\alpha)}] \end{pmatrix} \tag{3.39}$$

One ought to add an extra assumption to guarantee that our symmetrizer is defined and positive which is:

$$\exists\ h_{03} > 0 \ \text{ such that } \ Q_0(\epsilon\underline{\zeta}, \beta b^{(\alpha)}) + \epsilon^2 Q_1(\epsilon\underline{\zeta}, \beta b^{(\alpha)}, \underline{v}) \geq h_{03} > 0. \tag{H3}$$

For given $s \geq 0$ and $\mu, T > 0$, we denote by X^s the vector space $H^s(\mathbb{R}) \times H^{s+1}_\mu(\mathbb{R})$ endowed with the norm

$$\forall\ U = (\zeta, v) \in X^s, \quad |U|^2_{X^s} \equiv |\zeta|^2_{H^s} + |v|^2_{H^s} + \mu|\partial_x v|^2_{H^s},$$

The energy of the initial value problem (3.38) is now given by:

$$E^s(U)^2 = (\Lambda^s U, Z[\underline{U}]\Lambda^s U) = (\Lambda^s\zeta, \frac{Q_0(\epsilon\underline{\zeta}, \beta b^{(\alpha)}) + \epsilon^2 Q_1(\epsilon\underline{\zeta}, \beta b^{(\alpha)}, \underline{v})}{H(\epsilon\underline{\zeta})}\Lambda^s\zeta) + \Big(\Lambda^s v, \mathfrak{T}[\epsilon\underline{\zeta}, \beta b^{(\alpha)}]\Lambda^s v\Big). \tag{3.40}$$

In order to ensure the equivalency of X^s-norm with the energy of the symmetrizer it requires to add the additional assumption given in (H3).

3.6 Full justification of the new coupled model

According to the terminology of Lannes [84], the full justification of an asymptotic model follows from two requirements. The first one is that the Cauchy problem for both the full Euler system and the asymptotic model should be well-posed; and the second one is that the solutions with corresponding initial data should remain close. In this section we express every one of the elements for the full justification of our model. We do not state the proofs of the following results since they are proved using the same techniques as in [90] adapted to our new model.

Proposition 12 (Consistency)**.** *For all family $\mathcal{P}$ of parameters p satisfying* (3.10)*, let $U^\mathsf{p} = (\zeta^\mathsf{p}, \psi^\mathsf{p})^\top$ be a family of solutions of the full Euler system* (3.2) *such that there exists $T > 0$, $s \geq s_0 + 1$, $s_0 > 1/2$ for which $(\zeta^\mathsf{p}, \partial_x\psi^\mathsf{p})^\top$ is bounded in $L^\infty([0,T); H^{s+N})^2$ with sufficiently large N, and uniformly with respect to p. Moreover assume that $b \in H^{s+N}$ satisfy* (H0) *and there exists $h_{01} > 0$ such that*

$$h_1 = 1 - \epsilon\zeta^\mathsf{p} \geq h_{01} > 0, \quad h_2 = \frac{1}{\delta} + \epsilon\zeta^\mathsf{p} - \beta b^{(\alpha)} \geq h_{01} > 0.$$

Define v^p as in (3.5)*. Then $(\zeta^\mathsf{p}, v^\mathsf{p})$ is H^s-consistent with* (3.26)*, on $[0,T]$ with precision $\mathcal{O}(\mu^2)$.*

Theorem 3.6.1 (Existence and uniqueness). *Let* $\mathsf{p} \in \mathcal{P}$ *satisfy* (3.10) *and* $s \geq s_0 + 1$, $s_0 > 1/2$, *and assume* $U_0 = (\zeta_0, v_0)^\top \in X^s$, $b \in H^{s+1}$ *satisfies* (H0),(H1),(H2), *and* (H3). *The system of equations* (3.26) *admits a unique strong solution* $U = (\zeta, v)^\top \in C^0([0, T_{\max}); X^s) \cap C^1([0, T_{\max}); X^{s-1})$ *with the initial value* $(\zeta, v)\,|_{t=0} = (\zeta_0, v_0)$ *with* $T_{\max} > 0$ *is a maximal time uniformly bounded from below with respect to* $\mathsf{p} \in \mathcal{P}_{\mathrm{CH}}$. *The solution preserves the conditions* (H1),(H2) *and* (H3) *(with different lower bounds) for any* $t \in [0, T_{\max})$.

Moreover, there exists T, λ *and* $C_0 = C(h_{01}^{-1}, h_{02}^{-1}, h_{03}^{-1}, M, T, \left|U_0\right|_{X^s}, |b|_{H^{s+1}})$, *such that* $T_{\max} \geq \frac{T}{\max(\epsilon, \beta\alpha)}$, *and one has the energy estimates*

$\forall\ 0 \leq t \leq \frac{T}{\max(\epsilon, \beta\alpha)}$,

$$\left|U(t,\cdot)\right|_{X^s} + \left|\partial_t U(t,\cdot)\right|_{X^{s-1}} \leq C_0 e^{\max(\epsilon,\beta\alpha)\lambda t} + \max(\epsilon, \beta\alpha) C_0^2 \int_0^t e^{\max(\epsilon,\beta\alpha)\lambda(t-t')} dt' + \max(\epsilon, \beta\alpha) C_0$$

If $T_{\max} < \infty$, *one has*

$$|U(t,\cdot)|_{X^s} \longrightarrow \infty \quad as \quad t \longrightarrow T_{\max},$$

or one of the conditions (H1),(H2), (H3) *ceases to be true as* $t \longrightarrow T_{\max}$.

Theorem 3.6.2 (Stability). *Let* $\mathsf{p} \in \mathcal{P}$ *satisfy* (3.10) *and* $s \geq s_0 + 1$ *with* $s_0 > 1/2$, *and assume* $U_{1,0} = (\zeta_{1,0}, v_{1,0})^\top \in X^s$, $U_{2,0} = (\zeta_{2,0}, v_{2,0})^\top \in X^{s+1}$, *and* $b \in H^{s+1}$ *satisfies* (H0),(H1),(H2), *and* (H3). *Denote* U_j *the solution to* (3.26) *with* $U_j\,|_{t=0} = U_{j,0}$.
Then there exists $T, \lambda, C_0 = C(M, h_{01}^{-1}, h_{02}^{-1}, h_{03}^{-1}, \left|U_{1,0}\right|_{X^s}, |U_{2,0}|_{X^{s+1}}, |b|_{H^{s+1}})$ *such that* $\forall t \in [0, \frac{T}{\max(\epsilon, \beta\alpha)}]$,

$$\left|(U_1 - U_2)(t,\cdot)\right|_{X^s} \leq C_0 e^{\max(\epsilon,\beta\alpha)\lambda t} \left|U_{1,0} - U_{2,0}\right|_{X^s}.$$

Theorem 3.6.3 (Convergence). *Let* $\mathsf{p} \in \mathcal{P}$ *satisfy* (3.10) *and* $s \geq s_0 + 1$ *with* $s_0 > 1/2$, *and let* $U^0 \equiv (\zeta^0, \psi^0)^\top \in H^{s+N}(\mathbb{R})^2$, $b \in H^{s+N}$ *satisfy the hypotheses* (H0),(H1),(H2), *and* (H3), *with* N *sufficiently large. We suppose* $U \equiv (\zeta, \psi)^\top$ *a unique solution to the full Euler system* (3.2) *with initial data* $(\zeta^0, \psi^0)^\top$, *defined on* $[0, T_1]$ *for* $T_1 > 0$ [1],*and we suppose that* $U \equiv (\zeta, \psi)^\top$ *satisfies the assumptions of our consistency result, Proposition* (12). *Then there exists* $C, T > 0$, *independent of* p, *such that*

- *There exists a unique solution* $\underline{U} \equiv (\underline{\zeta}, \underline{v})^\top$ *to our new model* (3.26), *defined on* $[0, \frac{T}{\max(\epsilon,\beta\alpha)}]$ *and with initial data* $(\zeta^0, v^0)^\top$ *(provided by Theorem 3.6.1);*
- *With* v, *defined as in* (3.5), *one has for any* $t \leq \min(T_1, \frac{T}{\max(\epsilon,\beta\alpha)})$,

$$\left|(\zeta, v) - (\underline{\zeta}, \underline{v})\right|_{L^\infty([0,t];X^s)} \leq C\ \mu^2\ t.$$

3.7 Derivation of the unidirectional approximation

In what follows, we are interested in scalar asymptotic models for the propagation of internal waves contrarily to the aforementioned model, which consist in a system of evolution equations. Thus, we derive an approximate solution to the Green-Naghdi system (3.6) over variable topography, taking after the same strategy created for the water-wave problem in [34], and for the

1. To our knowledge, the local well-posedness of the full Euler system in the two-fluid configuration over a variable topography seems to be an open problem.

internal wave problem over flat topography in [47]. In fact, at the lowest order of approximation (that is dropping the first order terms in μ, ϵ and β), the Green-Naghdi system (3.6) becomes a linear wave equation of speed ± 1 and any initial disturbance of the interface splits up into two waves moving in opposite direction. In what follows we will focus on a given direction of the two counter-propagating waves.

More precisely, we prove that if one picks carefully the initial data (deformation of the interface as well as shear layer-mean velocity) so that only one wave is present in the dynamics of the system, then the flow is unidirectional, in the sense that the flow can be approximated as a solution of a scalar evolution equation for the deformation at the interface (see (3.48)), followed by a reconstruction of the shear layer-mean velocity from the deformation (in particular, the initial shear velocity is determined by the initial deformation).

Let us now state the steps for the derivation of the unidirectional approximation. In the interest of simplifying the calculations, we use the Green-Naghdi system (3.6) expressed using the variables $(\zeta, \underline{v})$, where we define $\underline{v} = \dfrac{h_1 h_2}{h_1 + \gamma h_2} v$. The system reads

$$\begin{cases} \partial_t \zeta \ + \ \partial_x \underline{v} \ = \ 0, \\ \\ \partial_t \Big(\dfrac{h_1 + \gamma h_2}{h_1 h_2} \underline{v} \ + \ \mu \underline{\mathcal{Q}}[h_1, h_2]\underline{v} \Big) \ + \ (\gamma + \delta) \partial_x \zeta \ + \ \dfrac{\epsilon}{2} \partial_x \Big(\dfrac{h_1^2 - \gamma h_2^2}{(h_1 h_2)^2} \underline{v}^2 \Big) \ = \\ \qquad\qquad \mu \epsilon \partial_x \big(\underline{\mathcal{R}}[h_1, h_2]\underline{v} \big) + \mu \dfrac{\gamma + \delta}{\mathrm{bo}} \partial_x^3 \zeta, \end{cases} \tag{3.41}$$

where we denote

$$\begin{aligned} \underline{\mathcal{Q}}[h_1, h_2]\underline{v} \quad &= \quad \mathcal{T}[h_2, \beta b^{(\alpha)}]\Big(\frac{1}{h_2} \underline{v} \Big) - \gamma \mathcal{T}[h_1, 0]\Big(\frac{-\underline{v}}{h_1} \Big), \\ &= \quad -\frac{1}{3h_2} \partial_x \Big(h_2^3 \partial_x \big(\frac{\underline{v}}{h_2} \big) \Big) + \frac{1}{2h_2} \beta \alpha \Big[\partial_x \Big(h_2^2 (\partial_x b)^{(\alpha)} \frac{\underline{v}}{h_2} \Big) - h_2^2 (\partial_x b)^{(\alpha)} \partial_x \big(\frac{\underline{v}}{h_2} \big) \Big] \\ &+ \quad \alpha^2 \beta^2 ((\partial_x b)^{(\alpha)})^2 \big(\frac{\underline{v}}{h_2} \big) - \gamma \Big[\frac{1}{3h_1} \partial_x \Big(h_1^3 \partial_x \big(\frac{\underline{v}}{h_1} \big) \Big) \Big], \end{aligned} \tag{3.42}$$

$$\begin{aligned} \underline{\mathcal{R}}[h_1, h_2]\underline{v} \quad &= \quad \frac{1}{2} \Big(- h_2 \partial_x \big(\frac{\underline{v}}{h_2} \big) + \beta \alpha (\partial_x b)^{(\alpha)} \big(\frac{\underline{v}}{h_2} \big) \Big)^2 - \frac{\gamma}{2} \Big(h_1 \partial_x \big(\frac{-\underline{v}}{h_1} \big) \Big)^2 \\ &- \quad \big(\frac{\underline{v}}{h_2} \big) \mathcal{T}[h_2, \beta b^{(\alpha)}]\Big(\frac{\underline{v}}{h_2} \Big) + \gamma \big(\frac{-\underline{v}}{h_1} \big) \mathcal{T}[h_1, 0]\Big(\frac{-\underline{v}}{h_1} \Big). \end{aligned} \tag{3.43}$$

We proceed by giving the following asymptotic expansions:

$$\frac{h_1 + \gamma h_2}{h_1 h_2} = \gamma + c + \epsilon \zeta \big(\gamma - c^2 \big) + \epsilon^2 \zeta^2 \big(\gamma + c^3 \big) + \epsilon^3 \zeta^3 \big(\gamma - c^4 \big) + \mathcal{O}(\epsilon^4), \tag{3.44}$$

$$\frac{h_1^2 - \gamma h_2^2}{(h_1 h_2)^2} = c^2 - \gamma - 2\epsilon \zeta \big(c^3 + \gamma \big) + 3\epsilon^2 \zeta^2 \big(c^4 - \gamma \big) + \mathcal{O}(\epsilon^3), \tag{3.45}$$

$$\begin{aligned}
\underline{\mathcal{Q}}[h_1,h_2]\underline{v} &= -d(\gamma+c)\partial_x^2\underline{v} - \epsilon d(\gamma-c^2)\partial_x^2(\zeta\underline{v}) \\
&+ \epsilon(\gamma+c)\Big(\eta\ \underline{v}\partial_x^2\zeta + \big(2\eta+(\gamma-1)g\big)\partial_x\zeta\partial_x\underline{v} + \big(\eta+\frac{2}{3}(\gamma-1)g\big)\zeta\partial_x^2\underline{v}\Big) \\
&+ \beta\big(\frac{\gamma}{3}f+\frac{2}{3}\delta^{-1}f\big)b^{(\alpha)}\Big((\gamma+c)\partial_x^2\underline{v}+\epsilon(\gamma-c^2)\partial_x^2(\zeta\underline{v})\Big) \\
&+ \beta\alpha(\gamma+c)\Big(2\eta_1(\partial_x b)^{(\alpha)}\partial_x\underline{v}\Big) \\
&- \beta^2\frac{1}{3}f{b^{(\alpha)}}^2\Big((\gamma+c)\partial_x^2\underline{v}+\epsilon(\gamma-c^2)\partial_x^2(\zeta\underline{v})\Big) \\
&+ \beta^2\alpha(\gamma+c)\Big(\frac{2\gamma}{3}f'b^{(\alpha)}(\partial_x b)^{(\alpha)}\partial_x\underline{v}\Big) \\
&+ \mathcal{O}(\epsilon^2,\beta\alpha\epsilon,\beta\alpha^{3/2}),
\end{aligned} \tag{3.46}$$

$$\underline{\mathcal{R}}[h_1,h_2]\underline{v} = (1-\gamma)g^2(\gamma+c)^2\left(\frac{1}{2}(\partial_x\underline{v})^2+\frac{1}{3}\underline{v}\partial_x^2\underline{v}\right)+\mathcal{O}(\epsilon,\beta\alpha), \tag{3.47}$$

with $c=c(\beta b^{(\alpha)})=\dfrac{\delta}{1-\delta\beta b^{(\alpha)}}$ and d, f, f', g, η and η_1 functions depending on $\beta b^{(\alpha)}$, defined in (3.11), (3.12), (3.13) and (3.14). We would like to mention that definition of the function $c(\beta b^{(\alpha)})$ forbids the value $\beta b^{(\alpha)}=\delta^{-1}$. That is to say the bottom should be restricted in a small neighborhood around this value.

It is clear that if ζ is to satisfy the following scalar evolution equation,

$$\begin{aligned}
\partial_t\zeta+\alpha_0\partial_x\zeta+\frac{1}{2}\partial_x(\alpha_0)\zeta+\epsilon\alpha_1\zeta\partial_x\zeta+\epsilon^2\alpha_2\zeta^2\partial_x\zeta+\epsilon^3\alpha_3\zeta^3\partial_x\zeta+\mu\varrho\partial_x^3\zeta+\mu\beta\alpha(\omega+\varrho')(\partial_x b)^{(\alpha)}\partial_x^2\zeta \\
+\mu\epsilon\partial_x\big(\varkappa_1\zeta\partial_x^2\zeta+\varkappa_2(\partial_x\zeta)^2\big)=0,
\end{aligned} \tag{3.48}$$

where α_i $(i=0,1,2,3)$, ϱ, ω, $\varkappa_1$ and $\varkappa_2$ are functions depending on $\beta b^{(\alpha)}$ to be determined later, then $\underline{v}$ shall satisfy the following

$$\begin{aligned}
\underline{v}=\alpha_0\zeta-\frac{1}{2}\int_{-\infty}^{x}\partial_x(\alpha_0)\zeta dx+\epsilon\frac{\alpha_1}{2}\zeta^2+\epsilon^2\frac{\alpha_2}{3}\zeta^3+\epsilon^3\frac{\alpha_3}{4}\zeta^4+\mu\varrho\partial_x^2\zeta \\
+\mu\beta\alpha\omega(\partial_x b)^{(\alpha)}\partial_x\zeta+\mu\epsilon\big(\varkappa_1\zeta\partial_x^2\zeta+\varkappa_2(\partial_x\zeta)^2\big),
\end{aligned} \tag{3.49}$$

so that the first equation of (3.41) is satisfied up to $\mathcal{O}(\beta\alpha\epsilon,\beta\alpha^{3/2})$ terms, using the fact that the system is at rest at infinity: $(\zeta,\underline{v}\to 0$ when $x\to\pm\infty)$.

We will proceed now by showing that the coefficients α_i $(i=0,1,2,3)$, ϱ, ω, $\varkappa_1$ and $\varkappa_2$ are precisely chosen so that the second equation of (3.41) is satisfied up to a remainder term $\mathcal{R}$ of size $\mathcal{O}(\mu^2,\mu\epsilon^2,\beta\alpha^{3/2},\beta\alpha\epsilon)$. Indeed, plugging (3.44),(3.45),(3.46),(3.47), (3.48) and (3.49) into

the second equation of (3.41), yields

$$
\begin{aligned}
&\big[-\alpha_0^2(\gamma+c)+(\gamma+\delta)\big]\partial_x\zeta\\
&\quad+\epsilon\big[3(c^2-\gamma)\alpha_0^2-2\alpha_0\alpha_1(\gamma+c)]\zeta\partial_x\zeta\\
&\quad+\epsilon^2\big[6(\gamma+c^3)\alpha_0^2-5(c^2-\gamma)\alpha_0\alpha_1+(\alpha_1^2+2\alpha_0\alpha_2)(\gamma+c)]\zeta^2\partial_x\zeta\\
&\quad+\epsilon^3\big[10(c^4-\gamma)\alpha_0^2-9(c^3+\gamma)\alpha_0\alpha_1+(2\alpha_1^2+\frac{14}{3}\alpha_2\alpha_0)(c^2-\gamma)-2(\alpha_3\alpha_0+\alpha_1\alpha_2)(\gamma+c)]\zeta^3\partial_x\zeta\\
&\quad+\mu\big[-2\varrho(\gamma+c)\alpha_0+\big(d-\beta(\frac{\gamma}{3}f+\frac{2}{3}\delta^{-1}f)b+\beta^2\frac{f}{3}b^2\big)(\gamma+c)\alpha_0^2-\frac{(\gamma+\delta)}{\mathrm{bo}}\big]\partial_x^3\zeta\\
&\quad+\mu\beta\alpha\big[-2\omega(\gamma+c)\alpha_0-(\gamma+c)2\eta_1\alpha_0^2-\beta(\gamma+c)\frac{2\gamma}{3}f'b^{(\alpha)}\alpha_0^2-(\gamma+c)\varrho'\alpha_0\big](\partial_x b)^{(\alpha)}\partial_x^2\zeta\\
&\quad+\mu\epsilon\big[4\varrho(c^2-\gamma)\alpha_0\\
&\qquad-\big(\frac{(\gamma-1)}{3}-2d(\gamma-c^2)+2\eta(\gamma+c)+2\beta(\frac{\gamma}{3}f+\frac{2}{3}\delta^{-1}f)b(\gamma-c^2)-2\beta^2\frac{f}{3}b^2(\gamma-c^2)\big)\alpha_0^2\\
&\qquad+\big(2d(\gamma+c)-2\beta(\frac{\gamma}{3}f+\frac{2}{3}\delta^{-1}f)b(\gamma+c)+2\beta^2\frac{f}{3}b^2(\gamma+c)\big)\alpha_0\alpha_1\\
&\qquad-2\varrho(\gamma+c)\alpha_1-2\varkappa_1(\gamma+c)\alpha_0\big]\zeta\partial_x^3\zeta\\
&\quad+\mu\epsilon\big[2\varrho(c^2-\gamma)\alpha_0\\
&\qquad+\big(\frac{4(1-\gamma)}{3}+6d(\gamma-c^2)-6\eta(\gamma+c)-6\beta(\frac{\gamma}{3}f+\frac{2}{3}\delta^{-1}f)b(\gamma-c^2)+6\beta^2\frac{f}{3}b^2(\gamma-c^2)\big)\alpha_0^2\\
&\qquad+\big(6d(\gamma+c)-6\beta(\frac{\gamma}{3}f+\frac{2}{3}\delta^{-1}f)b(\gamma+c)+6\beta^2\frac{f}{3}b^2(\gamma+c)\big)\alpha_0\alpha_1\\
&\qquad-3\varrho(\gamma+c)\alpha_1-2\varkappa_1(\gamma+c)\alpha_0-4\varkappa_2(\gamma+c)\alpha_0\big]\partial_x\zeta\partial_x^2\zeta\\
&\qquad=\mathcal{R}.
\end{aligned}
\tag{3.50}
$$

In order to cancel the left hand side of (3.50) we set,

$$\alpha_0=\alpha_0(\beta b^{(\alpha)})=\sqrt{\frac{\gamma+\delta}{\gamma+c}},\quad \alpha_1=\alpha_1(\beta b^{(\alpha)})=-\frac{3}{2}\alpha_0\frac{\gamma-c^2}{\gamma+c},\tag{3.51}$$

$$\alpha_2=\alpha_2(\beta b^{(\alpha)})=\frac{-5\alpha_1(\gamma-c^2)-6\alpha_0(\gamma+c^3)}{2(\gamma+c)}-\frac{\alpha_1^2}{2\alpha_0},\tag{3.52}$$

$$\alpha_3=\alpha_3(\beta b^{(\alpha)})=\frac{10(c^4-\gamma)\alpha_0^2-9(c^3+\gamma)\alpha_0\alpha_1+(\frac{14}{3}\alpha_2\alpha_0+2\alpha_1^2)(c^2-\gamma)}{2\alpha_0(\gamma+c)}-\frac{\alpha_1\alpha_2}{\alpha_0},\tag{3.53}$$

$$\varrho=\varrho(\beta b^{(\alpha)})=\frac{d}{2}\alpha_0-\frac{\gamma+\delta}{2\mathrm{bo}(\gamma+\mathrm{c})\alpha_0}-\frac{\beta(\gamma+2\delta^{-1})fb\alpha_0}{6}+\frac{\beta^2fb^2\alpha_0}{6},\tag{3.54}$$

$$\omega=\omega(\beta b^{(\alpha)})=-\eta_1\alpha_0-\beta\frac{\gamma}{3}f'b^{(\alpha)}\alpha_0-\frac{\varrho'}{2},\tag{3.55}$$

$$\varkappa_1=\varkappa_1(\beta b^{(\alpha)})=\frac{4(c^2-\gamma)\varrho+\big[\frac{(1-\gamma)}{3}+2\mathcal{A}\big]\alpha_0+2\mathcal{B}\alpha_1}{2(\gamma+c)}-\frac{\varrho\alpha_1}{\alpha_0},\tag{3.56}$$

$$\varkappa_2=\varkappa_2(\beta b^{(\alpha)})=\frac{(c^2-\gamma)\varrho+[\frac{2(1-\gamma)}{3}+3\mathcal{A}]\alpha_0+3\mathcal{B}\alpha_1}{2(\gamma+c)}-\frac{3\varrho\alpha_1}{4\alpha_0}-\frac{\varkappa_1}{2},\tag{3.57}$$

where we denote,

$$\mathcal{A} = \mathcal{A}(\beta b^{(\alpha)}) = d(\gamma - c^2) - \eta(\gamma + c) - \beta(\frac{\gamma}{3} f + \frac{2}{3}\delta^{-1} f) b(\gamma - c^2) + \beta^2 \frac{f}{3} b^2(\gamma - c^2),$$

$$\mathcal{B} = \mathcal{B}(\beta b^{(\alpha)}) = \big(d - \beta(\frac{\gamma}{3} f + \frac{2}{3}\delta^{-1} f) b + \beta^2 \frac{f}{3} b^2\big)(\gamma + c).$$

Let us now demonstrate that one can deduce from (3.48), a large family of models with the same order of precision (in the sense of consistency), taking after the strategies used for instance in [14, 34, 46], and that we review below. Such a large family of models may be used for mathematical purposes, since they might have very different properties (well-posedness, integrability, etc.).

BBM trick (Benjamin-Bona-Mahony [9]). We make use of the first approximation of (3.48):

$$\partial_t \zeta + \alpha_0 \partial_x \zeta + \frac{1}{2}\partial_x(\alpha_0)\zeta + \epsilon\alpha_1 \zeta \partial_x \zeta = \mathcal{O}(\mu, \epsilon^2),$$

so that one has, for any $\theta \in \mathbb{R}$,

$$\partial_x \zeta = (1-\theta)\partial_x \zeta - \frac{\theta}{\alpha_0}(\partial_t \zeta + \epsilon\alpha_1 \zeta \partial_x \zeta + \frac{1}{2}\partial_x(\alpha_0)\zeta) + \mathcal{O}(\mu, \epsilon^2).$$

Plugging this identity into (3.48) yields

$$\begin{aligned}\partial_t \zeta + \alpha_0 \partial_x \zeta + \frac{1}{2}\partial_x(\alpha_0)\zeta + \epsilon\alpha_1 \zeta \partial_x \zeta + \epsilon^2 \alpha_2 \zeta^2 \partial_x \zeta + \epsilon^3 \alpha_3 \zeta^3 \partial_x \zeta + \mu(1-\theta)\varrho \partial_x^3 \zeta - \mu\varrho\frac{\theta}{\alpha_0}\partial_x^2 \partial_t \zeta \\ + \mu\beta\alpha\big(\omega + \varrho' - \frac{\varrho}{2}\frac{\theta}{\alpha_0}\alpha_0'\big)(\partial_x b)^{(\alpha)}\partial_x^2 \zeta + \mu\epsilon\partial_x\big((\varkappa_1 - \theta\varrho\frac{\alpha_1}{\alpha_0})\zeta\partial_x^2\zeta + (\varkappa_2 - \theta\varrho\frac{\alpha_1}{\alpha_0})(\partial_x\zeta)^2\big) \\ = \mathcal{O}(\mu^2, \mu\epsilon^2, \beta\alpha^{3/2}, \beta\alpha\epsilon)\end{aligned} \tag{3.58}$$

Near identity change of variable. Let us consider

$$\zeta_{\theta,\lambda} \equiv \zeta_\theta - \mu\varrho\lambda\partial_x^2\zeta_\theta,$$

with ζ_θ satisfying (3.58) (with zero on the right hand side). Then $\zeta_{\theta,\lambda}$ satisfies

$$\begin{aligned}\partial_t \zeta + \alpha_0 \partial_x \zeta + \frac{1}{2}\partial_x(\alpha_0)\zeta + \epsilon\alpha_1 \zeta \partial_x \zeta + \epsilon^2 \alpha_2 \zeta^2 \partial_x \zeta + \epsilon^3 \alpha_3 \zeta^3 \partial_x \zeta + \mu((1-\theta)\varrho - \alpha_0\lambda\varrho)\partial_x^3 \zeta \\ - \mu(\varrho\frac{\theta}{\alpha_0} + \varrho\lambda)\partial_x^2\partial_t\zeta + \mu\beta\alpha\big(\omega + \varrho' - \frac{\varrho}{2}\frac{\theta}{\alpha_0}\alpha_0' - \alpha_0\varrho'\lambda - \frac{1}{2}\alpha_0'\varrho\lambda\big)(\partial_x b)^{(\alpha)}\partial_x^2\zeta \\ + \mu\epsilon\partial_x\big((\varkappa_1 - \theta\varrho\frac{\alpha_1}{\alpha_0} - \lambda\varrho\alpha_1)\zeta\partial_x^2\zeta + (\varkappa_2 - \theta\varrho\frac{\alpha_1}{\alpha_0})(\partial_x\zeta)^2\big) \\ = \mathcal{O}(\mu^2, \mu\epsilon^2, \beta\alpha^{3/2}, \beta\alpha\epsilon).\end{aligned} \tag{3.59}$$

Now for any $\theta, \lambda \in \mathbb{R}$, then ζ satisfies (3.59) (with zero on the r.h.s).

Remark 5. If we take $\beta = 0$ and $1/\mathrm{bo} = 0$ in (3.59) i.e if we consider a flat bottom with no surface tension, then one can recover the equation obtained by Duchêne in [47].
When $\gamma \to 0$, $\delta \to 1$ and if we take $\beta = 0$ and $1/\mathrm{bo} = 0$ in (3.59), then one recovers the one-fluid model introduced by Constantin and Lannes in [34], with $q = \dfrac{1-\theta}{6}$ and $\lambda = 0$, using notations therein.

One can easily remark that:

$$-\mu\theta\frac{\varrho}{\alpha_0}\partial_x^2\partial_t\zeta = -\mu\theta\partial_x^2\partial_t\zeta - \mu\theta(\frac{\varrho}{\alpha_0}-1)\partial_x^2\partial_t\zeta,$$
$$-\mu\varrho\lambda\partial_x^2\partial_t\zeta = -\mu\lambda\partial_x^2\partial_t\zeta - \mu\lambda(\varrho-1)\partial_x^2\partial_t\zeta,$$

thus after replacing $\partial_t\zeta$ of the second term in the r.h.s of both equalities, by its expression given in (3.59) and neglecting $\mathcal{O}(\mu\epsilon^2,\mu^2,\beta\alpha^{3/2},\beta\alpha\epsilon)$ terms, one gets

$$\begin{aligned}-\mu\theta\frac{\varrho}{\alpha_0}\partial_x^2\partial_t\zeta &= -\mu\theta\partial_x^2\partial_t\zeta + \mu\theta(\varrho-\alpha_0)\partial_x^3\zeta + \mu\epsilon\theta(\frac{\varrho}{\alpha_0}-1)\alpha_1\partial_x((\partial_x\zeta)^2+\zeta\partial_x^2\zeta)\\ &\quad+\mu\beta\alpha\theta(\frac{\varrho}{\alpha_0}-1)\frac{5}{2}(\partial_x b)^{(\alpha)}\alpha_0'\partial_x^2\zeta + \mathcal{O}(\mu\epsilon^2,\mu^2,\beta\alpha^{3/2},\beta\alpha\epsilon),\end{aligned}$$

$$\begin{aligned}-\mu\varrho\lambda\partial_x^2\partial_t\zeta &= -\mu\lambda\partial_x^2\partial_t\zeta + \mu\lambda(\varrho-1)\alpha_0\partial_x^3\zeta + \mu\epsilon\lambda(\varrho-1)\alpha_1\partial_x((\partial_x\zeta)^2+\zeta\partial_x^2\zeta)\\ &\quad+\mu\beta\alpha\lambda(\varrho-1)\frac{5}{2}(\partial_x b)^{(\alpha)}\alpha_0'\partial_x^2\zeta + \mathcal{O}(\mu\epsilon^2,\mu^2,\beta\alpha^{3/2},\beta\alpha\epsilon).\end{aligned}$$

After replacing these two terms in (3.59) by their expressions given above and neglecting $\mathcal{O}(\mu\epsilon^2,\mu^2,\beta\alpha^{3/2},\beta\alpha\epsilon)$ terms, one obtains

$$\begin{aligned}\partial_t\zeta + \alpha_0\partial_x\zeta + \frac{1}{2}\partial_x(\alpha_0)\zeta + \epsilon\alpha_1\zeta\partial_x\zeta + \epsilon^2\alpha_2\zeta^2\partial_x\zeta + \epsilon^3\alpha_3\zeta^3\partial_x\zeta + \mu(\varrho-\theta\alpha_0-\lambda\alpha_0)\partial_x^3\zeta - \mu(\theta+\lambda)\partial_x^2\partial_t\zeta\\ +\mu\beta\alpha\big(\omega+\varrho'+2\varrho\frac{\theta}{\alpha_0}\alpha_0' - \alpha_0\varrho'\lambda - \alpha_0'\theta\frac{5}{2}+2\lambda\varrho\alpha_0' - \frac{5}{2}\alpha_0'\lambda\big)(\partial_x b)^{(\alpha)}\partial_x^2\zeta\\ +\mu\epsilon\partial_x\big((\varkappa_1-\theta\alpha_1-\lambda\alpha_1)\zeta\partial_x^2\zeta + (\varkappa_2-\theta\alpha_1+\lambda(\varrho-1)\alpha_1)(\partial_x\zeta)^2\big) = 0.\end{aligned} \tag{3.60}$$

Remark 6. It is more advantageous to use the above equation in the study of the well-posedness of the Cauchy problem of (3.59) since the coefficient of the $(\partial_x^2\partial_t\zeta)$ term is no more variable. This new equation shares the same order of precision $\mathcal{O}(\epsilon^4,\mu\epsilon^2,\beta\alpha^{3/2},\beta\alpha\epsilon)$ as the standard one. When $\gamma\to 0$, $\delta\to 1$ and if we take $\beta\alpha=\mathcal{O}(\mu)$ and $1/\mathrm{bo}=0$ in (3.60), then one recovers the one-fluid model introduced in [71], with $q=\frac{1}{6}-\theta$ and $\lambda=0$, using notations therein.

Remark 7. Following [34] and [71], one could of course derive the unidirectional approximation on the velocity instead of the one on the deformation of the interface but the result is fundamentally the same and calculations are pretty complex in that case.

3.8 Mathematical analysis of the unidirectional approximation

3.8.1 Consistency

This section is dedicated to the study of the accuracy of the unidirectional approximate solution derived in section 3.7, in the Camassa-Holm regime. We show that, under some restrictions on the set of admissible dimensionless parameters, families of solutions of the unidirectional approximation (3.62) satisfies the Green-Naghdi system (3.6) up to a small residual, $\mathcal{O}(\mu^2)$. The restrictions on the set of admissible parameters $\mathsf{p}\in\mathcal{P}$ are as follows:

$$\epsilon=\mathcal{O}(\sqrt{\mu}),\quad \beta\alpha=\mathcal{O}(\sqrt{\mu}),\quad \beta\alpha^{3/2}=\mathcal{O}(\mu^2),\quad \beta\alpha\epsilon=\mathcal{O}(\mu^2). \tag{3.61}$$

We state here an L^∞-consistency result under very general assumptions on the topography parameters β and α (see (3.61)). H^s-consistency and full justification of the models will then be achieved under additional assumptions.

Proposition 13 (L^∞-Consistency)**.** *Let $b \in H^\infty(\mathbb{R})$ and set $\theta, \lambda \in \mathbb{R}$. For all family $\mathcal{P}$ of parameters p satisfying* (3.61)*, denote $(\zeta^{\mathsf{p}})_{\mathsf{p}\in\mathcal{P}} \in L^\infty([0, \frac{T}{\max(\epsilon,\beta\alpha)}], H^{s+5})$ with $s > 3/2$ the unique solution given by Theorem 3.8.2 of the equation,*

$$\partial_t\zeta + \alpha_0\partial_x\zeta + \frac{1}{2}\partial_x(\alpha_0)\zeta + \epsilon\alpha_1\zeta\partial_x\zeta + \epsilon^2\alpha_2\zeta^2\partial_x\zeta + \epsilon^3\alpha_3\zeta^3\partial_x\zeta + \mu\varrho^{\theta,\lambda}\partial_x^3\zeta - \mu(\theta+\lambda)\partial_x^2\partial_t\zeta$$
$$+\mu\beta\alpha\omega^{\theta,\lambda}(\partial_x b)^{(\alpha)}\partial_x^2\zeta + \mu\epsilon\partial_x\big(\varkappa_1^{\theta,\lambda}\zeta\partial_x^2\zeta + \varkappa_2^{\theta,\lambda}(\partial_x\zeta)^2\big) = 0, \qquad (3.62)$$

where α_i $(i = 0, 1, 2, 3)$ are precisely defined in (3.51)*,* (3.52) *and* (3.53)*,*
$\varrho^{\theta,\lambda} = \varrho - \theta\alpha_0 - \lambda\alpha_0$, $\omega^{\theta,\lambda} = \omega + \varrho' + 2\varrho\frac{\theta}{\alpha_0}\alpha_0' - \alpha_0\varrho'\lambda - \alpha_0'\theta\frac{5}{2} + 2\lambda\varrho\alpha_0' - \frac{5}{2}\alpha_0'\lambda$, $\varkappa_1^{\theta,\lambda} = \varkappa_1 - \theta\alpha_1 - \lambda\alpha_1$ *and* $\varkappa_2^{\theta,\lambda} = \varkappa_2 - \theta\alpha_1 + \lambda(\varrho - 1)\alpha_1$*. with ϱ, ω, $\varkappa_1$ and $\varkappa_2$ precisely defined in* (3.54),(3.55),(3.56) *and* (3.57)*.*

For given $M^*, h > 0$, we assume that there exists $T > 0$ such that $\|\zeta^{\mathsf{p}}\|_{L^\infty([0,\frac{T}{\max(\epsilon,\beta\alpha)}],H^{s+5})} \le M^*$ and for any $(t, x) \in [0, \frac{T}{\max(\epsilon,\beta\alpha)}] \times \mathbb{R}$,

$$h_1 = 1 - \epsilon\zeta^{\mathsf{p}} \ge h > 0, \quad h_2 = 1/\delta + \epsilon\zeta^{\mathsf{p}} - \beta b^{(\alpha)} \ge h > 0. \qquad (H1)$$

We define v^{p} as $v^{\mathsf{p}} = \dfrac{h_1 + \gamma h_2}{h_1 h_2}\underline{v}[\zeta^{\mathsf{p}}]$, with

$$\underline{v}[\zeta] = \alpha_0\zeta - \frac{1}{2}\int_{-\infty}^{x}\partial_x(\alpha_0)\zeta dx + \epsilon\frac{\alpha_1}{2}\zeta^2 + \epsilon^2\frac{\alpha_2}{3}\zeta^3 + \epsilon^3\frac{\alpha_3}{4}\zeta^4 + \mu\varrho\partial_x^2\zeta$$
$$+\mu\beta\alpha\omega(\partial_x b)^{(\alpha)}\partial_x\zeta + \mu\epsilon\big(\varkappa_1\zeta\partial_x^2\zeta + \varkappa_2(\partial_x\zeta)^2\big).$$

Then $(\zeta^{\mathsf{p}}, v^{\mathsf{p}})$ is L^∞-consistent with the Green-Naghdi system (3.6)*, on $[0, \frac{T}{\max(\epsilon,\beta\alpha)}]$, with precision $\mathcal{O}(\mu^2)$.*

Before stating the proof of Proposition 13 we introduce the following Lemma.

Lemma 3.8.1. *With ζ and b as in the statement of Proposition 13, the mapping $(t, x) \longrightarrow \int_{-\infty}^{x}\partial_x(\alpha_0)\zeta dx$ is well defined on $[0, \frac{T}{\max(\epsilon,\beta\alpha)}] \times \mathbb{R}$. Moreover one has that*

$$\Big|\int_{-\infty}^{x}\partial_x(\alpha_0)\zeta dx\Big|_{L^\infty([0,\frac{T}{\max(\epsilon,\beta\alpha)}]\times\mathbb{R})} \le Cst\ \sqrt{\alpha}\beta|\partial_x b|_2|\zeta|_2.$$

Proof. We used here the Cauchy-Schwarz inequality and the definition of $\alpha_0^2 = \dfrac{(\gamma+\delta)(1-\delta\beta b^{(\alpha)})}{\gamma(1-\delta\beta b^{(\alpha)})+\delta}$ in (3.51) to get

$$\int_{-\infty}^{x}\partial_x(\alpha_0)\zeta dx \le Cst\ \alpha\beta|(\partial_x b)^{(\alpha)}|_2|\zeta|_2 \le Cst\ \sqrt{\alpha}\beta|\partial_x b|_2|\zeta|_2.$$

□

Let us continue now by stating the proof of Proposition 13.

Proof. Let us denote first by $\mathcal{O}(\mu)$ any family of functions $(f^{\mathsf{p}})_{\mathsf{p}\in\mathcal{P}}$ bounded by:

$$|f^{\mathsf{p}}|_{L^\infty([0,\frac{T}{\max(\epsilon,\beta\alpha)}],H^r(\mathbb{R}))}\leq C\mu,$$

with C any positive constant, for all $\mathsf{p}\in\mathcal{P}$ and for different values of r. We denote also by $\mathcal{O}_{L^\infty}(\mu)$ any family of functions $(f^{\mathsf{p}})_{\mathsf{p}\in\mathcal{P}}$ bounded by:

$$|f^{\mathsf{p}}|_{L^\infty([0,\frac{T}{\max(\epsilon,\beta\alpha)}]\times\mathbb{R}))}\leq C\mu.$$

Of course similar notations are used for $\mathcal{O}(\mu^2)$ and $\mathcal{O}_{L^\infty}(\mu^2)$.

Since ζ^{p} is the unique solution of (3.62) and v^{p} is defined as above, it is clear that the first equation of (3.41) is satisfied up to $\mathcal{O}(\beta\alpha\epsilon,\beta\alpha^{3/2})=\mathcal{O}(\mu^2)$ terms, using the fact that the system is at rest at infinity: $\zeta,\underline{v}\to 0$ when $x\to\pm\infty$).

Remarking that the relations $\mathcal{O}(\beta\alpha^{3/2})=\mathcal{O}(\mu^2)$, and $\mathcal{O}(\beta\alpha\epsilon)=\mathcal{O}(\mu^2)$ and using Lemma 3.8.1 imply that

$$-\int_{-\infty}^{x}\partial_x(\alpha_0)\partial_t\zeta dx=\partial_x(\alpha_0)\alpha_0\zeta+\mathcal{O}_{L^\infty}(\mu^2),$$

then the remainder $\mathcal{R}$ in (3.50) can be bounded in $L^\infty([0,\frac{T}{\max(\epsilon,\beta\alpha)}]\times\mathbb{R})$, provided (H1) is satisfied, as

$$\begin{aligned}\big|\mathcal{R}\big|_{L^\infty([0,\frac{T}{\max(\epsilon,\beta\alpha)}]\times\mathbb{R})} &\leq C(h^{-1},\big|b\big|_{H^{s+1}},M^*,M_0)\times\max(\mu^2,\epsilon^4,\mu\epsilon^2,\beta\alpha^{3/2},\beta\alpha\epsilon)\\ &\leq C(h^{-1},\big|b\big|_{H^{s+1}},M^*,M_0)\times\mu^2.\end{aligned}$$

where we denote $M_0=\max\{\mu_{\max},\beta_{\max},\alpha_{\max},\delta_{\min}^{-1},\delta_{\max},\mathrm{bo}_{\min}^{-1}\}$.

ζ_θ, a solution of (3.58) (with zero on the right hand side), satisfies (3.48) with a remainder bounded by $\mathcal{O}(\max(\mu^2,\mu\epsilon^2,\beta\alpha^{3/2},\beta\alpha\epsilon))$. One can easily check that, defining $\underline{v}_\theta$ as a function of ζ_θ through (3.49), $(\zeta_\theta,\underline{v}_\theta)$ satisfies (3.50) up to a remainder $\mathcal{R}_\theta=\mathcal{O}(\max(\mu^2,\mu\epsilon^2,\beta\alpha^{3/2},\beta\alpha\epsilon))=\mathcal{O}(\mu^2)$. Proposition 13 is now proved for $\theta\in\mathbb{R}$ and $\lambda=0$.

Denoting $\zeta_{\theta,\lambda}$ the solution of (3.59) and defining $\underline{v}_{\theta,\lambda}$ as a function of $\zeta_{\theta,\lambda}$ through (3.49), then $(\zeta_{\theta,\lambda},\underline{v}_{\theta,\lambda})$ satisfies (3.50) up to a remainder $\mathcal{R}_{\theta,\lambda}=\mathcal{O}(\max(\mu^2,\mu\epsilon^2,\beta\alpha^{3/2},\beta\alpha\epsilon))=\mathcal{O}(\mu^2)$. Proposition 13 is now proved for any $\theta,\lambda\in\mathbb{R}$. □

3.8.2 Well-posedness

In this section we are going to study the well-posedness of a general Cauchy problem rather than solving the initial value problem of the scalar evolution equation (3.62). Relying on a precise study of the energy estimates of the linearized system, we demonstrate here the existence and uniqueness of family of solutions of the following general class of equations,

$$\begin{aligned}(1-\mu m\partial_x^2)\partial_t\zeta+a_0\partial_x\zeta+a_1\zeta+F(\epsilon\zeta)\partial_x\zeta+\mu\beta\alpha a_2\partial_x^2\zeta+\mu a_3\partial_x^3\zeta+\mu\epsilon a_4\zeta\partial_x^3\zeta\\ +\mu\epsilon\partial_x(a_5\zeta)\partial_x^2\zeta+\mu\epsilon\partial_x^2(a_5\zeta)\partial_x\zeta=0,\end{aligned}\tag{3.63}$$

where $m>0$, $a_i=a_i(\beta b^{(\alpha)})$ are smooth enough functions of $\beta b^{(\alpha)}$ and F a smooth mapping defined in a neighborhood of the origin, and vanishing at the origin.

In fact, taking $m=\theta+\lambda$, $a_0=\alpha_0$, $a_1=\dfrac{1}{2}\partial_x(\alpha_0)$, $F(x)=\alpha_1x+\alpha_2x^2+\alpha_3x^3$, $a_2=\omega^{\theta,\lambda}(\partial_xb)^{(\alpha)}$, $a_3=\varrho^{\theta,\lambda}$, $a_4=\varkappa_1^{\theta,\lambda}$, and $a_5=\dfrac{\varkappa_1^{\theta,\lambda}+2\varkappa_2^{\theta,\lambda}}{2}$, one recovers the equation given in (3.62).

We have to study the initial value problem beneath on a time scale $\mathcal{O}(\frac{1}{\max(\epsilon,\beta\alpha)})$.

$$\begin{cases} (1-\mu m\partial_x^2)\partial_t\zeta + a_0\partial_x\zeta + a_1\zeta + F(\epsilon\zeta)\partial_x\zeta + \mu\beta\alpha a_2\partial_x^2\zeta + \mu a_3\partial_x^3\zeta + \mu\epsilon a_4\zeta\partial_x^3\zeta \\ \qquad\qquad +\mu\epsilon\partial_x(a_5\zeta)\partial_x^2\zeta + \mu\epsilon\partial_x^2(a_5\zeta)\partial_x\zeta = 0, \\ \\ \zeta_{|t=0} = \zeta^0. \end{cases} \tag{3.64}$$

However, it is necessary to have $m > 0$, as our proof relies heavily on some precise energy estimates of the solution. To this end, we define the energy space X^s as $X^{s+1}(\mathbb{R}) = H^{s+1}(\mathbb{R})$ endowed with the following norm:

$$|\zeta|^2_{X^{s+1}} = |\zeta|^2_{H^s} + \mu m|\partial_x\zeta|^2_{H^s}.$$

Theorem 3.8.2 (Well-posedness)**.** *Let $s > 3/2$, $m > 0$ and $b \in H^\infty(\mathbb{R})$. For all family $\mathcal{P}$ of parameters p satisfying* (3.61) *and for all $\zeta^0 \in H^{s+1}$, there exists a time $T > 0$ and a unique family of solutions $(\zeta^{\mathsf{p}})_{\mathsf{p}\in\mathcal{P}}$ to* (3.64) *in $C([0, \frac{T}{\max(\epsilon,\beta\alpha)}], X^{s+1}(\mathbb{R})) \cap C^1([0, \frac{T}{\max(\epsilon,\beta\alpha)}], X^s(\mathbb{R}))$.*

Remark 8. To prove the well-posedness of our scalar evolution equation (3.62) which is a particular case of (3.63), we assume an infinity smooth bottom i.e $b \in H^\infty(\mathbb{R})$ for the sake of simplicity. Actually, we do not try to give some optimal regularity assumption on the bottom parametrization b. This could easily be done, but is of no interest for our present purpose.

Proof. For any smooth enough v, we define the "linearized" operator:

$$\begin{aligned}\mathcal{L}(v,\partial) = (1-\mu m\partial_x^2)\partial_t + a_0\partial_x + a_1 + F(\epsilon v)\partial_x + \mu\beta\alpha a_2\partial_x^2 + \mu a_3\partial_x^3 \\ +\mu\epsilon a_4 v\partial_x^3 + \mu\epsilon\partial_x(a_5 v)\partial_x^2 + \mu\epsilon\partial_x^2(a_5 v)\partial_x\end{aligned}$$

and the following initial value problem:

$$\begin{cases} \mathcal{L}(v,\partial)\zeta = \epsilon f, \\ \\ \zeta_{|t=0} = \zeta^0. \end{cases} \tag{3.65}$$

Existence and uniqueness of a solution to the linear system (3.65) are achieved in the same way as in [72, Appendix A] and we thus focus our attention on the proof of the energy estimates given in terms of the $|\ .\ |_{X^{s+1}}$ norm introduced above.
Differentiating $\frac{1}{2}e^{-\max(\epsilon,\beta\alpha)\lambda t}|\zeta|^2_{X^{s+1}}$ with respect to time, one gets using (3.65) and integrating by parts:

$$\begin{aligned}\frac{1}{2}e^{\max(\epsilon,\beta\alpha)\lambda t}\partial_t(e^{-\max(\epsilon,\beta\alpha)\lambda t}|\zeta|^2_{X^{s+1}}) \quad &= \quad -\frac{\max(\epsilon,\beta\alpha)\lambda}{2}|\zeta|^2_{X^{s+1}} - (\Lambda^s(a_0\partial_x\zeta),\Lambda^s\zeta) \\ &- (\Lambda^s(a_1\zeta),\Lambda^s\zeta) - \epsilon(\Lambda^s(V\partial_x\zeta),\Lambda^s\zeta) \\ &- \mu\beta\alpha(\Lambda^s(a_2\partial_x^2\zeta),\Lambda^s\zeta) - \mu(\Lambda^s(a_3\partial_x^3\zeta),\Lambda^s\zeta) \\ &- \mu\epsilon(\Lambda^s(a_4 v\partial_x^3\zeta),\Lambda^s\zeta) - \mu\epsilon\big(\Lambda^s((a_5 v)_x\partial_x\zeta),\Lambda^s\partial_x\zeta\big) \\ &+ \epsilon(\Lambda^s f,\Lambda^s\zeta),\end{aligned}$$

where $\Lambda = (1-\partial_x^2)^{1/2}$ and $V = \frac{1}{\epsilon}F(\epsilon v)$. Using the fact that for all skew-symmetric operator T (that is, $T^* = -T$), and all h smooth enough, one has that

$$(\Lambda^s(hTu),\Lambda^s u) = ([\Lambda^s,h]Tu,\Lambda^s u) - \frac{1}{2}([T,h]\Lambda^s u,\Lambda^s u),$$

we deduce applying this identity with ($T = \partial_x$ and $T = \partial_x^3$) and integrating by parts,

$$\begin{aligned}
\frac{1}{2}e^{\max(\epsilon,\beta\alpha)\lambda t}\partial_t(e^{-\max(\epsilon,\beta\alpha)\lambda t}|\zeta|^2_{X^{s+1}}) &= -\frac{\max(\epsilon,\beta\alpha)\lambda}{2}|\zeta|^2_{X^{s+1}} - ([\Lambda^s, a_0]\partial_x\zeta, \Lambda^s\zeta)\\
&+ \frac{1}{2}(\partial_x(a_0)\Lambda^s\zeta, \Lambda^s\zeta) - (\Lambda^s(a_1\zeta), \Lambda^s\zeta)\\
&- \epsilon([\Lambda^s, V]\partial_x\zeta, \Lambda^s\zeta) + \frac{\epsilon}{2}((\partial_x V)\Lambda^s\zeta, \Lambda^s\zeta)\\
&- \mu\beta\alpha([\Lambda^s, a_2]\partial_x^2\zeta, \Lambda^s\zeta) + \mu\beta\alpha(a_2\Lambda^s\partial_x\zeta, \Lambda^s\partial_x\zeta)\\
&+ \mu\beta\alpha(\partial_x(a_2)\Lambda^s\zeta, \Lambda^s\partial_x\zeta)\\
&- \mu([\Lambda^s, a_3]\partial_x^2\zeta - \frac{3}{2}\partial_x a_3\Lambda^s\partial_x\zeta - \partial_x^2 a_3\Lambda^s\zeta, \Lambda^s\partial_x\zeta)\\
&- \mu([\Lambda^s, \partial_x a_3]\partial_x^2\zeta, \Lambda^s\zeta)\\
&- \mu\epsilon([\Lambda^s, a_4 v]\partial_x^2\zeta - \frac{3}{2}\partial_x(a_4 v)\Lambda^s\partial_x\zeta - \partial_x^2(a_4 v)\Lambda^s\zeta, \Lambda^s\partial_x\zeta)\\
&- \mu\epsilon([\Lambda^s, \partial_x(a_4 v)]\partial_x^2\zeta, \Lambda^s\zeta) - \mu\epsilon\big(\Lambda^s((a_5 v)_x\partial_x\zeta), \Lambda^s\partial_x\zeta\big)\\
&+ \epsilon(\Lambda^s f, \Lambda^s\zeta).
\end{aligned} \tag{3.66}$$

Here we used similarly the following identities, for all h smooth enough one has that

$$[\Lambda^s, h]\partial_x^3\zeta = \partial_x([\Lambda^s, h]\partial_x^2\zeta) - [\Lambda^s, \partial_x h]\partial_x^2\zeta,$$

$$\frac{1}{2}(\partial_x^3 h\Lambda^s\zeta, \Lambda^s\zeta) = -(\partial_x^2 h\Lambda^s\zeta, \Lambda^s\partial_x\zeta).$$

We now turn to estimating the different terms of the r.h.s. of the previous identity (3.66).

Since $|\zeta|_{H^s} \leq |\zeta|_{X^{s+1}}$ and $\sqrt{\mu}|\partial_x\zeta|_{H^s} \leq \frac{1}{\sqrt{m}}|\zeta|_{X^{s+1}}$, one gets directly by the Cauchy–Schwarz inequality

$$\begin{aligned}
e^{\max(\epsilon,\beta\alpha)\lambda t}\partial_t(e^{-\max(\epsilon,\beta\alpha)\lambda t}|\zeta|^2_{X^{s+1}}) \leq C(\mu_{\max}, \frac{1}{m})(A(\zeta, v)|\zeta|_{X^{s+1}} + B(v)|\zeta|^2_{X^{s+1}}) - \max(\epsilon, \beta\alpha)\lambda|\zeta|^2_{X^{s+1}}\\
+2\max(\epsilon, \beta\alpha)|f|_{X^{s+1}}|\zeta|_{X^{s+1}},
\end{aligned}$$

with

$$\begin{aligned}
A(\zeta, v) &= |([\Lambda^s, a_0] - \{\Lambda^s, a_0\})\partial_x\zeta|_2 + |\{\Lambda^s, a_0\}\partial_x\zeta|_2 + \epsilon|[\Lambda^s, V]\partial_x\zeta|_2 + \beta\alpha|[\Lambda^s, a_2]\sqrt{\mu}\partial_x^2\zeta|_2\\
&+ |([\Lambda^s, a_3] - \{\Lambda^s, a_3\})\sqrt{\mu}\partial_x^2\zeta|_2 + |\{\Lambda^s, a_3\}\sqrt{\mu}\partial_x^2\zeta|_2 + |[\Lambda^s, \partial_x a_3]\sqrt{\mu}\partial_x^2\zeta|_2\\
&+ \epsilon|[\Lambda^s, a_4 v]\sqrt{\mu}\partial_x^2\zeta|_2 + \epsilon|[\Lambda^s, \sqrt{\mu}\partial_x(a_4 v)]\sqrt{\mu}\partial_x^2\zeta|_2 + \epsilon\sqrt{\mu}|\partial_x(a_5 v)\partial_x\zeta|_{H^s},
\end{aligned}$$

$$\begin{aligned}
B(v) &= |\partial_x a_0|_\infty + |a_1|_{W^{[s]+1,\infty}} + \epsilon|\partial_x V|_\infty + \beta\alpha|a_2|_{W^{1,\infty}}\\
&+ |\partial_x a_3|_{L^\infty} + |\partial_x^2 a_3|_{L^\infty} + \epsilon|a_4 v|_{W^{1,\infty}} + \epsilon\sqrt{\mu}|a_4 v|_{W^{2,\infty}},
\end{aligned}$$

where $[s]$ is the largest integer smaller or equal to s, and for all function G, $\{\Lambda^s, G\}$ stands for the Poisson bracket.

$$\{\Lambda^s, G\} = -s\partial_x G\Lambda^{s-2}\partial_x,$$

Let us recall the following commutator estimates, mainly due to Kato-Ponce [79], and improved by Lannes [82]: for all G and U smooth enough, one has:

$$\forall s > 3/2, \qquad \big|[\Lambda^s, G]U\big|_2 \leq \mathrm{Cst}|\partial_x G|_{H^{s-1}}|U|_{H^{s-1}},$$
$$\big|([\Lambda^s, G] - \{\Lambda^s, G\})U\big|_2 \leq \mathrm{Cst}|\partial_x^2 G|_{H^s}|U|_{H^{s-2}}.$$

We denote that since $s-1 > 1/2$, the imbedding $H^{s-1}(\mathbb{R}) \subset L^\infty(\mathbb{R})$ yields $|\partial_x V|_{H^{s-1}} = |F'(\epsilon v)\partial_x v|_{H^{s-1}} \leq C(F, |v|_{H^s})$. Since, $|\partial_x a_i|_{L^\infty} = \mathcal{O}(\beta\alpha)$ and $|\partial_x^2 a_i|_{H^s} = \mathcal{O}(\beta\alpha)$ (for $i = 0$ and $i = 3$), one can easily check that

$$A(\zeta, v) \leq \max(\epsilon, \beta\alpha) C(\mu_{\max}, \beta_{\max}, \alpha_{\max}, s, m, \frac{1}{m}, |b|_{H^{s'}}, F, |v|_{X^{s+1}})|\zeta|_{X^{s+1}},$$

and

$$B(v) \leq \max(\epsilon, \beta\alpha) C(\mu_{\max}, \beta_{\max}, \alpha_{\max}, s, m, \frac{1}{m}, |b|_{H^{s'}}, F, |v|_{X^{s+1}}),$$

for some $s' > s + 1/2$ large enough.

Therefore we obtain

$$e^{\max(\epsilon,\beta\alpha)\lambda t}\partial_t(e^{-\max(\epsilon,\beta\alpha)\lambda t}|\zeta|^2_{X^{s+1}}) \leq \max(\epsilon, \beta\alpha)(C(\mu_{\max}, \beta_{\max}, \alpha_{\max}, s, m, \frac{1}{m}, |b|_{H^{s'}}, F, |v|_{X^{s+1}}) - \lambda)|\zeta|^2_{X^{s+1}}$$
$$+2\max(\epsilon, \beta\alpha)|f|_{X^{s+1}}|\zeta|_{X^{s+1}}.$$

Thanks to the above inequality, one can choose $\lambda = \lambda_T$ large enough (how large depends on $\sup_{t\in[0,\frac{T}{\max(\epsilon,\beta\alpha)}]} C(\mu_{\max}, \beta_{\max}, \alpha_{\max}, s, m, \frac{1}{m}, |b|_{H^{s'}}, F, |v|_{X^{s+1}})$) so that the first term of the right-hand side of the above inequality to be negative for all $t \in [0, \frac{T}{\max(\epsilon,\beta\alpha)}]$, one deduces

$$\partial_t(e^{-\max(\epsilon,\beta\alpha)\lambda_T t}|\zeta|^2_{X^{s+1}}) \leq 2\max(\epsilon, \beta\alpha)e^{-\max(\epsilon,\beta\alpha)\lambda_T t}|f|_{X^{s+1}}|\zeta|_{X^{s+1}}.$$

Integrating this differential inequality yields

$$\forall t \in [0, \frac{T}{\max(\epsilon, \beta\alpha)}], \quad |\zeta(t)|_{X^{s+1}} \leq e^{\max(\epsilon,\beta\alpha)\lambda_T t}|\zeta^0|_{X^{s+1}} + 2\max(\epsilon, \beta\alpha)\int_0^t e^{\max(\epsilon,\beta\alpha)\lambda_T(t-t')}|f(t')|_{X^{s+1}}dt'.$$

Thanks to this energy estimate, we classically conclude (see e.g. [1]) to the existence of a time:

$$T = T(|\zeta^0|_{X^{s+1}}) > 0,$$

and a unique solution $\zeta \in C([0, \frac{T}{\max(\epsilon,\beta\alpha)}], X^{s+1}(\mathbb{R}))$ to (3.64) as the limit of the iterative scheme:

$$\zeta_0 = \zeta^0, \quad \text{and} \quad \forall n \in \mathbb{N}, \quad \begin{cases} \mathcal{L}(\zeta^n, \partial)\zeta^{n+1} = 0, \\ \\ \zeta^{n+1}_{|t=0} = \zeta^0. \end{cases}$$

Since ζ solves (3.63), we have $\mathcal{L}(\zeta, \partial)\zeta = 0$ and therefore

$$(\Lambda^{s-1}(1 - \mu m\partial_x^2)\partial_t\zeta, \Lambda^{s-1}\partial_t\zeta) = -(\Lambda^{s-1}\mathcal{K}(\zeta, \partial)\zeta, \Lambda^{s-1}\partial_t\zeta),$$

with $\mathcal{K}(\zeta, \partial) = \mathcal{L}(\zeta, \partial) - (1 - \mu m\partial_x^2)\partial_t$. Proceeding as above, one gets

$$|\partial_t\zeta|_{X^s} \leq C(|\zeta^0|_{X^{s+1}}, |\zeta|_{X^{s+1}}),$$

and it follows that the family of solution is also bounded in $C^1([0, \frac{T}{\max(\epsilon,\beta\alpha)}], X^s(\mathbb{R}))$. □

3.8.3 Wave breaking

It is known that the family of equations related to (3.62), can create singularities in finite time for a smooth initial data only in the form of wave breaking (see [34] for the free surface over flat topography case). There is two types of wave breaking, the first called "surging", if there exists a time $0 < T < \infty$ and solution ζ such that

$$\zeta \in L^\infty([0,T]\times\mathbb{R}) \quad \text{and} \quad \sup_{x\in\mathbb{R}}\{\partial_x\zeta(t,x)\} \to \infty \quad \text{as} \quad t \to T.$$

The second called "plunging", if there exists a time $0 < T < \infty$ and solution ζ such that

$$\zeta \in L^\infty([0,T]\times\mathbb{R}) \quad \text{and} \quad \inf_{x\in\mathbb{R}}\{\partial_x\zeta(t,x)\} \to -\infty \quad \text{as} \quad t \to T.$$

As in the one-layer case [71, Proposition 4], it is conceivable to give some facts on the explosion profile for the equation (3.62) for the interface between two layers of fluids. Indeed, diverse type of wave breaking are acquired under some particular conditions on the coefficients in (3.62) and under additional restriction on the parameter $\beta = \mathcal{O}(\mu^{3/2})$, thus the equation (3.62) reads after neglecting the $\mathcal{O}(\mu^2)$ terms:

$$\partial_t\zeta + \alpha_0\partial_x\zeta + \frac{1}{2}\partial_x(\alpha_0)\zeta + \epsilon\alpha_1\zeta\partial_x\zeta + \epsilon^2\alpha_2\zeta^2\partial_x\zeta + \epsilon^3\alpha_3\zeta^3\partial_x\zeta + \mu\varrho^{\theta,\lambda}\partial_x^3\zeta - \mu(\theta+\lambda)\partial_x^2\partial_t\zeta$$
$$+\mu\epsilon\partial_x\big(\varkappa_1^{\theta,\lambda}\zeta\partial_x^2\zeta + \varkappa_2^{\theta,\lambda}(\partial_x\zeta)^2\big) = 0, \qquad (3.67)$$

with

$$\alpha_0 = \alpha_0(\beta b^{(\alpha)}) = \sqrt{\frac{\gamma+\delta}{\gamma+c}}, \quad \alpha_1 = -\frac{3}{2}\frac{\gamma-\delta^2}{\gamma+\delta}, \quad \alpha_2 = \frac{21(\delta^2-\gamma)^2}{8(\gamma+\delta)^2} - \frac{3(\delta^3+\gamma)}{\gamma+\delta},$$
$$\alpha_3 = \frac{71(\delta^2-\gamma)^3}{16(\gamma+\delta^3)} - \frac{37(\delta^2-\gamma)(\delta^3+\gamma)}{4(\gamma+\delta)^2} + \frac{5(\delta^4-\gamma)}{\gamma+\delta}, \quad \varrho = \frac{1+\gamma\delta}{6\delta(\gamma+\delta)}, \quad \varrho^{\theta,\lambda} = \varrho - \frac{1}{2\text{bo}} - \theta - \lambda,$$

$$\varkappa_1^{\theta,\lambda} = \frac{4(\delta^2-\gamma)\varrho - \frac{1-\gamma}{3} + \alpha_1\frac{2(1+\gamma\delta)}{3\delta}}{2(\gamma+\delta)} - (\theta+\lambda)\alpha_1,$$

$$\varkappa_2^{\theta,\lambda} = \frac{(\delta^2-\gamma)\varrho - \frac{1-\gamma}{3} + \alpha_1\frac{(1+\gamma\delta)}{\delta}}{2(\gamma+\delta)} - \frac{3\varrho\alpha_1}{4} - \frac{\varkappa_1}{2} - (\theta+(1-\varrho)\lambda)\alpha_1.$$

Proposition 14. *Let $b \in H^\infty(\mathbb{R})$, $\zeta_0 \in H^3(\mathbb{R})$. If the maximal time of existence $T_m > 0$ of ζ solution of (3.67) with initial profile $\zeta(0,.) = \zeta_0$ is finite, then*

• *If $\theta+\lambda > 0$, $\alpha_3 > 0$ and $\varkappa_1^{\theta,\lambda} = 2\varkappa_2^{\theta,\lambda} > 0$, in finite time the singularities are of surging wave breaking type.*

• *If $\theta+\lambda > 0$, $\alpha_3 < 0$ and $\varkappa_1^{\theta,\lambda} = 2\varkappa_2^{\theta,\lambda} < 0$, in finite time the singularities are of plunging wave breaking type.*

Proof. The proof of [71, Proposition 4] can easily be adapted to more general coefficients in order to prove this Proposition, so we omit the proof here. □

3.8.4 Full justification

In the following section we will give a full justification of the unidirectional equation (3.62), under the following restrictions on the parameters ϵ, β, α, and μ:

$$\epsilon = \mathcal{O}(\sqrt{\mu}), \quad \beta\alpha = \mathcal{O}(\mu^2). \tag{3.68}$$

Under these stronger restrictions we are able to control the secular growth effects that prevented us from achieving the H^s-consistency and the full justification. We state here the H^s-consistency result:

Proposition 15 (H^s-Consistency)**.** *Let $b \in H^\infty(\mathbb{R})$ and set $\theta, \lambda \in \mathbb{R}$. For all family $\mathcal{P}$ of parameters p satisfying (3.68), denote $(\zeta^{\mathsf{p}})_{\mathsf{p}\in\mathcal{P}} \in L^\infty([0, \frac{T}{\epsilon}], H^{s+5})$ with $s > 3/2$ the unique solution given by Theorem 3.8.2 of the equation*

$$\begin{aligned}\partial_t\zeta + \alpha_0\partial_x\zeta + \epsilon\alpha_1\zeta\partial_x\zeta + \epsilon^2\alpha_2\zeta^2\partial_x\zeta + \epsilon^3\alpha_3\zeta^3\partial_x\zeta + \mu\varrho^{\theta,\lambda}\partial_x^3\zeta - \mu(\theta+\lambda)\partial_x^2\partial_t\zeta \\ +\mu\epsilon\partial_x\big(\varkappa_1^{\theta,\lambda}\zeta\partial_x^2\zeta + \varkappa_2^{\theta,\lambda}(\partial_x\zeta)^2\big) = 0,\end{aligned} \tag{3.69}$$

where α_i $(i = 0, 1, 2, 3)$ are precisely defined in (3.51), (3.52) and (3.53), $\varrho^{\theta,\lambda} = \varrho - \theta\alpha_0 - \lambda\alpha_0$, $\varkappa_1^{\theta,\lambda} = \varkappa_1 - \theta\alpha_1 - \lambda\alpha_1$ and $\varkappa_2^{\theta,\lambda} = \varkappa_2 - \theta\alpha_1 + \lambda(\varrho - 1)\alpha_1$. with ϱ, $\varkappa_1$ and $\varkappa_2$ precisely defined in (3.54),(3.56) and (3.57).

For given $M^*, h > 0$, we assume that there exists $T > 0$ such that $\|\zeta^{\mathsf{p}}\|_{L^\infty([0,\frac{T}{\epsilon}],H^{s+5})} \leq M^*$ and for any $(t, x) \in [0, \frac{T}{\epsilon}] \times \mathbb{R}$,

$$h_1 = 1 - \epsilon\zeta^{\mathsf{p}} \geq h > 0, \quad h_2 = 1/\delta + \epsilon\zeta^{\mathsf{p}} - \beta b^{(\alpha)} \geq h > 0. \tag{H1}$$

We define v^{p} as $v^{\mathsf{p}} = \dfrac{h_1 + \gamma h_2}{h_1 h_2}\underline{v}[\zeta^{\mathsf{p}}]$, with

$$\underline{v}[\zeta] = \alpha_0\zeta + \epsilon\frac{\alpha_1}{2}\zeta^2 + \epsilon^2\frac{\alpha_2}{3}\zeta^3 + \epsilon^3\frac{\alpha_3}{4}\zeta^4 + \mu\varrho\partial_x^2\zeta + \mu\epsilon\big(\varkappa_1\zeta\partial_x^2\zeta + \varkappa_2(\partial_x\zeta)^2\big), \tag{3.70}$$

where α_i $(i = 0, 1, 2, 3)$ are as above, and $\varrho = \varrho^{0,0}$, $\varkappa_1 = \varkappa_1^{0,0}$, $\varkappa_2 = \varkappa_2^{0,0}$.

Then $(\zeta^{\mathsf{p}}, v^{\mathsf{p}})$ is H^s-consistent with the Green-Naghdi system (3.6), on $[0, \frac{T}{\epsilon}]$, with precision $\mathcal{O}(\mu^2)$.

Proof. The proposition is obtained using the same techniques of the proof of Proposition 13, but under the stronger restrictions in (3.68), we remark that there is no $\partial_x\alpha_0\zeta$ term in the proof of Proposition 13 and the $\mathcal{O}_{L^\infty}(\mu^2)$ terms are now of order $\mathcal{O}(\mu^2)$ in $L^\infty([0, \frac{T}{\epsilon}], H^s(\mathbb{R}))$. Therefore there is no need of $\partial_x\alpha_0\zeta$ in the definition of $\underline{v}$ in (3.70). □

Remark 9. Following the proof of Proposition 12, one can easily check that the result of Proposition 15 holds with regards to our new Green-Naghdi system (3.26) in the present scaling (3.68), therefore we state the following convergence result.

Theorem 3.8.3 (Convergence)**.** *Let $b \in H^\infty(\mathbb{R})$ and set $\theta, \lambda \in \mathbb{R}$. Let $\mathsf{p} \in \mathcal{P}$ satisfy (3.68). Assume the hypothesis of Proposition 15 hold. If $(\theta + \lambda) > 0$, for all $\zeta_0^{\mathsf{p}} \in H^{s+s'}$, with s and s' sufficiently big, the following holds:*

• *There exists a unique family* $(\underline{v}^{\mathsf{p}}, \underline{\zeta}^{\mathsf{p}})_{\mathsf{p}\in\mathcal{P}}$*, uniformly bounded on* H^s *solving the new Green-Naghi equations* (3.26) *over time interval* $[0, \frac{T}{\epsilon}]$*, with initial condition* $(v^{\mathsf{p}}_{|t=0}, \zeta^{\mathsf{p}}_0)$*.*

• *There exists a unique family* $(v^{\mathsf{p}}, \zeta^{\mathsf{p}})_{\mathsf{p}\in\mathcal{P}}$*, given by the resolution of* (3.69) *over time interval* $[0, \frac{T}{\epsilon}]$*, with initial condition* ζ^{p}_0 *and* $v^{\mathsf{p}}_{|t=0}$ *satisfying* (3.70)*.*

Moreover, one has for all $\mathsf{p} \in \mathcal{P}$ *and for any* $t \leq \frac{T}{\epsilon}$*,*

$$|\underline{v}^{\mathsf{p}} - v^{\mathsf{p}}|_{L^\infty([0,t];H^s)} + |\underline{\zeta}^{\mathsf{p}} - \zeta^{\mathsf{p}}|_{L^\infty([0,t];H^s)} \leq Cst\ \mu^2\ t.$$

Proof. The first point of the theorem and the error estimate follow immediately from Theorem 3.6.1 and Theorem 3.6.2. The second point of the theorem is a direct consequence of Theorem 3.8.2. As indicated in Remark 9, we know that $(\zeta^{\mathsf{p}}, v^{\mathsf{p}})_{\mathsf{p}\in\mathcal{P}}$ is H^s-consistent with the new Green-Naghdi system (3.26). □

Remark 10. Our approximate solution described in Proposition 15 is fully justified as approximate solution of the new Green-Naghdi model (3.26). Thanks to Theorem 3.6.3 and Theorem 3.8.3, one can deduce using the triangular inequality that our approximate solution in the Camassa-Holm regime is fully justified as approximate solution of the full Euler system (3.2).

3.9 Full justification of the unidirectional approximation in the long wave regime

In this section, we give a full justification of the unidirectional approximation, restricted to the so-called long wave regime and under some restrictions on the topography variations. In fact, we consider ϵ, β, α and μ satisfying:

$$\epsilon = \mathcal{O}(\mu), \quad \beta\alpha = \mathcal{O}(\sqrt{\mu}), \quad \beta\alpha^{3/2} = \mathcal{O}(\mu^2) \quad \beta\alpha\epsilon = \mathcal{O}(\mu^2). \tag{3.71}$$

The flow can be approximated by neglecting the $\mathcal{O}(\epsilon^2, \mu\epsilon)$ terms in (3.48) and thus one obtains the so-called variable-depth KdV equation with non constant coefficients, which is a generalization of the KdV equation introduced in [46]. The equation is as follows:

$$\partial_t\zeta + \alpha_0\partial_x\zeta + \frac{1}{2}\partial_x(\alpha_0)\zeta + \epsilon\alpha_1\zeta\partial_x\zeta + \mu\varrho\partial_x^3\zeta + \mu\beta\alpha(\omega + \varrho')(\partial_x b)^{(\alpha)}\partial_x^2\zeta = 0, \tag{3.72}$$

where α_i $(i = 0, 1)$, ϱ and ω are precisely defined in (3.51), (3.54) and (3.55), and v defined as $v = \dfrac{h_1 + \gamma h_2}{h_1 h_2}\underline{v}[\zeta]$, with

$$\underline{v}[\zeta] = \alpha_0\zeta - \frac{1}{2}\int_{-\infty}^{x} \partial_x(\alpha_0)\zeta dx + \epsilon\frac{\alpha_1}{2}\zeta^2 + \mu\varrho\partial_x^2\zeta + \mu\beta\alpha\omega(\partial_x b)^{(\alpha)}\partial_x\zeta.$$

We would like to mention that, under the restrictions on the set of admissible dimensionless parameters given in (3.71), one can easily prove that families of solutions of the equation (3.72) are L^∞-consistent with the Boussinesq system for internal waves over variable topography, which directly descend from the Green-Naghdi model (3.6) under the present scaling. A well-posedness result to the generalized KdV equation with time and space dependent coefficients has been proved in [73], where they show that the control of the dispersive and "diffusion" terms is possible under some conditions on the behavior of the ratio of dispersive to "diffusion" coefficients

and if they use an adequate weight function determined with respect to the dispersive and "diffusion" coefficients to define the energy and under a condition of non-degeneracy of the dispersive coefficient.

Remark 11. If we take $\beta = 0$ and $1/\mathrm{bo} = 0$ in (3.72) i.e if we consider a flat bottom with no surface tension, then one can recover the equation obtained in [46] for the bi-fluidic case. If we assume that $\gamma \to 0$, $\delta \to 1$ and if we take $\beta = 0$ and $1/\mathrm{bo} = 0$ in (3.72), then one recover the equation which has been originally introduced in [81] and rigorously justified in [14] as a model for the propagation of surface gravity waves over flat topography and in the long wave regime. When $\gamma \to 0$, $\delta \to 1$ and if we take $\beta\alpha = \mathcal{O}(\mu)$ and $1/\mathrm{bo} = 0$ in (3.72), then one recovers the variable-depth KdV equation in the long wave scaling introduced and fully justified in [71].

We give first a proposition concerning the H^s-consistency result followed by the full justification. In order to control the secular growth effects as in Proposition 15, we consider stronger restrictions on the parameters ϵ, β, α, and μ:

$$\epsilon = \mathcal{O}(\mu), \quad \beta\alpha = \mathcal{O}(\mu^2). \tag{3.73}$$

Proposition 16 (H^s-Consistency)**.** *Let $b \in H^\infty(\mathbb{R})$. For all family $\mathcal{P}$ of parameters p satisfying (3.73), denote $(\zeta^{\mathsf{p}})_{\mathsf{p}\in\mathcal{P}} \in L^\infty([0, \frac{T}{\epsilon}], H^{s+5})$ with $s > 3/2$ the unique solution of the equation*

$$\partial_t\zeta + \alpha_0\partial_x\zeta + \epsilon\alpha_1\zeta\partial_x\zeta + \mu\varrho\partial_x^3\zeta = 0, \tag{3.74}$$

where α_i $(i = 0, 1)$ and ϱ are precisely defined in (3.51) and (3.54). For given $M^*, h > 0$, we assume that there exists $T > 0$ such that $\|\zeta^{\mathsf{p}}\|_{L^\infty([0,\frac{T}{\epsilon}],H^{s+5})} \leq M^*$ and for any $(t, x) \in [0, \frac{T}{\epsilon}] \times \mathbb{R}$,

$$h_1 = 1 - \epsilon\zeta^{\mathsf{p}} \geq h > 0, \quad h_2 = 1/\delta + \epsilon\zeta^{\mathsf{p}} - \beta b^{(\alpha)} \geq h > 0. \tag{H1}$$

We define v^{p} as $v^{\mathsf{p}} = \dfrac{h_1 + \gamma h_2}{h_1 h_2}\underline{v}[\zeta^{\mathsf{p}}]$, with

$$\underline{v}[\zeta] = \alpha_0\zeta + \epsilon\frac{\alpha_1}{2}\zeta^2 + \mu\varrho\partial_x^2\zeta, \tag{3.75}$$

where α_i $(i = 0, 1)$ and ϱ are as above.

Then $(\zeta^{\mathsf{p}}, v^{\mathsf{p}})$ is H^s-consistent with the Green-Naghdi system (3.6), on $[0, \frac{T}{\epsilon}]$, with precision $\mathcal{O}(\mu^2)$.

Proof. The proposition is obtained using the same techniques of the proof of Proposition 15 and also using the fact that if a family is consistent with the Boussinesq equations, it is also consistent with the Green-Naghdi equations (3.6) under the present scaling. □

Remark 12. Following the proof of Proposition 12, one can easily check that the result of Proposition 16 holds with regards to our new Green-Naghdi system (3.26) in the present scaling (3.73), therefore we state the following convergence result.

Theorem 3.9.1 (Convergence)**.** *Let $b \in H^\infty(\mathbb{R})$ and let $\mathsf{p} \in \mathcal{P}$ satisfy (3.73). Assume the hypothesis of Proposition 16 hold. For all $\zeta_0^{\mathsf{p}} \in H^{s+s'}$, with s and s' sufficiently big, the following holds:*

• *There exists a unique family* $(\underline{v}^{\mathsf{p}}, \underline{\zeta}^{\mathsf{p}})_{\mathsf{p}\in\mathcal{P}}$*, uniformly bounded on* H^s *solving the new Green-Naghi equations* (3.26) *over time interval* $[0, \frac{T}{\epsilon}]$*, with initial condition* $(v^{\mathsf{p}}_{|t=0}, \zeta^{\mathsf{p}}_0)$*.*

• *There exists a unique family* $(v^{\mathsf{p}}, \zeta^{\mathsf{p}})_{\mathsf{p}\in\mathcal{P}}$*, given by the resolution of* (3.74) *over time interval* $[0, \frac{T}{\epsilon}]$*, with initial condition* ζ^{p}_0 *and* $v^{\mathsf{p}}_{|t=0}$ *satisfying* (3.75)*.*

Moreover, one has for all $\mathsf{p} \in \mathcal{P}$ *and for any* $t \leq \frac{T}{\epsilon}$*,*

$$|\underline{v}^{\mathsf{p}} - v^{\mathsf{p}}|_{L^\infty([0,t];H^s)} + |\underline{\zeta}^{\mathsf{p}} - \zeta^{\mathsf{p}}|_{L^\infty([0,t];H^s)} \leq Cst\ \mu^2\ t.$$

Proof. The first point of the theorem and the error estimate follow immediately from Theorem 3.6.1 and Theorem 3.6.2. The second point of the theorem is a direct consequence of [71, Theorem 2], where a well-posedness result has been proved for a general class of KdV equation. Indeed the proof of [71, Theorem 2] can be adjusted without any difficulty to more general coefficients. As indicated in Remark 12, we know that $(v^{\mathsf{p}}, \zeta^{\mathsf{p}})_{\mathsf{p}\in\mathcal{P}}$ is H^s-consistent with the new Green-Naghdi system (3.26). □

Remark 13. Our approximate solution described in Proposition 16 is fully justified as approximate solution of the new Green-Naghdi model (3.26). Thanks to Theorem 3.6.3 and Theorem 3.9.1, one can deduce using the triangular inequality that our approximate solution in the long wave regime is fully justified as approximate solution of the full Euler system (3.2).

3.10 Conclusion

In this work, we generalized the result of full justification obtained in [49] and [90] to a more complex case of variable topography. In fact we assume a slowly varying topography with large amplitude. Using this additional assumption we construct a new model with a pleasant symmetrizable hyperbolic structure that allows to prove its well-posedness thanks to some precise energy estimates. Some reasonable restrictions on the bottom parametrization are required in order to ensure the validity of our model. Hence, a full justification result is a consequence of the consistency and stability results. Furthermore, our new model allows to fully justify any well-posed and consistent models. We apply this procedure to some new unidirectional scalar models in different regimes of slowly varying topography. The next step of this study may concern the full justification of new coupled and scalar models in a strong topography variations framework.

Deuxième partie

Résolution numérique

Chapitre 4

A numerical scheme for an improved Green–Naghdi model in the Camassa-Holm regime for the propagation of internal waves

In this chapter we introduce a new reformulation of the Green-Naghdi model in the Camassa-Holm regime for the propagation of internal waves over a flat topography derived by Duchêne, Israwi and Talhouk [*SIAM J. Math. Anal.*, 47(1), 240—290]. These new Green–Naghdi systems are adapted to improve the frequency dispersion of the original model, they share the same order of precision as the standard one but have an appropriate structure which makes them much more suitable for the numerical resolution. We develop a second order splitting scheme where the hyperbolic part of the system is treated with a high-order finite volume scheme and the dispersive part is treated with a finite difference approach. Numerical simulations are then performed to validate the model.

4.1 Introduction

This study deals with the propagation internal waves in the uni-dimensional setting located at the interface between two layers of fluids of different densities. The fluids are assumed to be incompressible, homogeneous, and immiscible, limited from above by a rigid lid and from below by a flat bottom. This type of fluid dynamics problem is encountered by researchers in oceanography when they study the wave near the shore. Because of the difference in the salinity of the different layers of water near the shore, it is useful to model the flow of salted water by a two layers incompressible fluids flow. The usual way of describing such a flow is to use the 3D-Euler equations for the different layers adding some thermodynamic and dynamic conditions at the interface. This system will be called the *full Euler system*. This system of partial differential equations is very rich but very difficult to manipulate both mathematically and numerically. This is the reason why reduced models have been derived to characterize the evolution of the solution in some physical and geometrical specific regimes. Many models for the water wave (air-water interface) system have already been derived and studied in the shallow-water regime, where we consider the wave length of the flow is large compared to the typical depth. We refer the reader to the following papers [8, 23, 85, 17, 84]. Earlier works have also set a very interesting

theoretical background for the two-fluid system see [16, 6, 47, 48, 49], for more details.

One of these reduced models is the Green-Naghdi system of partial differential equations (denoted GN in the following). Many numerical studies of the fully nonlinear GN equations for the one layer case have been proposed in the literature. Let us introduce some of these results. The GN model describing dispersive shallow water waves have been numerically studied in [88] after being written in terms of potential variables in a pseudo-conservative form and using a Godunov scheme. Bonneton *et al.* studied numerically in [18] the fully nonlinear and weakly dispersive GN model for shallow water waves of large amplitude over variable topography. The original model was firstly adjusted in a suitable way for numerical resolution with an improvement of the dispersive properties, then they proposed to use a finite volume-finite difference splitting scheme that decomposes the hyperbolic and dispersive parts of the equations. This similar approach was earlier introduced in [55] for the solution of the Boussinesq equations. In [30], a three-parameters GN system is derived, yielding further improvements of the dispersive properties. Let us mention also [96], where a highly accurate and stable numerical scheme based on the Galerkin / finite-element method was presented for the Serre system. The method is based on smooth periodic splines in space and an explicit fourth-order Runge-Kutta method in time. Recently, Lannes and Marche introduced in [86] a new class of two-dimensional GN equations over varying topography. These fully nonlinear and weakly dispersive equations have a mathematical structure more suitable for 2D simulations. Using the same splitting strategy initiated in [30], they develop a high order, well balanced, and robust numerical code for these new models. Finally, we would like to mention the recent work of Duchêne, Israwi and Talhouk [50], where they derive a new class of GN models with improved frequency dispersion for the propagation of internal waves at the interface between two layers of fluids. They numerically compute their class of GN models using spectral methods [111] for space discretization and the Matlab solver ode45, which is based on the fourth and fifth order Runge-Kutta-Merson method for time evolution. Their numerical simulations show how the different frequency dispersion of the modified GN models may affect the appearance of high frequency Kelvin-Helmholtz instabilities.

In this chapter, we present the numerical resolution of the GN model in the Camassa-Holm (medium amplitude) regime obtained and fully justified by Duchêne, Israwi and Talhouk in [49] using the same strategy initiated in [18, 86]. Let us recall that this model describes the propagation of one-dimensional internal waves at the interface between two layers of ideal fluids, limited by a rigid lid from above and a flat bottom from below. This model is first recast under a new formulation more suitable for numerical resolution with the same order of precision as the standard one but with improved frequency dispersion. More precisely, following [18] we derive a family of GN equations depending on a parameter α to be chosen in order to minimize the phase velocity error between the reduced model and the *full Euler system*. Then we propose a numerical scheme that decomposes the hyperbolic and dispersive parts of the equations. Following the same strategy adopted in [18, 86], we use a second order splitting scheme. The approximation $U^{n+1} = (\zeta^{n+1}, v^{n+1})$ is computed at time $t^{n+1} = t^n + \Delta t$ where ζ represents the deformation of the interface and v represent the *shear mean velocity* defined in Section 4.3, in terms of the approximation U^n at time t^n by solving

$$U^{n+1} = S_1(\Delta t/2)S_2(\Delta t)S_1(\Delta t/2)U^n,$$

where $S_1(.)$ is the operator associated to the hyperbolic part and $S_2(.)$ the operator associated to the dispersive part of the GN equations. For the numerical computation of $S_1(.)$, we use a finite volume method. We begin by the VFRoe method (see [24, 57, 58]), that is an approximate Godunov scheme. Unfortunately, the VFRoe scheme seems to be very diffusive. To this end,

we propose a second-order scheme following the classical "MUSCL" approach [112]. Finally, following [74] we implement a fifth-order accuracy "WENO" reconstruction in order to reach higher order accuracy in smooth regions and a good resolution around discontinuities since the second order schemes are known to degenerate to first order accuracy at smooth extrema. On the other hand, $S_2(.)$ is computed using a finite difference scheme discretized using second and fourth order formulas, whereas for time discretization we use classical second and fourth order Runge-Kutta methods according to the order of the space derivative in consideration. The computation of $S_2(\Delta t)$ in the above splitting scheme (dispersive part) requires the inversion of the following symmetric second order differential operator introduced in [49]

$$\mathfrak{T}[\epsilon\zeta]V \;=\; q_1(\epsilon\zeta)V \;-\; \mu\nu\partial_x\Big(q_2(\epsilon\zeta)\partial_x V\Big).$$

with $q_i(X) \equiv 1 + \kappa_i X$ $(i = 1, 2)$, where κ_i and ν are constants depending on three parameters: the ratio between the densities of the two layers, the ratio between their depth and the capillary effect of the interface. Moreover, it is known that third order derivatives involved in this model may create high frequencies instabilities, but the presence of the operator $\mathfrak{T}[\epsilon\zeta]^{-1}$ in the second equation stabilizes the model with respect to these perturbations, allowing for more robust numerical computations, see Section 4.3.4. The invertibility of this operator played also an important role in the well-posedness of these equations (see [72] for the one layer case and [49] for the two layers case). However, this operator is time dependent since it depends on the deformation of the interface $\zeta(t, x)$. In order to avoid the inversion of this operator at each time step keeping its stabilizing effects, we derive a new family of physical models that are equivalent to the standard one in the sense of consistency (same order of precision $\mathcal{O}(\mu^2)$), where we remove the time dependency of the operator $\mathfrak{T}$. The structure of the time-independent model leads to a small improvement in terms of computational time due to its simple one-dimensional structure. In fact, this strategy was originally initiated for numerical simulations of the fully nonlinear and weakly dispersive GN models in the two-dimensional case [86], in order to reduce significantly the computational time.

We organize the chapter as follows. In Section 4.2, we introduce the non-dimensonalized *full Euler system*. Section 4.3 is devoted to recall the GN model in the Camassa-Holm regime, where an equivalent time-independent reformulation is given with an improved frequency dispersion based on the choice of a parameter α. The stability issue of this new reformulation is discussed in the one and two layers cases. Section 4.4 is then devoted to the presentation of the numerical scheme. Firstly the hyperbolic/dispersive splitting is introduced. Then we describe the finite-volume spatial discretization of the hyperbolic part. The first-order finite volume scheme is given, an extension to the second-order accuracy is considered following the "MUSCL" approach and finally high-order accuracy around discontinuities is achieved thanks to the implementation of a fifth-order "WENO" reconstruction. The finite-difference discretization of the dispersive part is then detailed and the boundary conditions are briefly described. Finally, we present in Section 4.5 several numerical validations of our model. The one layer case is numerically validated: we compare the accuracy of the first, second and fifth orders of accuracy by studying the propagation of a solitary wave. To evaluate the influence of dispersive nonlinear terms, we consider the head-on collision of counter-propagating waves and the breaking of a Gaussian hump. Dealing with discontinuities is numerically validated by studying the dam-break problem in the one layer case. We highlight then the importance of the choice of the parameter α in improving the frequency dispersion of the model and compare our results with numerical experiments. Finally,

we validate the ability of our numerical scheme to deal with discontinuities when considering a dam-break problem in the two layers case.

4.2 Full Euler system

In this section, we briefly recall the derivation of the *full Euler system* governing the evolution equations of the two-layers flow and refer to [6, 16, 47, 48] for more details. The two-layers flow considered are assumed to be incompressible, homogeneous, immiscible perfect fluids of different densities under the sole influence of gravity.

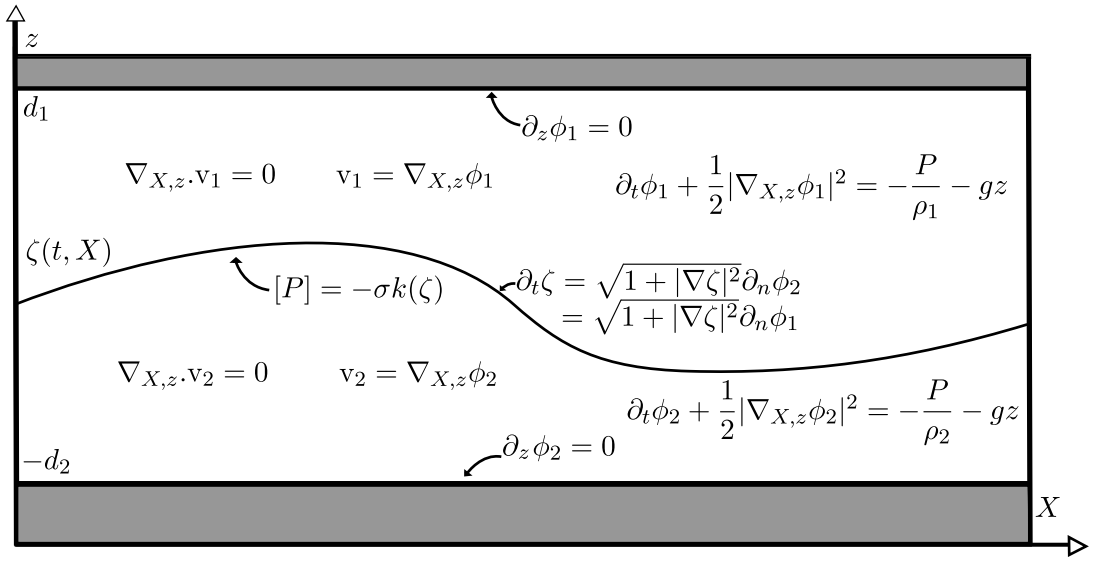

Figure 4.1. Domain of study and governing equations.

The study is restricted to the one-dimensional horizontal variable. The deformation of the interface between the two layers is represented by the graph of function a $\zeta(t,x)$ while the bottom and the top surfaces are assumed to be rigid and flat. The domains of the upper and lower fluid at time t (denoted, respectively, Ω_1^t and Ω_2^t), are given by

$$\begin{aligned}\Omega_1^t &= \{\ (x,z)\in\mathbb{R}\times\mathbb{R},\quad \zeta(t,x)\ \le\ z\ \le\ d_1\ \},\\ \Omega_2^t &= \{\ (x,z)\in\mathbb{R}\times\mathbb{R},\quad -d_2\ \le\ z\ \le\ \zeta(t,x)\ \}.\end{aligned}$$

In what follows, we assume that the domains remain strictly connected, that is there exists $h_0>0$ such that $d_1-\zeta(t,x)\ge h_0>0$ and $d_2+\zeta(t,x)\ge h_0>0$. The density and velocity fields of the upper and lower layers are denoted by $(\rho_i,\mathbf{v}_i)$, $(i=1,2)$ respectively. We assume the fluids to be incompressible, homogeneous and irrotational so that the velocity fields are divergence free and expressed as gradients of a potential denoted ϕ_i. The fluids being ideal, that is with no viscosity, we may assume that each fluid follows the Euler equations. Assuming that the surface, the bottom or the interface are impenetrable one deduces the kinematic boundary conditions. Finally, the set of equations is completed by the continuity of the stress tensor at the interface.

Altogether, the governing equations are given by the following system:

$$\begin{cases} \partial_x^2\phi_i \ + \ \partial_z^2\phi_i \ = \ 0 & \text{in } \Omega_i^t, \ i=1,2, \\ \partial_t\phi_i + \dfrac{1}{2}|\nabla_{x,z}\phi_i|^2 = -\dfrac{P_i}{\rho_i} - gz & \text{in } \Omega_i^t, \ i=1,2, \\ \partial_z\phi_1 \ = \ 0 & \text{on } \Gamma_{\rm t} \equiv \{(x,z), z=d_1\}, \\ \partial_t\zeta \ = \ \sqrt{1+|\partial_x\zeta|^2}\partial_n\phi_1 \ = \ \sqrt{1+|\partial_x\zeta|^2}\partial_n\phi_2 & \text{on } \Gamma \equiv \{(x,z), z=\zeta(t,x)\}, \\ \partial_z\phi_2 \ = \ 0 & \text{on } \Gamma_{\rm b} \equiv \{(x,z), z=-d_2\}, \\ \lim\limits_{\varepsilon\to 0}\Big(P(t,x,\zeta(t,x)+\varepsilon) - P(t,x,\zeta(t,x)-\varepsilon)\Big) = -\sigma k(\zeta) & \text{on } \Gamma, \end{cases} \tag{4.1}$$

where n denotes the unit upward normal vector at the interface.
The function $k(\zeta) = -\partial_x\Big(\dfrac{1}{\sqrt{1+|\partial_x\zeta|^2}}\partial_x\zeta\Big)$ denotes the mean curvature of the interface and σ the surface (or interfacial) tension coefficient.

To go further in the study of the flow of the two layers in order to build a numerical scheme for the asymptotic dynamics, we write the system in dimensionless form. To this end, we introduce dimensionless parameters and variables that reduce the setting to the physical regime under consideration. Firstly, let a be the maximum amplitude of the deformation of the interface and λ the wavelength of the interface. Then the typical velocity of small propagating internal waves (or wave celerity) is given by

$$c_0 \ = \ \sqrt{g\frac{(\rho_2-\rho_1)d_1d_2}{\rho_2 d_1 + \rho_1 d_2}}.$$

Consequently, we introduce the dimensionless variables:

$$\tilde{z} \ \equiv \ \frac{z}{d_1}, \qquad \tilde{x} \ \equiv \ \frac{x}{\lambda}, \qquad \tilde{t} \ \equiv \ \frac{c_0}{\lambda}t,$$

the dimensionless unknowns:

$$\tilde{\zeta}(\tilde{t},\tilde{x}) \ \equiv \ \frac{\zeta(t,x)}{a}, \qquad \tilde{\phi_i}(\tilde{t},\tilde{x},\tilde{z}) \ \equiv \ \frac{d_1}{a\lambda c_0}\phi_i(t,x,z) \quad (i=1,2),$$

and finally the dimensionless parameters:

$$\gamma \ = \ \frac{\rho_1}{\rho_2}, \quad \epsilon \ \equiv \ \frac{a}{d_1}, \quad \mu \ \equiv \ \frac{d_1^2}{\lambda^2}, \quad \delta \ \equiv \ \frac{d_1}{d_2}, \quad \text{bo} \ = \ \frac{g(\rho_2-\rho_1)d_1^2}{\sigma}.$$

In what follows we assume that the depth ratio δ do not approach zero or infinity which means that the two layers of fluid have comparable depth. Therefore, the choice of the reference vertical length is harmless so we decided to choose d_1. We would like to mention that $\text{Bo} = \mu\text{bo}$ where Bo is the classical Bond number. The significations of the different dimensionless parameters are the following :

- γ represents the ratio between the densities of the two layers,
- ϵ represents the amplitude of the interface between the two layers,
- μ represents the nonlinear effect of the shallowness approximation,
- δ represents the ratio between the depth of the two layers,
- bo represents the capillary effect of the interface.

Let us now remark that the system can be rewritten as two evolution equations coupling Zakharov's canonical variables [115, 39], (ζ, ψ) representing respectively the deformation of the interface and the trace of the dimensionless upper potential at the interface defined by $\psi \equiv \phi_1(t, x, \zeta(t, x))$.

In order to do so, we define the so-called Dirichlet-Neumann operators. The tildes are removed for the sake of readability.

Definition 4.2.1 (Dirichlet-Neumann operators)**.** Let $\zeta \in H^{t_0+1}(\mathbb{R})$, $t_0 > 1/2$, such that there exists $h > 0$ with $h_1 \equiv 1 - \epsilon\zeta \geq h > 0$ and $h_2 \equiv \frac{1}{\delta} + \epsilon\zeta \geq h > 0$, and let $\psi \in L^2_{\rm loc}(\mathbb{R}), \partial_x\psi \in H^{1/2}(\mathbb{R})$. Then we define:

$$\begin{aligned} G^\mu\psi &\equiv G^\mu[\epsilon\zeta]\psi \equiv \sqrt{1+\mu|\epsilon\partial_x\zeta|^2}\big(\partial_n\phi_1\big)\,|_{z=\epsilon\zeta} = -\mu\epsilon(\partial_x\zeta)(\partial_x\phi_1)\,|_{z=\epsilon\zeta} + (\partial_z\phi_1)\,|_{z=\epsilon\zeta}\,, \\ H^{\mu,\delta}\psi &\equiv H^{\mu,\delta}[\epsilon\zeta]\psi \equiv \partial_x\big(\phi_2\,|_{z=\epsilon\zeta}\,\big) = (\partial_x\phi_2)\,|_{z=\epsilon\zeta} + \epsilon(\partial_x\zeta)(\partial_z\phi_2)\,|_{z=\epsilon\zeta}\,, \end{aligned}$$

where, ϕ_1 and ϕ_2 are uniquely deduced from (ζ, ψ) as solutions of the following Laplace's problems:

$$\begin{cases} \big(\,\mu\partial_x^2 \,+\, \partial_z^2\,\big)\,\phi_1 = 0 & \text{in } \Omega_1 \equiv \{(x,z)\in\mathbb{R}^2,\ \epsilon\zeta(x) < z < 1\}, \\ \partial_z\phi_1 = 0 & \text{on } \Gamma_{\rm t} \equiv \{(x,z)\in\mathbb{R}^2,\ z = 1\}, \\ \phi_1 = \psi & \text{on } \Gamma \equiv \{(x,z)\in\mathbb{R}^2,\ z = \epsilon\zeta\}, \end{cases}$$

$$\begin{cases} \big(\,\mu\partial_x^2 \,+\, \partial_z^2\,\big)\,\phi_2 = 0 & \text{in } \Omega_2 \equiv \{(x,z)\in\mathbb{R}^2,\ -\frac{1}{\delta} < z < \epsilon\zeta\}, \\ \partial_n\phi_2 = \partial_n\phi_1 & \text{on } \Gamma, \\ \partial_z\phi_2 = 0 & \text{on } \Gamma_{\rm b} \equiv \{(x,z)\in\mathbb{R}^2,\ z = -\frac{1}{\delta}\}. \end{cases}$$

At this stage of the model, using the above definition and withouth making any assumption on the different dimensionless parameters, one can rewrite the nondimensionalized version of (4.1) as a system of two coupled evolution equations, which writes:

$$\begin{cases} \partial_t\zeta \,-\, \dfrac{1}{\mu}G^\mu\psi \;=\; 0, \\[2ex] \partial_t\Big(H^{\mu,\delta}\psi - \gamma\partial_x\psi\Big) \,+\, (\gamma+\delta)\partial_x\zeta \,+\, \dfrac{\epsilon}{2}\partial_x\Big(|H^{\mu,\delta}\psi|^2 - \gamma|\partial_x\psi|^2\Big) \\[2ex] \qquad\qquad = \;\mu\epsilon\partial_x\mathcal{N}^{\mu,\delta} - \mu\dfrac{\gamma+\delta}{\rm bo}\dfrac{\partial_x\big(k(\epsilon\sqrt{\mu}\zeta)\big)}{\epsilon\sqrt{\mu}}\,, \end{cases} \tag{4.2}$$

where we denote:

$$\mathcal{N}^{\mu,\delta} \;\equiv\; \frac{\big(\frac{1}{\mu}G^\mu\psi + \epsilon(\partial_x\zeta)H^{\mu,\delta}\psi\big)^2 \,-\, \gamma\big(\frac{1}{\mu}G^\mu\psi + \epsilon(\partial_x\zeta)(\partial_x\psi)\big)^2}{2(1+\mu|\epsilon\partial_x\zeta|^2)}.$$

We will refer to (4.2) as the *full Euler system*.

4.3 Green-Naghdi model in the Camassa-Holm regime

We now recall the new Green-Naghdi model in the Camassa-Holm regime recently derived by Duchêne, Israwi and Talhouk in [49]. This new model is derived after expanding the different

operators of the original Green-Naghdi model with respect to ϵ and μ. Then several additional transformations are made using the smallness assumption $\epsilon = \mathcal{O}(\sqrt{\mu})$ in order to produce an equivalent precise system of partial differential equations whose unknowns are ζ and v :

$$\begin{cases} \partial_t \zeta + \partial_x \left(\dfrac{h_1 h_2}{h_1 + \gamma h_2} v \right) \;=\; 0, \\ \\ \mathfrak{T}[\epsilon\zeta]\left(\partial_t v + \epsilon\varsigma v \partial_x v\right) + (\gamma+\delta) q_1(\epsilon\zeta)\partial_x \zeta \\ \qquad\qquad + \dfrac{\epsilon}{2} q_1(\epsilon\zeta)\partial_x \left(\dfrac{h_1^2 - \gamma h_2^2}{(h_1+\gamma h_2)^2}|v|^2 - \varsigma |v|^2 \right) = -\mu\epsilon \dfrac{2}{3}\dfrac{1-\gamma}{(\gamma+\delta)^2}\partial_x\big((\partial_x v)^2\big), \end{cases} \tag{4.3}$$

where $h_1 \equiv 1 - \epsilon\zeta$ (resp. $h_2 \equiv \dfrac{1}{\delta} + \epsilon\zeta$) denotes the depth of the upper (resp. lower) fluid, and v is the *shear mean velocity* defined by:

$$v \equiv \frac{1}{h_2}\int_{-\frac{1}{\delta}}^{\epsilon\zeta(t,x)} \partial_x \phi_2(t,x,z)\; dz - \frac{\gamma}{h_1}\int_{\epsilon\zeta(t,x)}^{1} \partial_x \phi_1(t,x,z)\; dz.$$

The operator $\mathfrak{T}$ is defined as:

$$\mathfrak{T}[\epsilon\zeta]V \;=\; q_1(\epsilon\zeta)V \;-\; \mu\nu\partial_x\Big(q_2(\epsilon\zeta)\partial_x V\Big),$$

with $q_i(X) \equiv 1 + \kappa_i X$ $(i = 1, 2)$ and ν, κ_1, κ_2, ς are defined below. Let us first introduce the following constants in order to ease the reading:

$$\lambda = \frac{1+\gamma\delta}{3\delta(\gamma+\delta)}\;, \quad \alpha = \frac{1-\gamma}{(\gamma+\delta)^2} \quad \text{and} \quad \beta = \frac{(1+\gamma\delta)(\delta^2-\gamma)}{\delta(\gamma+\delta)^3}\;. \tag{4.4}$$

Thus

$$\nu \;=\; \lambda - \frac{1}{\mathrm{bo}} \;=\; \frac{1+\gamma\delta}{3\delta(\gamma+\delta)} - \frac{1}{\mathrm{bo}},$$

$$(\lambda - \frac{1}{\mathrm{bo}})\kappa_1 \;=\; \frac{\gamma+\delta}{3}(2\beta - \alpha), \quad (\lambda - \frac{1}{\mathrm{bo}})\kappa_2 \;=\; (\gamma+\delta)\beta,$$

$$(\lambda - \frac{1}{\mathrm{bo}})\varsigma \;=\; \frac{2\alpha-\beta}{3} \;-\; \frac{1}{\mathrm{bo}}\frac{\delta^2-\gamma}{(\delta+\gamma)^2}.$$

The function f is defined as follows:

$$f : X \to \frac{(1-X)(\delta^{-1}+X)}{1 - X + \gamma(\delta^{-1}+X)},$$

so one has:

$$f(\epsilon\zeta) \;=\; \frac{h_1 h_2}{h_1 + \gamma h_2} \quad \text{and} \quad f'(\epsilon\zeta) \;=\; \frac{h_1^2 - \gamma h_2^2}{(h_1+\gamma h_2)^2}\;.$$

Additionally, let us denote:

$$\kappa = \frac{2}{3}\frac{1-\gamma}{(\delta+\gamma)^2} \quad \text{and} \quad q_3(\epsilon\zeta) = \frac{1}{2}\big(f'(\epsilon\zeta) - \varsigma\big) = \frac{1}{2}\Big(\frac{h_1^2 - \gamma h_2^2}{(h_1+\gamma h_2)^2} - \varsigma\Big)\;. \tag{4.5}$$

Problem (4.3) writes now in compact form:

$$\begin{cases} \partial_t\zeta + \partial_x\big(f(\epsilon\zeta)v\big) \;=\; 0, \\ \\ \mathfrak{T}\left(\partial_t v + \epsilon\varsigma v\partial_x v\right) + (\gamma+\delta)q_1(\epsilon\zeta)\partial_x\zeta + \epsilon q_1(\epsilon\zeta)\partial_x(q_3(\epsilon\zeta)v^2) + \mu\epsilon\kappa\partial_x\big((\partial_x v)^2\big) = 0. \end{cases} \tag{4.6}$$

Let us now recall the regime of validity of the system (4.6) as exactly given in [49]. In the first place, we consider the so-called *shallow water regime* for two layers of comparable depths:

$$\mathcal{P}_{\rm SW} \;\equiv\; \Big\{(\mu,\epsilon,\delta,\gamma,{\rm bo}):\; 0 \;<\; \mu \;\leq\; \mu_{\max},\; 0 \;\leq\; \epsilon \;\leq\; 1,\; \delta\in(\delta_{\min},\delta_{\max}),\\ 0 \;\leq\; \gamma \;<\; 1,\; {\rm bo}_{\min}\leq {\rm bo}\leq\infty\Big\}, \tag{4.7}$$

with given $0\leq\mu_{\max},\delta_{\min}^{-1},\delta_{\max},{\rm bo}_{\min}^{-1}<\infty$.

Two additional key restrictions are necessary for the validity of the model:

$$\mathcal{P}_{\rm CH}\equiv\left\{(\mu,\epsilon,\delta,\gamma,{\rm bo})\in\mathcal{P}_{\rm SW}:\; \epsilon\leq {\rm M}\sqrt{\mu} \quad\text{and}\quad \nu\equiv\frac{1+\gamma\delta}{3\delta(\gamma+\delta)}-\frac{1}{\rm bo}\geq\nu_0\right\}, \tag{4.8}$$

with given $0\leq M,\nu_0^{-1}<\infty$.

Duchêne, Israwi and Talhouk proved in [49], that the system (4.6) is well-posed (in the sense of Hadamard) in the energy space $X^s \;=\; H^s(\mathbb{R})\times H^{s+1}(\mathbb{R})$, endowed with the norm

$$\forall\, U=(\zeta,v)^\top\in X^s,\quad |U|_{X^s}^2\equiv|\zeta|_{H^s}^2+|v|_{H^s}^2+\mu|\partial_x v|_{H^s}^2.$$

This result is obtained for parameters in the *Camassa-Holm regime* (4.8) and under the following non-zero depth and ellipticity (for the operator $\mathfrak{T}$) conditions:

$$\exists h_{01}>0 \text{ such that, } \inf_{x\in\mathbb{R}} h_1\geq\; h_{01}\;>\;0,\quad \inf_{x\in\mathbb{R}} h_2\geq\; h_{01}\;>\;0. \tag{H1}$$

$$\exists h_{02}>0 \text{ such that, } \inf_{x\in\mathbb{R}} (1+\epsilon\kappa_1\zeta)\geq\; h_{02}\;>\;0,\quad \inf_{x\in\mathbb{R}} (1+\epsilon\kappa_2\zeta)\geq\; h_{02}\;>\;0. \tag{H2}$$

They also prove that this new asymptotic model model is fully justified by a convergence result in the Camassa-Holm regime.

4.3.1 Reformulation of the model

One can easily check that the operator $\mathfrak{T}$ can be written under the form:

$$\mathfrak{T}[\epsilon\zeta]V=(q_1(\epsilon\zeta)I+\mu\nu T[\epsilon\zeta])V \quad\text{with}\quad T[\epsilon\zeta]V=-\partial_x(q_2(\epsilon\zeta)\partial_x V).$$

Therefore, this operator is time dependant through the presence of the term ζ and at each time, this operator has to be inverted in order to solve equation (4.6) Thus we want to derive a new model equivalent to (4.3) up to a lower order in ϵ or μ but with a structure adapted to construct a numerical scheme for its resolution.

Let us first denote :

$$Q_1(v)=\kappa\partial_x((\partial_x v)^2), \tag{4.9}$$

such that one can rewrite problem (4.6) as :

$$\begin{cases} \partial_t\zeta + \partial_x\big(f(\epsilon\zeta)v\big) \;=\; 0, \\ \Big(q_1(\epsilon\zeta)I + \mu\nu T[\epsilon\zeta]\Big)\Big(\partial_t v + \epsilon\varsigma v\partial_x v\Big) + (\gamma+\delta)q_1(\epsilon\zeta)\partial_x\zeta + \epsilon q_1(\epsilon\zeta)\partial_x(q_3(\epsilon\zeta)v^2) + \mu\epsilon Q_1(v) = 0. \end{cases} \tag{4.10}$$

As we said before since the operator $(q_1(\epsilon\zeta)I + \mu\nu T[\epsilon\zeta])$ depends on $\zeta(t,x)$, one has to remove this time dependency to avoid its inversion at each time.

Firstly, let us write the operator $T[\epsilon\zeta]$ under the form:

$$T[\epsilon\zeta]V = -\partial_x(q_2(\epsilon\zeta)\partial_x V) = T[0]V + \epsilon S[\zeta]V,$$

with

$$T[0]V = -\partial_x^2 V \quad \text{and} \quad S[\zeta]V = -\kappa_2\partial_x(\zeta\partial_x V).$$

Expanding the term $\Big(q_1(\epsilon\zeta)I + \mu\nu T[\epsilon\zeta]\Big)\Big(\partial_t v + \epsilon\varsigma v\partial_x v\Big)$ in problem (4.10) leads to :

$$\begin{cases} \partial_t\zeta + \partial_x\big(f(\epsilon\zeta)v\big) \;=\; 0, \\ \Big(I + \mu\nu T[0]\Big)\Big(\partial_t v + \epsilon\varsigma v\partial_x v\Big) + (\gamma+\delta)q_1(\epsilon\zeta)\partial_x\zeta + \epsilon q_1(\epsilon\zeta)\partial_x(q_3(\epsilon\zeta)v^2) + \mu\epsilon Q_1(v) \\ +\mu\epsilon\nu S[\zeta]\left(\partial_t v + \epsilon\varsigma v\partial_x v\right) + \epsilon\kappa_1\zeta\left(\partial_t v + \epsilon\varsigma v\partial_x v\right) = 0. \end{cases} \tag{4.11}$$

But we have: $\mu\epsilon\nu S[\zeta]\left(\partial_t v + \epsilon\varsigma v\partial_x v\right) = \mu\epsilon\nu S[\zeta]\partial_t v + \mathcal{O}(\mu\epsilon^2)$. By assumption the term $\mathcal{O}(\mu\epsilon^2)$ is of order $\mathcal{O}(\mu^2)$; thus Problem (4.11) is equivalent to the following system:

$$\begin{cases} \partial_t\zeta + \partial_x\big(f(\epsilon\zeta)v\big) \;=\; 0, \\ \Big(I + \mu\nu T[0]\Big)\Big(\partial_t v + \epsilon\varsigma v\partial_x v\Big) + (\gamma+\delta)q_1(\epsilon\zeta)\partial_x\zeta + \epsilon q_1(\epsilon\zeta)\partial_x(q_3(\epsilon\zeta)v^2) + \mu\epsilon Q_1(v) \\ +\mu\epsilon\nu S[\zeta]\left(\partial_t v\right) + \epsilon\kappa_1\zeta\left(\partial_t v + \epsilon\varsigma v\partial_x v\right) = 0. \end{cases} \tag{4.12}$$

4.3.2 Improved Green-Naghdi equations

As done by many authors, see [113, 91, 33], the frequency dispersion of problem (4.12) can be improved by adding some terms of order $\mathcal{O}(\mu^2)$ to the momentum equation. The accuracy of the model is not affected by this manipulation since this equation is precise up to terms of the same order as the added ones, namely $\mathcal{O}(\mu^2)$.

Going back to problem (4.10), one notices that:

$$q_1(\epsilon\zeta)\left(\partial_t v + \epsilon\varsigma v\partial_x v\right) + (\gamma+\delta)q_1(\epsilon\zeta)\partial_x\zeta + \epsilon q_1(\epsilon\zeta)\partial_x(q_3(\epsilon\zeta)v^2) + \mathcal{O}(\mu) = 0. \tag{4.13}$$

We can now divide (4.13) by $q_1(\epsilon\zeta)$ to obtain:

$$\partial_t v = -\epsilon\varsigma v\partial_x v - (\gamma+\delta)\partial_x\zeta - \epsilon\partial_x(q_3(\epsilon\zeta)v^2) - \frac{\mathcal{O}(\mu)}{q_1(\epsilon\zeta)}. \tag{4.14}$$

Let us fix $\alpha \in \mathbb{R}$. Multiplying (4.14) by $(1-\alpha)$ leads to:

$$\partial_t v = \alpha\partial_t v - (1-\alpha)[\epsilon\varsigma v\partial_x v + (\gamma+\delta)\partial_x\zeta + \epsilon\partial_x(q_3(\epsilon\zeta)v^2)] - (1-\alpha)\frac{\mathcal{O}(\mu)}{q_1(\epsilon\zeta)}. \tag{4.15}$$

Replacing $\partial_t v$ by its expression given in (4.15) in the second equation of (4.12) and regrouping the $\mathcal{O}(\mu^2)$ terms yields to the following equation:

$$(I+\mu\nu T[0])\left(\alpha\partial_t v-(1-\alpha)[\epsilon\varsigma v\partial_x v+(\gamma+\delta)\partial_x\zeta+\epsilon\partial_x(q_3(\epsilon\zeta)v^2)]-(1-\alpha)\frac{\mathcal{O}(\mu)}{q_1(\epsilon\zeta)}+\epsilon\varsigma v\partial_x v\right)$$
$$+(\gamma+\delta)q_1(\epsilon\zeta)\partial_x\zeta+\epsilon q_1(\epsilon\zeta)\partial_x(q_3(\epsilon\zeta)v^2)+\mu\epsilon Q_1(v)+\mu\epsilon\nu S[\zeta]\partial_t v+\epsilon\kappa_1\zeta\left(\partial_t v+\epsilon\varsigma v\partial_x v\right)+\mathcal{O}(\mu^2)=0$$

After straightforward computations,

$$\begin{aligned}(I+\mu\nu\alpha T[0])\left(\partial_t v+\epsilon\varsigma v\partial_x v\right)+(\alpha-1)[\partial_t v+\epsilon\varsigma v\partial_x v+(\gamma+\delta)\partial_x\zeta+\epsilon\partial_x(q_3(\epsilon\zeta)v^2)]\\ +(\alpha-1)\mu\nu T[0]\big((\gamma+\delta)\partial_x\zeta+\epsilon\partial_x(q_3(\epsilon\zeta)v^2)\big)+(\gamma+\delta)q_1(\epsilon\zeta)\partial_x\zeta+\epsilon q_1(\epsilon\zeta)\partial_x(q_3(\epsilon\zeta)v^2)\\ +\mu\epsilon Q_1(v)+\mu\epsilon\nu S[\zeta]\partial_t v+\epsilon\kappa_1\zeta\left(\partial_t v+\epsilon\varsigma v\partial_x v\right)-(1-\alpha)\frac{\mathcal{O}(\mu)}{q_1(\epsilon\zeta)}+\mathcal{O}(\mu^2)=0\end{aligned}\quad(4.16)$$

Replacing in (4.16), $\epsilon\kappa_1\zeta\left(\partial_t v+\epsilon\varsigma v\partial_x v\right)$ by $\epsilon\kappa_1\zeta\Big(-(\gamma+\delta)\partial_x\zeta-\epsilon\partial_x(q_3(\epsilon\zeta)v^2)-\frac{\mathcal{O}(\mu)}{q_1(\epsilon\zeta)}\Big)$, we have:

$$\begin{aligned}(I+\mu\nu\alpha T[0])\left(\partial_t v+\epsilon\varsigma v\partial_x v\right)+(I-\mu\nu(1-\alpha)T[0])(\gamma+\delta)\partial_x\zeta+\epsilon\partial_x(q_3(\epsilon\zeta)v^2))\\ +\mu\epsilon Q_1(v)+\mu\epsilon\nu S[\zeta]\partial_t v-\epsilon\kappa_1\zeta\frac{\mathcal{O}(\mu)}{q_1(\epsilon\zeta)}+\mathcal{O}(\mu^2)=0.\end{aligned}\quad(4.17)$$

One deduces easily that,

$$\begin{aligned}(I-\mu\nu(1-\alpha)T[0])(\gamma+\delta)\partial_x\zeta+\epsilon\partial_x(q_3(\epsilon\zeta)v^2))=\frac{1}{\alpha}\big((\gamma+\delta)\partial_x\zeta+\epsilon\partial_x(q_3(\epsilon\zeta)v^2)\big)\\ +\frac{\alpha-1}{\alpha}(I+\mu\nu\alpha T[0])((\gamma+\delta)\partial_x\zeta+\epsilon\partial_x(q_3(\epsilon\zeta)v^2)).\end{aligned}\quad(4.18)$$

Plugging (4.18) in (4.17) one has:

$$\begin{aligned}(I+\mu\nu\alpha T[0])\big[\partial_t v+\epsilon\varsigma v\partial_x v+\frac{\alpha-1}{\alpha}\big((\gamma+\delta)\partial_x\zeta+\epsilon\partial_x(q_3(\epsilon\zeta)v^2)\big)\big]+\frac{1}{\alpha}\big((\gamma+\delta)\partial_x\zeta+\epsilon\partial_x(q_3(\epsilon\zeta)v^2)\big)\\ +\mu\epsilon Q_1(v)+\mu\epsilon\nu S[\zeta]\partial_t v-\epsilon\kappa_1\zeta\frac{\mathcal{O}(\mu)}{q_1(\epsilon\zeta)}+\mathcal{O}(\mu^2)=0\end{aligned}\quad(4.19)$$

Remembering that $\mu\nu T[0](\partial_t v+\epsilon\varsigma v\partial_x v)+\mu\epsilon Q_1(v)+\mu\epsilon\nu S[\zeta]\partial_t v=\mathcal{O}(\mu)$, and regrouping the $\mathcal{O}(\mu\epsilon^2)$ terms, (4.19) becomes:

$$\begin{aligned}(I+\mu\nu\alpha T[0])\big[\partial_t v+\epsilon\varsigma v\partial_x v+\frac{\alpha-1}{\alpha}\big((\gamma+\delta)\partial_x\zeta+\epsilon\partial_x(q_3(\epsilon\zeta)v^2)\big)\big]+\frac{1}{\alpha}\big((\gamma+\delta)\partial_x\zeta+\epsilon\partial_x(q_3(\epsilon\zeta)v^2)\big)\\ +\mu\epsilon Q_1(v)+\mu\epsilon\nu S[\zeta](\partial_t v)-\epsilon\kappa_1\zeta\mu\nu T[0](\partial_t v)+\mathcal{O}(\mu^2,\mu\epsilon^2)=0\end{aligned}\quad(4.20)$$

Expanding in terms of ϵ and μ, and looking for the term $\partial_t v$, we get:

$$\partial_t v=-(I+\mu\nu\alpha T[0])^{-1}[(\gamma+\delta)\partial_x\zeta]+\mathcal{O}(\epsilon,\mu)\quad(4.21)$$

Replacing $\partial_t v$ by its expression obtained in (4.21) in the last two terms of the equation (4.20) the Green–Naghdi equations with improved dispersion can therefore be written as (up to the order

$\mathcal{O}(\mu^2)$) :

$$\begin{cases} \partial_t\zeta + \partial_x\big(f(\epsilon\zeta)v\big) \;=\; 0, \\ \\ (I+\mu\nu\alpha T[0])\big[\partial_t v + \epsilon\varsigma v\partial_x v + \dfrac{\alpha-1}{\alpha}\big((\gamma+\delta)\partial_x\zeta + \epsilon\partial_x(q_3(\epsilon\zeta)v^2)\big)\big] \\ +\dfrac{1}{\alpha}\big((\gamma+\delta)\partial_x\zeta + \epsilon\partial_x(q_3(\epsilon\zeta)v^2)\big) + \mu\epsilon Q_1(v) + \mu\epsilon\nu Q_2(\zeta) + \mu\epsilon\nu Q_3(\zeta) = 0. \end{cases} \tag{4.22}$$

with

$$Q_2(\zeta) = -S[\zeta]\Big(I+\mu\nu\alpha T[0]\Big)^{-1}[(\gamma+\delta)\partial_x\zeta], \tag{4.23}$$

and

$$Q_3(\zeta) = \kappa_1\zeta T[0]\Big(I+\mu\nu\alpha T[0]\Big)^{-1}[(\gamma+\delta)\partial_x\zeta]. \tag{4.24}$$

In [30], a three-parameter family of Green–Naghdi equations in the one layer case is derived yielding additional improvements of the dispersive properties. In this chapter we stick to the one-parameter family (4.22). This new formulation does not contain any third-order derivative, thus one can expect more stable and robust numerical computations.

4.3.3 Choice of the parameter α

The choice of the parameter α is motivated by the agreement of the dispersion properties of the *full Euler system* and the improved Green-Naghdi system (4.22) in term of the dispersion relation. Therefore, we have first to find the dispersion relation for the improved Green-Naghdi system, then the dispersion relation for the *full Euler system* and finally to find an optimal parameter α_{opt} to ensure a good agreement between these two relations.

The dispersion relation associated to the improved GN formulation

The system (4.22) can be written under the following form:

$$\begin{cases} \partial_t\zeta + \partial_x\big(f(\epsilon\zeta)v\big) \;=\; 0, \\ \\ (I+\mu\nu\alpha T[0])\big[\partial_t v + \epsilon\varsigma v\partial_x v + \dfrac{\alpha-1}{\alpha}\big((\gamma+\delta)\partial_x\zeta + \epsilon\partial_x(q_3(\epsilon\zeta)v^2)\big)\big] \\ +\dfrac{1}{\alpha}\big((\gamma+\delta)\partial_x\zeta + \epsilon\partial_x(q_3(\epsilon\zeta)v^2)\big) + \mu\epsilon Q_1(v) + \mu\epsilon\nu Q_2(\zeta) + \mu\epsilon\nu Q_3(\zeta) = 0, \end{cases} \tag{4.25}$$

where the operators Q_1, Q_2 and Q_3 are explicitly given in (4.9), (4.23) and (4.24). Looking at the linearization of (4.25) around the rest state $(\zeta, v) = (0, 0)$, one derives the dispersion relation associated to (4.25).
This relation is obtained by looking for plane wave solutions of the form $(\zeta, v) = (\underline{\zeta}, \underline{v})e^{i(kx-wt)}$, with k the spatial wave number and ω the time pulsation, of the linearized equations.

The first equation of (4.25) gives:

$$-iw\underline{\zeta} + \frac{1}{(\gamma+\delta)}ik\underline{v} = 0\ .$$

Thus we first obtain:

$$\underline{v} = \frac{w(\gamma+\delta)}{k}\underline{\zeta}. \tag{4.26}$$

From the second equation of (4.25) we have:

$$(1+\mu\nu\alpha k^2)\Big(-iw\underline{v}+\frac{\alpha-1}{\alpha}(\gamma+\delta)ik\underline{\zeta}\Big)+\frac{1}{\alpha}(\gamma+\delta)ik\underline{\zeta}=0.$$

This equation may be written as:

$$-iw\underline{v}+(\gamma+\delta)ik\underline{\zeta}-\mu\nu\alpha iwk^2\underline{v}+\mu\nu(\alpha-1)(\gamma+\delta)ik^3\underline{\zeta}=0. \tag{4.27}$$

Replacing $\underline{v}$ in (4.27) by its expression given in (4.26) we obtain:

$$-w^2\frac{(\gamma+\delta)}{k}\underline{\zeta}+(\gamma+\delta)k\underline{\zeta}-\mu\nu\alpha wk^2\frac{w(\gamma+\delta)}{k}\underline{\zeta}+\mu\nu(\alpha-1)(\gamma+\delta)k^3\underline{\zeta}=0. \tag{4.28}$$

After straightforward computations, we obtain the following dispersion relation of the new GN formulation for $\alpha \geq 1$:

$$w_{\alpha,GN}=\pm|k|\sqrt{\frac{1+\mu\nu(\alpha-1)k^2}{1+\mu\nu\alpha k^2}} \tag{4.29}$$

Defining the linear phase velocity associated to (4.29) as:

$$C^p_{GN}(k)=\frac{w(k)}{|k|},$$

we choose α such that the phase velocity stays close to the reference phase velocity $C^p_S(k)$ coming from Stokes linear theory. Thanks to this approach, the error on the phase velocity is minimized for any discrete value of $\mu|k|$ and the corresponding local optimal value of α, denoted by α_{opt} is computed. In order to do so, we have firstly to obtain the dispersion relation of the original *full Euler system.*

The dispersion relation associated to the full-Euler system

Let us recall the *full-Euler system* given in (4.2):

$$\begin{cases} \partial_t\zeta \;-\; \dfrac{1}{\mu}G^\mu\psi \;=\; 0, \\[2ex] \partial_t\Big(H^{\mu,\delta}\psi-\gamma\partial_x\psi\Big) \;+\; (\gamma+\delta)\partial_x\zeta \;+\; \dfrac{\epsilon}{2}\partial_x\Big(|H^{\mu,\delta}\psi|^2-\gamma|\partial_x\psi|^2\Big) \\ \qquad\qquad = \mu\epsilon\partial_x\mathcal{N}^{\mu,\delta}-\mu\dfrac{\gamma+\delta}{\mathrm{bo}}\dfrac{\partial_x\big(k(\epsilon\sqrt{\mu}\zeta)\big)}{\epsilon\sqrt{\mu}}\;, \end{cases} \tag{4.30}$$

where

$$\mathcal{N}^{\mu,\delta} \;\equiv\; \frac{\big(\frac{1}{\mu}G^\mu\psi+\epsilon(\partial_x\zeta)H^{\mu,\delta}\psi\big)^2 \;-\; \gamma\big(\frac{1}{\mu}G^\mu\psi+\epsilon(\partial_x\zeta)(\partial_x\psi)\big)^2}{2(1+\mu|\epsilon\partial_x\zeta|^2)},$$

and

$$\begin{aligned} G^\mu\psi \;&\equiv\; G^\mu[\epsilon\zeta]\psi\equiv\sqrt{1+\mu|\epsilon\partial_x\zeta|^2}\big(\partial_n\phi_1\big)\,|_{z=\epsilon\zeta}=-\mu\epsilon(\partial_x\zeta)(\partial_x\phi_1)\,|_{z=\epsilon\zeta}+(\partial_z\phi_1)\,|_{z=\epsilon\zeta}\;, \\ H^{\mu,\delta}\psi \;&\equiv\; H^{\mu,\delta}[\epsilon\zeta,\beta b]\psi\equiv\partial_x\big(\phi_2\,|_{z=\epsilon\zeta}\,\big)=(\partial_x\phi_2)\,|_{z=\epsilon\zeta}+\epsilon(\partial_x\zeta)(\partial_z\phi_2)\,|_{z=\epsilon\zeta}\;, \end{aligned}$$

where ϕ_1 and ϕ_2 are uniquely defined (up to a constant for ϕ_2) as the solutions in $H^2(\mathbb{R})$ of the following Laplace's problems.

$$\begin{cases} \left(\mu\partial_x^2 + \partial_z^2 \right) \phi_1 = 0 & \text{in } \Omega_1 \equiv \{(x,z) \in \mathbb{R}^2,\ \epsilon\zeta(x) < z < 1\}, \\ \partial_z\phi_1 = 0 & \text{on } \Gamma_{\rm t} \equiv \{(x,z) \in \mathbb{R}^2,\ z = 1\}, \\ \phi_1 = \psi & \text{on } \Gamma \equiv \{(x,z) \in \mathbb{R}^2,\ z = \epsilon\zeta\}, \end{cases} \tag{4.31}$$

$$\begin{cases} \left(\mu\partial_x^2 + \partial_z^2 \right) \phi_2 = 0 & \text{in } \Omega_2 \equiv \{(x,z) \in \mathbb{R}^2,\ -\frac{1}{\delta} < z < \epsilon\zeta\}, \\ \partial_n\phi_2 = \partial_n\phi_1 & \text{on } \Gamma, \\ \partial_z\phi_2 = 0 & \text{on } \Gamma_{\rm b} \equiv \{(x,z) \in \mathbb{R}^2,\ z = -\frac{1}{\delta}\}. \end{cases} \tag{4.32}$$

To obtain the dispersion relation associated to the *full-Euler system*, we first have to linearize it around the rest state that is $\zeta = 0\,,\, v = 0$. We have thus to compute the two operators G^μ and $H^{\mu,\delta}$ at the rest state. Therefore we have firstly to linearize the two previous equations (4.31)-(4.32), then write the linear system in the wave number space by performing a Fourier transform. After performing some algebraic computations, we will obtain the dispersion relation. Let us remark that the two equations (4.31) and (4.32) are very similar except for the boundary conditions, and the space domain Ω_1 and Ω_2. Therefore we have chosen to perform the complete analysis for the two equations.

• Linearizing (4.31) around the rest state ($\zeta = 0$) gives:

$$\begin{cases} \left(\mu\partial_x^2 + \partial_z^2 \right) \phi_1 = 0 & \text{in } \Omega_1 \equiv \{(x,z) \in \mathbb{R}^2,\ 0 < z < 1\}, \\ \partial_z\phi_1 = 0 & \text{on } \Gamma_{\rm t} \equiv \{(x,z) \in \mathbb{R}^2,\ z = 1\}, \\ \phi_1 = \psi & \text{on } \Gamma \equiv \{(x,z) \in \mathbb{R}^2,\ z = 0\}, \end{cases} \tag{4.33}$$

Applying the Fourier transform with respect to x, one has:

$$\begin{cases} -\mu|k|^2\widehat{\phi_1} + \partial_z^2\widehat{\phi_1} = 0 & \text{in } \Omega_1 \equiv \{(x,z) \in \mathbb{R}^2,\ 0 < z < 1\}, \\ \partial_z\widehat{\phi_1} = 0 & \text{on } \Gamma_{\rm t} \equiv \{(x,z) \in \mathbb{R}^2,\ z = 1\}, \\ \widehat{\phi_1} = \widehat{\psi} & \text{on } \Gamma \equiv \{(x,z) \in \mathbb{R}^2,\ z = 0\}, \end{cases} \tag{4.34}$$

One can easily remark that (4.34) is an ordinary linear differential equation of order 2 whose solution has the following form (since $\mu k^2 \geq 0$):

$$\widehat{\phi_1}(k) = A(k)\cosh(\sqrt{\mu}|k|z) + B(k)\sinh(\sqrt{\mu}|k|z).$$

Writing the boundary condition at $z = 0$ i.e. $\widehat{\phi_1}|_{z=0} = \widehat{\psi}$ and at $z = 1$ i.e. $(\partial_z\widehat{\phi_1})|_{z=1} = 0$ we obtain:

$$A(k) = \widehat{\psi}(k) \quad \text{and} \quad B(k) = -\tanh(\sqrt{\mu}|k|)\widehat{\psi}(k)\ .$$

Thus we obtain:

$$\widehat{\phi_1}(k) = \Big[\cosh(\sqrt{\mu}|k|z) - \tanh(\sqrt{\mu}|k|)\sinh(\sqrt{\mu}|k|z)\Big]\widehat{\psi}(k)\ .$$

Therefore as:

$$\widehat{G^\mu[0]\psi} = (\partial_z\widehat{\phi_1})|_{z=0} = -\sqrt{\mu}|k|\tanh(\sqrt{\mu}|k|)\widehat{\psi}(k),$$

we finally have:

$$G^\mu[0]\psi = -\sqrt{\mu}|k|\tanh(\sqrt{\mu}|k|)\psi(k). \tag{4.35}$$

• Linearizing (4.32) around the rest state ($\zeta = 0$) gives:

$$\begin{cases} \left(\mu\partial_x^2 \ + \ \partial_z^2 \right) \ \phi_2 = 0 & \text{in } \Omega_2 \equiv \{(x,z) \in \mathbb{R}^2, \ -\frac{1}{\delta} < z < 0\}, \\ \partial_z\phi_2 = \partial_z\phi_1 = G^\mu[0]\psi & \text{on } \Gamma \equiv \{(x,z) \in \mathbb{R}^2, \ z = 0\}, \\ \partial_z\phi_2 = 0 & \text{on } \Gamma_{\rm b} \equiv \{(x,z) \in \mathbb{R}^2, \ z = -\frac{1}{\delta}\}. \end{cases} \tag{4.36}$$

Applying the Fourier transform with respect to x, one has:

$$\begin{cases} -\mu|k|^2\widehat{\phi_2} + \partial_z^2\widehat{\phi_2} = 0 & \text{in } \Omega_2 \equiv \{(x,z) \in \mathbb{R}^2, \ -\frac{1}{\delta} < z < 0\}, \\ \partial_z\widehat{\phi_2} = \widehat{G^\mu[0]\psi} = -\sqrt{\mu}|k|\tanh(\sqrt{\mu}|k|)\widehat{\psi(k)} & \text{on } \Gamma \equiv \{(x,z) \in \mathbb{R}^2, \ z = 0\}, \\ \partial_z\widehat{\phi_2} = 0 & \text{on } \Gamma_{\rm b} \equiv \{(x,z) \in \mathbb{R}^2, \ z = -\frac{1}{\delta}\}. \end{cases} \tag{4.37}$$

One can easily remark that (4.37) is an ordinary differential equation of order 2 whose solution has the following form (since $\mu k^2 \geq 0$):

$$\widehat{\phi_2}(k) = A(k)\cosh(\sqrt{\mu}|k|z) + B(k)\sinh(\sqrt{\mu}|k|z).$$

Writing the boundary condition at $z = 0$ i.e. $(\partial_z\widehat{\phi_2})|_{z=0} = -\sqrt{\mu}|k|\tanh(\sqrt{\mu}|k|)\widehat{\psi(k)}$ and at $z = -1/\delta$ i.e. $(\partial_z\widehat{\phi_2})|_{z=-1/\delta} = 0$ we obtain:

$$B(k) = -\tanh(\sqrt{\mu}|k|)\widehat{\psi}(k) \quad \text{and} \quad -A(k)\sinh\left(\frac{\sqrt{\mu}|k|}{\delta}\right) + B(k)\cosh\left(\frac{\sqrt{\mu}|k|}{\delta}\right) = 0 \ .$$

Replacing $B(k)$ by its expression, we obtain:

$$A(k) = -\frac{\tanh\left(\sqrt{\mu}|k|\right)}{\tanh\left(\frac{\sqrt{\mu}|k|}{\delta}\right)}\widehat{\psi}(k).$$

Since $\widehat{\phi_2}(k)|_{z=0} = A(k)$ we have thus: $\phi_2(k)|_{z=0} = -\dfrac{\tanh\left(\sqrt{\mu}|k|\right)}{\tanh\left(\frac{\sqrt{\mu}|k|}{\delta}\right)}\psi(k)$.

Therefore,

$$H^{\mu,\delta}[0]\psi = \partial_x(\phi_2|_{z=0}) = -\frac{\tanh\left(\sqrt{\mu}|k|\right)}{\tanh\left(\frac{\sqrt{\mu}|k|}{\delta}\right)}\partial_x\psi. \tag{4.38}$$

Having obtained the two operators G^μ and $H^{\mu,\delta}$ at the rest state, (4.35) and (4.38), we can now proceed to compute the dispersion relation for the *full Euler system*.
One derives the dispersion relation associated to (4.30) by looking for plane wave solutions of the form $(\zeta, \psi) = (\underline{\zeta}, \underline{\psi})e^{i(kx-wt)}$ to the linearized equations around the rest state $(\zeta, \psi) = (0, 0)$.

The linearisation of the *full Euler system*, (4.30) at the rest state, $\zeta = 0$, $\psi = 0$, writes under the form:

$$\begin{cases} \partial_t\zeta \ - \ \dfrac{1}{\mu}G^\mu[0]\psi \ = \ 0, \\ \\ \partial_t\Big(H^{\mu,\delta}[0]\psi - \gamma\partial_x\psi\Big) \ + \ (\gamma+\delta)\partial_x\zeta = -\mu\dfrac{\gamma+\delta}{\rm bo}\dfrac{\partial_x\big(k(\epsilon\sqrt{\mu}\zeta)\big)}{\epsilon\sqrt{\mu}} \ , \end{cases} \tag{4.39}$$

Replacing $G^{\mu}[0]\psi$ by its expression given by (4.35) in the first equation of the system (4.39), we firstly have:

$$-iw\underline{\zeta} + \frac{1}{\sqrt{\mu}}|k|\tanh\Big(\sqrt{\mu}|k|\Big)\underline{\psi} = 0.$$

Thus,

$$\underline{\zeta} = \frac{1}{\sqrt{\mu}iw}|k|\tanh\Big(\sqrt{\mu}|k|\Big)\underline{\psi}. \tag{4.40}$$

Replacing $H^{\mu}[0]\psi$ by its expression given by (4.38) in the second equation of the system (4.39), we obtain:

$$-\frac{\tanh\Big(\sqrt{\mu}|k|\Big)}{\tanh\Big(\frac{\sqrt{\mu}|k|}{\delta}\Big)}\partial_t(\partial_x\psi) - \gamma\partial_t(\partial_x\psi) + (\gamma+\delta)\partial_x\zeta - \mu\frac{\gamma+\delta}{\mathrm{bo}}\partial_x^3\zeta = 0.$$

Thus,

$$-\frac{\tanh\Big(\sqrt{\mu}|k|\Big)}{\tanh\Big(\frac{\sqrt{\mu}|k|}{\delta}\Big)}wk\underline{\psi} - \gamma wk\underline{\psi} + (\gamma+\delta)ik\underline{\zeta} + \mu\frac{\gamma+\delta}{\mathrm{bo}}ik^3\underline{\zeta} = 0.$$

After straightforward computations and replacing $\underline{\zeta}$ by its expression given in (4.40) we finally obtain the following dispersion relation:

$$w_{F.E}^2 = \frac{(\gamma+\delta)|k|\tanh\Big(\sqrt{\mu}|k|\Big)(1+\frac{\mu}{\mathrm{bo}}k^2)\tanh\Big(\sqrt{\mu}\frac{|k|}{\delta}\Big)}{\sqrt{\mu}[\tanh\Big(\sqrt{\mu}|k|\Big)+\gamma\tanh\Big(\sqrt{\mu}\frac{|k|}{\delta}\Big)]}. \tag{4.41}$$

Phase velocity agreement

One can easily remark that the Taylor expansions of the two previous dispersion relations (4.29) and (4.41) are equivalent for small wavenumbers,

$$w_{\alpha,GN}^2 \equiv w_{F.E}^2 \simeq k^2 - \mu\nu k^4 + \mathcal{O}(\mu^2k^6).$$

Indeed, for small wavenumber one has:

$$\begin{aligned} w_{\alpha,GN}^2 &= k^2\Big(\frac{1+\mu\nu(\alpha-1)k^2}{1+\mu\nu\alpha k^2}\Big) \\ &\approx k^2(1+\mu\nu(\alpha-1)k^2)(1-\mu\nu\alpha k^2+\mathcal{O}((\sqrt{\mu}k)^4)) \\ &\approx k^2(1-\mu\nu\alpha k^2+\mu\nu(\alpha-1)k^2+\mathcal{O}((\sqrt{\mu}k)^4)) \\ &\approx k^2-\mu\nu k^4+\mathcal{O}(\mu^2k^6). \end{aligned}$$

and

$$\begin{aligned}
w_{FE}^2 &= \frac{(\gamma+\delta)|k|\tanh(\sqrt{\mu}|k|)(1+\frac{\mu}{\mathrm{bo}}k^2)\tanh(\sqrt{\mu}\frac{|k|}{\delta})}{\sqrt{\mu}[\tanh(\sqrt{\mu}|k|)+\gamma\tanh(\sqrt{\mu}\frac{|k|}{\delta})]} \\
&\approx \frac{(\gamma+\delta)|k|\big[\sqrt{\mu}k-\frac{(\sqrt{\mu}k)^3}{3}+\mathcal{O}((\sqrt{\mu}k)^5)\big](1+\frac{\mu}{\mathrm{bo}}k^2)\big[\frac{\sqrt{\mu}k}{\delta}-\big(\frac{\sqrt{\mu}k}{\delta}\big)^3\frac{1}{3}+\mathcal{O}((\sqrt{\mu}k)^5)\big]}{\sqrt{\mu}\Big[\sqrt{\mu}k-\frac{(\sqrt{\mu}k)^3}{3}+\mathcal{O}((\sqrt{\mu}k)^5)+\gamma\Big(\frac{\sqrt{\mu}k}{\delta}-\big(\frac{\sqrt{\mu}k}{\delta}\big)^3\frac{1}{3}+\mathcal{O}((\sqrt{\mu}k)^5)\Big)\Big]} \\
&\approx k^2+\mu k^4\Big[\frac{1}{\mathrm{bo}}-\frac{\delta^2(1+\gamma\delta)}{3\delta^3(\gamma+\delta)}\Big]+\mathcal{O}(\mu^2k^6) \\
&\approx k^2-\mu\nu k^4+\mathcal{O}(\mu^2k^6).
\end{aligned}$$

Therefore for small wavenumbers and in the whole range of regime, the choice of α does not influence the dispersion relation (4.29). In the desired simulations, we are interested in small wave length (i.e large wavenumbers) dispersion characteristics and thus we would like to find an optimal value of α in order to observe the same dispersion properties for the reduced Green-Naghdi model that the *full Euler* original problem satisfies. Therefore, we are interested in values of α such that $C_{GN}^p(k) = C_{F.E}^p(k)$ for large value of k. We can thus compute α_{opt} from the equality: $w_{\alpha,GN}^2 = w_{F.E}^2$.
Let us denote $X = \sqrt{\mu}|k|$. The previous equality writes:

$$\frac{1+\nu X^2(\alpha_{opt}-1)}{1+\nu X^2\alpha_{opt}} = \frac{(\gamma+\delta)\tanh(X)(1+\frac{X^2}{\mathrm{bo}})\tanh(\frac{X}{\delta})}{X[\tanh(X)+\gamma\tanh(\frac{X}{\delta})]} = g(X).$$

After straightforward computations we obtain the follwing expression for the value of α_{opt}:

$$\alpha_{opt} = \frac{g(X)-1+\nu X^2}{\nu X^2(1-g(X))}.$$

In Figure 4.2 (top), α_{opt} is plotted against the spatial wave number k, for $k \in [0,4]$ and $\mu = 1$, for the one and two layers cases. For the one layer case we set $\gamma = 0$, $\delta = 1$ and $\mathrm{bo}^{-1} = 0$ whereas for the two layers case we set $\gamma = 0.95$, $\delta = 0.5$ and $\mathrm{bo}^{-1} = 5\times10^{-5}$. We would like to mention that $\alpha_{opt} \to 1$ in both cases when considering very large values of k, this fact is confirmed by the numerical simulation done in Section 4.5.2, see Figure 4.18, where we notice similar observations at time $t = 20\ s$. Therefore, we will use an optimal value of α different of 1 only when looking at the dispersion effects for intermediate wave numbers. This is highlighted, when comparing to the numerical experiments done in [50] (for more details see Section 4.5.2). In Figure 4.2 (bottom), the ratio $\dfrac{C_{GN}^p(k)}{C_S^p(k)}$ (i.e linear phase velocity error), is plotted against the spatial wave number k for $k \in [0,4]$, in the one and two layer cases.

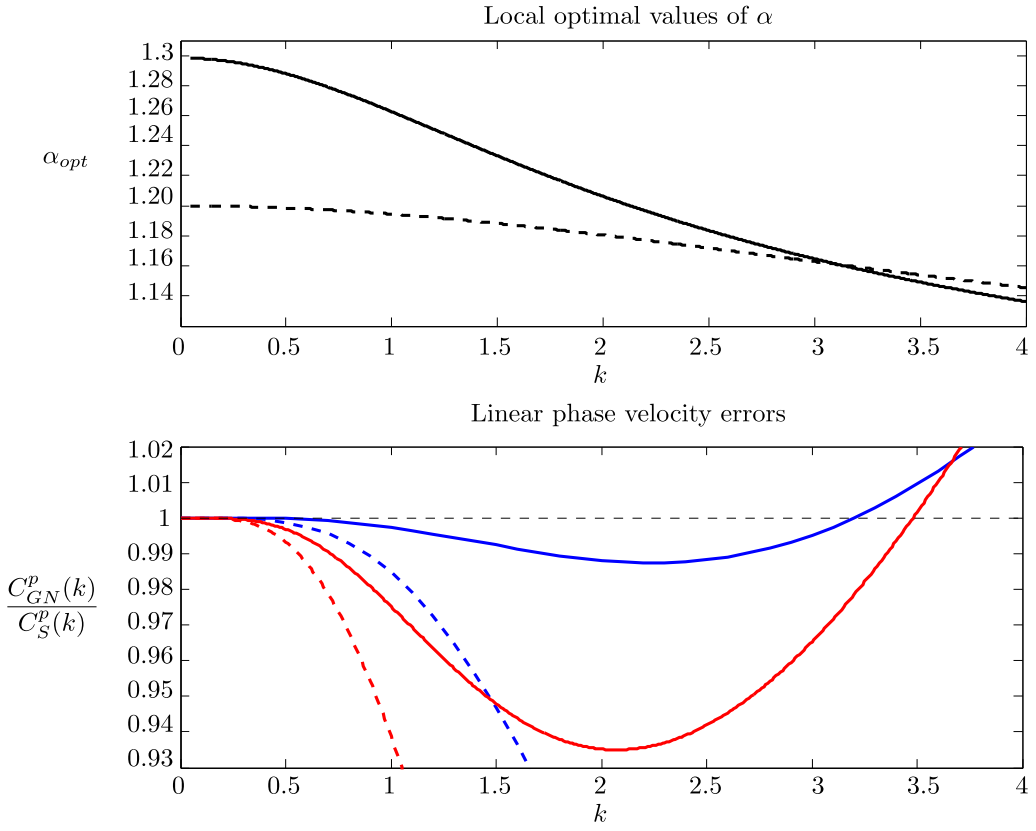

Figure 4.2. Top: local optimal values of α for $k \in [0, 4]$, for the two layers case (full line) and one layer case (dashed line). Bottom: linear phase velocity errors in the one layer case (blue) and two layers case (red) for $\alpha_{opt} = 1.159$ (full blue line) and $\alpha_{opt} = 1.498$ (full red line) and $\alpha = 1$ (dashed line)

4.3.4 High frequencies instabilities

In what follows, a qualitative discussion on the stability of the improved model (4.22) is given. We study the high frequencies instabilities in the one layer case, as well as in the two layers case. As $\mu << 1$, a simple expansion of the operator $(I + \mu\nu\alpha T[0])^{-1}$ shows that we have:

$$(I + \mu\nu\alpha T[0])^{-1}[(\gamma + \delta)\partial_x\zeta] = (\gamma + \delta)\partial_x\zeta + \mathcal{O}(\mu).$$

Thus, we could replace $Q_2(\zeta)$ by $\widetilde{Q}_2(\zeta) = -S[\zeta]\big((\gamma+\delta)\partial_x\zeta\big)$, and $Q_3(\zeta)$ by $\widetilde{Q}_3(\zeta) = \kappa_1\zeta T[0][(\gamma+\delta)\partial_x\zeta]$ in the second equation of (4.22), keeping the same order of precision $\mathcal{O}(\mu^2)$. This simple expansion would avoid the inversion of $(I+\mu\nu\alpha T[0])$ (resolution of an extra linear system) in the computation of Q_2 and Q_3 but it leads to instabilities. Indeed, this is due to the fact that the two terms $\widetilde{Q}_2(\zeta)$ and $\widetilde{Q}_3(\zeta)$ contain third order derivatives in ζ that may create high frequencies instabilities.

Remark 14. In order to recover the dimensionalized version of system (4.22), one has to set $\mu = \epsilon = 1$ and add the acceleration of gravity term g when necessary to obtain the following

system:

$$\begin{cases} \partial_t\zeta + \partial_x\big(f(\zeta)v\big) \;=\; 0, \\ \\ (I+\nu\alpha T[0])\big[\partial_t v + \varsigma v\partial_x v + \dfrac{\alpha-1}{\alpha}\big((\gamma+\delta)g\partial_x\zeta + \partial_x(q_3(\zeta)v^2)\big)\big] \\ +\dfrac{1}{\alpha}\big((\gamma+\delta)g\partial_x\zeta + \partial_x(q_3(\zeta)v^2)\big) + Q_1(v) + \nu Q_2(\zeta) + \nu Q_3(\zeta) = 0, \end{cases} \tag{4.42}$$

with

$$Q_2(\zeta) = \kappa_2\partial_x\Big(\zeta\partial_x\big((I+\nu\alpha T[0])^{-1}[(\gamma+\delta)g\partial_x\zeta]\big)\Big) \tag{4.43}$$

and

$$Q_3(\zeta) = \kappa_1\zeta T[0](I+\nu\alpha T[0])^{-1}[(\gamma+\delta)g\partial_x\zeta]. \tag{4.44}$$

Firstly, we discuss the stability of the model (4.42) in the one layer case without surface tension. To this end, we set $\gamma = 0$, $\delta = 1$ and $\dfrac{1}{\text{bo}} = 0$. Thus system (4.42) becomes:

$$\begin{cases} \partial_t\zeta + \partial_x\big((1+\zeta)v\big) \;=\; 0, \\ \\ (I+\dfrac{\alpha}{3}T[0])\big[\partial_t v + v\partial_x v + \dfrac{\alpha-1}{\alpha}g\partial_x\zeta\big] + \dfrac{1}{\alpha}g\partial_x\zeta + Q_1(v) + Q_2(\zeta) + \dfrac{1}{3}Q_3(\zeta) = 0, \end{cases} \tag{4.45}$$

with

$$Q_1(v) = \frac{2}{3}\partial_x((\partial_x v)^2),$$

$$Q_2(\zeta) = \partial_x\Big(\zeta\partial_x\big((I+\frac{\alpha}{3}T[0])^{-1}[g\partial_x\zeta]\big)\Big), \tag{4.46}$$

$$Q_3(\zeta) = \zeta T[0](I+\frac{\alpha}{3}T[0])^{-1}[g\partial_x\zeta]. \tag{4.47}$$

When linearizing system (4.45) around constant state solution $(\underline{\zeta}, \underline{v})$, one obtains the following linear system in $(\tilde{\zeta}, \tilde{v})$:

$$\begin{cases} \partial_t\tilde{\zeta} + (1+\underline{\zeta})\partial_x\tilde{v} + \underline{v}\partial_x\tilde{\zeta} \;=\; 0, \\ \\ (I-\dfrac{\alpha}{3}\partial_x^2)\big[\partial_t\tilde{v} + \underline{v}\partial_x\tilde{v} + \dfrac{\alpha-1}{\alpha}g\partial_x\tilde{\zeta}\big] + \dfrac{1}{\alpha}g\partial_x\tilde{\zeta} + \dfrac{2}{3}g\underline{\zeta}\partial_x^2\Big((I-\dfrac{\alpha}{3}\partial_x^2)^{-1}\partial_x\tilde{\zeta}\Big) = 0. \end{cases} \tag{4.48}$$

Looking for plane wave solution of the form $(\tilde{\zeta}, \tilde{v}) = e^{i(kx-wt)}(\zeta^0, v^0)$ as solution of the above system, one obtains the following dispersion relation:

$$\frac{(w-k\underline{v})^2}{g(1+\underline{\zeta})k^2} = \frac{1+\frac{(\alpha-1)}{3}k^2 - \dfrac{2k^2\underline{\zeta}}{3(1+\frac{\alpha}{3}k^2)}}{1+\frac{\alpha}{3}k^2}. \tag{4.49}$$

When we consider the linearization of our new model around the rest state $(\underline{\zeta}, \underline{v}) = (0, 0)$, the dispersion relation (4.49) becomes:

$$w^2 = gk^2\frac{1+\frac{(\alpha-1)}{3}k^2}{1+\frac{\alpha}{3}k^2}.$$

In this case the perturbations are always stable if $\alpha \geq 1$. We refer to Section 4.3.3 for the discussion concerning the choice of α in order to improve the dispersive properties of the model. Now, replacing $Q_2(\zeta)$ defined in (4.46) by $\widetilde{Q}_2(\zeta) = \partial_x\Big(\zeta\partial_x\big(g\partial_x\zeta\big)\Big)$ and $Q_3(\zeta)$ defined in (4.47) by $\widetilde{Q}_3(\zeta) = \kappa_1\zeta T[0][g\partial_x\zeta]$ in the second equation of (4.45), modifies the dispersion relation (4.49) and we obtain instead:

$$\frac{(\tilde{w} - k\underline{v})^2}{g(1+\underline{\zeta})k^2} = \frac{1 + \frac{(\alpha-1)}{3}k^2 - \frac{2k^2\underline{\zeta}}{3}}{1 + \frac{\alpha}{3}k^2}. \tag{4.50}$$

One can easily check that if $\underline{\zeta} > \dfrac{(\alpha-1)}{2}$, the numerator of the right hand side of the dispersion relation (4.50) will become negative for sufficiently large values of k^2. Thus the root of $\tilde{w}$ will become complex inducing a high frequency instability of the model, see Figure 4.3. On the other hand, the numerator of the r.h.s of the dispersion relation (4.49) is positive for sufficiently large values of k^2, due to the existence of the term $-\dfrac{2k^2\underline{\zeta}}{3(1+\frac{\alpha}{3}k^2)}$, thus w is always real at high frequencies.

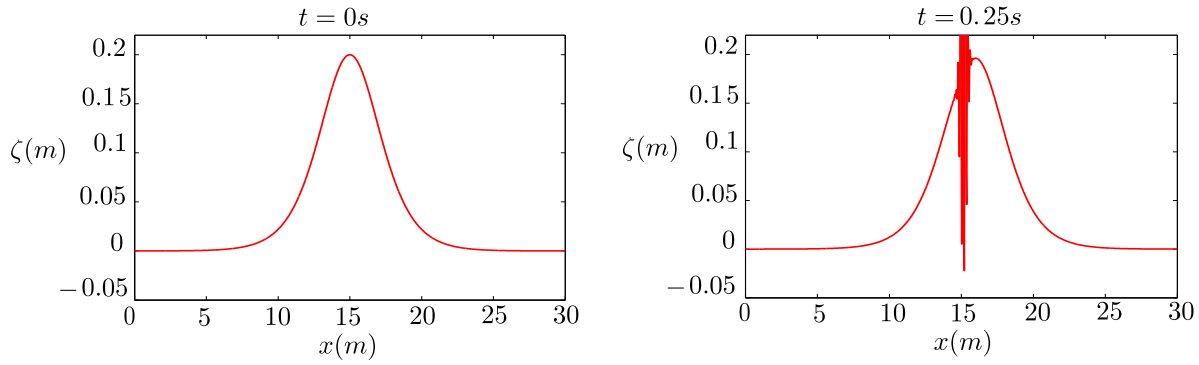

Figure 4.3. High frequencies instabilities in the one layer case due to third order derivatives.

Let us now discuss the stability issue of the model (4.42) in the two layers case without surface tension. When linearizing system (4.42) around motionless steady state solution ($\underline{\zeta} = \text{cst}, \underline{v} = 0$) and after following the same method as above, one obtains the following dispersion relation:

$$\frac{w^2}{gf(\underline{\zeta})k^2} = \frac{(\gamma+\delta)\Big(1 + \nu(\alpha-1)k^2 - \nu\dfrac{(\kappa_2-\kappa_1)k^2\underline{\zeta}}{(1+\nu\alpha k^2)}\Big)}{1+\nu\alpha k^2}. \tag{4.51}$$

Replacing $Q_2(\zeta)$ defined in (4.43) by $\widetilde{Q}_2(\zeta) = \partial_x\Big(\zeta\partial_x\big(g(\gamma+\delta)\partial_x\zeta\big)\Big)$ and $Q_3(\zeta)$ defined in (4.44) by $\widetilde{Q}_3(\zeta) = \kappa_1\zeta T[0][g(\gamma+\delta)\partial_x\zeta]$ in the second equation of (4.42), modifies the dispersion relation (4.51) and we obtain instead:

$$\frac{\tilde{w}^2}{gf(\underline{\zeta})k^2} = \frac{(\gamma+\delta)(1 + \nu(\alpha-1)k^2 - \nu(\kappa_2-\kappa_1)k^2\underline{\zeta})}{(1+\nu\alpha k^2)}. \tag{4.52}$$

In this case, there exists a critical ratio for the depth of the two layers. Indeed, when $\delta^2 < \gamma$, one has $\kappa_2 < \kappa_1$, thus the perturbations are always stable if $\alpha \geq 1$. Whereas, when $\delta^2 \geq \gamma$ i.e

assuming $\gamma = 0.5$, $\delta = 0.8$ and $\dfrac{1}{\text{bo}} = 0$, one has $\kappa_2 > \kappa_1$, thus the perturbations are unstable if $\underline{\zeta} > \dfrac{\alpha - 1}{\kappa_2 - \kappa_1}$. In fact, under the previous conditions the numerator of the right hand side of the dispersion relation (4.52) will become negative for sufficiently large values of k^2. Thus the root of $\tilde{w}$ will become complex inducing a high frequency instability of the model, see Figure 4.4. On the other hand, the numerator of the r.h.s of the dispersion relation (4.51) is positive for sufficiently large values of k^2, due to the existence of the term $-\nu\dfrac{(\kappa_2 - \kappa_1)k^2\underline{\zeta}}{(1 + \nu\alpha k^2)}$, thus w is always real at high frequencies. This ensures the numerical stability of the model (4.42) which will be considered in the rest of this work.

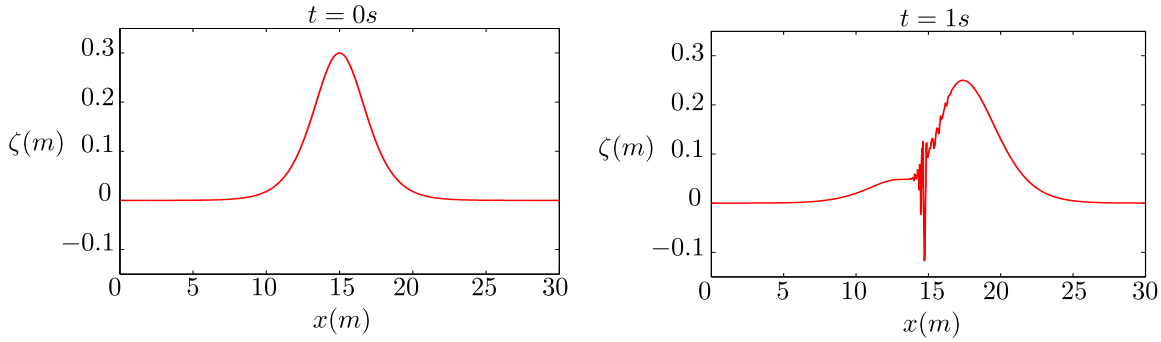

Figure 4.4. High frequencies instabilities in the two layers case due to third order derivatives.

4.4 Numerical methods

This section is devoted to the numerical methods developped to solve the improved Green-Naghdi equations (4.22). As pointed out by many authors [18, 86] the improved dispersion Green-Naghdi equations (4.22) is well-adapted to the implementation of a splitting scheme separating the hyperbolic and the dispersive parts of the equations. We present in Section 4.4.1 this splitting scheme inspired by [18, 86]. We explain in Sections 4.4.2 and 4.4.3 how we treat respectively the hyperbolic and dispersive parts of the equations.

We decided to treat the hyperbolic part by a finite volume method of Roe type. We will construct first order, second order "MUSCL" type method and finally 5th order "WENO" method. The high order method is suitable to compute correctly the maximum value of the height ζ and the discontinuities by limiting the diffusive effects. As we will show in the numerical validations, the high order scheme is also suitable to catch correctly the dispersive effects.

The dispersive part of the proposed splitting method is solved using a classical finite difference method.

4.4.1 The splitting scheme

Let us recall the improved Green-Naghdi system that we consider:

$$\begin{cases} \partial_t\zeta + \partial_x\big(f(\epsilon\zeta)v\big) \;=\; 0, \\ \\ (I+\mu\nu\alpha T[0])\big[\partial_t v + \epsilon\varsigma v\partial_x v + \dfrac{\alpha-1}{\alpha}\big((\gamma+\delta)\partial_x\zeta + \epsilon\partial_x(q_3(\epsilon\zeta)v^2)\big)\big] \\ +\dfrac{1}{\alpha}\big((\gamma+\delta)\partial_x\zeta + \epsilon\partial_x(q_3(\epsilon\zeta)v^2)\big) + \mu\epsilon Q_1(v) + \mu\nu Q_2(\zeta) + \mu\epsilon\nu Q_3(\zeta) = 0. \end{cases} \tag{4.53}$$

q_3 defined by (4.5),Q_1, Q_2 and Q_3 are defined by (4.9), (4.23) and (4.24).

We decompose the solution operator $S(.)$ associated to (4.53) at each time step Δt by the following second order splitting scheme:

$$S(\Delta t) = S_1(\Delta t/2)S_2(\Delta t)S_1(\Delta t/2)$$

where $S_1(.)$ is the solution operator associated to the hyperbolic part, and $S_2(.)$ the solution operator associated to the dispersive part of the equations (4.53).

• $S_1(t)$ is the solution operator associated to the hyperbolic part namely the nonlinear shallow water equations, NSWE:

$$\begin{cases} \partial_t\zeta + \partial_x\big(f(\epsilon\zeta)v\big) \;=\; 0, \\ \\ \partial_t v + \epsilon\varsigma v\partial_x v + \dfrac{\alpha-1}{\alpha}\big((\gamma+\delta)\partial_x\zeta + \epsilon\partial_x(q_3(\epsilon\zeta)v^2)\big) + \dfrac{1}{\alpha}\big((\gamma+\delta)\partial_x\zeta + \epsilon\partial_x(q_3(\epsilon\zeta)v^2)\big) = 0. \end{cases} \tag{4.54}$$

Using the definition of $q_3(\epsilon\zeta)$ given in (4.5), one can easily check that $\dfrac{\varsigma}{2} + q_3(\epsilon\zeta) = \dfrac{f'(\epsilon\zeta)}{2}$. Thus we rewrite the NSWE system (4.54) in the following condensed form:

$$\begin{cases} \partial_t\zeta + \partial_x\big(f(\epsilon\zeta)v\big) \;=\; 0, \\ \\ \partial_t v + \partial_x\Big(\dfrac{\epsilon f'(\epsilon\zeta)}{2}v^2 + (\gamma+\delta)\zeta\Big) = 0. \end{cases} \tag{4.55}$$

We recall that, $f(\epsilon\zeta) = \dfrac{h_1h_2}{h_1+\gamma h_2}$ and $f'(\epsilon\zeta) = \dfrac{h_1^2-\gamma h_2^2}{(h_1+\gamma h_2)^2}$, with $h_1 = 1-\epsilon\zeta$ and $h_2 = 1/\delta+\epsilon\zeta$.

• $S_2(t)$ is the solution operator associated to the remaining (dispersive) part of the equations.

$$\begin{cases} \partial_t\zeta \;=\; 0, \\ \\ (I+\mu\nu\alpha T[0])\big[\partial_t v - \dfrac{1}{\alpha}\big((\gamma+\delta)\partial_x\zeta + \epsilon\partial_x(q_3(\epsilon\zeta)v^2)\big)\big] \\ +\dfrac{1}{\alpha}\big((\gamma+\delta)\partial_x\zeta + \epsilon\partial_x(q_3(\epsilon\zeta)v^2)\big) + \mu\epsilon Q_1(v) + \mu\nu Q_2(\zeta) + \mu\epsilon\nu Q_3(\zeta) = 0. \end{cases} \tag{4.56}$$

In this study, S_1 is computed using a finite volume method while S_2 is computed using a classical finite-difference method.

In order to discretize system (4.53), the numerical domain is an interval of length L denoted $[0, L]$. Let $N \in \mathbb{N}^*$, and let us consider the following mesh on $[0, L]$. Cells are denoted for every

$i \in [0, N+1]$, by $m_i = (x_{i-1/2}, x_{i+1/2})$, with $x_i = \dfrac{x_{i-1/2} + x_{i+1/2}}{2}$ and $h_i = x_{i+1/2} - x_{i-1/2}$ the space mesh. The "fictitious" cells m_0 and m_{N+1} denote the boundary cells and the mesh interfaces located at $x_{1/2} = 0$ and $x_{N+1/2} = L$ are respectively the upstream and the downstream ends (see Figure 4.5).

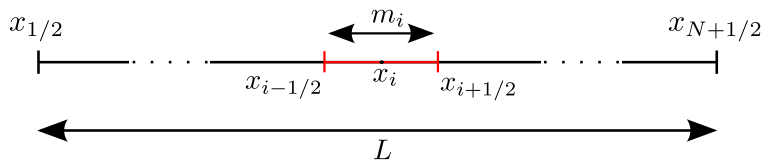

Figure 4.5. The space discretization.

We denote $\Delta x = \min_{i=1,N} h_i$.

We also consider a time discretization t^n defined by $t^{n+1} = t^n + \Delta t$ with Δt the time step.

4.4.2 Finite volume scheme

For the sake of simplicity in the notations, it is convenient to rewrite the hyperbolic system (4.55) in the following form:

$$\partial_t U + \partial_x(F(U)) = 0, \tag{4.57}$$

with the following conservative variables and flux function:

$$U = \begin{pmatrix} \zeta \\ v \end{pmatrix}, \quad F(U) = \begin{pmatrix} f(\epsilon\zeta)v \\ \dfrac{\epsilon f'(\epsilon\zeta)}{2} v^2 + (\gamma + \delta)\zeta \end{pmatrix}. \tag{4.58}$$

The Jacobian matrix is given by:

$$A(U) = d(F(U)) = \begin{pmatrix} \epsilon f'(\epsilon\zeta)v & f(\epsilon\zeta) \\ (\gamma+\delta) + \epsilon^2 \dfrac{f''(\epsilon\zeta)}{2} v^2 & \epsilon f'(\epsilon\zeta)v \end{pmatrix}, \tag{4.59}$$

where $f''(\epsilon\zeta) = -\dfrac{2\gamma(h_1+h_2)^2}{(h_1+\gamma h_2)^3}$.

A simple computation shows that the homogeneous system (4.57) is strictly hyperbolic provided that:

$$\begin{cases} \inf\limits_{x\in\mathbb{R}} h_1 > 0, \\ \inf\limits_{x\in\mathbb{R}} h_2 > 0, \\ \inf\limits_{x\in\mathbb{R}} \left[(\gamma+\delta) - \dfrac{\gamma(h_1+h_2)^2}{(h_1+\gamma h_2)^3} \epsilon^2 v^2 \right] > 0. \end{cases} \tag{4.60}$$

As a matter of fact, these conditions simply consist in assuming that the deformation of the interface is not too large and imposing a smallness assumption on ϵv. Notice that theses conditions

correspond exactly to the hyperbolicity condition for the shallow water system provided in [65].

As a consequence, the solutions may develop shock discontinuities. In order to rule out the unphysical solutions, the system (4.57) must be supplemented by entropy inequalities, (see for instance [19] and references therein for more details). The Cauchy problem associated to (4.57) is the following:

$$\begin{cases} \partial_t U + \partial_x(F(U)) \;=\; 0, \qquad t \geq 0, x \in \mathbb{R}. \\ \\ U(0,x) = U_0(x), \qquad x \in \mathbb{R}. \end{cases} \tag{4.61}$$

We are interested in the approximation of (4.61) by the finite volume method.

We denote $\overline{U}_i = (\zeta_i, v_i)$, the cell-centered approximation of U on the cell m_i at time t given by:

$$\overline{U}_i = \frac{1}{h_i} \int_{m_i} U(t,x)\, dx \ .$$

The piecewise constant representation of U is given by, $U(t,x) = \overline{U}_i \mathbb{1}_{m_i}(x)$.

We denote $\overline{U}_i^n = (\zeta_i^n, v_i^n)$, the cell-centered approximation of U on the cell m_i at time t^n given by:

$$\overline{U}_i^n = \frac{1}{h_i} \int_{m_i} U(t^n,x)\, dx \ .$$

The spatial discretization of the homogeneous system (4.54) can be recast under the following classical semi-discrete finite-volume formalism:

$$\frac{d\overline{U}_i(t)}{dt} + \frac{1}{h_i}\Big(\widetilde{F}(\overline{U}_i, \overline{U}_{i+1}) - \widetilde{F}(\overline{U}_{i-1}, \overline{U}_i)\Big) = 0 \tag{4.62}$$

where $\widetilde{F}$ is a numerical flux function based on a conservative flux consistent with the homogeneous NSWE:

$$F_{i+1/2} = \widetilde{F}(\overline{U}_i, \overline{U}_{i+1}) \approx F(U(t, x_{i+1/2})). \tag{4.63}$$

VFRoe method. In what follows, we consider the numerical approximation of the hyperbolic system of conservation laws in the form of (4.57). To this end, we adopt the VFRoe method (see [24, 57, 58]) which is an approximate Godunov scheme. It relies on the exact resolution of the following linearized Riemann problem:

$$\begin{cases} \partial_t U + \widetilde{A}(\overline{U}_i^n, \overline{U}_{i+1}^n)\partial_x U \;=\; 0, \\ \\ U(0,x) = \begin{cases} \overline{U}_i^n \quad if \quad x < x_{i+1/2}, \\ \\ \overline{U}_{i+1}^n \quad if \quad x > x_{i+1/2}, \end{cases} \end{cases} \tag{4.64}$$

where $\widetilde{A}(\overline{U}_i^n, \overline{U}_{i+1}^n) = A\left(\dfrac{\overline{U}_i^n + \overline{U}_{i+1}^n}{2}\right)$.

By solving the linearized Riemann problem we obtain $\overline{U}_{i+1/2}^* = U(x = x_{i+1/2}, t = t_n)$, the interface value between two neighbouring cells.

In what follows, we will detail the choice of the numerical flux for different order of approximation.

The only change is in the computation of the interface values $\overline{U}^*_{i+1/2}$ which depends on the right and the left states of the linearized Riemann problem. For the sake of simplicity, we will still denote by $\widetilde{F}$ these numerical fluxes.

CFL condition It is always necessary to impose what is called a CFL condition (for Courant, Friedrichs, Levy) on the timestep to prevent the blow up of the numerical values. It comes usually under the form

$$a_{i+1/2}\Delta t \leq \Delta x, \quad i = 1, \ldots, N, \tag{4.65}$$

where $a_{i+1/2} = \max_{i\in[1,N]}(j = 1, 2, |\lambda_j(\widetilde{U}_i)|)$ and $\lambda_j(\widetilde{U}_i)$ are the eigenvalues of $A\big(\widetilde{U}_i = \dfrac{\overline{U}^n_i + \overline{U}^n_{i+1}}{2}\big)$. The restriction (4.65) enables in practice to compute the timestep at each time level t_n, in order to determine the new time level $t_{n+1} = t_n + \Delta t$ (within this view, Δt is not constant, it is computed in an adaptive fashion).

Consistency. The numerical flux $\widetilde{F}(U_l, U_r)$ is called consistent with (4.57) if

$$\widetilde{F}(U, U) = F(U) \quad \text{for all U.} \tag{4.66}$$

First order finite-volume scheme

The semi-discrete equation (4.62) is discretised by an explicit Euler (in time) method to obtain :

$$\overline{U}^{n+1}_i = \overline{U}^n_i - \frac{\Delta t}{h_i}(F^n_{i+1/2} - F^n_{i-1/2}), \tag{4.67}$$

where the numerical flux is defined directly as the value of the exact flux at the interface value, namely:

$$\begin{aligned} F^n_{i+1/2} &= \widetilde{F}(\overline{U}^n_i, \overline{U}^n_{i+1}) = F(\overline{U}^*_{i+1/2}) \\ F^n_{i-1/2} &= \widetilde{F}(\overline{U}^n_{i-1}, \overline{U}^n_i) = F(\overline{U}^*_{i-1/2}). \end{aligned} \tag{4.68}$$

Let us remark that by construction the numerical flux given by (4.68) ensures the consistency property.

In the sequel, we will suppose that the space discretisation is uniform.

Algorithm. In the following, we state the algorithm for computing the discrete values $\overline{U}^{n+1}_i$ at t^{n+1}. Given the initial data and boundary conditions and the number $CFL \leq 1$, we start with the known discrete averaged values $(\overline{U}^n_i)$ for $i = 0, ..., N+1$ at t^n. As long as $(t < T)$ one has to do:

1) Computation of $\widetilde{A}_i$ for $i = 0, ..., N$ where $\widetilde{A}_i = A\left(\dfrac{\overline{U}^n_i + \overline{U}^n_{i+1}}{2}\right)$.

2) Computation of r^1_i,r^2_i and λ^1_i, λ^2_i set respectively as the eigenvectors and eigenvalues of $\widetilde{A}_i$.

3) Computation of Δt, such that $\dfrac{\Delta t}{\Delta x} \leq \dfrac{CFL}{a_{i+1/2}}$.

4) Computation of $\overline{U}^*_{i-1/2}$ for $i = 1, ..., N+1$ by solving the linearized Riemann problem.

In fact we have 3 cases:

• if λ_i^1,λ_i^2<0 then $\overline{U}_{i-1/2}^* = \overline{U}_i^n$.

• if λ_i^1,λ_i^2>0 then $\overline{U}_{i-1/2}^* = \overline{U}_{i-1}^n$.

• if $\lambda_i^1 < 0$, $\lambda_i^2 > 0$ then for:

$$\begin{cases} x < \lambda_i^1 t \quad \text{one has} \quad \overline{U}_{i-1/2}^* = \overline{U}_{i-1}^n, \\ \\ x > \lambda_i^1 t \quad \text{or} \quad x < \lambda_i^2 t \quad \text{one has} \quad \overline{U}_{i-1/2}^* = \overline{U}_i^n - (R^{-1}[U])_2 r_i^2 = \overline{U}_{i-1}^n + (R^{-1}[U])_1 r_i^1, \\ \\ x > \lambda_i^2 t \quad \text{one has} \quad \overline{U}_{i-1/2}^* = \overline{U}_i^n, \end{cases} \tag{4.69}$$

with $R = (r_i^1 | r_i^2)$ and $[U] = \overline{U}_i^n - \overline{U}_{i-1}^n$.

5) Computation of $F(\overline{U}_{i-1/2}^*)$.

6) Computation of $\overline{U}_i^{n+1} = \overline{U}_i^n - \dfrac{\Delta t}{\Delta x}(F_{i+1/2}^n - F_{i-1/2}^n)$ for $i = 1, ..., N$.

We repeat this algorithm for the new level of time $(t^{n+1} + \Delta t)$, until we reach the required final time T.

Second order finite-volume scheme: MUSCL-RK2

A drawback of the Roe scheme (such as Godunov) is to be very diffusive. A remedy for this situation is through the extension of the scheme to the second order in space, associated to a second order Runge-Kutta scheme in time. In fact, we would like to reduce both numerical dissipation and dispersion within the hyperbolic component $S_1(.)$. To this end, high order reconstructed states at each interface have to be considered, following the classical "MUSCL" approach [112] (Monotonic Upstream Scheme for Conservation Laws). To prevent the spurious oscillations that would occur around discontinuities or shocks, we suggest to use the "minmod" limiter, designed to generate slope limited, reconstructed left and right states for each cell that are used to calculate the flux at the interfaces. The implementation of this scheme is very easy and provides a natural extension of the Roe scheme described above. In fact, the main interests seem to be, after the tests, a gain of precision and stability.

The steps of the second-order reconstruction are as follows:
1. Using the discrete averaged values $\overline{U}_i^n$, we construct the slopes S_i^n using the "minmod" limiter as the reconstruction must be non oscillatory in some sense, see [59]. We consider:

$$S_i^n = minmod\left(\frac{\overline{U}_{i+1} - \overline{U}_i}{x_{i+1} - x_i}, \frac{\overline{U}_i - \overline{U}_{i-1}}{x_i - x_{i-1}}\right) \tag{4.70}$$

where the function *minmod* is defined on $\mathbb{R}^2$ by

$$minmod(a,b) = \begin{cases} min(|a|,|b|)sgn(a) \quad \text{if} \quad sgn(a) = sgn(b), \\ \\ 0 \quad \text{else.} \end{cases}$$

2. On the cell $m_i =]x_{i-1/2}, x_{i+1/2}[$, the solution is approached by:

$$U^n(x) = \overline{U}_i^n + (x - x_i)S_i^n.$$

3. We compute the numerical flux at the interfaces:

$$F_{i+1/2}^n = \widetilde{F}(\overline{U}_i^{n,+}, \overline{U}_{i+1}^{n,-}) \quad \text{and} \quad F_{i-1/2}^n = \widetilde{F}(\overline{U}_{i-1}^{n,+}, \overline{U}_i^{n,-})$$

with:

$$\begin{cases} \overline{U}_i^{n,+} &= \overline{U}_i^n + \dfrac{\Delta x}{2} S_i^n \\ \\ \overline{U}_{i+1}^{n,-} &= \overline{U}_{i+1}^n - \dfrac{\Delta x}{2} S_{i+1}^n. \end{cases}$$

4. We compute $\widetilde{U}_i^{n+1}$ by the application of (4.67), thus the scheme is given as follows:

$$\widetilde{U}_i^{n+1} = \overline{U}_i^n - \frac{\Delta t}{\Delta x}(F_{i+1/2}^n - F_{i-1/2}^n).$$

As far as time discretization is concerned, we use the second-order explicit Runge–Kutta "RK2" method which is described in the following. Given the ODE $\dfrac{dy}{dt} = f(t, y)$, one has,

$$y^{n+1} \quad = \quad y^n + \frac{h}{2}\Big(f(t^n, y^n) + f(t^{n+1}, \tilde{y}^{n+1})\Big), \tag{4.71}$$

with $\tilde{y}^{n+1} = y^n + hf(t^n, y^n)$, and $t^{n+1} = t^n + h$.
Applying (4.71) to (4.67), we obtain the following modified scheme "MUSCL-RK2":

$$\overline{U}_i^{n+1} = \overline{U}_i^n - \frac{\Delta t}{2\Delta x}(F_{i+1/2}^n - F_{i-1/2}^n + F_{i+1/2}^{n+1} - F_{i-1/2}^{n+1}), \tag{4.72}$$

with

$$F_{i+1/2}^{n+1} = \widetilde{F}(\widetilde{U}_i^{n+1,+}, \widetilde{U}_{i+1}^{n+1,-}) \quad \text{and} \quad F_{i-1/2}^{n+1} = \widetilde{F}(\widetilde{U}_{i-1}^{n+1,+}, \widetilde{U}_i^{n+1,-}) \ ,$$

$-\widetilde{F}$: the numerical flux determined as in the first order VFRoe method, given by (4.68).
$-\widetilde{U}_i^{n+1}$ is computed as follows:

$$\widetilde{U}_i^{n+1} = \overline{U}_i^n - \frac{\Delta t}{\Delta x}(F_{i+1/2}^n - F_{i-1/2}^n).$$

$-\widetilde{U}_i^{n+1,+} = \widetilde{U}_i^{n+1} + \dfrac{\Delta x}{2}\widetilde{S}_i^{n+1}$.
$-\widetilde{U}_{i+1}^{n+1,-} = \widetilde{U}_{i+1}^{n+1} - \dfrac{\Delta x}{2}\widetilde{S}_{i+1}^{n+1}$.
$-\widetilde{S}_i^{n+1}$ and $\widetilde{S}_{i+1}^{n+1}$ are associated respectively to $\widetilde{U}_i^{n+1}$ and $\widetilde{U}_{i+1}^{n+1}$ by (4.70).

Higher order finite-volume scheme: WENO5-RK4

The second order schemes are known to degenerate to first order accuracy at smooth extrema. To reach higher order accuracy in smooth regions and a good resolution around discontinuities, we implement fifth-order accuracy "WENO" reconstruction, following [74, 107], where Jiang and Shu constructed third and fifth order finite difference "WENO" schemes in multi-space dimensions

with a general framework for the design of the smoothness indicators and nonlinear weights. To automatically achieve high order accuracy and non-oscillatory property near discontinuities, "WENO" schemes use the idea of adaptive stencils in the reconstruction procedure based on the local smoothness of the numerical solution. We would like to mention also the previous studies [30, 18, 86], where it is shown that for the study of dispersive waves, it is necessary to use high-order schemes to prevent the corruption of the dispersive properties of the model by some dispersive truncation errors linked to second-order schemes. Using the same reconstruction proposed in [18], we consider a cell m_i, and the corresponding constant averaged value $\overline{U}_i^n = (\overline{\zeta}_i^n, \overline{v}_i^n)$, with a constant space step Δx. This approach, provides high order reconstructed left and right values $\overline{U}_i^{n,-}$ and $\overline{U}_i^{n,+}$, built following the five points stencil, and introduced as follows:

$$\overline{U}_i^{n,+} = \overline{U}_i^n + \frac{1}{2}\overline{\delta U}_i^{n,+} \quad \text{and} \quad \overline{U}_i^{n,-} = \overline{U}_i^n - \frac{1}{2}\overline{\delta U}_i^{n,-}, \tag{4.73}$$

where $\overline{\delta U}_i^{n,+}$ and $\overline{\delta U}_i^{n,-}$ are defined as follows:

$$\begin{aligned}\overline{\delta U}_i^{n,+} &= \frac{2}{3}(\overline{U}_{i+1}^n - \overline{U}_i^n) + \frac{1}{3}(\overline{U}_i^n - \overline{U}_{i-1}^n) - \frac{1}{10}(-\overline{U}_{i-1}^n + 3\overline{U}_i^n - 3\overline{U}_{i+1}^n + \overline{U}_{i+2}^n) \\ &\quad - \frac{1}{15}(-\overline{U}_{i-2}^n + 3\overline{U}_{i-1}^n - 3\overline{U}_i^n + \overline{U}_{i+1}^n)\end{aligned} \tag{4.74}$$

$$\begin{aligned}\overline{\delta U}_i^{n,-} &= \frac{2}{3}(\overline{U}_i^n - \overline{U}_{i-1}^n) + \frac{1}{3}(\overline{U}_{i+1}^n - \overline{U}_i^n) - \frac{1}{10}(-\overline{U}_{i-2}^n + 3\overline{U}_{i-1}^n - 3\overline{U}_i^n + \overline{U}_{i+1}^n) \\ &\quad - \frac{1}{15}(-\overline{U}_{i-1}^n + 3\overline{U}_i^n - 3\overline{U}_{i+1}^n + \overline{U}_{i+2}^n)\end{aligned} \tag{4.75}$$

and the coefficients $\frac{2}{3}$, $\frac{1}{3}$, $\frac{-1}{10}$ and $\frac{-1}{15}$ are set in order to obtain better dissipation and dispersion properties in the truncature error. We consider the following modified scheme:

$$\overline{U}_i^{n+1} = \overline{U}_i^n - \frac{\Delta t}{\Delta x}\Big(\widetilde{F}(\overline{U}_i^{n,+}, \overline{U}_{i+1}^{n,-}) - \widetilde{F}(\overline{U}_{i-1}^{n,+}, \overline{U}_i^{n,-})\Big). \tag{4.76}$$

To reduce spurious oscillations near discontinuities, we apply the same limitation procedure as in [18], preserving the scheme positivity and the high order accuracy. Thus scheme (4.76) becomes

$$\overline{U}_i^{n+1} = \overline{U}_i^n - \frac{\Delta t}{\Delta x}\Big(\widetilde{F}({}^L\overline{U}_i^{n,+}, {}^L\overline{U}_{i+1}^{n,-}) - \widetilde{F}({}^L\overline{U}_{i-1}^{n,+}, {}^L\overline{U}_i^{n,-})\Big). \tag{4.77}$$

We define the limited high-order values as follows:

$${}^L\overline{U}_i^{n,+} = \overline{U}_i^n + \frac{1}{2}L_i^+(\overline{U}^n) \quad \text{and} \quad {}^L\overline{U}_i^{n,-} = \overline{U}_i^n - \frac{1}{2}L_i^-(\overline{U}^n). \tag{4.78}$$

Using the following limiter,

$$L(u,v,w) = \begin{cases} min(|u|,|v|,2|w|)\ sgn(u) & \text{if} \quad sgn(u) = sgn(v), \\ 0 \quad \text{else}, \end{cases}$$

we define the limiting process as,

$$L_i^+(\overline{U}^n) = L(\delta\overline{U}_i^n, \delta\overline{U}_{i+1}^n, \overline{\delta U}_i^{n,+}) \quad \text{and} \quad L_i^-(\overline{U}^n) = L(\delta\overline{U}_{i+1}^n, \delta\overline{U}_i^n, \overline{\delta U}_i^{n,-}),$$

with $\delta\overline{U}^n_{i+1} = \overline{U}^n_{i+1} - \overline{U}^n_i$ and $\delta\overline{U}^n_i = \overline{U}^n_i - \overline{U}^n_{i-1}$ are upstream and downstream variations, and $\overline{\delta U}^{n,+}_i$ and $\overline{\delta U}^{n,-}_i$ taken from (4.74) and (4.75).

The limited high order reconstructions stated above must be performed on both conservative variables $\overline{U}^n_i = (\overline{\zeta}^n_i, \overline{v}^n_i)$. We would like to mention that the resulting finite volume scheme preserve motionless steady states, $\zeta = \text{cst}$ and $v = 0$.

As far as time discretization is concerned, we use the fourth-order explicit Runge–Kutta "RK4" method which is described in the following. Given the ODE $\dfrac{dy}{dt} = f(t, y)$, one has,

$$\begin{aligned} k_1 &= f(t^n, y^n), \\ k_2 &= f(t^n + \frac{h}{2}, y^n + h\frac{k_1}{2}), \\ k_3 &= f(t^n + \frac{h}{2}, y^n + h\frac{k_2}{2}), \\ k_4 &= f(t^n + h, y^n + hk_3), \\ y^{n+1} &= y^n + \frac{h}{6}\big(k_1 + 2k_2 + 2k_3 + k_4\big), \end{aligned} \tag{4.79}$$

with $t^{n+1} = t^n + h$. Applying (4.79) to (4.77), one gets the "WENO5-RK4" scheme.

4.4.3 Finite difference scheme for the dispersive part

First of all, let us detail how to construct nodal values of the unknowns (which are the ones used for a finite difference discretization) from the cell-averaged value computed by a finite volume scheme and vice versa.

We denote by U^n_i the nodal value of U at the ith node $(x_{i+1/2})_{i\in[0,N]}$ and at time t_n i.e. U^n_i is an approximation of $U(x_{i+1/2}, t^n)$. The finite volume-finite difference mix imply to switch between the cell-averaged and nodal values for each unknown and at each time step. To this end, we use the fifth-order accuracy "WENO" reconstruction, that allows to approximate the nodal values (i.e finite difference unknowns) $(U^n_i)_{i=1,N+1}$ in terms of the cell-averaged values (i.e finite volume unknowns) $(\overline{U}^n_i)_{i=1,N}$. The relation is given by:

$$U^n_i = \frac{1}{30}\overline{U}^n_{i-2} - \frac{13}{60}\overline{U}^n_{i-1} + \frac{47}{60}\overline{U}^n_i + \frac{9}{20}\overline{U}^n_{i+1} - \frac{1}{20}\overline{U}^n_{i+2} + \mathcal{O}(\Delta x^5), \quad 1 \le i \le N+1, \tag{4.80}$$

with adaptations at the boundaries following the method presented in Section 4.4.4. One can easily recover the relation that allows to determine the cell-averaged values $(\overline{U}^n_i)_{i\in[1:N]}$ in terms of the nodal values $(U^n_i)_{i\in[1:N+1]}$.

We can easily check that (4.80) preserve the steady state at rest and that this formula is precise up to order $\mathcal{O}(\Delta x^5)$ terms, thus preserving the global order of the scheme.

We can now proceed by explaining how we compute the solution operator $S_2(.)$ associated to the dispersive part of the equations. Let us recall the system (4.56) corresponding to the operator $S_2(.)$, given in Section (4.4.1).

$$\begin{cases} \partial_t\zeta = 0, \\ \\ \partial_t v - \dfrac{1}{\alpha}\big((\gamma+\delta)\partial_x\zeta + \epsilon\partial_x(q_3(\epsilon\zeta)v^2)\big) \\ +(I + \mu\nu\alpha T[0])^{-1}\Big[\dfrac{1}{\alpha}\big((\gamma+\delta)\partial_x\zeta + \epsilon\partial_x(q_3(\epsilon\zeta)v^2)\big) + \mu\epsilon Q_1(v) + \mu\nu Q_2(\zeta) + \mu\epsilon\nu Q_3(\zeta)\Big] = 0. \end{cases} \tag{4.81}$$

where the operators Q_1, Q_2 and Q_3 are explicitly given in (4.9), (4.23) and (4.24). For the sake of simplicity, we detail the numerical resolution of (4.81) using an explicit Euler in time scheme. Standard extensions to second and fourth order Runge-Kutta method has been used according to the order of the space derivative operators as done in the previous section.

The finite discretization of the system (4.81) leads to the following discrete problem:

$$\begin{cases} \dfrac{\zeta^{n+1}-\zeta^n}{\Delta t} = 0, \\ \dfrac{v^{n+1}-v^n}{\Delta t} - \dfrac{1}{\alpha}(\gamma+\delta)D_1(\zeta^n) - 2\dfrac{\epsilon}{\alpha}q_3(\epsilon\zeta^n)v^nD_1(v^n) - \dfrac{\epsilon^2}{\alpha}q_3'(\epsilon\zeta^n)D_1(\zeta^n)(v^n)(v^n) \\ +(I-\mu\nu\alpha D_2)^{-1}\Big[\dfrac{1}{\alpha}(\gamma+\delta)D_1(\zeta^n) + 2\dfrac{\epsilon}{\alpha}q_3(\epsilon\zeta^n)v^nD_1(v^n) + \dfrac{\epsilon^2}{\alpha}q_3'(\epsilon\zeta^n)D_1(\zeta^n)(v^n)(v^n) \\ +\mu\epsilon Q_1(v^n) + \mu\nu\epsilon Q_2(\zeta^n) + \mu\epsilon\nu Q_3(\zeta^n)\Big] = 0, \end{cases} \tag{4.82}$$

with

$$Q_1(v^n) = 2\kappa D_1(v^n)D_2(v^n),$$

$$Q_2(\zeta^n) = \kappa_2 D_1\Big[\zeta^n D_1\Big((I-\mu\nu\alpha D_2)^{-1}(\gamma+\delta)D_1(\zeta^n)\Big)\Big],$$

$$Q_3(\zeta^n) = -\kappa_1\zeta^n D_2\Big[(I-\mu\nu\alpha D_2)^{-1}(\gamma+\delta)D_1(\zeta^n)\Big].$$

The system (4.82) is solved at each time step using a classical finite-difference technique, where the matrices D_1 and D_2 are the classical centered discretizations of the derivatives ∂_x and ∂_x^2 given below.

The first formula is the second-order formula called "DF2", where the spatial derivatives are given as follows:

$$(\partial_x U)_i = \frac{1}{2\Delta x}(U_{i+1} - U_{i-1}),$$

$$(\partial_x^2 U)_i = \frac{1}{\Delta x^2}(U_{i+1} - 2U_i + U_{i-1}).$$

For time discretization, the second-order formula "DF2" is associated to a second-order classical Runge-Kutta "RK2" scheme, and thus one obtains the "DF2-RK2" scheme.

The second formula is the fourth-order formula called "DF4" where the spatial derivatives are given as follows:

$$(\partial_x U)_i = \frac{1}{12\Delta x}(-U_{i+2} + 8U_{i+1} - 8U_{i-1} + U_{i-2}),$$

$$(\partial_x^2 U)_i = \frac{1}{12\Delta x^2}(-U_{i+2} + 16U_{i+1} - 30U_i + 16U_{i-1} - U_{i-2}).$$

For time discretization, the fourth-order formula "DF4" is associated to a fourth-order classical Runge-Kutta "RK4" scheme, and thus one obtains the "DF4-RK4" scheme.

4.4.4 Boundary conditions

In the following section, we show how to treat the boundary conditions for the hyperbolic and dispersive parts of the splitting scheme. Suitable relations are imposed on both cell-averaged and nodal quantities. We only treat either periodic boundary conditions or reflective boundary

conditions. We detail now how we have implemented these boundary conditions for the hyperbolic part and the dispersive part of the numerical scheme.

For the hyperbolic part, we have introduced "ghosts cells" respectively at the upstream and downstream boundaries of the domain. The imposed relations on the cell-averaged quantities are the following:

• $\overline{U}_{-k+1} = \overline{U}_{N-k+1}$, and $\overline{U}_{N+k} = \overline{U}_k$, $k \geq 1$, for periodic conditions on upstream and downstream boundaries.

• $\overline{\zeta}_{-k+1} = \overline{\zeta}_{-k}$, $\overline{v}_{-k+1} = -\overline{v}_{-k}$ for $k \geq 0$ and $\overline{\zeta}_{N+k-1} = \overline{\zeta}_{N+k}$, $\overline{v}_{N+k-1} = -\overline{v}_{N+k}$ for $k \geq 1$, for reflective conditions on the left and right boundaries.

For the dispersive part of the splitting, the boundary conditions are simply imposed on the nodal values that are located outside of the domain, in order to maintain centered formula at the boundaries, while keeping a regular structure in the discretized model:

• $U_{-k+1} = U_{N-k+1}$, and $U_{N+k} = U_k$, $k \geq 1$, for periodic conditions on upstream and downstream boundaries.

• $\zeta_{-k+1} = \zeta_{-k}$, $v_{-k+1} = -v_{-k}$ for $k \geq 0$ and $\zeta_{N+k-1} = \zeta_{N+k}$, $v_{N+k-1} = -v_{N+k}$ for $k \geq 1$, for reflective conditions on upstream and downstream boundaries.

4.5 Numerical validations

In this section, several numerical tests are performed in both one and two layers cases in order to validate the numerical efficiency and accuracy of the improved Green-Naghdi model (4.42). We first consider several numerical tests in the one layer case without any surface tension i.e $\mathrm{bo}^{-1} = 0$. We begin by studying the propagation of a solitary wave over a flat bottom. We compare our numerical solution with an analytic one (up to an $\mathcal{O}(\mu^2)$ remainder) at several times and for different orders of discretizations and show that our numerical scheme is very efficient and accurate. To evaluate the influence of the nonlinear and dispersive terms we study the collision between two solitary waves traveling in opposite directions (head-on collision). We then study the breaking of a Gaussian hump into two solitary waves. Finally, we study the dam-break problem supplemented by a comparison between the second and fifth order accuracy in order to show the ability of the higher order numerical scheme in dealing with discontinuities. We used the value $\alpha = 1$ in the aforementioned cases. In fact, we obtained very similar results when performing the same simulations with $\alpha_{opt} = 1.159$. Secondly, two numerical simulations are performed in the two layers cases. In the first one, we compare our results with numerical data from [50], where we show that a very good matching is observable if α is carefully chosen as in Section 4.3.3. We then consider the dam-break problem in the two layers cases, where we test the ability of the splitting scheme to compute dispersive shock waves with high accuracy. We would like to mention that in all the numerical tests, we use the WENO5 reconstruction for the hyperbolic part of the splitting scheme and a fourth order finite difference scheme "DF4" for the dispersive part, both associated to a fourth-order classical Runge-Kutta "RK4" time scheme. In every numerical simulation presented in the following section, we choose to use a CFL number equal to 1 in the algorithm stated in page 122, in order to obtain a stable numerical scheme.

4.5.1 Numerical validations in the one layer case

Propagation of a solitary wave

Here, we test the accuracy of our numerical scheme (4.42) with $\alpha = 1$, by using the exact solitary wave solutions of the one layer Green-Naghdi equations in the one-dimensional setting over a flat bottom (see [86]), given in variables with dimensions, by

$$\begin{cases} \zeta(t,x) = a\ \mathrm{sech}^2(k(x-ct)), \\ \\ v(t,x) = c\Big(\dfrac{\zeta(t,x)}{d_2+\zeta(t,x)}\Big), \\ \\ k = \dfrac{\sqrt{3a}}{2d_2\sqrt{d_2+a}}, \quad c = \sqrt{g(d_2+a)}, \end{cases} \tag{4.83}$$

where we recall that d_2 is depth of the fluid when considering the one layer case. Such solitary waves are also solution of the improved Green-Naghdi model (4.42) up to an $\mathcal{O}(\mu^2)$ remainder. We consider the propagation of a solitary wave initially centered at $x_0 = 20\ m$, of relative amplitude $a = 0.2\ m$, over a constant water depth $d_2 = 1\ m$. The computational domain is 200 m in length and discretized with 1280 cells. The single solitary wave propagates from left to right. In this test, since the solitary wave is initially far from boundaries, the boundary conditions do not affect the computation, thus we choose to impose periodic boundary conditions on each boundary for the sake of simplicity. We compare the water surface profile of our numerical solution provided by the model (4.42) (after setting the parameters $\gamma = 0$ and $\delta = 1$ corresponding to the one layer case), with the exact one given by (4.83) at several times using the first, second and fifth order discretizations (see Figure 4.6). One can easily remark that the fifth order discretization "WENO5-DF4-RK4" provides very accurate solutions and reduces both numerical dissipation and dispersion, contrarily to the first order discretization "FV1-DF2-Euler" which seems to be very diffusive. Indeed, looking at the amplitude and shape of the solitary wave at $t = 50\ s$ in the bottom of Figure 4.6, we can observe an excellent agreement between numerical and exact solutions, unlike the second order discretization "MUSCL-DF2-RK2" (middle of Figure 4.6), generating a less accurate numerical solution. The preservation of the amplitude and shape of the solitary wave computed using the fifth order scheme, even after 200 m indicate that the governing equations have been accurately discretized in space and time.

In what follows, we quantify the numerical accuracy of our numerical scheme by computing the numerical solution for this particular test case for an increasing number of cells N, over a duration $T = 5\ s$. Starting with $N = 80$ number of cells, we successively multiply the number of cells by two. The relative errors $E_{L^2}(\zeta)$ and $E_{L^2}(v)$ on the water surface deformation and the averaged velocity presented in Table 4.1 are computed at $t = 5\ s$, using the discrete L^2 norm $\|.\|_2$:

$$E_{L^2}(\zeta) = \frac{\|\zeta_{num} - \zeta_{sol}\|_2}{\|\zeta_{sol}\|_2}; \qquad E_{L^2}(v) = \frac{\|v_{num} - v_{sol}\|_2}{\|v_{sol}\|_2}, \tag{4.84}$$

where (ζ_{num}, v_{num}) are the numerical solutions and (ζ_{sol}, v_{sol}) are the analytical ones coming from (4.83). Very accurate results are thus obtained as an evaluation of the capacity of our numerical method to compute in a stable way the propagation of a solitary wave.

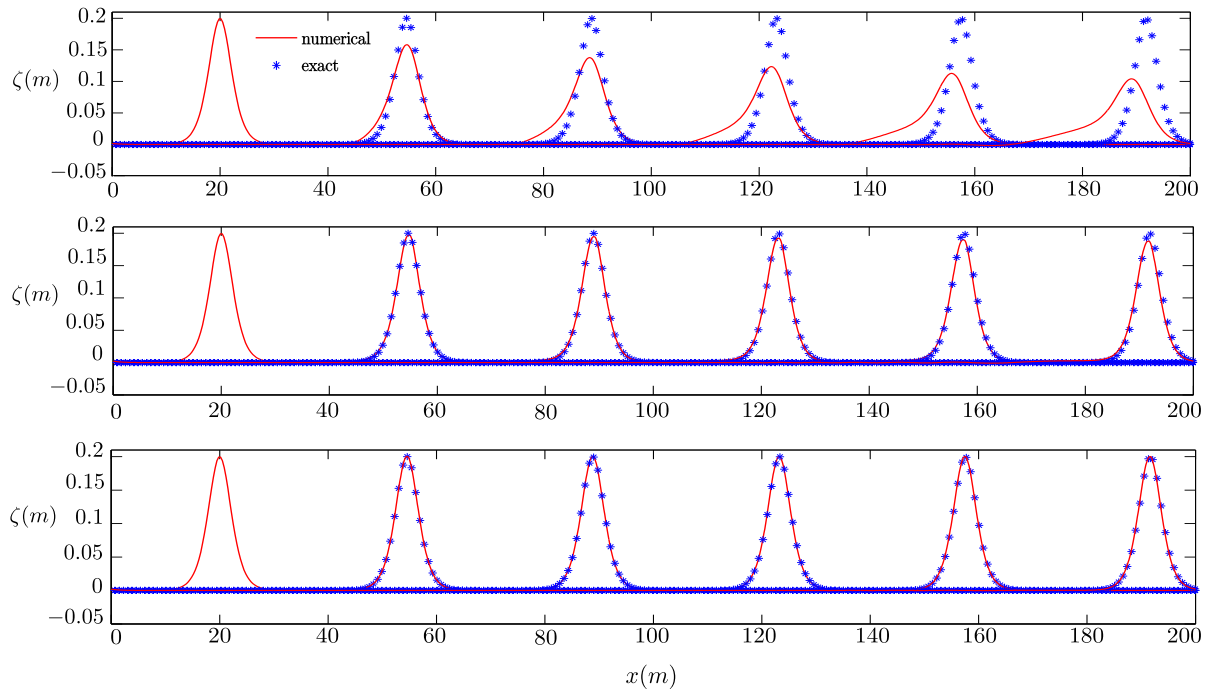

Figure 4.6. Propagation of a solitary wave over a flat bottom: water surface profiles at t=0, 10, 20, 30, 40 and 50s. Top: FV1-DF2-Euler, middle: MUSCL-DF2-RK2 and bottom: WENO5-DF4-RK4.

	FV1-DF2-Euler		MUSCL-DF2-RK2		WENO5-DF4-RK4	
N	$E_{L^2}(\zeta)$	$E_{L^2}(v)$	$E_{L^2}(\zeta)$	$E_{L^2}(v)$	$E_{L^2}(\zeta)$	$E_{L^2}(v)$
80	5.79×10^{-1}	5.56×10^{-1}	5.57×10^{-1}	5.30×10^{-1}	4.32×10^{-1}	4.02×10^{-1}
160	4.30×10^{-1}	4.07×10^{-1}	3.54×10^{-1}	3.27×10^{-1}	1.94×10^{-1}	1.67×10^{-1}
320	3.04×10^{-1}	2.83×10^{-1}	1.76×10^{-1}	1.54×10^{-1}	6.45×10^{-2}	5.25×10^{-2}
640	1.95×10^{-1}	1.79×10^{-1}	5.96×10^{-2}	5.00×10^{-2}	1.16×10^{-2}	9.30×10^{-3}
1280	1.14×10^{-1}	1.04×10^{-1}	1.38×10^{-2}	1.20×10^{-2}	3.60×10^{-3}	3.40×10^{-3}

Table 4.1. Propagation of a solitary wave over a flat bottom: relative L^2-error table for the conservative variables.

Remark 15. We believe that the main reason for not obtaining the predicted order in each space discretization might be due to the fact that the analytic solution given in (4.83) satisfies the model (4.42) up to an $\mathcal{O}(\mu^2)$ remainder, that is to say it is an approximate solution. A remedy for this situation could be through an "iterative cleaning" technique that acts to damp the high frequency oscillations (i.e the oscillatory dispersive tails) that appears due to the remainder term of size $\mathcal{O}(\mu^2)$. This technique has been used by several authors, see for instance [11, 15, 99]. In this chapter, we do not try to give some optimal convergence result and the filtering technique is left to future work.

Head-on collision of counter-propagating waves

We now investigate the interaction of solitary waves which allows us to evaluate the impact of non linearities and dispersive terms. To this end, we study the head-on collision of two solitary waves traveling in opposite directions. The initial data for the two counter-propagating solitary waves are given in (4.83). Many authors have set different models and numerical methods in order to numerically study this problem (see [37, 51, 96]). Unlike solitary waves in integrable systems, the one for the *full Euler* equations are often followed by a non zero residual wave after interactions. The resulting residual has the form of dispersive trailing waves of small amplitude. In this test, we study the interaction of two solitary waves of equal amplitudes propagating in an opposite direction, initially located at $x = 100\ m$ and $x = 300\ m$. The spatial domain is $400\ m$ in length discretized using 1200 cells. Periodic conditions are imposed on each boundary.

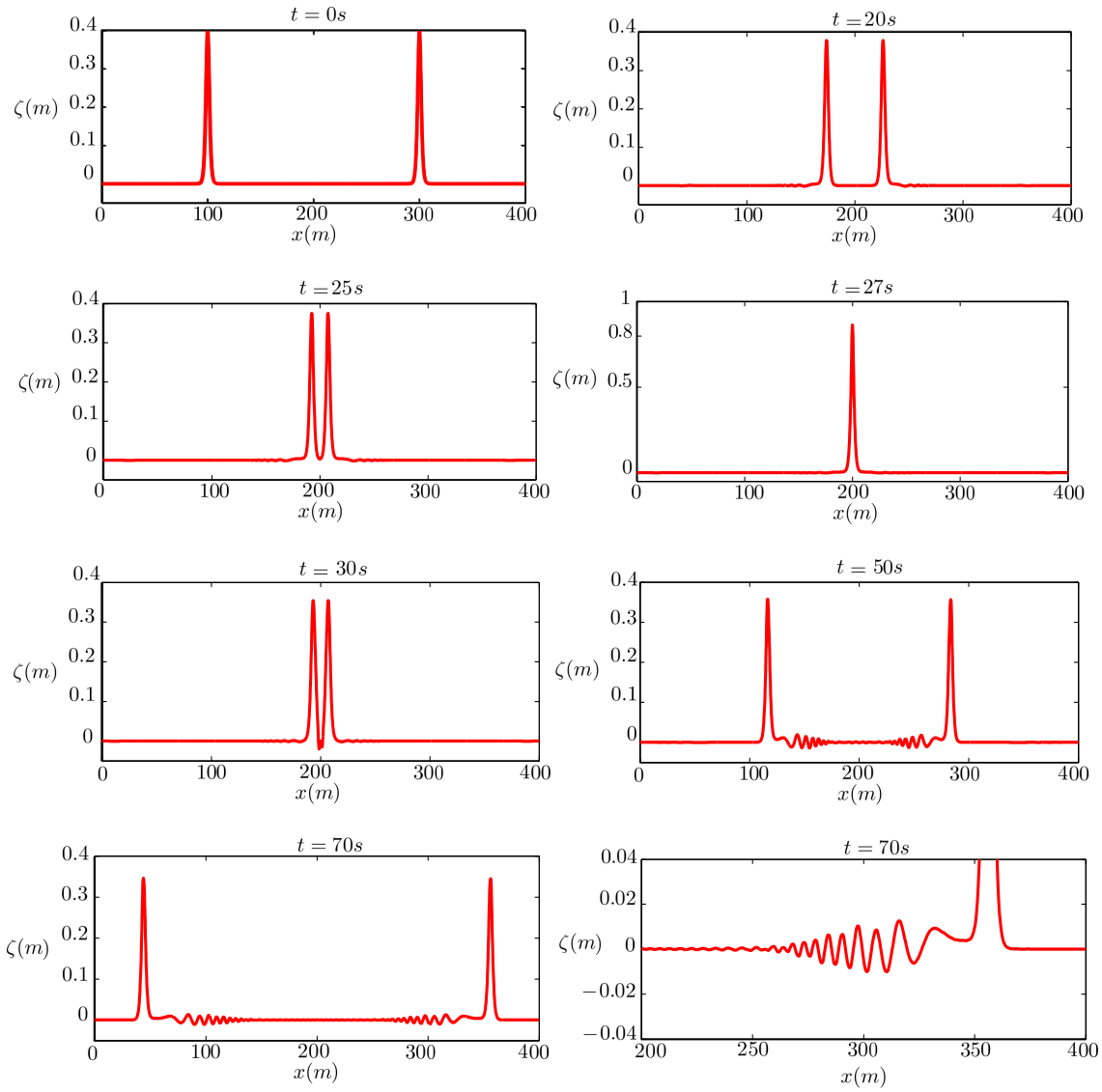

Figure 4.7. Head on collision of two counter-propagating solitary waves: water surface profiles at several times during the propagation.

The results are shown in Figure 4.7 at different propagation times. Before the collision, at times $t = 20\ s$ and $t = 25\ s$ one can observe two dispersive tails of very small amplitude located to the left and right of each solitary wave. The generation of such dispersive tails is due to the $\mathcal{O}(\mu^2)$ remainder term as mentioned in Remark 15. As expected, the waves collide to reach a maximum height larger than the sum of the amplitudes of the two incident solitary waves at the time $t = 27\ s$. After the collision, dispersive tails with small amplitudes appear clearly when zooming at $t = 70\ s$, illustrating an appropriate characterization of the nonlinear interactions. Capturing this dynamics validate the high precision of our numerical scheme. The head-on collision is also studied in [96, 51], leading to similar observations.

Breaking of a Gaussian hump

In this test, we consider the following initial data representing a heap of water,

$$\zeta(0,x) = ae^{-\frac{1}{\lambda}(x-\frac{L}{2})^2}, \quad v(0,x) = 0,$$

where a represents the amplitude, λ represents the width and L represents the length of the domain. Figure 4.8, shows the overall behavior of the solutions using $a = 0.4\ m$ and $\lambda = 40\ m$ and $L = 400\ m$ discretized with 2000 cells using periodic boundary conditions. The initial hump breaks up into two large solitary waves and smaller dispersive tails. These waves and the dispersive tails travel in opposite directions.

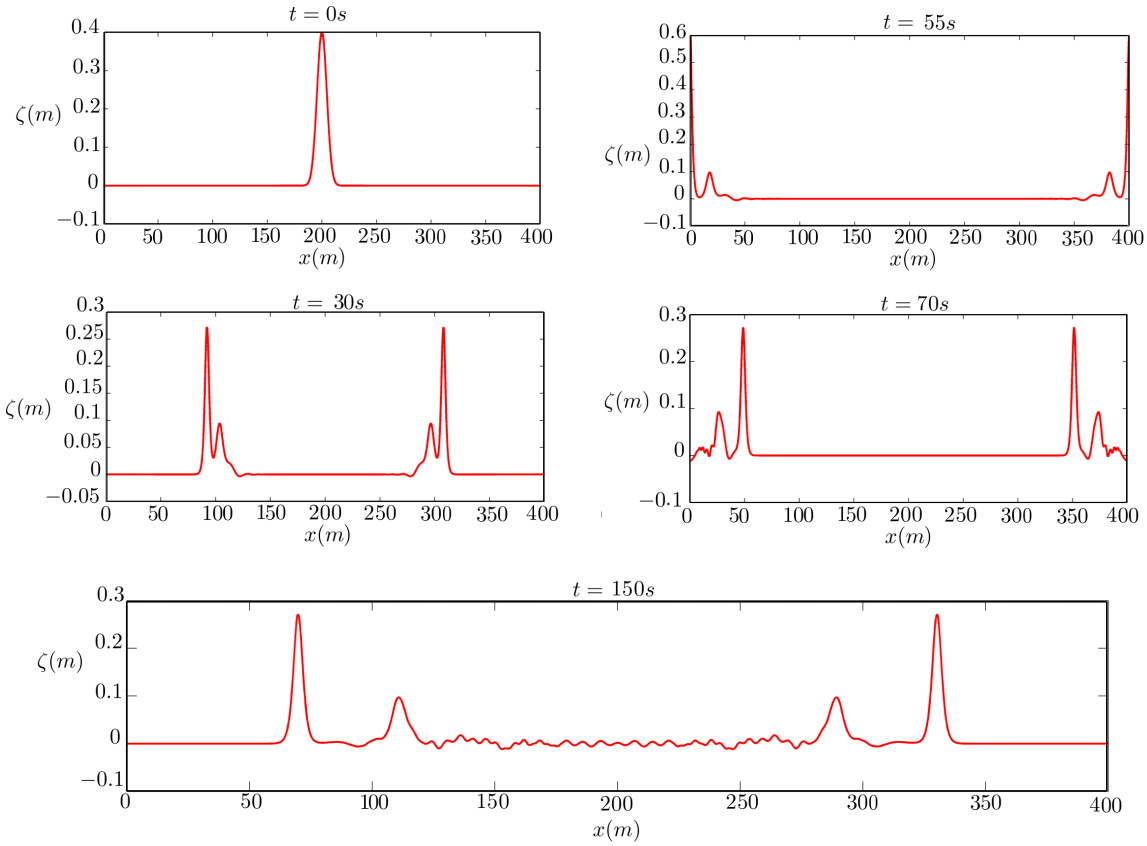

Figure 4.8. Breakup of a Gaussian hump into two solitary waves traveling in opposite directions and dispersive tails.

The results shown in Figure 4.8, tends to confirm the ability of our numerical scheme to capture this dynamics accurately. Indeed, this typical behaviour is also studied in [96], leading to very similar observations.

Dam-break problem in the one layer case

We consider now a dam-break problem in the one layer case in order to test the ability of our numerical scheme to deal with discontinuities. In general, discontinuous initial data of this type generates dispersive shock waves due to the dispersive effects [88]. Analytic and computational studies of the dispersive shock waves in fully-nonlinear dispersive shallow water systems were carried out in [54, 88]. We would like to mention also the previous studies [30, 18, 86], where it is shown that for the study of dispersive waves, it is necessary to use high-order schemes to prevent the corruption of the dispersive properties of the model by some dispersive truncation errors linked to second-order schemes. Indeed, this test is supplemented by a comparison between the second and fifth order accuracy exhibiting the ability of higher order schemes to capture the rapid oscillations in dispersive shock waves. We use the following initial data:

$$\zeta(0,x) = a[1+\tanh(250-|x|)], \quad v(0,x) = 0, \tag{4.85}$$

where $a = 0.2091\ m$. The computational domain is the interval $x \in (-700, 700)$ and discretized using 2800 cells. We choose to impose periodic boundary conditions.

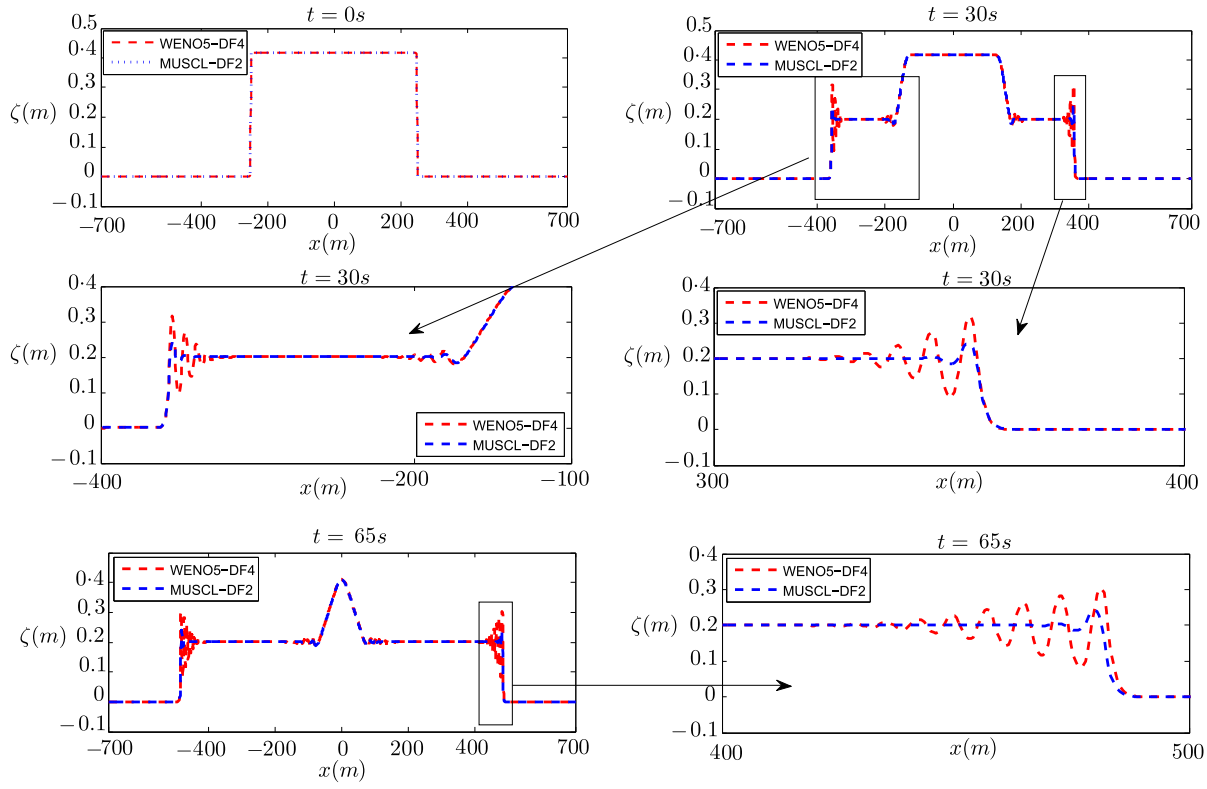

Figure 4.9. Dam break in the one layer case: water surface profiles at several times

Figure 4.9 shows the results of the numerical simulations with two different orders of discretization, “MUSCL-DF2-RK2” and “WENO5-DF4-RK4”, generating two dispersive tails prop-

agating in opposite direction, on the left and right side of the "dam", and two rarefaction waves that travel towards the center. A zoom on the shock and rarefaction waves at $t = 30\ s$ and $t = 65\ s$, shows clearly the corruption of the dispersive properties by the second order scheme. The dam-break problem was also studied in [54, 88] and seems to fit well with our numerical observations. The numerical model proposed in [96] computes using a finite element method all the nonlinear dispersive terms, in particular the third order ones. These third order derivatives are present in our model but in order to improve the frequency dispersion we have proposed to factorize these terms, making it possible not to compute them. This formulation has the inconvenience of numerical diffusion. This is the reason why the dispersive tails observed in the dam-break problem in [96] have larger amplitude oscillations.

4.5.2 Numerical validations in the two layers case

Kelvin-Helmholtz instabilities

In this case, we would like to highlight the importance of the choice of the parameter α in order to improve the frequency dispersion of the model (4.22), through the simulation of a sufficiently regular initial wave, following the numerical experiments performed in [50]. In the aforementioned paper they introduce a new class of Green-Naghdi type models for the propagation of internal waves with improved frequency dispersion in order to prevent high-frequency Kelvin-Helmholtz instabilities. These models are obtained by regularizing the original Green-Naghdi one by slightly modifying the dispersion components using a class of Fourier multipliers. They represent three different choices of the Fourier multipliers, each one yields to a specific Green-Naghi model which they denote as follows:

• "original" as the classical Green-Naghi model introduced in [32].

• "regularized" which is a well-posed system for sufficiently small and regular data, even in absence of surface tension. In addition its dispersion relation fit the one of *full Euler system* at order $\mathcal{O}(\mu^3)$.

• "improved" whose dispersion relation is the same as the one of the *full Euler system*.

Using the spectral methods [111] for the space discretization and the Matlab solver ode45, which is based on the fourth and fifth order Runge-Kutta-Merson method for time evolution, they numerically compute several of their Green-Naghdi systems. Several computations are made, with and without surface tension in order to observe how the different frequency dispersion may affect the appearance of Kelvin-Helmholtz instabilities.

In order to compare with the numerical experiments done in [50] we choose to use the initial data $\zeta(0,x) = \ -e^{-4|x|^2}$ and $v(0,x) = 0$ (represented by the dashed lines). The dimensionless parameters are set as follows: $\mu = 0.1$, $\epsilon = 0.5$, $\delta = 0.5$, $\gamma = 0.95$ and $\mathrm{bo}^{-1} = 5 \times 10^{-5}$. The computational domain is the interval $x \in (-4, 4)$ discretized with 512 cells using periodic boundary conditions. In all the following simulations we compute our numerical solution using the fifth order accuracy scheme "WENO5-DF4-RK4".

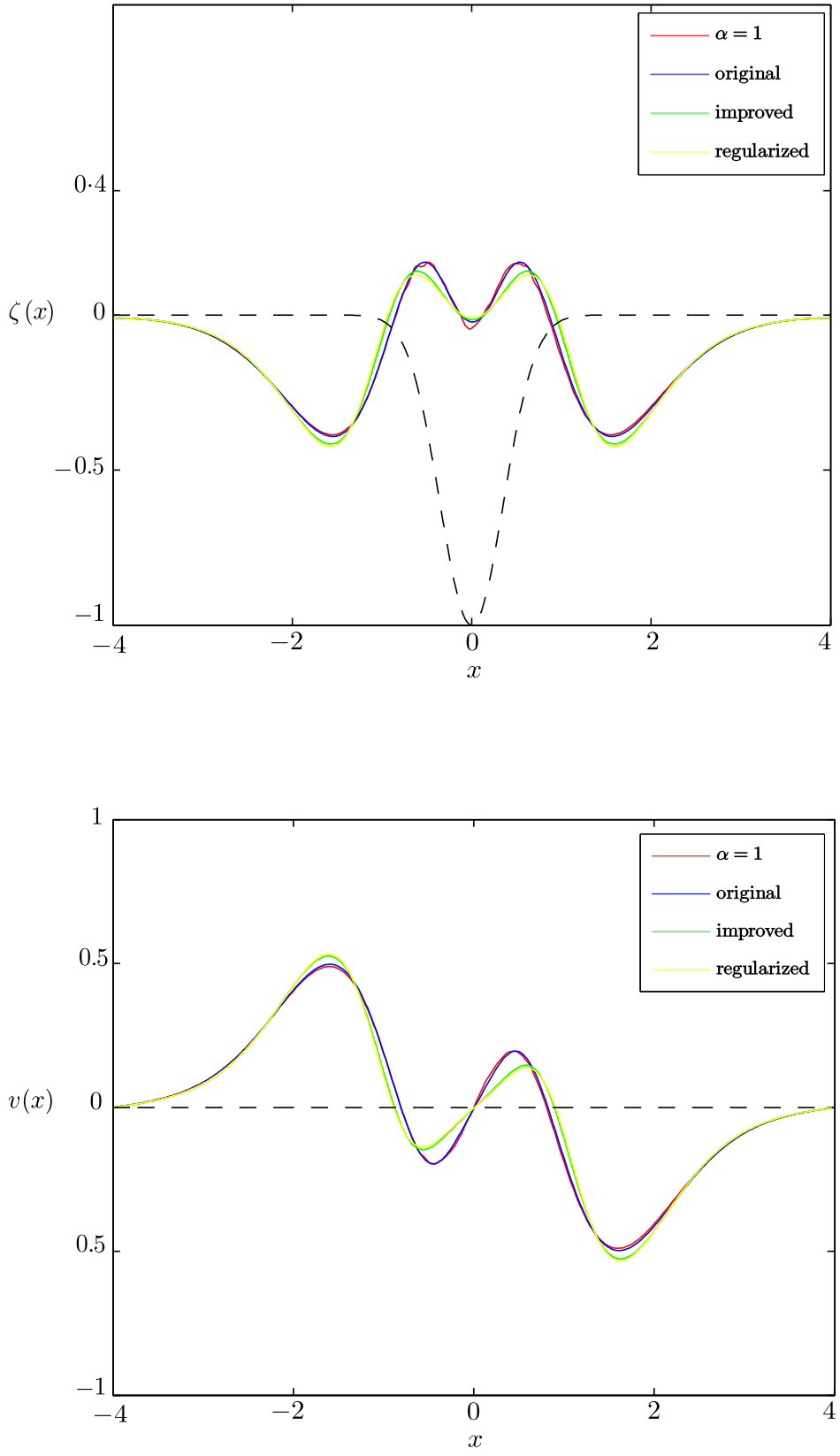

Figure 4.10. Comparison with the Green-Naghdi models, with surface tension, at time $t = 2$, for $\alpha = 1$.

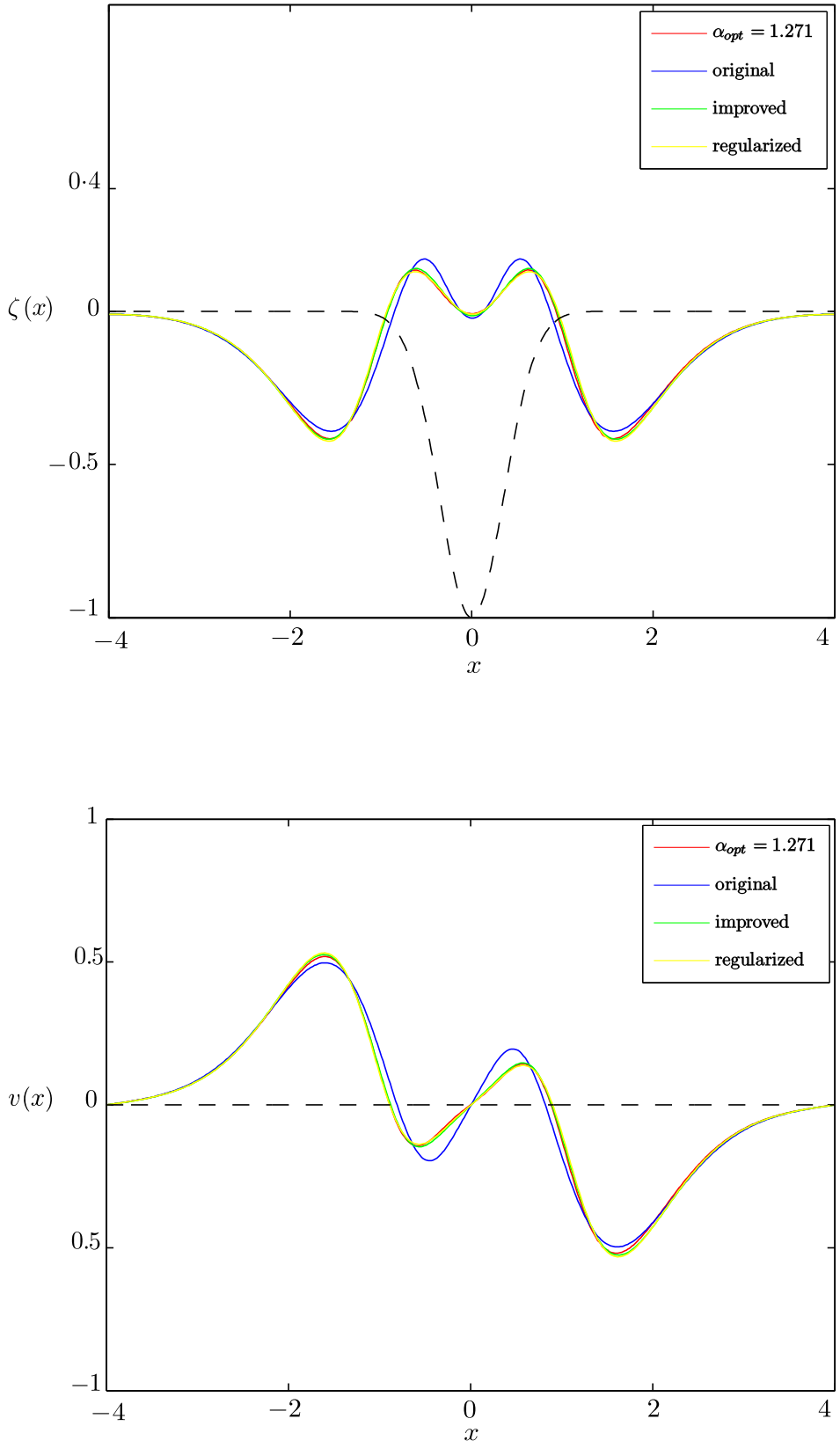

Figure 4.11. Comparison with the Green-Naghdi models, with surface tension, at time $t = 2$, for $\alpha_{opt} = 1.271$.

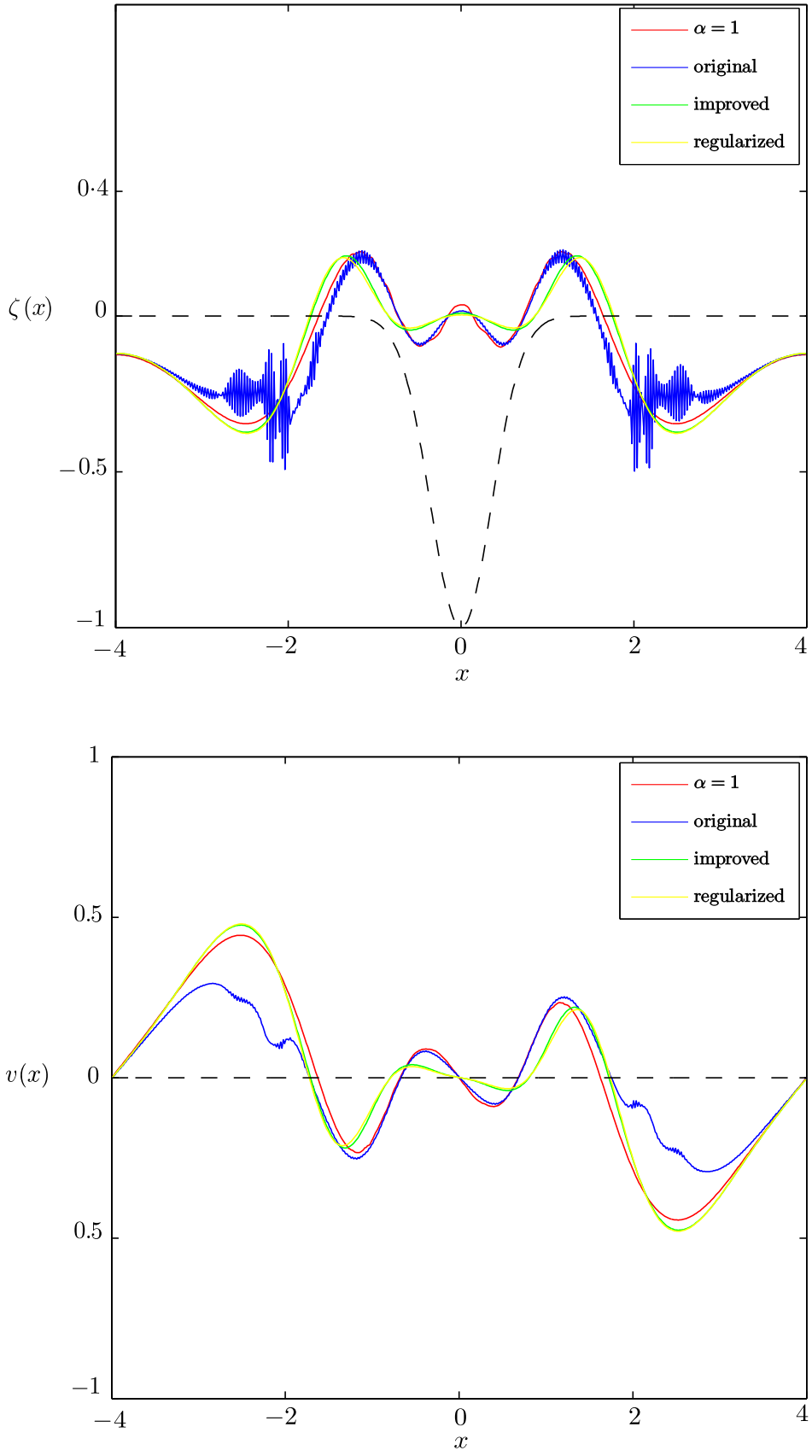

Figure 4.12. Comparison with the Green-Naghdi models, with surface tension, at time $t = 3$, for $\alpha = 1$.

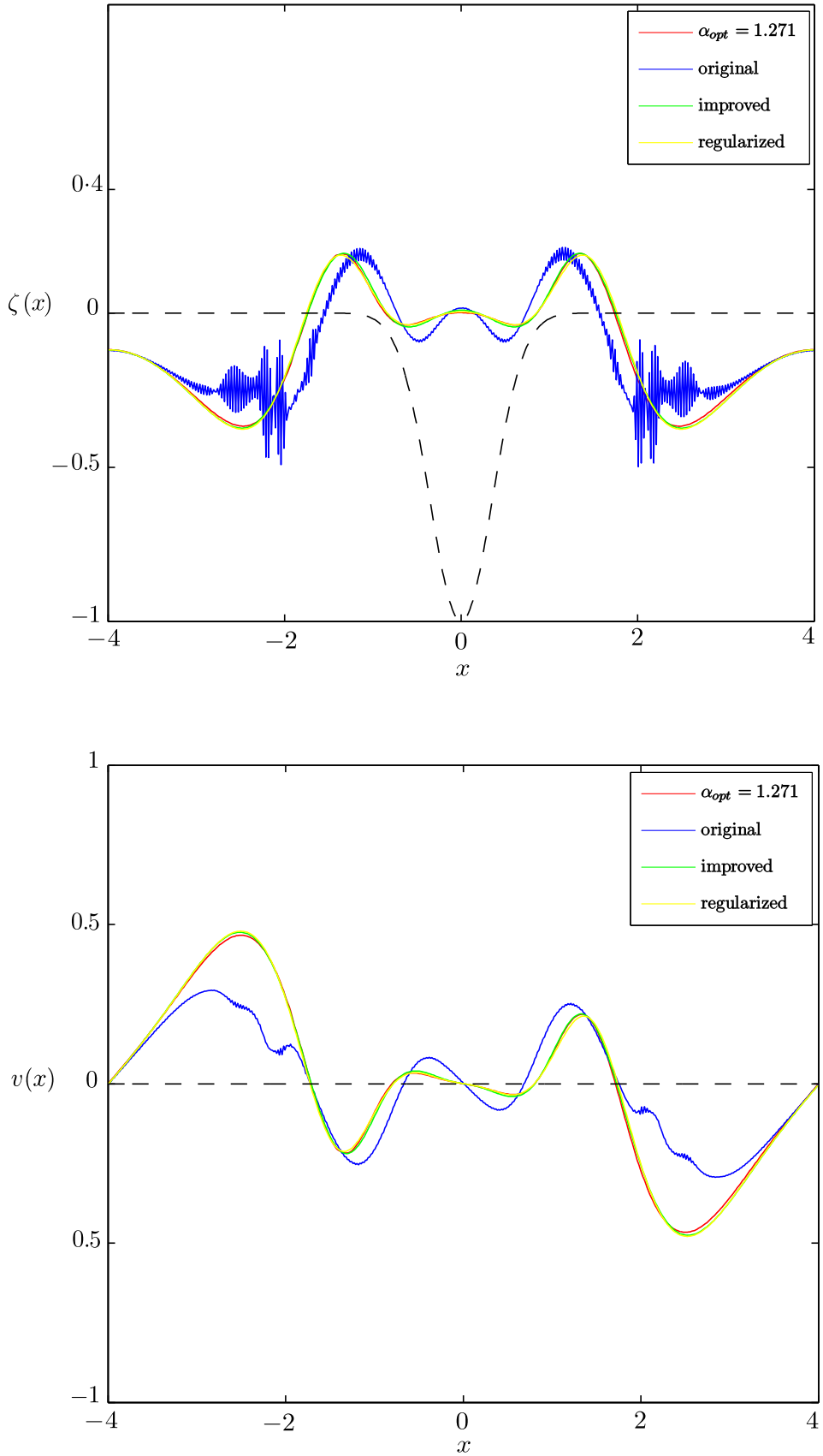

Figure 4.13. Comparison with the Green-Naghdi models, with surface tension, at time $t = 3$, for $\alpha_{opt} = 1.271$.

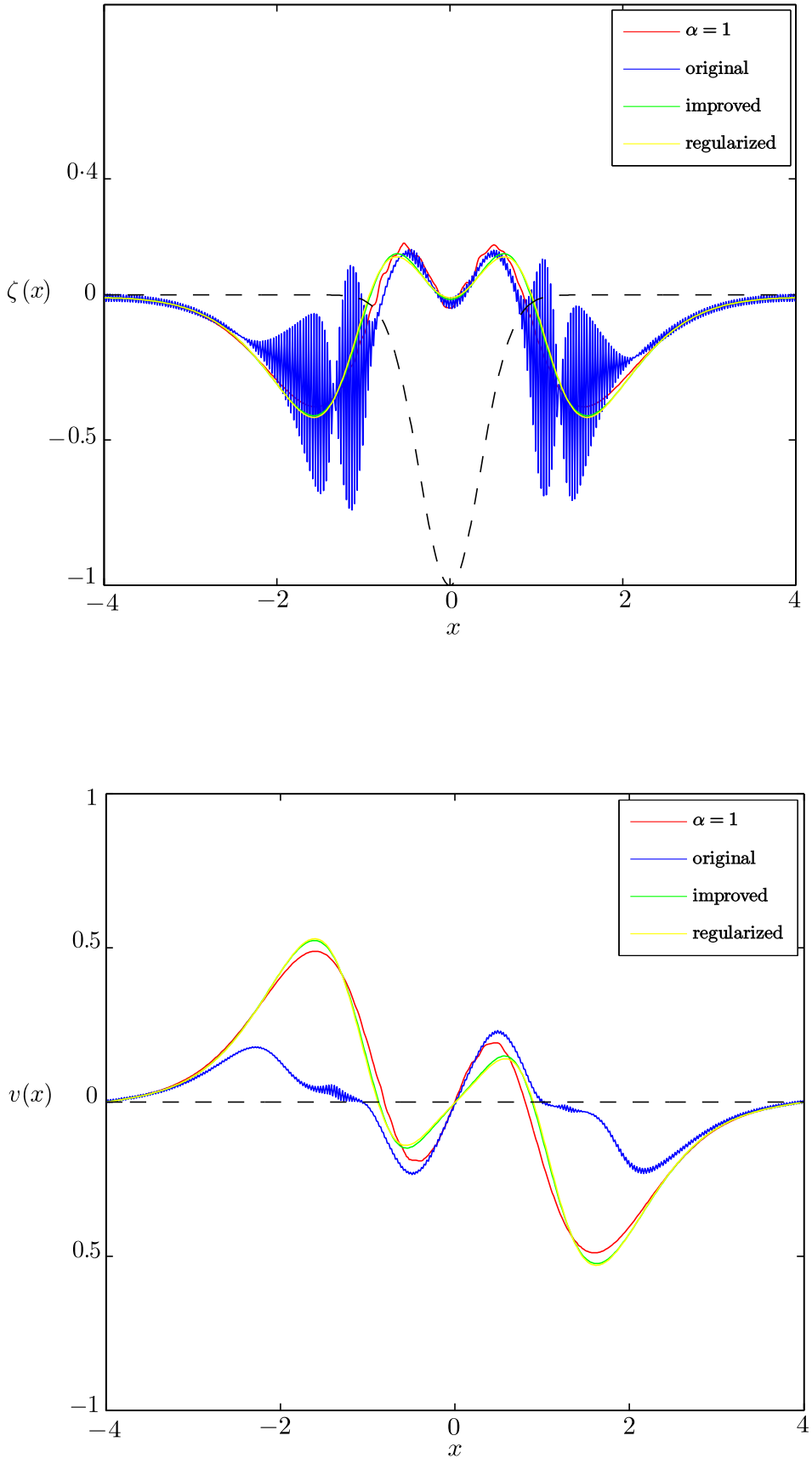

Figure 4.14. Comparison with the Green-Naghdi models, without surface tension ($\mathrm{bo}^{-1} = 0$), at time $t = 2$, for $\alpha = 1$.

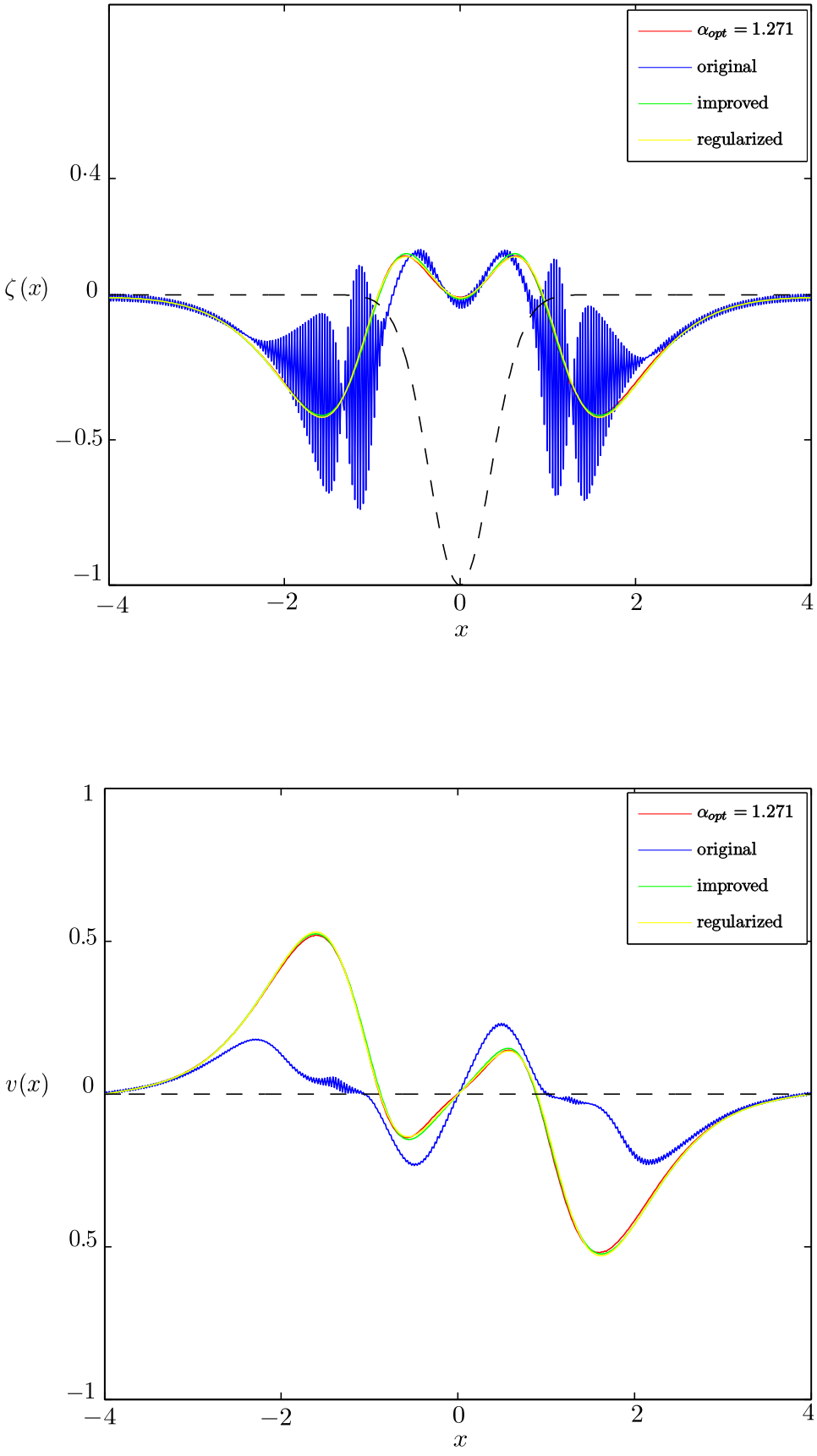

Figure 4.15. Comparison with the Green-Naghdi models, without surface tension ($\mathrm{bo}^{-1} = 0$), at time $t = 2$ for $\alpha_{opt} = 1.271$.

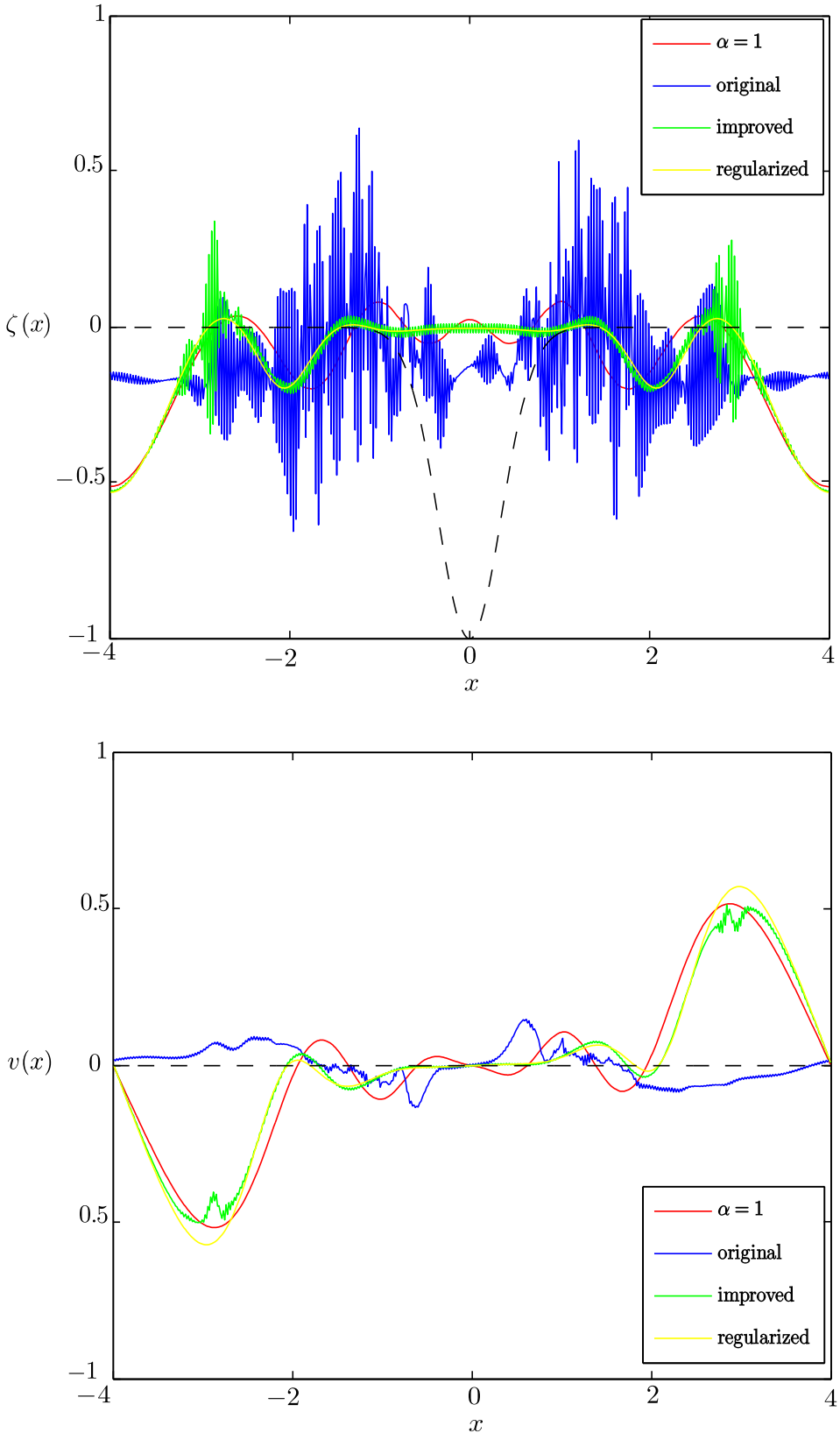

Figure 4.16. Comparison with the Green-Naghdi models, without surface tension ($\text{bo}^{-1} = 0$), at time $t = 5$ for $\alpha = 1$.

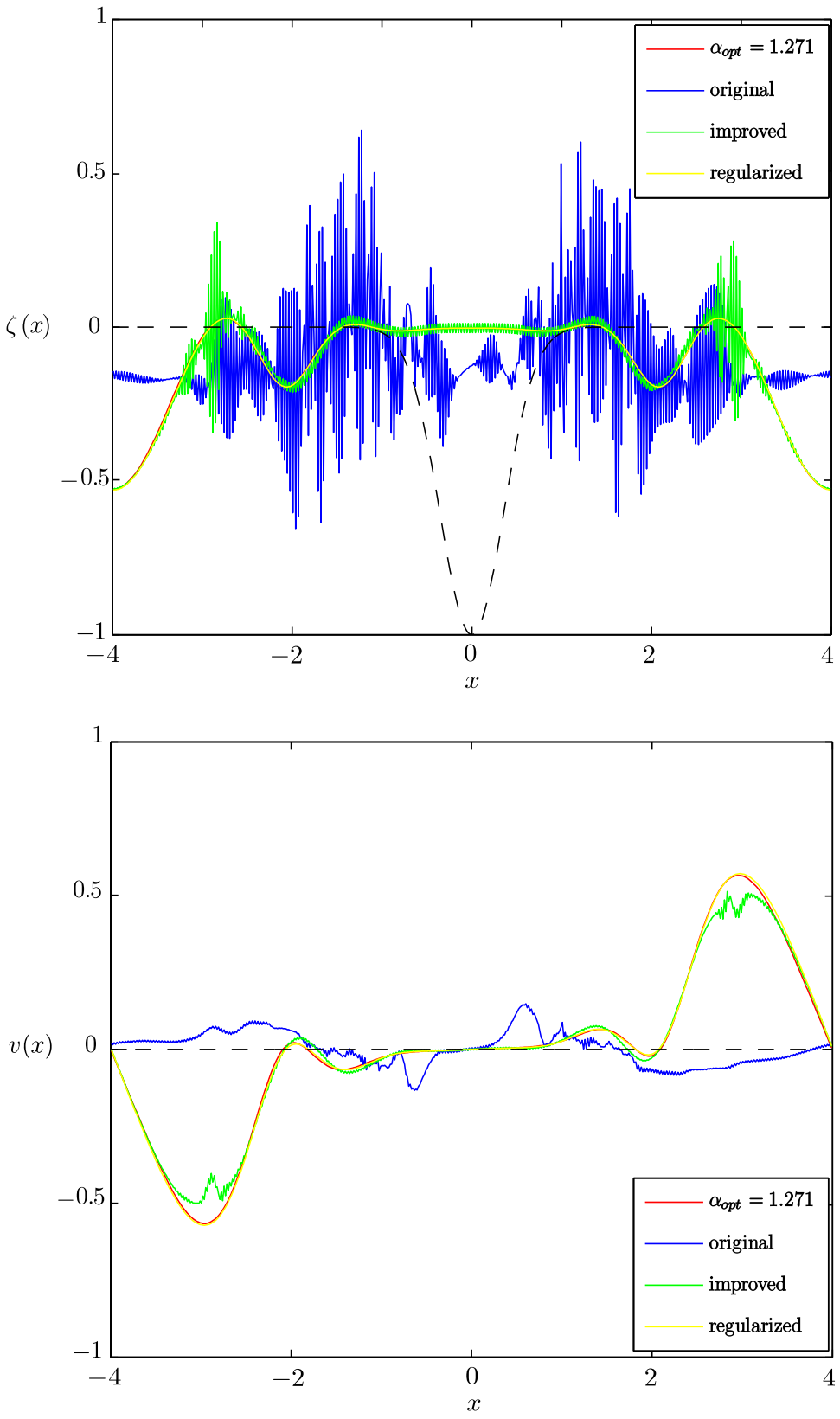

Figure 4.17. Comparison with the Green-Naghdi models, without surface tension ($\mathrm{bo}^{-1} = 0$), at time $t = 5$ for $\alpha_{opt} = 1.271$.

Figures 4.10 and 4.11 show the comparisons between our numerical solution and the Green-Naghdi models solutions obtained in [50], with a small amount of surface tension, at time $t = 2$ for $\alpha = 1$ and $\alpha_{opt} = 1.271$ respectively.

The same simulation is performed for a larger time $t = 3$ and the same comparisons are shown in Figures 4.12 and 4.13 for $\alpha = 1$ and $\alpha_{opt} = 1.271$ respectively. We observe an excellent agreement between our numerical solution computed for $\alpha_{opt} = 1.271$ and both "improved" and "regularized" models at $t = 2$ and $t = 3$ which is not the case when choosing $\alpha = 1$. As expected, at $t = 3$ the original model induces Kelvin-Helmholtz instabilities. Meanwhile, the flows predicted by the regularized and improved models and by our model (4.22) with $\alpha_{opt} = 1.271$ remain smooth and are very similar. Figure 4.14 shows that the numerical solutions computed for $\alpha = 1$ without surface tension at time $t = 2$ and the "improved" and "regularized" models are not in agreement. On the other hand an excellent agreement is observable in Figure 4.15 when choosing $\alpha_{opt} = 1.271$. One can remark in Figure 4.15 that the flow of the original model is completely destroyed in absence of the surface tension due to Kelvin-Helmholtz instabilities.

However, at a larger time ($t = 5$), figure 4.17 shows that in absence of surface tension ($\text{bo}^{-1} = 0$) Kelvin-Helmholtz instabilities will destroy completely both "original" and "improved" models. Meanwhile the numerical solution computed for $\alpha_{opt} = 1.271$ and for the "regularized" models remain smooth and very similar contrarily to the case when $\alpha = 1$ (see figure 4.16).

The overall observations show the importance of the choice of the parameter α as in Section 4.3.3 in improving the frequency dispersion. Indeed, when choosing $\alpha_{opt} = 1.271$, we observe an excellent matching between our numerical solutions and those obtained by the "improved" model before the latter is completely destroyed in absence of surface tension due to the Kelvin-Helmholtz instabilities. As well, our numerical solution matches the one computed by the "regularized" model even for a large time and with or without surface tension. This is not the case when choosing $\alpha = 1$. In fact, the "improved" model has the same dispersion relation as the one of the *full Euler system* and the dispersion relation of the "regularized" model fit the one of the *full Euler system* to an $\mathcal{O}(\mu^3)$ order. This explains the reason behind the matching when choosing an optimal value for α.

Dam-break problem in the two layers case

This simulation concerns a test of the ability of our numerical scheme (4.42) to handle discontinuities when considering a dam-break problem in the two layers case. To this end, we use the same initial data as in the one layer case given by (4.85), where $a = 0.2091\ m$.

The simulations are performed on the interval $x \in (-700, 700)$, discretized with 2800 cells imposing periodic conditions on each boundary. The dimensionless parameters representing the ratio between the depth and the ratio between the densities of the two layers are set respectively as follows: $\delta = 0.5$, $\gamma = 0.95$. Taking into account a small amount of surface tension, we set $\text{bo}^{-1} = 5 \times 10^{-5}$. We would like to mention that the simulations are computed using $\alpha = 1$. As expected, the same simulations performed when choosing $\alpha_{opt} = 1.1498$ yielded the same result since $\alpha_{opt} \to 1$ when considering large wave numbers as explained in Section 4.3.3.

Figure 4.18 shows the results of the numerical simulation at several times, generating two dis-

persive tails propagating towards the center and two rarefaction waves that travel in opposite directions, on each side of the "dam". A zoom on the dispersive tails is proposed at $t = 55\ s$ and $t = 75\ s$. Indeed, capturing this phenomenon accurately exhibit the high accuracy of our numerical scheme.

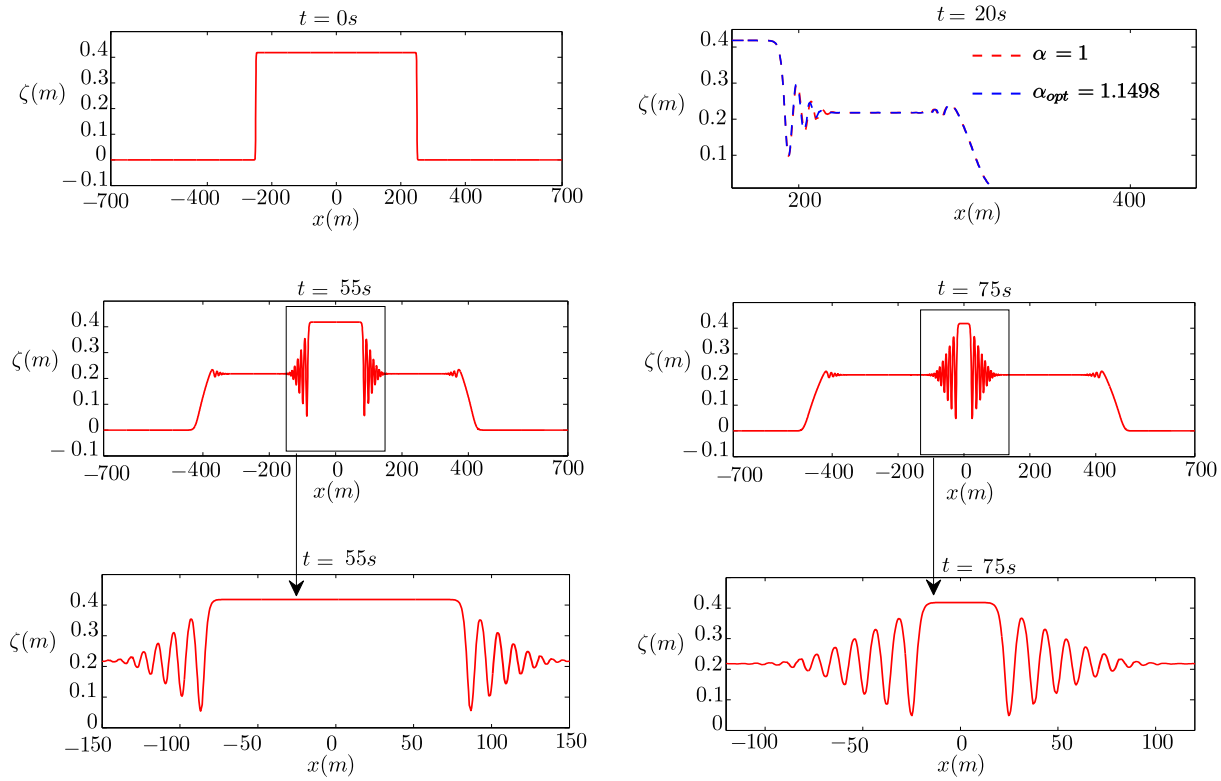

Figure 4.18. Dam break in the two layers case: water surface profiles at several times

4.6 Conclusion

In this work, we presented a numerical scheme for the Green-Naghdi model in the Camassa-Holm regime. This model is first reformulated under more appropriate structure, where the time dependency of a second order differential operator present in the model is removed, keeping the stabilizing effects of its inversion. Furthermore, we improved the frequency dispersion of the original model keeping the same order of precision thanks to a parameter α to be precisely chosen. Additionally, our model do not contain third order derivatives that may create high frequencies instabilities. We then propose an efficient, precise and stable numerical splitting scheme that decomposes the hyperbolic and dispersive parts of the equations. The hyperbolic part is treated with a finite-volume method, where we consider the following schemes with different orders of accuracy: the first order finite-volume scheme based on a VFRoe method, the second order finite volume scheme following the classical "MUSCL" approach and finally a fifth-order "WENO" reconstruction. On the other hand, we treat the dispersive part with a finite-difference scheme, using second and fourth order formulas. Concerning time discretization we use classical second and fourth order Runge-Kutta methods, according to the order of the space derivative in consideration. Finally, we present several numerical validations in the one and two layers cases,

showing the numerical efficiency and accuracy of our scheme and exhibiting its ability to reduce numerical dispersion and dissipation and to deal with discontinuities. The next step of this study may concern the extension of this numerical scheme to a more general configuration of variable topography. We believe that this splitting strategy may be applied in the variable bottom case.

Conclusions et perspectives

Dans cette thèse, nous nous sommes intéressés aux modèles asymptotiques unidimensionnels qui décrivent la propagation des ondes internes à l'interface entre deux couches de fluides idéaux de densités différentes. Le premier objectif concernait la modélisation et l'étude théorique (existence, unicité et convergence de solutions) de deux classes de modèles asymptotiques pour deux régimes de variations topographiques différents. Le second objectif concernait la résolution numérique d'un modèle asymptotique existant dans la littérature dans le cadre d'un fond plat. Ces deux objectifs ont été remplis dans deux parties distinctes.

La première partie de cette thèse a été consacrée à la dérivation et à la justification mathématique de modèles asymptotiques de type Green-Naghdi dans le régime de Camassa-Holm (interface de moyenne amplitude). Dans ce cadre et en suivant la même stratégie initiée en [49] nous avons construit à partir du système de Green-Naghdi original un *modèle couplé* consistant avec le *système d'Euler complet* prenant en compte une variation topographique de moyenne amplitude. Cette construction est basée sur un développement asymptotique des termes dispersifs et sur l'introduction d'un nouvel opérateur différentiel symétrique et inversible. Après quelques transformations supplémentaires nous avons obtenu un modèle qui possède une structure quasi-linéaire symétrisable. Nous avons montré le caractère bien posé de ce modèle (au sens de Hadamard) dans des espaces de Sobolev avec une méthode d'énergie suivant la théorie classique des systèmes hyperboliques. L'adaptation du symétriseur nous a permis d'annuler l'utilisation des hypothèses de petitesse sur les déformations à l'interface et au fond dans les résultats d'existence, d'unicité et de stabilité, indépendamment de leurs nécessités dans la dérivation du modèle. Grâce au résultat de stabilité nous avons justifié rigoureusement notre modèle par un résultat de convergence en montrant que la solution de notre modèle approche celle du *système d'Euler complet* avec une précision d'ordre $\mathcal{O}(\mu^2)$.

Dans un second temps, nous avons généralisé le résultat de justification rigoureuse obtenu précédemment au cas d'une topographie qui peut varier lentement mais avec une large amplitude. Notamment, nous avons supposé cette fois une topographie variable qui peut admettre une grande longueur d'onde et une large amplitude. Suivant les mêmes techniques mentionnées ci-dessus, nous avons construit un *modèle couplé* équivalent (au sens de la consistance) au système de Green-Naghdi original. Des restrictions raisonnables ont été imposées sur la déformation du fond afin de garantir la validité du nouveau modèle obtenu. Le caractère bien posé du nouveau modèle a été montré en utilisant des méthodes d'énergie classiques pour les systèmes hyperboliques symétrisables. Finalement, à l'aide du résultat de consistance ainsi que celui de stabilité, nous avons abouti à un résultat de convergence montrant qu'en partant de données initiales correspondantes la solution de notre modèle reste proche de celle du *système d'Euler complet* au cours du temps. De plus, le nouveau modèle que nous avons obtenu offre un outil important pour la justification rigoureuse d'autres modèles bien posés et consistants. Nous avons appliqué cette procédure à des nouveaux *modèles asymptotiques unidirectionnels* caractérisés par des équations

scalaires décrivant la propagation des ondes internes solitaires dans une direction donnée et sur une topographie variable. Nous avons montré que la nouvelle approximation unidirectionnelle obtenue dans le régime de Camassa-Holm satisfait le système de Green-Naghdi original à un petit reste sous certaines hypothèses de petitesse sur la déformation du fond. Ensuite, le caractère bien posé de cette équation scalaire a été montré à l'aide des estimations d'énergie pour un temps assez large. Ce type d'équations scalaires peut créer des singularités sous forme de déferlement dans un temps fini et pour une donné initiale régulière. Ceci a été montré pour l'approximation unidirectionnelle dans le régime de Camassa-Holm restreint au cas d'une lente variation topographique et sous certaines conditions particulières sur les paramètres. Sous des hypothèses plus fortes sur la topographie, nous avons justifié rigoureusement cette approximation par un résultat de convergence. Enfin, nous avons récupéré et justifié rigoureusement une approximation unidirectionnelle dans un régime plus restreint d'ondes longues.

Dans la deuxième partie de cette thèse, nous nous sommes attachés à la résolution numérique d'un *modèle couplé* existant dans la littérature (voir [49]) et qui correspond au modèle dérivé dans la première partie dans le cadre d'un fond plat. Ce modèle décrit la propagation des ondes internes à l'interface entre deux couches de fluides de densités différentes limitées par un toit rigide en haut et par un fond plat en bas. Nous avons réécrit ce modèle d'une manière équivalente (même ordre de précision) mais plus adaptée à la résolution numérique. Plus précisément, nous avons éliminé la dépendance en temps de l'opérateur différentiel symétrique de sorte qu'il soit inversé une seule fois durant le calcul. Nous avons montré dans la suite que l'inversion de cette opérateur ajoute un effet de stabilisation. Les propriétés de dispersion ont été améliorées à l'aide de l'introduction d'un nouveau paramètre choisi précisément de sorte que la relation de dispersion de la nouvelle formulation corresponde à celle du système complet. De plus, la nouvelle formulation ne contient plus de dérivées d'ordre trois qui peuvent créer des instabilités hautes fréquences. Pour la résolution numérique de la nouvelle formulation, nous avons proposé suivant la même stratégie utilisée en [18, 86] un schéma de "splitting" d'ordre deux séparant la partie hyperbolique et la partie dispersive du modèle. Nous avons traité la partie hyperbolique en utilisant une méthode de volumes finis où nous avons considéré trois schémas d'ordres de précision différents : un schéma du premier ordre basé sur une méthode de VFRoe, un schéma du second ordre suivant la méthode classique "MUSCL" et finalement un schéma "WENO" d'ordre cinq. La partie dispersive a été calculée numériquement avec un schéma aux différences finies d'ordre deux et quatre. En ce qui concerne la discrétisation en temps, nous avons utilisé des méthodes classiques de Runge-Kutta d'ordre deux et quatre selon l'ordre de discrétisation en espace considéré. Pour la validation de note schéma nous avons choisi d'effectuer plusieurs simulations numériques dans le cas d'une couche et de deux couches de fluides. Dans la plupart des simulations, nous avons utilisé des conditions aux bords périodiques. Nous avons illustré l'efficacité, la précision, la stabilité et la capacité de notre schéma à réduire la dissipation en étudiant la propagation d'une onde de surface solitaire et en comparant la solution de notre modèle à une solution analytique pour les trois différents ordres de discrétisation. La collision de deux ondes de surface se propageant en des directions opposées ainsi que la rupture d'une onde gaussienne tendent à confirmer la haute précision de notre schéma. Le capacité à traiter les discontinuités a été montrée en considérant le problème de rupture de barrage dans les deux cas d'une couche et de deux couches de fluide. Finalement, en comparant à des données numériques issues de [50], nous avons montré l'importance du choix du nouveau paramètre pour améliorer les propriétés de dispersion.

Perspectives

Les perspectives et pistes de recherches qui apparaissent à l'issue de cette thèse portent à la fois sur des aspects de modélisation, de justification mathématique ainsi que numérique.

Concernant la modélisation, nous envisageons dans un premier lieu étendre les *modèles couplés* de type Green-Naghdi dans le régime de Camassa-Holm dérivés aux Chapitres 2 et 3 au cas d'un fond variable avec une grande amplitude. Notamment, essayer d'enlever l'hypothèse de lente variation afin d'obtenir un modèle prenant en compte une variation topographique généralisée. Il serait également possible d'appliquer ceci aux *modèles unidirectionnels scalaires* dérivés au Chapitre 3. Par conséquent, il serait intéressant de justifier rigoureusement tous ces modèles en temps long.

D'un point de vue numérique, une perspective intéressante serait de proposer un schéma numérique afin de pouvoir étendre les simulations numériques du Chapitre 4 au cas de topographie variable. Une première étape serait de considérer les variations topographiques de moyenne amplitude. Nous aimerions également résoudre numériquement les modèles unidirectionnels scalaires du Chapitre 3. Ce travail dans le cadre des ondes internes avec fond variable n'est pas encore réalisé à ce jour. Finalement, il est important d'essayer d'atteindre l'ordre de précision attendu dans les simulations numériques du Chapitre 4. Pour ce faire nous aimerions mettre en œuvre une technique de filtrage communément appelée "cleaning technique" qui sert à nettoyer les queues de dispersion durant la propagation d'une onde solitaire et qui sont de l'ordre de l'erreur.

Bibliographie

[1] S. Alinhac and P. Gérard. *Opérateurs pseudo-différentiels et théorème de Nash-Moser*. Savoirs Actuels. InterEditions, Paris ; Éditions du Centre National de la Recherche Scientifique (CNRS), Meudon, 1991.

[2] B. Alvarez-Samaniego and D. Lannes. Large time existence for 3D water-waves and asymptotics. *Invent. Math.*, 171(3) :485–541, 2008.

[3] B. Alvarez-Samaniego and D. Lannes. A Nash-Moser theorem for singular evolution equations. Application to the Serre and Green-Naghdi equations. *Indiana Univ. Math. J.*, 57(1) :97–131, 2008.

[4] D. M. Ambrose. Well-posedness of vortex sheets with surface tension. *SIAM J. Math. Anal.*, 35(1) :211–244 (electronic), 2003.

[5] D. M. Ambrose and N. Masmoudi. Well-posedness of 3D vortex sheets with surface tension. *Commun. Math. Sci.*, 5(2) :391–430, 2007.

[6] C. T. Anh. Influence of surface tension and bottom topography on internal waves. *Math. Models Methods Appl. Sci.*, 19(12) :2145–2175, 2009.

[7] R. Barros and W. Choi. On regularizing the strongly nonlinear model for two-dimensional internal waves. *Phys. D*, 264 :27–34, 2013.

[8] E. Barthélemy. Nonlinear shallow water theories for coastal waves. *Surveys in Geophysics*, 25(3) :315–337, 2004.

[9] T. B. Benjamin, J. L. Bona, and J. J. Mahony. Model equations for long waves in nonlinear dispersive systems. *Philos. Trans. Roy. Soc. London Ser. A*, 272(1220) :47–78, 1972.

[10] T. B. Benjamin and T. J. Bridges. Reappraisal of the Kelvin-Helmholtz problem. I. Hamiltonian structure. *J. Fluid Mech.*, 333 :301–325, 1997.

[11] J. L. Bona and M. Chen. A Boussinesq system for two-way propagation of nonlinear dispersive waves. *Phys. D*, 116(1-2) :191–224, 1998.

[12] J. L. Bona, M. Chen, and J.-C. Saut. Boussinesq equations and other systems for small-amplitude long waves in nonlinear dispersive media. I. Derivation and linear theory. *J. Nonlinear Sci.*, 12(4) :283–318, 2002.

[13] J. L. Bona, M. Chen, and J.-C. Saut. Boussinesq equations and other systems for small-amplitude long waves in nonlinear dispersive media. II. The nonlinear theory. *Nonlinearity*, 17(3) :925–952, 2004.

[14] J. L. Bona, T. Colin, and D. Lannes. Long wave approximations for water waves. *Arch. Ration. Mech. Anal.*, 178(3) :373–410, 2005.

[15] J. L. Bona, V. A. Dougalis, and D. E. Mitsotakis. Numerical solution of KdV-KdV systems of Boussinesq equations. I. The numerical scheme and generalized solitary waves. *Math. Comput. Simulation*, 74(2-3) :214–228, 2007.

[16] J. L. Bona, D. Lannes, and J.-C. Saut. Asymptotic models for internal waves. *J. Math. Pures Appl. (9)*, 89(6) :538–566, 2008.

[17] P. Bonneton, E. Barthelemy, F. Chazel, R. Cienfuegos, D. Lannes, F. Marche, and M. Tissier. Recent advances in Serre-Green Naghdi modelling for wave transformation, breaking and runup processes. *Eur. J. Mech. B Fluids*, 30(6) :589–597, 2011.

[18] P. Bonneton, F. Chazel, D. Lannes, F. Marche, and M. Tissier. A splitting approach for the fully nonlinear and weakly dispersive Green-Naghdi model. *J. Comput. Phys.*, 230(4) :1479–1498, 2011.

[19] F. Bouchut. *Nonlinear stability of finite volume methods for hyperbolic conservation laws and well-balanced schemes for sources*. Frontiers in Mathematics. Birkhäuser Verlag, Basel, 2004.

[20] J. Boussinesq. Théorie de l'intumescence liquide appelée onde solitaire ou de translation se propageant dans un canal rectangulaire. *C.R. Acad. Sci. Paris Sér. A-B*, 72 :755–759, 1871.

[21] J. Boussinesq. Théorie des ondes et des remous qui se propagent le long d'un canal rectangulaire horizontal, en communiquant au liquide contenu dans ce canal des vitesses sensiblement pareilles de la surface au fond. *J. Math. Pures Appl.*, 17 :55–108, 1872.

[22] D. Bresch and M. Renardy. Well-posedness of two-layer shallow-water flow between two horizontal rigid plates. *Nonlinearity*, 24(4) :1081–1088, 2011.

[23] M. Brocchini and N. Dodd. Nonlinear shallow water equation modeling for coastal engineering. *Journal of Waterway, Port, Coastal, and Ocean Engineering*, 134(2) :104–120, 2008.

[24] T. Buffard, T. Gallouët, and J.-M. Hérard. A sequel to a rough Godunov scheme : application to real gases. *Comput. & Fluids*, 29(7) :813–847, 2000.

[25] C. Burtea. New long time existence results for a class of Boussinesq-type systems. *J. Math. Pures Appl. (9)*, 106(2) :203–236, 2016.

[26] R. Camassa, W. Choi, H. Michallet, P.-O. Rusas, and J. K. Sveen. On the realm of validity of strongly nonlinear asymptotic approximations for internal waves. *Journal of Fluid Mechanics*, 549 :1–23, 2 2006.

[27] R. Camassa and D. D. Holm. An integrable shallow water equation with peaked solitons. *Phys. Rev. Lett.*, 71(11) :1661–1664, 1993.

[28] F. Chazel. Influence of bottom topography on long water waves. *M2AN Math. Model. Numer. Anal.*, 41(4) :771–799, 2007.

[29] F. Chazel. On the Korteweg-de Vries approximation for uneven bottoms. *Eur. J. Mech. B Fluids*, 28(2) :234–252, 2009.

[30] F. Chazel, D. Lannes, and F. Marche. Numerical simulation of strongly nonlinear and dispersive waves using a Green-Naghdi model. *J. Sci. Comput.*, 48(1-3) :105–116, 2011.

[31] W. Choi and R. Camassa. Weakly nonlinear internal waves in a two-fluid system. *J. Fluid Mech.*, 313 :83–103, 1996.

[32] W. Choi and R. Camassa. Fully nonlinear internal waves in a two-fluid system. *J. Fluid Mech.*, 396 :1–36, 1999.

[33] R. Cienfuegos, E. Barthélemy, and P. Bonneton. A fourth-order compact finite volume scheme for fully nonlinear and weakly dispersive Boussinesq-type equations. II. Boundary conditions and validation. *Internat. J. Numer. Methods Fluids*, 53(9) :1423–1455, 2007.

[34] A. Constantin and D. Lannes. The hydrodynamical relevance of the Camassa-Holm and Degasperis-Procesi equations. *Arch. Ration. Mech. Anal.*, 192(1) :165–186, 2009.

[35] W. Craig. An existence theory for water waves and the Boussinesq and Korteweg-de Vries scaling limits. *Comm. Partial Differential Equations*, 10(8) :787–1003, 1985.

[36] W. Craig and M. D. Groves. Normal forms for wave motion in fluid interfaces. *Wave Motion*, 31(1) :21–41, 2000.

[37] W. Craig, P. Guyenne, J. Hammack, D. Henderson, and C. Sulem. Solitary water wave interactions. *Phys. Fluids*, 18(5) :057106, 25, 2006.

[38] W. Craig, P. Guyenne, and H. Kalisch. Hamiltonian long-wave expansions for free surfaces and interfaces. *Comm. Pure Appl. Math.*, 58(12) :1587–1641, 2005.

[39] W. Craig and C. Sulem. Numerical simulation of gravity waves. *J. Comput. Phys.*, 108(1) :73–83, 1993.

[40] W. Craig, C. Sulem, and P.-L. Sulem. Nonlinear modulation of gravity waves : a rigorous approach. *Nonlinearity*, 5(2) :497–522, 1992.

[41] B. de Saint-Venant. Théorie du mouvement non-permanent des eaux, avec application aux crues des rivières et à l'introduction des marées dans leur lit. *C.R. Acad. Sci. Paris*, 73 :147–154, 1871.

[42] M. W. Dingemans. *Water wave propagation over uneven bottoms. 2. , Non-linear wave propagation*, volume 13 of *Advanced series on ocean engineering*. World Scientific, Cornell Univ., Hollister Hall, 1997.

[43] V. D. Djordjevic and L. G. Redekopp. The fission and disintegration of internal solitary waves moving over two-dimensional topography. *Journal of Physical Oceanography*, 8(6) :1016–1024, 1978.

[44] V. Duchêne. Asymptotic shallow water models for internal waves in a two-fluid system with a free surface. *SIAM J. Math. Anal.*, 42(5) :2229–2260, 2010.

[45] V. Duchêne. Asymptotic models for the generation of internal waves by a moving ship, and the dead-water phenomenon. *Nonlinearity*, 24(8) :2281–2323, 2011.

[46] V. Duchêne. Boussinesq/Boussinesq systems for internal waves with a free surface, and the KdV approximation. *ESAIM Math. Model. Numer. Anal.*, 46(1) :145–185, 2012.

[47] V. Duchêne. Decoupled and unidirectional asymptotic models for the propagation of internal waves. *Math. Models Methods Appl. Sci.*, 24(1) :1–65, 2014.

[48] V. Duchêne, S. Israwi, and R. Talhouk. Shallow water asymptotic models for the propagation of internal waves. *Discrete Contin. Dyn. Syst. Ser. S*, 7(2) :239–269, 2014.

[49] V. Duchêne, S. Israwi, and R. Talhouk. A new fully justified asymptotic model for the propagation of internal waves in the Camassa-Holm regime. *SIAM J. Math. Anal.*, 47(1) :240–290, 2015.

[50] V. Duchêne, S. Israwi, and R. Talhouk. A new class of two-layer green–naghdi systems with improved frequency dispersion. *to appear in Studies in Applied Mathematics*, 2016.

[51] A. Duran and F. Marche. Discontinuous-Galerkin discretization of a new class of Green-Naghdi equations. *Commun. Comput. Phys.*, 17(3) :721–760, 2015.

[52] D. G. Ebin. Ill-posedness of the Rayleigh-Taylor and Helmholtz problems for incompressible fluids. *Comm. Partial Differential Equations*, 13(10) :1265–1295, 1988.

[53] V. W. Ekman. On dead water. *Sci. Results Norw. North Polar Expedi. 1893-96 5*, 15 :1–152, 1904.

[54] G. A. El, R. H. J. Grimshaw, and N. F. Smyth. Unsteady undular bores in fully nonlinear shallow-water theory. *Phys. Fluids*, 18(2) :027104, 17, 2006.

[55] K. S. Erduran, S. Ilic, and V. Kutija. Hybrid finite-volume finite-difference scheme for the solution of Boussinesq equations. *Internat. J. Numer. Methods Fluids*, 49(11) :1213–1232, 2005.

[56] L.-L. Fu and B. Holt. *Seasat views oceans and sea ice with synthetic aperture radar.* NASA/JPL-PUB-81-120, California Inst. of Tech. ; Pasadena, 1982.

[57] T. Gallouët, J.-M. Hérard, and N. Seguin. Some recent finite volume schemes to compute Euler equations using real gas EOS. *Internat. J. Numer. Methods Fluids*, 39(12) :1073–1138, 2002.

[58] T. Gallouët, J.-M. Hérard, and N. Seguin. Some approximate Godunov schemes to compute shallow-water equations with topography. *Comput. & Fluids*, 32(4) :479–513, 2003.

[59] E. Godlewski and P.-A. Raviart. *Hyperbolic systems of conservation laws*, volume 3/4 of *Mathématiques & Applications (Paris) [Mathematics and Applications]*. Ellipses, Paris, 1991.

[60] A. E. Green and P. M. Naghdi. A derivation of equations for wave propagation in water of variable depth. *J. Fluid Mech.*, 78 :237–246, 11 1976.

[61] R. Grimshaw. Internal solitary waves. In *Advances in fluid mechanics V*, volume 40 of *Adv. Fluid Mech.*, pages 209–218. WIT Press, Southampton, 2004.

[62] R. Grimshaw, E. Pelinovsky, and O. Poloukhina. Higher-order korteweg-de vries models for internal solitary waves in a stratified shear flow with a free surface. *Nonlinear Processes in Geophysics*, 9(3/4) :221–235, 2002.

[63] J. Grue, A. Jensen, P.-O. Rusas, and J. K. Sveen. Properties of large-amplitude internal waves. *J. Fluid Mech.*, 380.

[64] P. Guyenne. Large-amplitude internal solitary waves in a two-fluid model. *Comptes Rendus Mécanique*, 334(6) :341 – 346, 2006.

[65] P. Guyenne, D. Lannes, and J.-C. Saut. Well-posedness of the Cauchy problem for models of large amplitude internal waves. *Nonlinearity*, 23(2) :237–275, 2010.

[66] K. R. Helfrich and W. K. Melville. On long nonlinear internal waves over slope-shelf topography. *J. Fluid Mech.*, 167 :285–308, 6 1986.

[67] K. R. Helfrich and W. K. Melville. Long nonlinear internal waves. In *Annual review of fluid mechanics. Vol. 38*, volume 38 of *Annu. Rev. Fluid Mech.*, pages 395–425. Annual Reviews, Palo Alto, CA, 2006.

[68] K. R. Helfrich, W. K. Melville, and J. W. Miles. On interfacial solitary waves over slowly varying topography. *J. Fluid Mech.*, 149 :305–317, 1984.

[69] T. Iguchi, N. Tanaka, and A. Tani. On the two-phase free boundary problem for two-dimensional water waves. *Math. Ann.*, 309(2) :199–223, 1997.

[70] S. Israwi. Derivation and analysis of a new 2D Green-Naghdi system. *Nonlinearity*, 23(11) :2889–2904, 2010.

[71] S. Israwi. Variable depth KdV equations and generalizations to more nonlinear regimes. *M2AN Math. Model. Numer. Anal.*, 44(2) :347–370, 2010.

[72] S. Israwi. Large time existence for 1D Green-Naghdi equations. *Nonlinear Anal.*, 74(1) :81–93, 2011.

[73] S. Israwi and R. Talhouk. Local well-posedness of a nonlinear KdV-type equation. *C. R. Math. Acad. Sci. Paris*, 351(23-24) :895–899, 2013.

[74] G.-S. Jiang and C.-W. Shu. Efficient implementation of weighted ENO schemes. *J. Comput. Phys.*, 126(1) :202–228, 1996.

[75] R. S. Johnson. Camassa-Holm, Korteweg-de Vries and related models for water waves. *J. Fluid Mech.*, 455 :63–82, 2002.

[76] B. Kadomtsev and V. Petviashvili. On the stability of solitary waves in weakly dispersing media. In *Sov. Phys. Dokl*, volume 15, pages 539–541, 1970.

[77] T. Kakutani and N. Yamasaki. Solitary waves on a two-layer fluid. *Journal of the Physical Society of Japan*, 45(2) :674–679, 1978.

[78] V. Kamotski and G. Lebeau. On 2D Rayleigh-Taylor instabilities. *Asymptot. Anal.*, 42(1-2) :1–27, 2005.

[79] T. Kato and G. Ponce. Commutator estimates and the Euler and Navier-Stokes equations. *Comm. Pure Appl. Math.*, 41(7) :891–907, 1988.

[80] C. G. Koop and G. Butler. An investigation of internal solitary waves in a two-fluid system. *J. Fluid Mech.*, 112 :225–251, 1981.

[81] D. J. Korteweg and G. de Vries. On the change of form of long waves advancing in a rectangular canal, and on a new type of long stationary waves. *Philos. Mag. (5)*, 39(240) :422–443, 1895.

[82] D. Lannes. Sharp estimates for pseudo-differential operators with symbols of limited smoothness and commutators. *J. Funct. Anal.*, 232(2) :495–539, 2006.

[83] D. Lannes. A stability criterion for two-fluid interfaces and applications. *Arch. Ration. Mech. Anal.*, 208(2) :481–567, 2013.

[84] D. Lannes. *The water waves problem*, volume 188 of *Mathematical Surveys and Monographs*. American Mathematical Society, Providence, RI, 2013. Mathematical analysis and asymptotics.

[85] D. Lannes and P. Bonneton. Derivation of asymptotic two-dimensional time-dependent equations for surface water wave propagation. *Physics of Fluids*, 21(1) :016601, 2009.

[86] D. Lannes and F. Marche. A new class of fully nonlinear and weakly dispersive Green-Naghdi models for efficient 2D simulations. *J. Comput. Phys.*, 282 :238–268, 2015.

[87] D. Lannes and J.-C. Saut. Weakly transverse Boussinesq systems and the Kadomtsev-Petviashvili approximation. *Nonlinearity*, 19(12) :2853–2875, 2006.

[88] O. Le Métayer, S. Gavrilyuk, and S. Hank. A numerical scheme for the Green-Naghdi model. *J. Comput. Phys.*, 229(6) :2034–2045, 2010.

[89] G. Lebeau. Régularité du problème de Kelvin-Helmholtz pour l'équation d'Euler 2d. *ESAIM Control Optim. Calc. Var.*, 8 :801–825 (electronic), 2002. A tribute to J. L. Lions.

[90] R. Lteif, S. Israwi, and R. Talhouk. An improved result for the full justification of asymptotic models for the propagation of internal waves. *Commun. Pure Appl. Anal.*, 14(6) :2203–2230, 2015.

[91] P. A. Madsen, R. Murray, and O. R. Sørensen. A new form of the boussinesq equations with improved linear dispersion characteristics. *Coastal Engineering*, 15(4) :371 – 388, 1991.

[92] Z. L. Mal′tseva. Unsteady long waves in a two-layer fluid. *Dinamika Sploshn. Sredy*, (93-94) :96–110, 193, 1989.

[93] Y. Matsuno. A unified theory of nonlinear wave propagation in two-layer fluid systems. *Journal of the Physical Society of Japan*, 62(6) :1902–1916, 1993.

[94] H. Michallet and E. Barthélemy. Experimental study of interfacial solitary waves. *J. Fluid Mech.*, 366 :159–177, 7 1998.

[95] J. W. Miles. On the Korteweg-de Vries equation for a gradually varying channel. *J. Fluid Mech.*, 91(1) :181–190, 1979.

[96] D. Mitsotakis, B. Ilan, and D. Dutykh. On the Galerkin/finite-element method for the Serre equations. *J. Sci. Comput.*, 61(1) :166–195, 2014.

[97] M. Miyata. An internal solitary wave of large amplitude. *La mer*, 23(2) :43–48, 1985.

[98] F. Nansen. *Farthest North : The Epic Adventure of a Visionary Explorerr*. Library of Congress Cataloging-in-Publication Data, 1897.

[99] H. Y. Nguyen and F. Dias. A Boussinesq system for two-way propagation of interfacial waves. *Phys. D*, 237(18) :2365–2389, 2008.

[100] L. A. Ostrovsky and Y. A. Stepanyants. Do internal solitions exist in the ocean ? *Reviews of Geophysics*, 27(3) :293–310, 1989.

[101] L. A. Ostrovsky and Y. A. Stepanyants. Internal solitons in laboratory experiments : Comparison with theoretical models. *Chaos*, 15(3), 2005.

[102] S. R. Pudjaprasetya and E. van Groesen. Unidirectional waves over slowly varying bottom. II. Quasi-homogeneous approximation of distorting waves. *Wave Motion*, 23(1) :23–38, 1996.

[103] A. Ruiz de Zárate, D. G. A. Vigo, A. Nachbin, and W. Choi. A higher-order internal wave model accounting for large bathymetric variations. *Stud. Appl. Math.*, 122(3) :275–294, 2009.

[104] J.-C. Saut and L. Xu. The Cauchy problem on large time for surface waves Boussinesq systems. *J. Math. Pures Appl. (9)*, 97(6) :635–662, 2012.

[105] F. Serre. Contribution à l'étude des écoulements permanents et variables dans les canaux. *La Houille Blanche*, 6 :830–872, 1953.

[106] J. Shatah and C. Zeng. A priori estimates for fluid interface problems. *Comm. Pure Appl. Math.*, 61(6) :848–876, 2008.

[107] C.-W. Shu. Essentially non-oscillatory and weighted essentially non-oscillatory schemes for hyperbolic conservation laws. In *Advanced numerical approximation of nonlinear hyperbolic equations (Cetraro, 1997)*, volume 1697 of *Lecture Notes in Math.*, pages 325–432. Springer, Berlin, 1998.

[108] C. Sulem and P.-L. Sulem. Finite time analyticity for the two- and three-dimensional Rayleigh-Taylor instability. *Trans. Amer. Math. Soc.*, 287(1) :127–160, 1985.

[109] C. Sulem, P.-L. Sulem, C. Bardos, and U. Frisch. Finite time analyticity for the two- and three-dimensional Kelvin-Helmholtz instability. *Comm. Math. Phys.*, 80(4) :485–516, 1981.

[110] M. Tissier, P. Bonneton, F. Marche, F. Chazel, and D. Lannes. A new approach to handle wave breaking in fully non-linear boussinesq models. *Coastal Engineering*, 67 :54 – 66, 2012.

[111] L. N. Trefethen. *Spectral methods in MATLAB*, volume 10 of *Software, Environments, and Tools*. Society for Industrial and Applied Mathematics (SIAM), Philadelphia, PA, 2000.

[112] B. van Leer. Towards the ultimate conservative difference scheme. V. A second-order sequel to Godunov's method. *J. Comput. Phys.*, 135(2) :227–248, 1997.

[113] J. M. Witting. A unified model for the evolution nonlinear water waves. *J. Comput. Phys.*, 56(2) :203–236, 1984.

[114] L. Xu. Intermediate long wave systems for internal waves. *Nonlinearity*, 25(3) :597–640, 2012.

[115] V. E. Zakharov. Stability of periodic waves of finite amplitude on the surface of a deep fluid. *Journal of Applied Mechanics and Technical Physics*, 9(2) :190–194, 1968.